PHYSICO-CHEMICAL STUDIES OF BLOCK COPOLYMERS IN AQUEOUS SOLUTION

Jonathan Keith Armstrong

(B.Sc. Hons. Applied Chemistry)

A thesis submitted in partial fulfillment of the requirements of the University of Greenwich for the degree of Doctor of Philosophy

School of Chemical and Life Sciences,

University of Greenwich,

Woolwich, London, SE18 6PF, U.K.

July 1997

DEDICATION

To my parents:

Keith and Gwyneth Armstrong

ABSTRACT

PHYSICO-CHEMICAL STUDIES OF BLOCK COPOLYMERS IN AQUEOUS SOLUTION

The dilute aqueous solution behaviour of oxyethylene/oxypropylene copolymers has been investigated as a function of temperature (275-370K), copolymer concentration (0.1-5% w/v) and copolymer composition [polyoxypropylene (POP) and polyoxyethylene (POE) homopolymers (750-4000gmol^{-1}) and diblock copolymers (3450-13300gmol^{-1}), poloxamers (POE-POP-POE triblock copolymers, 1100-14000gmol^{-1}) and poloxamines (ethylene diamine alkoxylates, 1650-26000gmol^{-1})] using the macroscopic techniques of high sensitivity differential scanning calorimetry (HSDSC), and differential scanning densitometry (DSD) and also using the technique of ^{1}H and ^{13}C-NMR. The observed phase transitions from HSDSC data are indicative of an aggregation process and are consequent upon changes associated with POP involving dehydration, a conformational change and aggregation. For POP homopolymers, the phase transition results in phase separation of the polymer (cloud point) but for the diblock copolymers, poloxamers and poloxamines these copolymers remain in solution due to the effects of the POE portion of the copolymer. The phase transition temperature (T_m) decreases and the calorimetric enthalpy (ΔH_{cal}) increases with increasing molecular mass of the POP block and show no relationship to the POE content. DSD data of poloxamers in water at a concentration of 1% (w/v) show a sharp increase in partial specific volume ($\overline{v}$) with increasing temperature, the mid-point of the transition in agreement with the T_m observed by HSDSC. The partial specific volume change ($\Delta\overline{v}$) approach zero as the POE:POP ratio approaches 1:0 indicative that the phase transition is associated with changes in the POP portion of the copolymer. T_1 relaxation NMR data for poloxamer 237 in D_2O as a function of temperature shows a gradual increase in relaxation times for -$\underline{C}H_2$- and -$\underline{C}$H(Me)- resonances with increasing temperature due to increased molecular motion, but a sharp decrease of the -CH($\underline{Me}$)- relaxation time was observed at the T_m relating to a change in conformation of the POP portion of the copolymer. The effects of cosolutes (NaCl, Na_2HPO_4/NaH_2PO_4 , urea and guanidinium chloride) and cosolvents (methanol, ethanol, n-propanol, n-butanol and formamide) on the observed phase transition of poloxamers have been investigated using HSDSC. Sodium chloride, phosphate buffer, n-propanol and n-butanol favour aggregation of the copolymer reflected in a lowering the T_m and an increase in ΔH_{cal}. Conversely, urea, guanidinium chloride, methanol, ethanol and formamide prevent the onset of aggregation reflected in an increase in T_m and a lowering of ΔH_{cal}. The effects of cosolutes and cosolvents on the aggregation behaviour of poloxamers are explained in terms of enhancing or breaking water structure or by possibly replacing water molecules in the solvation sphere of the POP portion of the copolymer. The calorimetric output has been analysed using a model fitting procedure based upon a mass action description to obtain estimates for thermodynamic parameters which chracterise the aggregation process. These important parameters include $T_{1/2}$, the temperature at which the aggregation process is half completed, ΔH_{cal} , ΔH_{vH} , the van't Hoff enthalpy and *n* the aggregation number. The modelled excess heat capacity data are in good agreement with the experimental calorimetric outputs. An enthalpy-entropy compensation plot for all data obtained indicate that the solvent-solute interactions that are responsible for the phase transitions observed by HSDSC are the same for all of the copolymers investigated regardless of the copolymer composition and concentration.

Jonathan Keith Armstrong

STATEMENT

The work described in this thesis was carried out in the laboratories of the School of Biological and Chemical Sciences, University of Greenwich, between 1990 and 1994. Except where otherwise stated, it is entirely the work of the author.

ACKNOWLEDGMENTS

I would firstly and foremostly like to thank my supervisor, Professor Babur Z. Chowdhry for his guidance, scientific input, friendship, unrelenting enthusiasm, and support throughout this period in my life. I would also like to thank my co-supervisor Dr Steve Leharne, for his enthusiasm, scientific input, guidance and many useful discussions, Dr. John Mitchell for his enthusiasm and scientific input, and Professor Tony Beezer for many useful scientific discussions. I would also like to thank Dr. N. Rees for performing the NMR experiments. I would like to thank Professor Dr. Peter Laggner and the post-docs and technicians in his lab for enabling the densitometric experiments to occur, and for making my stay at the Austrian Academy of Sciences in Graz an enjoyable and useful experience.

To those people whose great friendship will always mean so much to me and whose support (especially when I needed it) helped me get through those "difficult times" we collectively faced; namely (and not in any particular order): Kathy and Dom, Jyoti, Paul, Fash, Stuart, Ronan, Sham, Babs, Steve and anyone else who I may have forgotten to mention - to all of you, thankyou.

CONTENTS

	Page Number
Abstract	**i**
Statement	**ii**
Acknowledgments	**ii**
Abbreviations	**vi**
List of Figures and Tables	**vii**
Data Accuracy	**xii**
Nomenclature and Coding of the Poloxamers and Poloxamines	**xiii**
Thesis Guide	**xiv**
Chapter 1 General Overview	**1**
1.1 Polymers	1
1.1.1 Introduction	1
1.1.2 Polymer Synthesis	2
1.2 Analysis of Polymers	2
1.2.1 Molecular Mass Distribution	2
1.2.2. Infra-red Analysis	3
1.2.3 Nuclear Magnetic Resonance (NMR)	4
1.2.4 Thermal Analysis	5
1.2.4.1 Differential Thermal Analysis (DTA)	5
1.2.4.2 Thermogravimetric Analysis (TGA)	6
1.2.4.3 Hot-Stage Microscopy (HSM)	6
1.2.4.4 Thermomechanical Analysis (TMA)	7
1.2.4.5 Dynamic Mechanical Analysis (DMA)	7
1.2.4.6 Torsional Braid Analysis (TBA)	8
1.2.4.7 Less Common Techniques of Thermal Analysis	8
1.2.4.8 Summary	9
1.3 Overview of Poloxamers and Poloxamines	9
1.3.1 Synthesis	9
1.3.2 Applications and Uses of Poloxamers in the Pharmaceutical Industry	13
1.3.2.1 Model Drug Delivery Systems (Dilute Systems)	13
1.3.2.2 Drug Delivery from Polymeric Gels	15
1.3.3 Clinical Uses of Poloxamers	16
1.3.4 Miscellaneous Uses of Poloxamers	18
1.3.4.1 Poloxamer Effects on Bacterial and Protein Adhesion to Surfaces	18
1.3.4.2 Poloxamer Effects on Cell Cultures	18
1.3.4.3 Other Applications of Poloxamers and Poloxamines	20
1.3.5 Fundamental Studies on the Solution Behaviour of Poloxamers	21
1.3.4.1 Preliminary Techniques	22
1.3.4.2 Literature Review of Current Research	23

1.4 References 34
Chapter 2 Theoretical Basis of Techniques 40
2.1 Calorimetry 40
2.1.1 High Sensitivity Differential Scanning Calorimetry (HSDSC) 41
2.1.2 HSDSC Data 44
2.1.2.1 Analysis of HSDSC Data 44
2.1.2.2 Two State Processes 45
2.1.2.3 Non-Two State Processes 47
(a) $\Delta H_{cal} < \Delta H_{vH}$ 47
(b) $\Delta H_{cal} > \Delta H_{vH}$ 48
(c) Irreversible Processes 48
2.1.3 Microcal MC-2 HSDSC 48
2.1.3.1 Cell Feed-Back 49
2.1.3.2 Data Accumulation and Analysis 50
2.1.4 Applications and Uses of HSDSC 52
2.2 Densitometric Analysis 53
2.2.1 General Considerations 53
2.2.2 Principle of the Mechanical Oscillator Technique 54
2.2.3 Experimental Procedure 56
2.2.4 Applications and Uses of Differential Scanning Densitometry 57
2.3 Nuclear Magnetic Resonance (NMR) 58
2.3.1 Principles of NMR 58
2.3.2 Applications and Uses of NMR 63
2.4 Overview 64
2.4.1 Objectives of Research 65
2.5 References 66

Chapter 3 General Experimental Section 68
3.1 Materials 68
3.1.1 Polymers 68
3.1.2 Cosolutes and Cosolvents 68
3.1.3 Molecular Mass Distribution 68
3.2 Experimental 72
3.2.1 General 72
3.2.2 High sensitivity Differential Scanning Calorimetry (HSDSC) 73
3.2.3 Differential Scanning Densitometry (DSD) 74
3.2.4 Nuclear Magnetic Resonance (NMR) 75
3.2.5 Fractionation of Poloxamer 407 75
3.3 References 76

Chapter 4 Polyoxyethylene and Polyoxypropylene Homopolymers 77
4.1 General 77
4.2 Experimental 79

4.3 Results and Discussion 80
4.3.1 Polyoxypropylenes and Polyoxyethylenes in Water 80
4.3.2 The Effects of Sodium Chloride on High Molecular Mass Polyoxyethylene 83
4.3.3 Polyoxypropylene Mixtures 85
4.4 Tables 86
4.5 References 88

Chapter 5 Polyoxyethylene-Polyoxypropylene Diblock Copolymers 90
5.1 Results and Discussion 90
5.1.1 Diblock Copolymers in Water 90
5.2 Tables 92
5.3 References 92

Chapter 6 Polyoxyethylene-Polyoxypropylene-Polyoxyethylene Triblock Copolymers (Poloxamers) 93
6.1 Calorimetric Studies 93
6.1.1 Results and Discussion 93
6.1.1.1 Poloxamers at 5mgmL^{-1} and Constant Oxypropylene Concentration 93
6.1.1.2 Empirical Relationships 102
6.1.1.3 Effects of Copolymer Concentration 103
6.1.1.4 Effects of Fractionation of Poloxamer 407 105
6.2 Nuclear Magnetic Resonance Studies 106
6.3 Densitometric Studies 109
6.3.1 Experimental 109
6.3.2 High Sensitivity DSC 109
6.3.3 Differential Scanning Densitometry (DSD) 110
6.4 Cosolute Effects 114
6.4.1 Effects of Sodium Chloride and Phosphate Buffer 114
6.4.2 Effects of Urea and Guanidinium Chloride 119
6.5 Effects of Cosolvents 122
6.6 Summary 125
6.6 Tables 127
6.7 References 136

Chapter 7 Ethylene Diamine Alkoxylates (Poloxamines) 138
7 1 Introduction 138
7.2 Experimental 139
7.2.1 High Sensitivity Differential Scanning Calorimetry (HSDSC) 139
7.2.2 Turbidimetric Analysis 139
7.2.3 Titrimetric Analysis 140
7.2.4 Nuclear Magnetic Resonance (NMR) 140

7.3 Results and Discussion 140
7.3.1 Background 140
7.3.2 Thermal Analysis 142
7.3.2.1 Scan Rate Effects for T701 144
7.3.2.2 Reversibility 144
7.3.2.3 Concentration Effects 145
7.3.2.4 pH Effects 145
7.3.3 Titrimetric Analysis 146
7.3.4 Turbidimetric Analysis 147
7.3.5 Sodium Chloride Effects 148
7.3.6 NMR Studies 149
7.4 Conclusions 151
7.5 Tables 151
7.6 References 154

Chapter 8 Modelling of the Calorimetric Phase Transitions 156
8.1 Introduction 156
8.1.1 Modelling of the Temperature Dependence of an Aggregation Process 156
8.1.2 Modelling of the Temperature Dependence of Phase Separation 157
8.1.3 Data Analysis 158
8.2 Results and Discussion 160
8.2.1 Establishing a Model for the Calorimetric Transitions 160
8.2.2 Phase Separation 164
8.2.3 Solubility Behaviour of Polyoxypropylene 165
8.2.4 Simulations of $C_{p,xs}$ Temperature Plots 167
8.2.5 The Effect of Concentration on the Thermodynamics of Phase Transitions 168
8.2.6 Comparison with POE-POP-POE Block Copolymers 169
8.2.7 Entropy-Enthalpy Compensation 169
8.2.8 Modelling of the Phase Transitions for Diblocks, Poloxamers and Poloxamines 170
8.2.8.1 Copolymers in Water at a Concentration of 5mgmL^{-1} 170
8.2.8.2 Concentration Effects 171
8.2.8.3 Cosolute and Cosolvent Effects 171
8.3 Concluding Remarks 172
8.4 Tables 173
8.5 References 179

Chapter 9 - Summary 180
Addendum 184
Conference Presentations 184
Full Publications 185

ABBREVIATIONS AND SYMBOLS

Abbreviation/Symbol	Definition
CFB	cell feed-back
$C_{p,max}$	maximum excess heat capacity
$C_{p,xs}$	excess heat capacity
DMA	dynamic mechanical analysis
DPPC	dipalmitoylphosphatidylcholine
DSC	differential scanning calorimetry
DSD	differential scanning densitometry
DSPC	distearylphosphatidylcholine
DTA	differential thermal analysis
$\overline{E}_2^0$	molal expansibility
EVA	evolved gas analysis
FTIR	Fourier Transform infra-red
GPC	gel permeation chromatography
ΔH_{cal}	calorimetric enthalpy
ΔH_{vH}	van't Hoff enthalpy
HSDSC	high sensitivity differential scanning calorimetry
HSM	hot stage microscopy
NMR	nuclear magnetic resonance
OE	oxyethylene
OP	oxypropylene
POE	polyoxyethylene
PEO	poly(ethylene oxide) (MW > 20000 gmol-1)
POP	polyoxypropylene
ppm	parts per million
ΔS	entropy
$T_{1/2}$	transition temperature mid-point, corresponding to $\Delta H_{cal}/2$
T_m	transition temperature mid-point, corresponding to $C_{p,max}$
$\Delta T_{1/2}$	transition half width
TBA	torsional braid analysis
TGA	thermogravimetric analysis
THF	tetrahydrofuran
TMA	thermomechanical analysis
TS	thermosonimetry
$\overline{v}$	partial specific volume
$\overline{v}(c)$	molar partial specific volume
$\Delta\overline{v}$	partial specific volume change

List of Figures and Tables

FIGURES

Figure Number	Legend	Page Number
Figure 1.1	*Classification of Polymers*	1
Figure 1.2	*Molecular mass distribution of poloxamer 235 (Pluronic P85) as determined by GPC, mixed PL-gel columns, mobile phase of tetrahydrofuran with antioxidant, flow rate 1mLmin^{-1}, ambient temperature and a refractive index detector.*	3
Figure 1.3	*Generalised structures of a poloxamer and a poloxamine.*	10
Figure 1.4	*Poloxamer synthesis.*	11
Figure 1.5	*Side reactions during polyoxypropylene synthesis.*	12
Figure 1.6	*Generalised diagram to demonstrate the complex nature of the aqueous solution behaviour of the poloxamers (only the main phases that can occur are shown). Where M = hydrated POP/POE single chain (n = 1), P_s = hydrated POP/POE associated POP (n > 1), A= hydrated POE, dehydrated + aggregated POP (n > 1), A_{gel} = hydrated and entangled POE, dehydrated + associated POP, (n >> 1), B = dehydrated POE/POP (CP) (n >> 1), T = temperature, c = concentration.*	21
Figure 2.1	*Classification of Calorimeters.*	41
Figure 2.2	*Schematic representation of the Microcal MC-2 Calorimetric Unit.*	50
Figure 2.3	*Idealised HSDSC Output.*	52
Figure 2.4	*Vector diagram of force harmonic oscillation (a) a balanced system, and (b) an unbalanced system.*	55
Figure 2.5	*Idealised Differential Scanning Densitometric scan, where T_β and T_α denote the start and end of the observed phase transition, the half width* $\Delta T_{1/2} = T_{\left(\bar{v}+\frac{\Delta\bar{v}}{4}\right)} - T_{\left(\bar{v}-\frac{\Delta\bar{v}}{4}\right)}$ *and the transition temperature T_m = T at* $\alpha^{max}(\alpha = \frac{1}{\bar{v}} \bullet \frac{d\bar{v}}{dT})$.	57
Figure 2.6	*Spin-state orientations of the hydrogen nucleus in a magnetic field, H_0.*	58
Figure 2.7	*Deshielding effects of neighbouring groups on the downfield shift for proton NMR.*	60
Figure 2.8	*The interaction between two dipoles in field B_0.*	62
Figure 4.1	*HSDSC scans of POP in double distilled water at a concentration of 5mgmL^{-1}, at a scan rate of 60Kh^{-1}.*	81
Figure 4.2	*Reversibility of the phase transitions of (a) POP 1000 gmol^{-1} and (b) POP 2000 gmol^{-1}, at a concentration of 5 mgmL^{-1} in double distilled water, scanned at ±30Kh^{-1}.*	81
Figure 4.3	*Calorimetric scan of POE of molecular mass 1000 gmol^{-1}, at a concentration of 5mgmL^{-1} in double distilled water, scanned at 60 Kh^{-1}.*	82
Figure 4.4	*Calorimetric traces obtained for POE of molecular mass 1x10^6 gmol^{-1} at a concentration of 2.5mgmL^{-1} in aqueous sodium chloride solution, at a scan rate of 60Kh^{-1}.*	84
Figure 5.1	*Calorimetric scans of diblock copolymers in double distilled water at a concentration of 5mgmL^{-1} and at a scan rate of 60Kh^{-1} (Each scan is identified by the molecular mass of the copolymer)*	91
Figure 6.1a	*Calorimetric traces of poloxamers in double distilled water at a concentration of 5mgmL^{-1}, scanned at 60Kh^{-1}.*	94
Figure 6.1b	*Calorimetric traces of poloxamers in double distilled water at a concentration of 5mgmL^{-1}, scanned at 60Kh^{-1}.*	95
Figure 6.2	*The relationship between the phase transition temperature and POE or POP content of the poloxamers for the phase transitions obtained at a concentration of 5mgmL^{-1} in double distilled water and at a scan rate of 60 Kh^{-1}.*	96
Figure 6.3	*Calorimetric scan to show the reversibility of the phase transition of poloxamer P333 in double distilled water at a scan rate of ± 30Kh^{-1}.*	96
Figure 6.4	*A plot to show the relationship between the calorimetric enthalpy per average monomer unit versus oxypropylene/oxyethylene ratio.*	97

List of Figures continued..

		Page Number
Figure 6.5	*A plot to show the relationship between the calorimetric enthalpy per average oxypropylene unit, averaged for each series of poloxamer, plotted against the percentage POE content.*	97
Figure 6.6	*A plot to show the dependence of the difference between the cloud point and phase transition temperature on the POE content of the poloxamers.*	98
Figure 6.7	*Calorimetric scans of poloxamer P237 at various copolymer concentrations (1 to 50mgmL^{-1}) in double distilled water at a scan rate of 60Kh^{-1}.*	104
Figure 6.8	*The effect of copolymer concentration on the phase transition temperature in double distilled water, at a scan rate of 60Kh^{-1}.*	104
Figure 6.9	*GPC output of the molecular mass distribution of P407 following fractionation of the copolymer by partitioning between hexane and dichloromethane.*	105
Figure 6.10	*Calorimetric scans of P407, and fractioned P407 recovered from hexane and dichloromethane.*	105
Figure 6.11	*OP methyl ^{13}C NMR shift positions (ppm) from 293K to 333K for P237 at a concentration of 10mgmL^{-1} in D_2O. Shifts relative to DSS. Temperatures (K): (a) 293, (b) 303K, (c) 305K, (d) 307K, (e) 308K, (f) 309K, (g) 311K, (h) 313K and (i) 333K.*	106
Figure 6.12	*T_1 relaxation measurements for P237 from 288K to 333K: ●, CH_2 (OP), □ CH (OP), ▲ CH_2 (OE), Δ, CH_3 (OP).*	107
Figure 6.13	*Partial specific volume ($\bar{v}$) of the poloxamers in double quartz distilled water at a concentration of 10mgmL^{-1} at a scan rate of 30Kh^{-1}.*	111
Figure 6.14	*Calorimetric traces and partial specific volume ($\bar{v}$) of poloxamers P215 and P333 at a concentration of 10mgmL^{-1}, in pure water, at a scan rate of 30Kh^{-1}.*	112
Figure 6.15	*Molal expansibility ($\bar{E}_2^0$) of poloxamer P333 in double quartz distilled water (10mgmL^{-1}) as a function of temperature.*	114
Figure 6.16	*Calorimetric scans of P237 in sodium chloride solutions (0 - 1.71M) at a copolymer concentration of 5mgmL^{-1}, at a scan rate of 60Kh^{-1}.*	115
Figure 6.17	*The effect of sodium chloride concentration on the phase transition temperature and cloud point of P237 and P407 at a copolymer concentration of 5mgmL^{-1}.*	115
Figure 6.18	*Calorimetric scans of P237 at various copolymer concentrations (1 to 20mgmL^{-1}) in 1.03M NaCl at a scan rate of 60Kh^{-1}.*	118
Figure 6.19	*The effect of concentration of P237 (1 to 20mgmL^{-1}) on the phase transition temperature and cloud point in 1.03M sodium chloride.*	119
Figure 6.20	*Calorimetric scans of poloxamer P237 in urea solutions (0 - 7.83M) at a copolymer concentration of 5mgmL^{-1}, at a scan rate of 60Kh^{-1}.*	120
Figure 6.21	*The effects of sodium chloride, phosphate buffer (pH 7.2), urea and guanidinium chloride concentration on the phase transition temperature of poloxamer P237 (5mgmL^{-1}) in aqueous solution.*	120
Figure 6.22	*The effect of methanol on the observed phase transition of P237 at a copolymer concentration of 5mgmL^{-1}.*	122
Figure 6.23	*The effect of ethanol on the observed phase transition of P237 at a copolymer concentration of 5mgmL^{-1}.*	122
Figure 6.24	*The effect of propanol on the observed phase transition of P237 at a copolymer concentration of 5mgmL^{-1}.*	122
Figure 6.25	*The effect of butanol on the observed phase transition of P237 at a copolymer concentration of 5mgmL^{-1}.*	122
Figure 6.26	*The effect of methanol on the observed phase transition of P237 at a copolymer concentration of 20mgmL^{-1}.*	123
Figure 6.27	*The effect of formamide on the observed phase transition of P237 at a copolymer concentration of 5mgmL^{-1}.*	123
Figure 6.28	*The effects of alcohol concentration on the calorimetric enthalpy and phase transition temperature of P237 at a concentration 5mgmL^{-1}, scanned at 60Kh^{-1}. (□ MeOH, ■ EtOH, ◊ PrOH, ◆ BuOH)*	124
Figure 6.29	*The effects of hydrazine on the phase transition temperature and calorimetric enthalpy of P237 in aqueous solution at a concentration of 5mgmL^{-1}.*	124

List of Figures continued..

		Page Number
Figure 6.30	*Plot of the calorimetric enthalpy as a function of T_m.*	124
Figure 7.1	*Calorimetric scans of poloxamines in double distilled water at a concentration of $5mgmL^{-1}$ and at a scan rate of $60Kh^{-1}$.*	143
Figure 7.2	*The relationship between the calorimetric enthalpy and oxypropylene/oxyethylene ratio of the poloxamines.*	144
Figure 7.3	*A plot to show the dependence of the difference between the main phase transition and cloud point to the oxyethylene content of the poloxamines.*	144
Figure 7.4	*Calorimetric scan to show the reversibility of T904 in double distilled water at a concentration of $5mgmL^{-1}$, at a scan rate of $\pm 30\ Kh^{-1}$.*	145
Figure 7.5	*The effects of pH on the observed phase transition of T701 in dilute aqueous solution ($5mgmL^{-1}$), scanned at $60Kh^{-1}$.*	146
Figure 7.6	*Graphs to show the effect of pH on the phase transition temperature of T701 and the corresponding back-titration of an acidified solution of T701 with 0.01M NaOH.*	147
Figure 7.7	*Turbidimetric scans of poloxamines T701 and T904 at 540nm and at a concentration of $5mgmL^{-1}$ in double distilled water, scanned at a scan rate of $60Kh^{-1}$. The corresponding calorimetric runs are superimposed showing the relationship between the two techniques.*	148
Figure 7.8	*Calorimetric scans of T304 at a concentration of $5mgmL^{-1}$ in solutions of sodium chloride.*	149
Figure 7.9	*Proton NMR of T701 and T904 in D_2O as a function of temperature.*	150
Figure 7.10	*^{13}C NMR of T701 and T904 in D_2O as a function of temperature.*	150
Figure 8.1	*Simulated calorimetric traces for (a) aggregation and (b) phase separation. Calorimetric traces obtained for (c) P215 and (d) Polyoxyethylene ($1x10^6\ gmol^{-1}$).*	160
Figure 8.2	*Effect of molecular mass on the thermodynamic parameters of T_m (□) and ΔH_{cal} (□).*	163
Figure 8.3	*Variation of $C_{p,xs}$ with temperature for POP of molecular mass 1000. The open circles represent simulated $C_{p,xs}$ values; the solid line represents experimental data.*	163
Figure 8.4	*Effect of concentration of aqueous solutions of POP 1000 on the thermodynamic parameters of T_m ( ) and ΔH_{cal} (□).*	166
Figure 8.5	*The variation of ΔH_{vH} with $T_{1/2}$. The data was obtained for POP 1000 solutions of various concentrations.*	166
Figure 8.6	*van 't Hoff plot for aqueous solutions of POP 1000.*	167
Figure 8.7	*Enthalpy-entropy compensation plot for all polymer solutions investigated.*	167
Figure 9.1	*A plot of the calorimetrically observed phase transition temperature versus POP content for all of the polymer samples investigated at a concentration of $5mgmL^{-1}$ and at a scan rate of $60Kh^{-1}$.*	180
Figure 9.2	*Entropy-enthalpy compensation plot for the observed phase transition of the polymers studied in dilute aqueous solution by HSDSC.*	180
Figure 9.3	*Summary of the different solvation states observed for block copolymers of POP and POE in dilute aqueous solution.*	181

TABLES

Table Number	Title	Page Number
Table 1.3.1	*Early industrial uses of oxyalkylene block copolymers. Technical Data on Pluronic and Tetronic Nonionics, Wyandotte Chemical Corporation, Wyandotte, Michigan.*	11
Table 1.3.2	*Critical micelle concentration values of poloxamers at 298K in a 0.5% aqueous solution of benzopurpurin 4B.*	23
Table 1.3.3	*Summarised review of current literature.*	24
Table 3.1	*Coding and Molecular Masses of the Poloxamers.*	70
Table 3.2	*Coding and Molecular Masses of the Poloxamines.*	71
Table 3.3	*Molecular Masses and Suppliers of Homopolymers and Diblock Copolymers.*	71

List of Tables continued..

		Page Number
Table 4.1	*Solubility of some Polyethers in Water.*	78
Table 4.2	*Thermodynamic parameters for the solution-phase transitions of polyoxypropylenes at a concentration of 5mgmL^{-1} in double distilled water, at a scan rate of 60Kh^{-1}.*	86
Table 4.3	*The effects of scan rate on the thermodynamic parameters for the solution-phase transition of polyoxypropylene (1000 gmol^{-1}) in double distilled water at a concentration of 5mgmL^{-1}.*	86
Table 4.4	*The effects of polymer concentration on the thermodynamic parameters for the solution-phase transition of polyoxypropylene (1000 gmol^{-1}).*	87
Table 4.5	*The effects of polymer mixtures on the solution-phase transition temperature of polyoxypropylenes at a concentration of 5mgmL^{-1} in double distilled water, and at a scan rate of 60Kh^{-1}.*	87
Table 5.1	*Thermodynamic parameters for the solution-phase transitions of POP-POE diblock copolymers in double distilled water at a concentration of 5mgmL^{-1}, at a scan rate of 60Kh^{-1}.*	92
Table 5.2	*The effects of scan rate and reversibility of the solution-phase transition of POP-POE diblock copolymer (13333 gmol^{-1}) in double distilled water at a concentration of 5mgmL^{-1}.*	92
Table 6.1	*Thermodynamic parameters for the solution-phase transitions of poloxamers in double distilled water at a concentration of 5mgmL^{-1}, at a scan rate of 60Kh^{-1}.*	127
Table 6.2	*Thermodynamic parameters for the solution-phase transitions of poloxamers in double distilled water at a constant oxypropylene concentration of 5mgmL^{-1}, at a scan rate of 60Kh^{-1}.*	128
Table 6.3	*Thermodynamic parameters for the solution-phase transitions of poloxamers in double distilled water at varying copolymer concentrations(1-50mgmL^{-1}), at a scan rate of 60Kh^{-1}.*	129
Table 6.4	*Thermodynamic parameters of fractioned samples of P407. Fractionation achieved by partitioning of P407 between hexane and dichloromethane, and subsequent separation and drying. Calorimetric data for unfractioned and fractioned samples were obtained from scans at a copolymer concentration of 5mgmL^{-1} in double distilled water and at a scan rate of 60Kh^{-1}.*	130
Table 6.5	*Thermodynamic parameters derived by HSDSC and DSD for the solution-phase transitions of poloxamers in double distilled water at a concentration of 10 mgmL^{-1} and at a scan rate of 30Kh^{-1}.*	130
Table 6.6	*Theoretical and experimental partial specific volumes of the poloxamers (cm^{3}g^{-1}) at a concentration of 10mgmL^{-1} in water.*	131
Table 6.7	*Thermodynamic parameters derived by HSDSC solution-phase transitions of poloxamers in sodium chloride at a copolymer concentration of 5mgmL^{-1} and at a scan rate of 60Kh^{-1}.*	132
Table 6.8	*Thermodynamic parameters derived by HSDSC solution-phase transitions of poloxamer P237 in phosphate buffer (pH 7.2) at a copolymer concentration of 5mgmL^{-1} and at a scan rate of 60Kh^{-1}.*	133
Table 6.9	*Thermodynamic parameters derived by HSDSC for the solution-phase transitions of poloxamer P237 in 1.03M sodium chloride at copolymer concentrations of 1 to 20mgmL^{-1} at a scan rate of 60Kh^{-1}.*	133
Table 6.10	*Thermodynamic parameters derived by HSDSC solution-phase transitions of poloxamer P237 in urea and guanidinium chloride solutions at a copolymer concentration of 5mgmL^{-1} and at a scan rate of 60Kh^{-1}.*	134
Table 6.11	*Thermodynamic parameters derived by HSDSC solution-phase transitions of poloxamer P237 in methanol, ethanol, propanol, butanol and formamide solutions at a copolymer concentration of 5mgmL^{-1} and at a scan rate of 60Kh^{-1}.*	135
Table 7.1	*Thermodynamic parameters associated with the calorimetrically observed phase transitions of poloxamines at concentration of 5mgmL^{-1} in double distilled water, scanned at 60Kh^{-1}.*	151
Table 7.2	*Thermodynamic parameters associated with the calorimetrically observed phase transitions of poloxamines at constant oxypropylene concentration in double distilled water, scanned at 60Kh^{-1}.*	152

List of Tables continued..

		Page Number
Table 7.3	*The effects of scan rate on the thermodynamic parameters associated phase transitions of T701 at concentration of 5mgmL^{-1} in double distilled water.*	152
Table 7.4	*Reversibility of the phase transition of T904 at a concentration of 5mgmL^{-1} in double distilled water, scanned at ± 30Kh^{-1}.*	152
Table 7.5	*The effects of copolymer concentration (1-20 mgmL^{-1} in double distilled water) and pH (0.03M buffer at a copolymer concentration of 5 mgmL^{-1})on the thermodynamic parameters associated with the phase transitions of T701, scanned at 60Kh^{-1}.*	153
Table 7.6	*The effects of sodium chloride on the thermodynamic parameters associated with the phase transition of T304 at a copolymer concentration of 5mgmL^{-1}, scanned at 60Kh^{-1}.*	154
Table 8.1	*The Effect of Molecular Mass on the Overall Thermodynamic Parameters for the Observed Phase Transitions of Poloyoxypropylene in Aqueous Solution.*	173
Table 8.2	*Values for Number of POP Molecules in Clusters and Number of Clusters Involved in Aggregation.*	173
Table 8.3	*Thermodynamic Parameters for POP 1000 as a Function of Concentration.*	173
Table 8.4	*Thermodynamic Parameters for the Diblock Copolymers in Water at a Concentration of 5mgmL^{-1} .*	174
Table 8.5	*Thermodynamic Parameters for the Phase Transitions Observed for Poloxamines in Water at a Concentration of 5mgmL^{-1} .*	174
Table 8.6	*Thermodynamic Parameters for the Phase Transitions Observed for Poloxamers in Water at a Concentration of 5mgmL^{-1} .*	175
Table 8.7	*The Effects of Concentration on the Thermodynamic Parameters for the Phase Transitions of Poloxamers in Water.*	176
Table 8.8	*The Effects of Cosolutes on the Thermodynamic Parameters Derived for P237 in Aqueous Solution at a Concentration of 5mgmL^{-1}.*	177
Table 8.9	*The Effects of Cosolvents on the Thermodynamic Parameters Derived for P237 in Aqueous Solution at a Concentration of 5mgmL^{-1}.*	178

Data Accuracy

The data presented in this thesis are within the following accuracy limits of the technique of high sensitivity differential scanning calorimetry and differential scanning densitometry:

T_m = ±0.1K

$T_{1/2}$ = ±0.1K

CP = ±0.1K

$\Delta T_{1/2}$ = ±0.2K

C_p^{max} = ±3%

ΔH_{cal} = ±3%

ΔH_{vH} = ±3%

ΔS_{cal} = ±3%

$\Delta \bar{v}$ = ±5%

$\bar{v}$ = ±5%

Nomenclature and Coding of the Poloxamers and Poloxamines

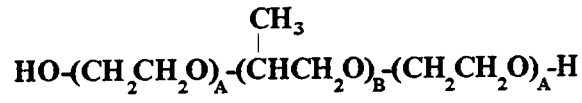

Poloxamer

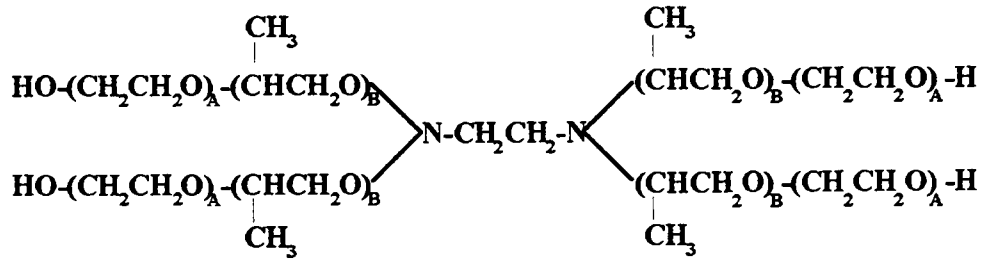

Poloxamine

Generalised Structure of a Poloxamer and a Poloxamine

Poloxamers:

Generic Names: Poloxamer, proxanol, oxyalkylene block copolymer.

Industrial Names: Pluronic, Synperonic PE Nonionic Surfactant.

Generic Coding: e.g., P188

"P" represents poloxamer.

The final digit x 10 = percentage polyoxyethylene content (w/w) i.e., 8 x 10 = 80%.

The first two digits x 100 = approximate molecular mass of the polyoxypropylene block, i.e., 18 x 100 = 1800gmol^{-1}.

Industrial Coding: (Pluronic Code) e.g., F68

The first letter represents the physical state of the polymer:

F = Flake, P = Paste, L = Liquid.

The final digit x 10 = percentage polyoxyethylene content (w/w).

The first digit(s) represent the molecular mass of the polyoxypropylene block, determined from the "Pluronic Grid" (BASF Technical Data).

Poloxamines:

Generic Names: Poloxamine, ethylene diamine alkoxylate.

Industrial Names: Tetronic, Synperonic T Nonionic Surfactant.

Generic Coding: None.

Industrial Coding: (Tetronic Code) e.g., T908

The first letter represents a Tetronic copolymer.

The final digit x 10 = percentage polyoxyethylene content (w/w).

The remaining digits represent the total molecular mass of the polyoxypropylene blocks, determined from the "Tetronic Grid" (BASF Technical Data).

Thesis Guide

Chapter 1 (pp1-39) gives a general overview of polymers, from structural analysis using infra-red and nuclear magnetic resonance (nmr) spectroscopy to thermal analysis. This chapter also includes a detailed survey of the literature on the applications and uses of poloxamers and poloxamines, and finally a tabulated summary of the current research into their solution behaviour is presented.

Chapter 2 (pp 40-67) discusses the techniques used for the studies presented in this thesis (scanning microcalorimetry, differential scanning densitometry and nuclear magnetic resonance) and presents the nature of the data that can be directly or indirectly derived from these techniques. At the end of this chapter a brief overview of the specific aims of the project are presented.

Chapter 3 (pp 68-76) presents the experimental methodology employed for each of the techniques used. The molecular masses and polyoxypropylene/polyoxyethylene contents of the polymers used are also tabulated in this chapter.

In Chapters 4, 5, 6 and 7 (pp 77-155) the data derived from calorimetric, densitometric, and nmr experiments for the aqueous solution behaviour of polyoxypropylene/polyoxyethylene homopolymers (chapter 4), diblocks (chapter 5), poloxamers (chapter 6) and poloxamines (chapter 7) are presented and discussed.

Chapter 8 (pp 156-179) presents the modelling of the calorimetrically observed phase transitions using a mass action model. Please note that the modelled data presented in Tables 8.1 - 8.9 is from a single analysis of a single transition, and the comparable experimental data presented in the previous chapters are averaged data from 5 analyses of each scan. Hence, there is a slight variation between the two sets of thermodynamic data.

Chapter 9 (pp 180-183) briefly summarises the aqueous solution behaviour of these homo- and co-polymers in aqueous solution, observed using the technique of high sensitivity differential scanning calorimetry.

CHAPTER 1 - GENERAL OVERVIEW

1.1 Polymers

1.1.1 Introduction.

Polymer science is a multidisciplinary area which encompasses the fields of biology, chemistry and physics. The development of polymer science since the late 19th century has not been uniform but exponential, with the most dramatic expansion occurring in the last 30 years. The quantity of polymeric materials marketed by the chemical industry far exceeds the amount of all other synthetic materials. The economic impact of these materials is such that over one half of the chemists employed by industry are in some way associated with the production of polymers. Before 1930, polymers were believed to be colloidal aggregates of many small molecules. Their properties were attributed to various attractive forces which held the components together. The pioneering work of Staudinger provided a basis for the modern understanding of polymers by showing that polymers are actually molecules. Flory and co-workers helped to develop the field further by applying physico-chemical methods to the study of the properties of macromolecules.[1]

Despite the diversity in structure and function of polymers, they can be broadly classified according to the scheme shown in Figure 1.1.

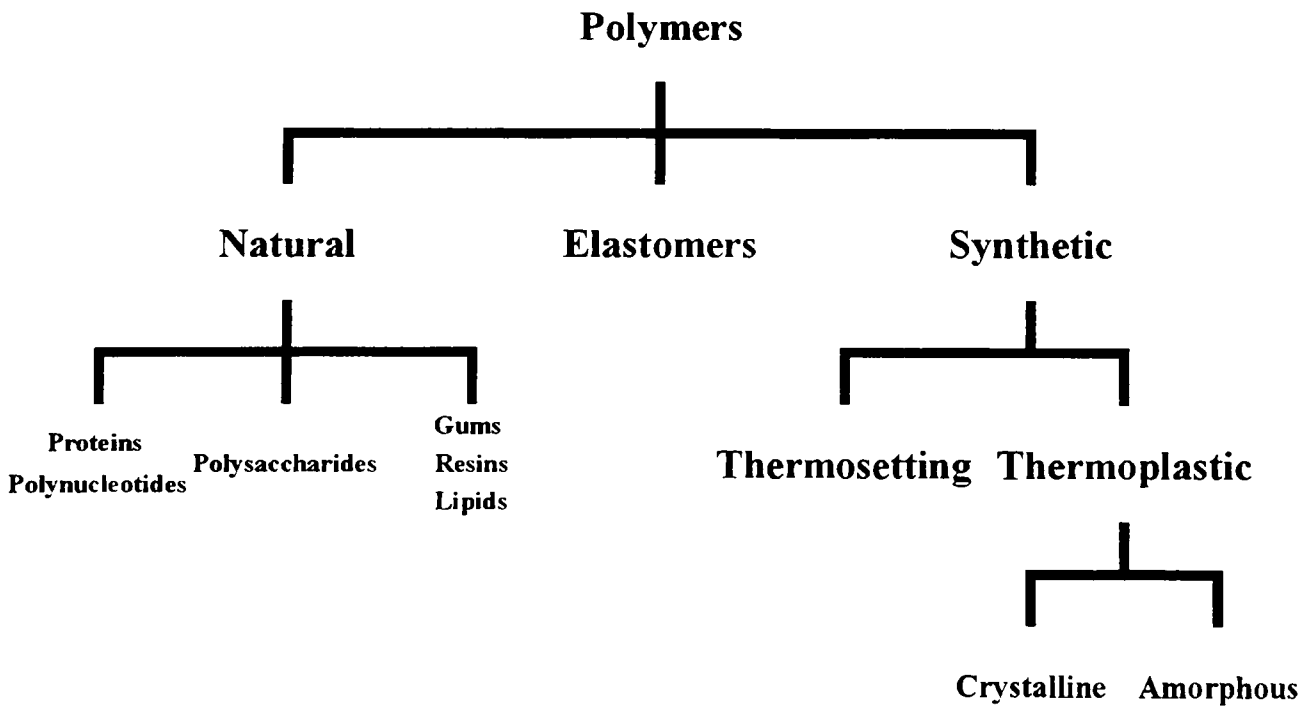

Figure 1.1 Classification of Polymers

1.1.2 **Polymer Synthesis**

In order for a monomer to polymerise, the monomer must be capable of reacting with two or more other monomers. Classification of such reactions is provided by considering the underlying polymerisation mechanisms:

(a) step polymerisations - in which the polymer chains grow stepwise by reactions that can occur between any two molecular species.

(b) chain polymerisations - in which a polymer chain grows only by reaction of monomer with a reactive end-group and usually require an initial reaction between monomer and an initiator to start the growth of a chain.

In step polymerisations the degree of polymerisation increases steadily throughout the reaction, but the monomer is rapidly consumed in the early stages. In chain polymerisations, high degrees of polymerisation are attained at low monomer conversions, the monomer being consumed steadily throughout the reaction. The synthesis of poloxamers is discussed in detail in Section 1.3.1.

1.2 Analysis of Polymers

1.2.1 **Molecular Mass Distribution**

The methods used to determine the molecular mass (M) are either relative or absolute. Relative methods require calibration with samples of known M and include viscosity and vapour pressure osmometry. The absolute methods are often classified by the type of average M they yield i.e., colligative methods yield number averages (M_n), light scattering and ultracentrifugation yield higher averages, weight and z-average (M_w and M_z) respectively.

The methods of molar mass determination cited above are time consuming and molecular weight distributions of polymer samples is generally determined by gel permeation chromatography (GPC) whereby fractionation of a polymer sample is achieved by passing a polymer solution through a series of columns containing a stationary phase of packed spheres (often beads of crosslinked polystyrene) whose pore size can be controlled. With a wide distribution of pore sizes in any support gel a separation into molecular size is obtained because the larger molecules

dissolved in the solvent carrier cannot diffuse into the pores, and are rapidly eluted while the smaller molecules penetrate further with decreasing size and are retarded correspondingly. A typical chromatography profile for a triblock ABA copolymer of polyoxyethylene (A) and polyoxypropylene (B) (poloxamer) is shown in figure 1.2 showing the M_w, M_n and M_z values with a polydispersity ratio (M_w / M_n) of 1.2. The conditions of the experiment being: mixed PL-gel columns (30cm), a mobile phase of tetrahydrofuran, flow rate of 1mLmin^{-1} at ambient temperature and refractive index detector.

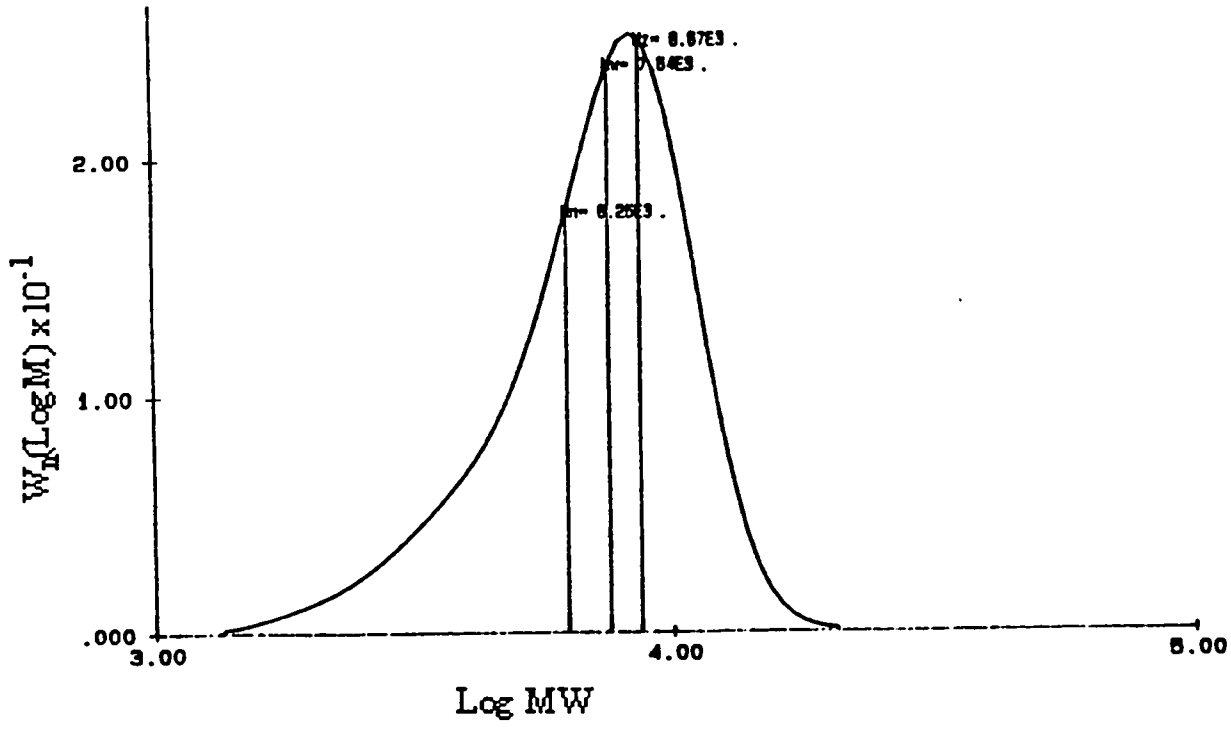

Figure 1.2 Molecular mass distribution of poloxamer 235 (Pluronic P85) as determined by GPC, mixed PL-gel columns, mobile phase of tetrahydrofuran with antioxidant, flow rate 1mLmin^{-1}, ambient temperature and a refractive index detector.

1.2.2 **Infrared Analysis**

Infrared spectroscopy is a widely used technique to analyse the composition of polymer samples or to determine the conformation of polymers in solution. Infrared techniques are often employed with separatory techniques e.g. mass spectroscopy, gas chromatography, high performance liquid chromatography etc. in order to analyse various fractions contained within a polymer sample.

The simplest application of infrared spectroscopy is for polymer identification. Comparison of the positions of absorptions in the infrared spectrum of a polymer sample with the characteristic absorption regions leads to identification of the bonds and functional groups present in the polymer.

In addition to identification, the technique has been used to elucidate certain aspects of polymer microstructure. The degree of branching in a branched polymer can be determined provided that the characteristic absorptions due to the branches can be identified.

Examples of the use of infrared spectroscopy to study polymeric systems include polymer composition,[2-6] e.g. the determination of the composition of styrene-methylmethacrylate random copolymers.[5] Various reactions have been studied by infrared spectroscopy[7-11] e.g., the heat curing reaction of glycerol-terminated urethane prepolymers,[8] and cross linking of unsaturated polyester resins with styrene.[11] Molecular structures and orientation have been investigated using infrared spectroscopy[12-18] e.g., transient structural changes of high, low and linear low density polyethylene,[16] the study of orientation in highly crosslinked epoxy/amine networks above their glass transition temperature, [14] and the effect of temperature on intermolecular orientational correlations between chain segments in strained polyisoprene.[18] Studies of hydrogen bonding in polymeric systems have also been investigated using infrared[19-27] e.g., hydrogen bonding in polybenzimidazole/polyimide systems using low molecular weight monofunctional probes,[25] and weak symmetrical hydrogen bonding of carbonyl groups in *rhodobacter-sphaeroides* reaction centres.[26]

1.2.3 **Nuclear Magnetic Resonance Spectroscopy (NMR).**

The theoretical basis of NMR will be discussed in detail in section 2.3. NMR spectroscopy is one of the most useful methods for structural elucidation of molecules. The technique provides information about molecular structure through examination of the magnetic properties of specific atoms within molecules. NMR spectroscopy can be carried out on nuclei with odd numbered masses(^{1}H, ^{11}B, ^{13}C, ^{15}N, ^{19}F, ^{31}P etc.) as well as those with an even mass but an odd atomic number (^{2}H, ^{10}B, ^{14}N etc.). Both ^{1}H and ^{13}C NMR are widely used for routine purposes such as polymer identification, confirmation of molecular structure, purity analysis and evaluation of average copolymer composition.

Applications of NMR to polymeric systems include the study of the compatibility and miscibility of polymer blends[28-32] e.g. the miscibility of several methacrylate polymers with poly(vinyl chloride) determined by ^{1}H NMR relaxation measurements[33] and miscibility of

poly(styrene-co-maleic anhydride) blends using distortionless enhancement fourier transform-NMR[34]. The study of the morphology of polymers[27,35-38] e.g. of isotactic propylene by ^{13}C NMR techniques[36] as well as of blends of films of polytetrafluoroethylene and ultra-high molecular weight polyethylene.[37] The degree of crystallinity for linear polypropylene was determined by ^{13}C NMR[39] and ^{1}H NMR.[40] Three dimensional NMR was used to determine the polymer chain conformation of vinylacetate-vinylidene cyanide alternating copolymers.[41] NMR has also been used to examine the reactivity ratios of copolymers,[42,43] as well as the formation of cross-links[45,46] and network formation as a result of curing.[47,48]

1.2.4 **Thermal Analysis.**

A variety of techniques are available for analysis of the thermal behaviour of polymers. The widely applicable modes i.e., differential thermal analysis (DTA), thermogravimetric analysis (TGA), hot-stage microscopy (HSM), thermomechanical analysis (TMA) and dynamic mechanical analysis (DMA) are discussed in addition to some less common techniques such as evolved gas analysis (EVA), thermosonimetry (TS) and combination techniques e.g. TG -mass spectroscopy. Differential scanning calorimetry (DSC) will be discussed in section 2.1.

1.2.4.1 **Differential Thermal Analysis (DTA).**

DTA is often considered inferior to the related technique DSC as it can only readily provide qualitative data. All commercial instruments measure the differential temperature of the sample against a thermally inert reference material (e.g., alumina) and is continuously recorded a function of temperature. As the temperature of the block is raised at a constant rate (5-20 K min^{-1}) the sample temperature, T_s, and that of the reference, T_r, will remain equivalent until a change in the sample takes place. If the change is exothermic, T_s will exceed T_r for a short period but if it is endothermic T_s will temporarily lag behind T_r. This temperature difference ΔT is recorded where changes such as melting or crystallisation are recorded as peaks. Since the heat capacities of sample and reference are different, ΔT is never actually zero and a change in heat capacity such as that associated with a glass transition, will cause a shift in the baseline. Other changes such as sample decomposition,[49,50] curing[51] and the existence of different polymorphic forms[52,53] can also

be detected. As ΔT measured in DTA is a function of the thermal conductivity and bulk density of the sample, it is non-quantitative and relatively uninformative.

1.2.4.2 **Thermogravimetric Analysis (TGA).**

TGA utilises a thermobalance, which allows for ongoing monitoring of sample weight as a function of temperature. This may involve the use of a controlled heating or cooling programme: the sample may also be examined at a fixed temperature as a function of time. Thermal decomposition of the polymer resulting in the evolution of volatile or gaseous components e.g., carbon dioxide, or loss of water of crystallisation from hydrates are measured as a decrease in mass.

There are three classes of thermobalance,[54] namely deflection type instruments, null type instruments and resonance-frequency-change instruments. The latter method is highly specialised and the principle of operation is that changes in mass of sample deposited on the surface of a highly polished crystal results in a shift of an oscillatory frequency.

The most widely available instruments utilise the null balance principle. Movement of the balance beam from its null position is sensed and restoring force applied to restore the beam to its null position. The change is restoring force, proportional to the change in the sample mass is monitored. All types of samples (powders, liquids, films and fibres) can be analysed with static or dynamic atmospheres provided by most gases.[56,57] Ambient or reduced pressure operation is also possible. An example of TGA is the TGS-2 (Perkin-Elmer).[58]

1.2.4.3 **Hot Stage Microscopy (HSM).**

HSM, also known as thermoanalytical microscopy, is a valuable supportive tool when used in conjunction with other techniques. It can be utilised to ascertain the nature of events leading to endotherms or exotherms on DSC traces or weight changes in TGA.[59-63]

Decomposition with gas evolution, and especially loss of water of crystallisation from hydrates, can be studied by mounting crystals in silicone oil and manually observing the sample using a microscope during a temperature programme. Gas or vapour bubbles can sometimes be

observed emanating from crystals at temperatures correlating with decomposition or desolvation endotherms/exotherms in DSC or DTA.

1.2.4.4 **Thermomechanical Analysis (TMA).**

TMA can measure dimensional changes in a sample (such as expansion or contraction) as a function of temperature, under a programmed temperature change, or as a function of time when the sample is subjected to isothermal conditions.[64-67] TMA measures deformation of a sample under a constant load, whereas volumetric-change determination (expansion or contraction) is a thermodilatometric measurement. Both techniques can be carried out in the same instrument, usually by employing different probes. Events such as expansion, deformation, flexure, softening and stretching of the sample, may be determined.

1.2.4.5 **Dynamic Mechanical Analysis (DMA).**

A special subset of TMA is provided by DMA or dynamic thermomechanometry. The DuPont DMA983[54] is widely used to measure the mechanical response of a material as it is deformed under an oscillatory load. Thus the viscoelastic behaviour of a material can be characterised. Four modes of operation are possible: fixed frequency, stress relaxation, resonant frequency and creep. The fixed frequency operation can provide for reliable determination of frequency dependence and end-use performance prediction whereas the resonant frequency mode allows for detection of subtle transitions. Stress relaxation will measure the ultra-low frequency molecular relaxation of polymers and composites whilst creep analysis will measure flow at constant stress. The latter allows determination of load bearing stability of materials. TMA is widely applicable to the characterisation of polymeric materials[68-72] allowing for assessment of expansion coefficients, glass transition temperature and, with DMA, detection of subtle transitions in polymers not observed by routine DSC or TMA.

1.2.4.6 **Torsional Braid Analysis (TBA).**

One final subset of TMA is TBA which utilises the torsional mode and torsional strain as the applied stimulus. The measured responses are the decay of the oscillation frequency as the modulus parameter and the rate of decay as the parameter for damping. TBA was devised from a freely oscillating torsional pendulum which possessed advantages, such as inherent simplicity, the use of a low frequency (~1Hz), which permits easy comparison with static methods such as DSC and DTA, and the high resolution of transitions. TBA has been developed to use small amounts of samples (~10mg), supported on an inert multifilamented substrate, the braid. The specimens are prepared by dissolving the polymer in an organic solvent and impregnating the braid, which consists of 3000-4000 filaments. Gillham,[73] considered that this argument allowed the 'picking up' of relatively large amounts of solution and minimised flow due to gravity. Due to the small specimen size compared with the torsional pendulum, far more rapid heating rates may be employed, and as an inert support is used, the method may be used to discriminate transitions in the liquid, rubbery and solid states.[74-77]

1.2.4.7 **Less Common Techniques of Thermal Analysis.**

Evolved gas analysis (EVA) is used where a knowledge of the type and amount of gases produced during a heating programme can be determined. EVA is generally achieved by interfacing DTA or TGA to a mass spectrometer or fourier-transform infra-red spectrometer.[78-81]

Thermosonimetry (TS) measures the noise produced during changes in crystalline materials (generally) subjected to a heating or cooling programme. Sound can be produced by propagation of cracks in crystals, which can arise from thermal stress or eruption of gases or vapours. Crystallisation from a melt can also produce such noise signals. The emitted sounds arise from thermal stresses which are imposed on the substance by the temperature programme and the induced strains may be released by processes such as chemical decomposition, melting and solid state transformation.[82-85] However, mechanical strain-release processes involve motions and creation of structural imperfections; for example, microcracks, dislocations or grain boundaries occur which are considerably less energetic than chemical and physical processes. These, although undetected by DSC or DTA methodologies, were detected by TS.[82] TS cannot be used

quantitatively, however, measurements of amplitudes, amplitude distributions and frequency distributions may be used to determine the nature of the material under examination.

1.2.4.8 **Summary.**

Reaction / Technique	DSC	DTA	HSM	TGA	TMA	DMA
Melting Points	+	+	+	–	+	+
Desolvation - Bound	+	+	+	+	–	–
Desolvation - Adsorbed	+	+	+	+	–	–
Glass Transition	+	+	–	–	+	+
Heats of Transition	+	(+)	–	–	–	–
Purity Determination	+	(+)	(+)	–	–	–
Compatibility	+	+	(+)	(+)	+	+
Decomposition Kinetics	+	+	–	+	–	–
Polymorphic Transitions	+	+	+	–	–	–

Key: + applicable; - inapplicable; (+) potential application

1.3 Overview of Poloxamers and Poloxamines.

1.3.1 **Synthesis.**

Oxyalkylene block copolymers were the earliest examples of sequential anionic block copolymerisation to be produced commercially[86] (figure 1.3). The Wyandotte Chemical Corporation (BASF) marketed these materials under the name 'Pluronic' and 'Tetronic' copolymers and they are now also marketed by ICI under the tradenames of Synperonic PE and T non-ionic surfactants. Copolymers of this type were first described in 1951 and their preparation described in a number of patents.[87] These oxyethylene-oxypropylene block copolymers are liquids at low molecular masses and pastes or solids at the higher end of the scale. Their molecular masses range from 1000 to 26000gmol^{-1}

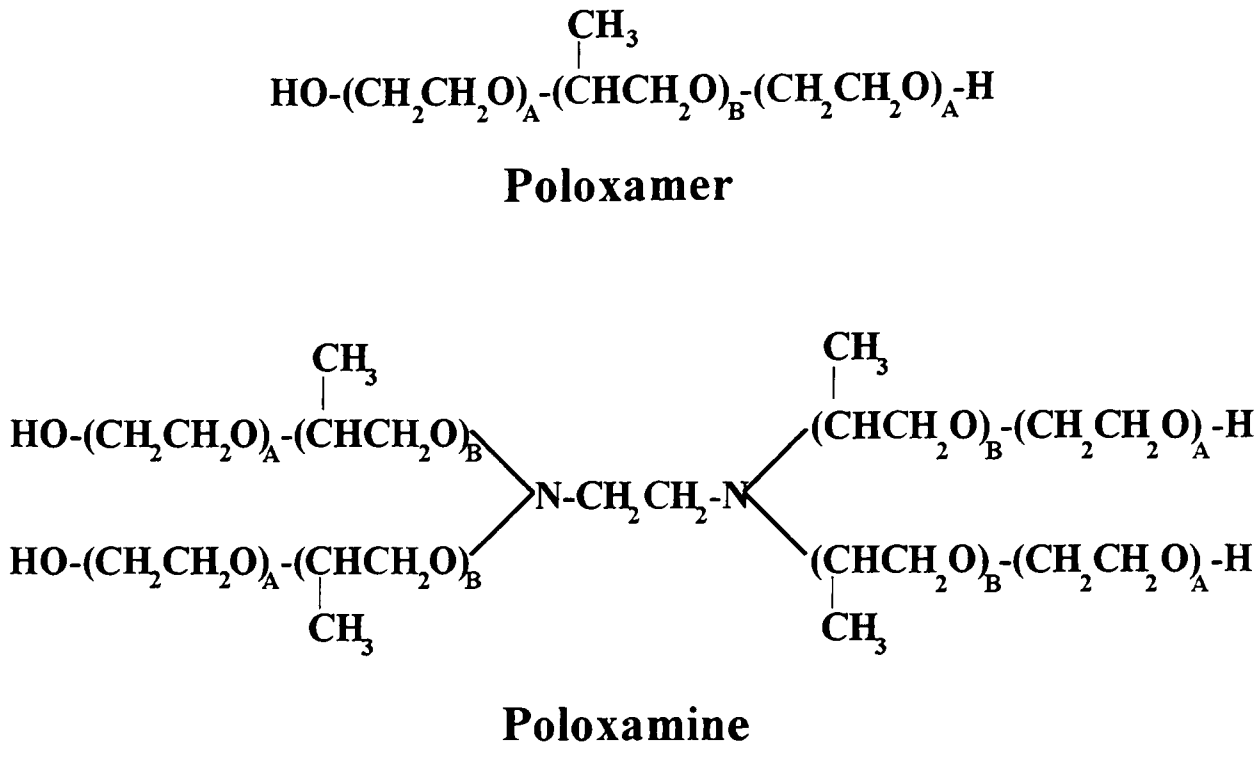

Figure 1.3 Generalised structures of a poloxamer and a poloxamine.

The hydrophobic nature of the polyoxypropylene segments gives the copolymers oil or organic solvent solubility whereas the polyoxyethylene exhibits water solubility. The contrasting properties and inert nature of these block copolymers has led the diverse industrially important applications of these copolymers as detergents, emulsifiers and demulsifying agents.[87-89] Early examples of industrial uses of these compounds are shown in Table 1.3.1.

Poloxamers are synthesised by the sequential addition of propylene oxide to propylene glycol in the presence of hydroxide (e.g., KOH) in an inert and anhydrous atmosphere under pressure and at about 393K. After the initial polymerisation is complete, ethylene oxide is then reacted with the polyoxypropylene. The alkaline catalyst is neutralised and usually removed from the final product. Polyoxypropylene changes from a water soluble to a water insoluble polymer as the molecular mass exceeds 750gmol^{-1}. The addition of ethylene oxide in the final step provides water solubility to the molecule (figure 1.4). An antioxidant 2,6-di-*tert*-butyl-4-hydroxytoluene (BHT) is added to the copolymer at a concentration of about 500ppm in order to inhibit oxidation of the copolymer when exposed to air.

Table 1.3.1 Early industrial uses of oxyalkylene block copolymers. Technical Data on Pluronic and Tetronic Nonionics, Wyandotte Chemical Corporation, Wyandotte, Michigan.

POLYMER	**INDUSTRIAL USE**
P101, P181	Viscosity control for the drilling of boreholes; Wyandotte 1960
P103, P123, P183, P212 + Poloxamines	Breaking of crude oil emulsions; Wyandotte 1960
P182	Reduction of viscosity in SBS/acrylic emulsions; Wyandotte 1960
P182	Viscosity control for coating pigment dispersions in the paper industry; Wyandotte 1960
P184	Wetting of pulp for the paper industry; US Patent 2,805,169, Mitchell and Rayonier
P188	Acid boiler descalant; Wyandotte 1954
P188, P238	Gas drilling - foaming enabled removal of water from the gas well; Wyandotte 1960

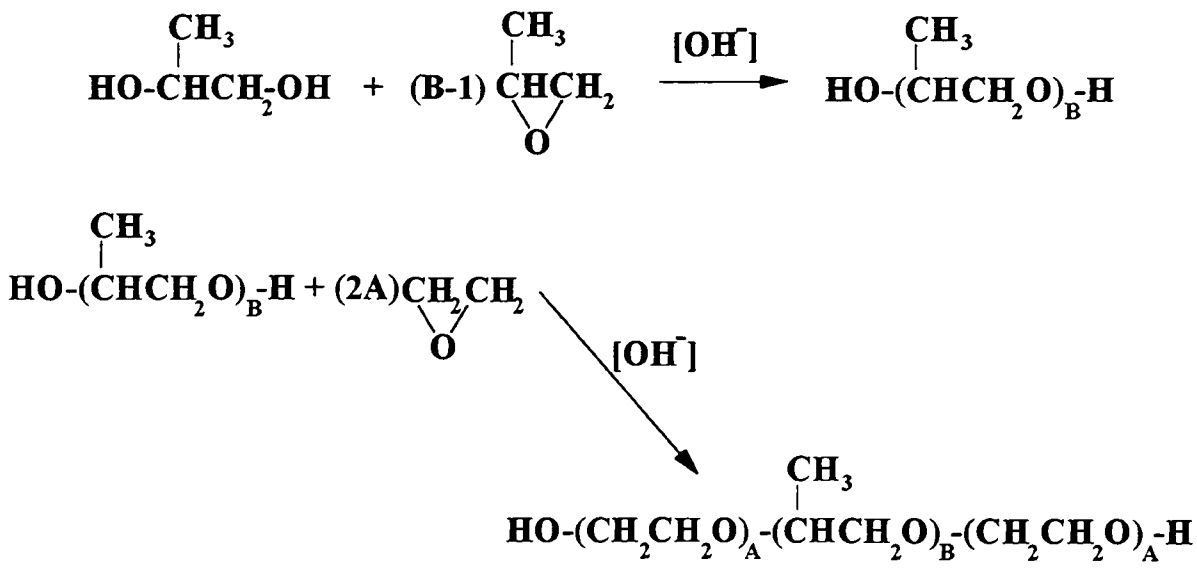

Figure 1.4 Poloxamer synthesis

The synthesis of poloxamines[90] is essentially the same as that shown for poloxamers, the difference being in the initial synthesis where propylene glycol is replaced with an ethylene diamine initiator. Structurally, the poloxamines differ from poloxamers in that they have four oxyalkylene chains, rather than two, since four active hydrogens are present in the initiator. These surfactants also differ from the poloxamers in that they have two tertiary nitrogen atoms. The synthesis of poloxamers and poloxamines is terminated only by complete consumption of the monomer, and unlike many common polymer syntheses the polymer chains are not capped (to avoid depolymerisation), thus the terminal groups for these polymers are primary hydroxyl groups.

During the first stage of addition of propylene oxide to propylene glycol, a rearrangement can occur which results in the formation of allyl alcohol and some propenyl alcohol (figure 1.5), this leads to the synthesis of monofunctional initiated surfactant i.e., a diblock copolymer.

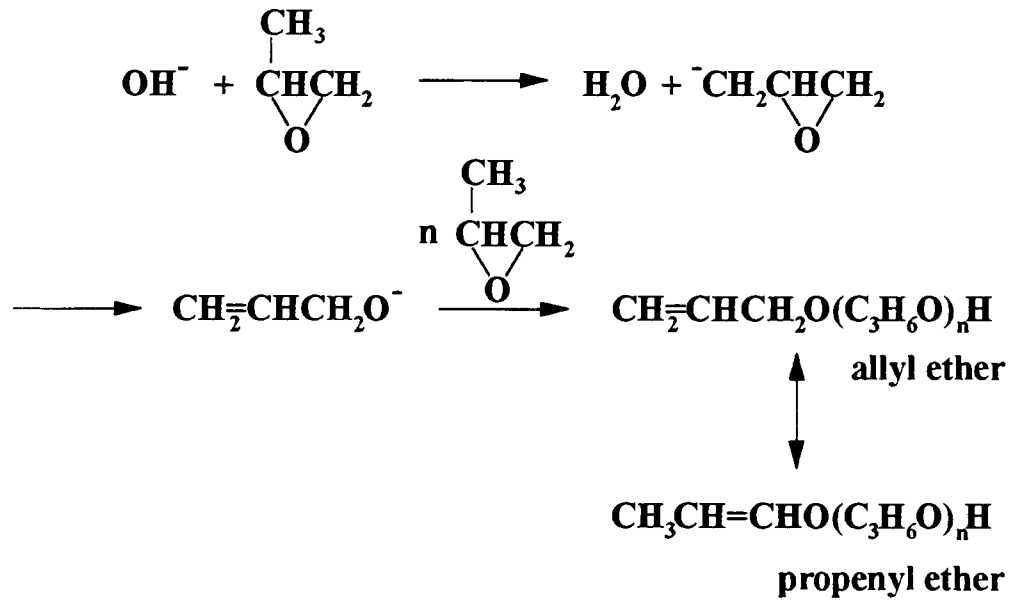

Figure 1.5 Side reactions during polyoxypropylene synthesis.

It is also apparent that there are quite large variations in molecular weight profile for polymers produced by different manufacturers e.g., poloxamer P407.[91] Price and Booth, from the Manchester Polymer Centre, have extensively studied the synthesis[92-94] and subsequent analysis and physico-chemical properties[95-100] of block copolymers of polyoxyethylene and polyoxypropylene for the synthesis of block copolymers. They have shown that the addition of crown-ether (18-crown-6 ether) for the anionic copolymerisation process alleviates certain proton extraction reactions that would otherwise result in initiation of new chains resulting in a high polydispersity ratio.

1.3.2 **Applications and uses of Poloxamers in the Pharmaceutical Industry.**

Poloxamers and poloxamines are finding increasing applications and potential applications[101] in the pharmaceutical industry due to their properties as surfactants and apparent low toxicity[88,102-104] (lethal dose for 50% of the population (LD_{50})>2g kg^{-1} oral dose (rats)). They are widely employed as emulsifiers and viscosity stabilisers in creams and pastes for dermatological use (e.g., emulsification of octylmethoxycinnamate, a sunscreen agent[105]) and in drug formulations[106-109] to control particle size[110] and are used as solubilising agents for non water soluble drugs.[111]

1.3.2.1 **Model Drug Delivery Systems (Dilute Systems).**

The effects of poloxamers and poloxamines as coatings for labelled microspheres has been investigated using intravenous administration and subsequent monitoring of the distribution of the microspheres throughout the subject under examination.

Polystyrene spheres (60nm diameter) coated with poloxamers P188, P338, secretory immunoglobulin and egg lecithin all show that the hydrophilic coatings help to depress liver uptake and prolonged circulatory times compared to uncoated spheres. The most profound effects were observed for polystyrene spheres coated with poloxamer P338 with a 48% reduction in liver uptake; and polystyrene spheres were observed to be sequestered in the bone marrow.[112] Similar effects were observed for the coating of polystyrene spheres (70nm in diameter) with poloxamer P407 where prevention of hepatic sequestration was observed with redirection of a significant portion of the polystyrene spheres to the bone marrow and spleen in rats.[113] However, no effects of reduction in hepatic sequestration has been observed for mixing of poloxamers and poloxamines with phospholipid vesicles (DSPC)[113] or poly(butyl-2-cyanoacrylate) nanoparticles.[114] A significant decrease in phagocytosis of polystyrene particles by mononuclear phagocytes coated with poloxamer P338 and poloxamine T908 was demonstrated, the integrity and viability of the phagocytes was unaffected by the presence of the copolymer coatings.[115] Intravenous delivery in rats of P407 + adriamycin loaded proliposomes compared to adriamycin loaded proliposomes showed a significant decrease in adsorption of the P407 loaded proliposomes in reticuloendothelial rich organs (liver, spleen) and an increased adsorption in non-reticuloendothelial rich organs (kidney, lung, heart).[116]

Also significant differences have been observed in reduction of microsphere uptake by the liver for poloxamers obtained from different manufacturers due to significant differences in the molecular weight profiles for poloxamer P407,[91] only one of the poloxamers showed the positive effects previously observed.[113] The coating of the polystyrene spheres was analysed by photon correlation spectroscopy, sedimentation and fluorescence anisotropy decay techniques and showed that poloxamer and poloxamine coatings (P338 and T908) were not displaced by proteins (human albumin, fibrinogen or whole plasma).[117] The hydrodynamic thickness of the polymer layer was found to be proportional to both the polyoxyethylene content and molecular weight. It was hypothesised that the polyoxyethylene extends further into solution when adsorbed onto smaller particles.[117] The results showed that adsorption was via the hydrophobic polyoxypropylene and the microsphere surface, and the adsorption of P338 appeared to be more strongly bound than the coating with T908.[118]

Poloxamers have also been used in the preparation of isohexacyanoacrylate or isobutylcyanoacrylate nanoparticles and the results showed that nanoparticles of mean diameter <50nm were obtained at low pH (10^{-3} -10^{-1} M HCl) in the presence of a 2% w/v solution of P188 in the polymerisation medium.[119]

Poloxamers with a high percentage polyoxyethylene content (P238, P407) were observed to greatly increase mucoadhesion for polymer coated isohexacyanoacrylate nanospheres to rat ileum segments under liquid flow due to adhesion between the polyoxyethylene and mucin network.[120]

P338 modified lipid emulsions, for intravenous drug delivery, have been shown to direct lipophilic drugs away from the reticuloendothelial system of the liver and spleen and target other tissues such as inflammatory tissues.[111] P235 has been used as a drug delivery vehicle for daunorubicin and has been shown *in vitro* to be effective in treating multi-drug resistant (MDR) ovarian cancer cell lines,[121,122] the cytotoxic activity increased up to 700 times in the presence of 0.01-1% P235. The copolymer also increased the cytotoxic effects of other MDR type drugs (doxorubicin, epirubicin, vinbalstine and mitomycin C) by a factor of 20-1000.[122] Gene delivery to control vascular smooth muscle proliferation following angioplasty has been

shown to be enhanced using P407 as a gene delivery vehicle using an *in vitro* model, thus potentially reducing required exposure times and total drug concentration.[123] P407 has been shown to be a potentially useful vehicle in the preservation of biological activity and sustained release of protein pharmaceuticals using urease as a model enzyme for intraperitoneal injections in the rat.[124] Prolonged release of diclofenac has been achieved by coating 3-ply walled microcapsules with P188, inhibiting uptake by the reticuloendothelium system.[125]

Poloxamer aggregates have been investigated as drug delivery vehicles.[126] Using fluorescent and light scattering techniques, the aggregation behaviour of P188, P235 and P338 was examined and the aggregates formed were observed to have an average hydrodynamic radius of 15-35nm with aggregation numbers ranging from one to several dozen dependent on the nature of the poloxamer. The application of poloxamers as micro-containers for drug delivery was proposed (e.g. delivery of haloperidol to the brain[127]).

1.3.2.2 **Drug Delivery from Polymeric Gels.**

Poloxamers and poloxamines with high molecular weights and high percentages of oxyethylene form thermoreversible gels in aqueous systems of high concentrations (>20% w/v). Prolonged plasma levels of indomethacin delivered via rectal administration from poloxamine T908 gels has been demonstrated when compared to commercial suppositories,[128] topical release of indomethacin has also been shown to be enhanced by using P407.[129] Control of drug release has been demonstrated for P407/cellulose acetate phthalate blends using theophylline as a model drug,[130] the release rate was controlled by the thickness and P407 content of the gel. Model systems using phenolsulphophthalein as a tracer showed a zero order release rate from a P407 gel for subcutaneous release in rats, a sustained plateau was attained within 15 minutes which lasted for 8-9 hours.[131] A sharp reduction in erosion of a polymeric drug delivery system by incorporation of P331 in a polymer matrix (cellulose acetate phthalate), led to sustained release of metronidazole effective over several days.[132] The drug release rate from poloxamer gels has been shown to decrease with increasing hydrophobic nature of the drug e.g., alkylnicotinates[133] explained by storage interrelations between drug and poloxamer. Sustained release of recombinant biological response modifiers from poloxamer gels has been investigated due to brief intervascular half life of most recombinant proteins and their associated rapid clearance from the circulation. Utilisation of

the thermoreversible gel properties of poloxamers has been shown to be of potential for the sustained delivery of such proteins e.g. Interleukin-2.[134,135] Poly(L-lactic acid)/poloxamer blends have been shown to reduce the initial "burst" release of protein when used as release matrices and also a significant extension of the protein release period was observed.[136, 137]

Transdermal drug delivery was modelled using methanol and octanol through mouse skin using a range of poloxamers and poloxamines. However, neither differences in molecular weight nor varying hydrophobe/lipophobe balance (HLB) values appeared to play a major role in transdermal drug delivery using the hairless mouse skin model.[138]

1.3.3 **Clinical Uses of Poloxamers.**

The first clinical use of poloxamers stemmed from the application of poloxamer 188 as an emulsifier in phospholipid emulsions.[139, 140] The observation of reduced fat emboli *in vivo* and stabilisation of the phospholipid emulsion led to the extensive use of P188 as an additive in disc pump oxygenators for extracorporeal circulation for cardiopulmonary bypass operations.[141-144] P188 reduced haemolysis,[141-144] and systemic fat emboli[143] during these operations. P188 was also of benefit as an "antisludging" agent for improving blood flow in the microcirculation in experimental models of haemorrhagic shock[145-148] and cold injury.[149, 150] P188 was later used as an emulsion stabiliser and emulsifier in formulations such as Fluosol®[151-153] (an artificial blood substitute containing 2% (w/v) P188). Further research into the role of poloxamers has led to their widespread use as potential vehicles for drug delivery both in transdermal and intravenous systems. Also the effects of the surfactant properties of the poloxamers on red-blood cell aggregation and reduction of whole blood viscosity have been investigated for the treatment of a variety of clinical disorders characterised by acute vaso-occlusion or impaired blood flow (e.g., myocardial infarction,[154-156] sickle cell disease[157]).

Poloxamers have been found to significantly reduce blood viscosity,[158] as well as reducing platelet adhesiveness during cardio-pulmonary bypass alterations.[159,160] Adjunctive therapy with P188 infusion in patients receiving thrombolytic therapy for acute myocardial infarction resulted in significantly smaller infarcts, greater myocardial salvage, improved left ventricular function and a reduced incidence of in-hospital reinfarction.[156] P188 has been shown to inhibit red blood cell-

induced platelet aggregation in citrated whole blood under conditions of gentle shear and was a more effective inhibitor than 2-chloradenosine and an ADP depleting substrate/enzyme system (phosphoenolpyruvate/pyruvate kinase).[161-163] It was concluded that P188 protected red blood cells from mechanical trauma by non-specific adsorption of copolymer to the cell surface, and that this effect prevented mechanical damage and hence leakage of ADP from red blood cells.[161] A significant reduction in infarct size and an increase in blood flow within the ischemic endocardium 3h after reperfusion in rabbits subjected to hyperoxic reperfusion was observed for P188 treated animals compared to control groups.[164] P188 was shown to have a significant impact in improving neurologic outcome after long periods of deep hypothermic circulatory arrest in the dog model,[165] after 150 minutes of hypothermic circulatory arrest (10°C) 50% of dogs in the control group did not survive whereas no deaths were reported in the P188 treatment group. Due to the surface active and gelation properties, and the apparent low toxicity of poloxamers they have found potential uses in reducing post surgical adhesion reformation in patients undergoing pelvic reconstructive procedures for infertility.[166] Post-surgical adhesion was also significantly reduced using P407 in place of cellulose (Interceed TC7®) using a rat uterine horn model.[167] A 50% reduction in the formation of leptomeningeal adhesion formation was observed when P407 was used following intra-spinal surgery in the rabbit, the results suggest that P407 may have potential to prevent adhesive arachnoiditis following surgery for disc, tumor and myelomenigocele.[168] The role of P188 infused for 48 hours was investigated following ischemic spinal chord injury (modelled by occlusion of the thoracic aorta and both subclavian arteries for 13 minutes).[169] P188 showed no significant effect compared to placebo for the mean histologic scores (P188 = 1.08±0.33, placebo = 1.54±0.41) indicating that P188 does not prevent paraplegia or improve long-term neurologic outcome.[169] The use of P188 in a formulation for the preservation of vein grafts in cardiovascular surgery was shown to be more effective than saline, St Thomas' cardioplegic buffer or Krebs-Henseleit's buffer; It was concluded that the new formulation containing P188 would reduce the frequency of vein graft narrowing and occlusion post-operatively.[170] P188 and P407 administered topically and intravenously have been shown to significantly reduce wound contraction and improve healing following incisional[171] or full skin thickness burn[172,173] wound in rats.

1.3.4 **Miscellaneous Uses of Poloxamers.**

1.3.4.1 **Poloxamer Effects on Bacterial and Protein Adhesion to Surfaces**.

The inhibition of protein adsorption and bacterial adhesion to surfaces is of great importance in the implantation of prosthetics, drug delivery and materials used in topical contact e.g., contact lenses, and for investigations where a biocompatible surface is advantageous for the study of protein or cellular behaviour and mechanisms.

Poloxamers have been shown to greatly inhibit adherence of three strains of *Staphylococcus epidermidis* to polystyrene surfaces, inhibition increased with increasing molecular weight of the hydrophobic POP block and percentage POE content, and inhibition of up to 97% was observed compared to uncoated surfaces.[174] A 92%, 50-60% and 50-70% inhibition in contact-lens adhesion of *Pseudomonas aeruginosa*, several *staphylococcul* strains and Gram-negative strains respectively was observed for P407 treated surfaces, and it was concluded that the poloxamer could potentially prevent implant related infections and keratitis associated with contact lens wear.[175] P407 has also been shown to inhibit the adsorption of granulocyte colony stimulating factor to poly(vinyl chloride).[176] Currently, the effect of P188 as a surface coating of silicone elastomer shunts to prevent bacterial adhesion is being evaluated for implantation of shunts in children with hydrocephalus in order to drain excess cerebrospinal fluid from the ventricular system into the peritoneal cavity.[177] Inhibition of fibrinogen and platelet adhesion to glass coated with poloxamers was demonstrated, the inhibition only occurred with poloxamers containing at least 56 oxypropylene monomeric units, and was independent of the oxyethylene content, no inhibition of fibrinogen or platelet adhesion was observed for polyoxyethylene homopolymer.[178] Poloxamers have been evaluated as to their effect on inhibiting protein adsorption to glass surfaces in capillary electrophoresis, it was concluded that they prevent protein adsorption and provide high efficiency separations.[179]

1.3.4.2 **Poloxamer Effects on Cell Cultures.**

Various effects of poloxamers on cell cultures have been reported, early studies include the effect of P188 on the growth of fibroplasts in suspension agitated on a rotary shaker.[180] Protein precipitation inhibited fibroplast growth by 25-100%, the addition of P188 to the suspending

medium resulted in zero protein precipitation and hence significantly enhanced cell growth at all of the concentrations of P188 studied.[180] The delivery of exogenous labelled [γ-^{32}P]ATP into intact Jurkat cells was enhanced using P235 as a delivery vehicle which resulted in a large increase of protein phosphorylation and did not affect cell viability.[181] Also, polycation-mediated cell uptake of plasmid DNA and cell transfection on MH 3T3, MDCK and Jurkat cell lines were significantly enhanced in the presence of P235.[182] However, the effects of a medium containing 0.05% (w/v) P188 was shown to decrease cell viability of *hybridoma* cells in continuous culture by about 12% and the growth inhibition was concluded to be due to a lowering of the rates of DNA synthesis[183] which is in contrast to the increased growth of cultured fibroblasts, melanoma cells[184] and human lymphocytes[185] when poloxamers were incorporated in the culture medium. P188 has been demonstrated to protect cells from mechanical damage in bioreactors[186-188] and has been shown to significantly increase the growth rate of cells in bioreactor culture processes, e.g., a two-fold increase recombinant protein production for media supplemented with P188 from *Bombyx mori* insect cells.[189] Increased antibiotic production by improved oxygen delivery to immobilised *Streptomyces coelicolor* was investigated using a 10% perfluorocarbon emulsion, the use of P188 as an emulsifier resulted in approximately double the antibiotic concentration compared to control and 10% perfluorocarbon without poloxamer.[190]

P188 has also been shown to significantly increase root, callus and protoplast growth of *Solanum dulcamara* at optimum concentrations of 0.01, 0.1 and 0.1% w/v respectively.[191] Higher concentrations (1.0% w/v) and poloxamer solutions stored for 5 days at 277 and 195K were observed to inhibit plant growth. Root and callus soluble carbohydrates and proteins were increased by exposure to freshly prepared media containing poloxamer. Similarly, the specific activities of malate dehydrogenase and acid phosphate were increased in P188 treated callus and roots. Supplementation of media with 0.001-0.1% (w/v) P188 has been shown to significantly increase the mean fresh weight gain of cultured leaf explants of chrysanthemum "Tone Maid" and "Early Charm" by 74 and 34% respectively.[192] Shoot regeneration was increased by 40% for *Hypericum perforatum L* supplemented with 0.001% P188,[193] and has also been shown to have significant effects on promotion of shoot regeneration from Jute cotyledons,[194,195] and increased protoplast plating efficiency for albino *Petunia hybrida* (a 37% increase).[196] The production of anthroquinones from cultures of *Morinda citrifolia* was increased twofold by supplementation of the media with 0.035-2% (w/v) P188 compared to controls.[197,198]

The thermoreversible properties of P407 have been utilised to study microbial coal solubilisation.[199] Cultures of *Streptomyces setonii*, *Candida sp.*, *Trametes versicolor* grown on media containing P407 (>18% w/v) and powdered coal. After a period of time, the solubilised coal products and insoluble materials were separated by cooling the medium and centrifuging at 277K, at which temperature the poloxamer gel liquefies allowing simple separation of solubilised coal products.

1.3.4.3 **Other Applications of Poloxamers and Poloxamines**.

The isolation of viable Nematode larvae from faecal contamination, cast larval sheaths, and non-viable larvae using P188 treated cellulose strips was reported for 2 hookworm species (*Necator americanus* and *Ancylostoma ceylanicum*).[200] The marked increases in isolation of viable Nematode larvae was proposed to be due to reduction of the surface tension on the surface of poloxamer-treated strips facilitating the downward migration of larvae along the strips.

The solubilisation of polycyclic aromatic hydrocarbon was investigated with regard to recovery of contaminants from coastal/surface and groundwater pollutants.[201] Solubilisation was observed to depend strongly on the structure of polymers and their relative composition ratios for 5 poloxamers and 5 poloxamines studied. Poloxamines were observed to solubilise aromatic hydrocarbons (napthalene, phenanthrene, pyrene) to a lesser extent than poloxamers due to configurational constraints resulting in less apolar environments. P185 has been shown to be an effective agent in the recovery of polychlorobiphenyls (PCBs) from a sample of Ashtabula river sediment, determined by an equilibrium phase distribution model of the PCB between soil organic carbon and micelles.[202]

Poloxamers have also been demonstrated to be effective at controlling cattle bloat. A 69% decrease in alfalfa bloat was observed in Jersey cattle fed with poloxamer at a concentration of 23mgkg^{-1} of bodyweight compared to control groups.[203]

1.3.5 **Fundamental Studies on the Solution Behaviour of Poloxamers.**

The solution behaviour of poloxamers has been studied by using a variety of physico-chemical techniques. Studies of poloxamer behaviour in aqueous solution is complicated by the similarity in nature between the polyoxypropylene and polyoxyethylene portion of the polymer and the absence of chromophores or bulky side groups resulting in difficulties in a conclusive interpretation of experimental results. The general behaviour of poloxamers in aqueous solution is summarised in figure 1.6, although several phase changes are omitted (e.g., micellar reorganisations in the gel phase).

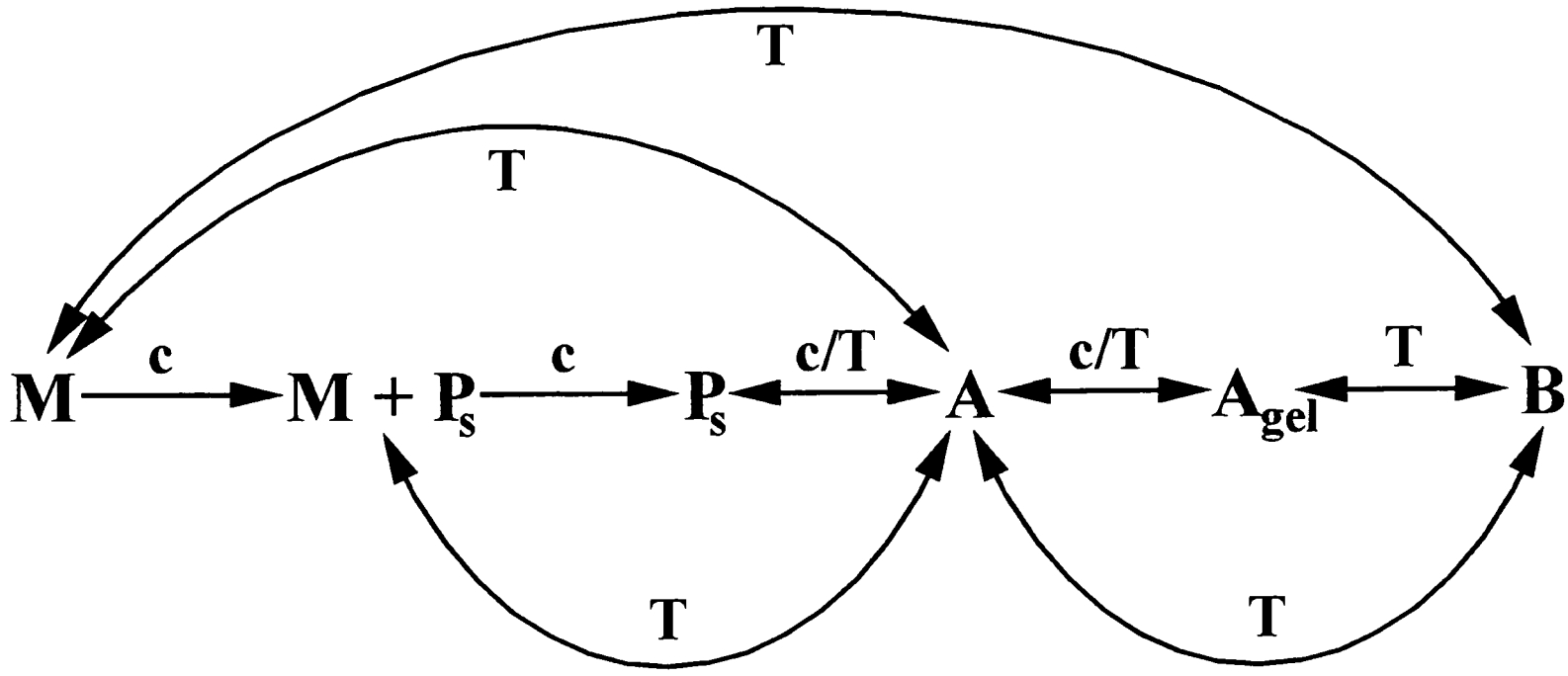

Figure 1.6 Generalised diagram to demonstrate the complex nature of the aqueous solution behaviour of the poloxamers (only the main phases that can occur are shown). Where M = hydrated POP/POE single chain (n = 1), P_s = hydrated POP/POE associated POP (n > 1), A= hydrated POE, dehydrated + aggregated POP (n > 1), A_{gel} = hydrated and entangled POE, dehydrated + associated POP, (n >> 1), B = dehydrated POE/POP (CP) (n >> 1), T = temperature, c = concentration.

The phase behaviour of poloxamers in aqueous solution is dependent on molecular weight and polyoxypropylene/polyoxyethylene ratio. e.g., poloxamers with a low relative POE content do not gel and tend to precipitate at low temperatures.

Methods used to study the phase behaviour of poloxamers in dilute aqueous solution include static and dynamic light scattering, photon correlation spectroscopy, ^{13}C and ^{1}H nuclear magnetic resonance, infrared and Raman spectroscopy, calorimetry, densitometry, dilatometry, fluorescence spectroscopy, ultrasonic absorption, neutron scattering, small angle X-ray scattering, GPC as well as the classical techniques of viscometry, vapour pressure osmometry, cryoscopy and surface tension measurements.

1.3.5.1 **Preliminary Techniques.**

Following the commercial availability of poloxamers in the 1950's research into the solution behaviour of the poloxamers yielded conflicting and inconclusive results despite the wide applications of these new compounds. The critical micelle concentration of the poloxamers was determined by Schmolka and Raymond[204, 205] by measuring the changes in the absorption spectrum of benzopurpurin 4B -surfactant complex (Table 1.3.2). The values obtained were, in several cases, confirmed by surface tension measurements. For surfactants of MW 1100 - 15500 $gmol^{-1}$ the cmc varied from 3.0 to 11.1μM (e.g., 6.8 μM for P182, MW= 2500 $gmol^{-1}$ measured at 298K). This value is much lower than the cmc value for P182 shown by Becker[206] (cmc of P182 = 24gL^{-1} in water ~ 9.6mM). A temperature increase from 298 to 313K increased the cmc of P184 from 5.6 to 11.5 μM, and the addition of 0.1M NaCl caused an increase from 5.6 to 10.4 μM (dye absorption method).[204]

Cowie and Sirianni[207] gave additional information on the micellar behaviour of poloxamers in aqueous and non-aqueous solutions. Light scattering measurements on P188, P108, P338 and P238 (MW 8750, 4750, 16250, 11000 $gmol^{-1}$ respectively) in benzene, dioxane, butyl chloride and water showed most evidence of micelle formation for P188. The micellar molecular weights were 35700 and 69600 $gmol^{-1}$ respectively (with asymmetry corrections 49000 and 95000 $gmol^{-1}$) in benzene and in dioxane, 11300 $gmol^{-1}$ in butyl chloride and 18600 $gmol^{-1}$ in water, corresponding to aggregation numbers of 4, 8, 1 and approximately 2 respectively. In benzene saturated with water the micellar molecular weight of P188 increased to 64000 $gmol^{-1}$, which was probably caused by the sorption of water by the polyoxyethylene chain. P108 gave rise to mainly tetramer formation in benzene, trimer formation in dioxane and dimer form in water; P338 and 238 both gave rise to dimer and trimer formation in some solvents.

1.3.5.2 **Literature Review of Current Research.**

Due to the complexity of the nature of poloxamers in aqueous solution, studies on the solution behaviour of these yield different and in some cases conflicting interpretations dependent on the polymer studied, concentration and temperature. Therefore it is convenient to present a review of the current literature in tabular form, loosely grouped under the principal technique used. The complexity of poloxamer solution behaviour is emphasised by the construction of phase diagrams,[208, 209] using the technique of small angle neutron scattering 6 distinct phases were observed for poloxamer 235 over a temperature range of 273 - 363K and up to a concentration of 25% w/v.[209] Neutron scattering data for poloxamers in aqueous solution has also been recently reviewed by Mortensen.[210] In addition to the review of the literature presented here, Alexandridis and Hatton,[211] and Almgren *et al.*[212] have recently published comprehensive reviews of the behaviour of poloxamers in aqueous solutions and at interfaces, the reviews also summarise the various models that have been proposed to interpret the observed behaviour of the poloxamers.

Table 1.3.2 Critical micelle concentration values of poloxamers at 298K in a 0.5% aqueous solution of benzopurpurin 4B (Schmolka and Raymond, 1965).[204]

Poloxamer	**POP base MW**	**Product MW**	**cmc mMl^{-1}**	**$mgml^{-1}$**
P101	940	1100	3.0	3.3
P105	940	1890	9.5	18
P108	940	5020	5.2	26
P122	1175	1620	11.1	18
P124	1175	2200	8.6	19
P181	1750	2000	8.0	16
P182	1750	2500	6.8	17
P184	1750	2875	5.6	16
P186	1750	3915	6.4	25
P188	1750	8000	6.9	55
P215	2050	4160	9.1	38
P234	2250	4520	8.9	40
P235	2250	4600	8.1	37
P238	2250	10750	5.1	55
P282	2750	3480	5.5	19
P334	3250	6050	7.3	44
P338	3250	15550	4.7	73

Table 1.3.3 Summarised review of current literature.

Technique	Copolymer	Conditions	Conclusion	Ref
Surface + Interfacial Tension, Static + Dynamic Light Scattering, Viscosity, Electric Birefringence, DSC (Micro-DSC Setaram), Small Angle Neutron Scattering (SANS).	P407, P403 P334	*0 - 25% w/v in water - 5% w/v in water*	Formation of micelles with increasing temperature. Micellar size increases with increasing temperature hydrodynamic radius is almost independent of temperature. Above 15% w/v all systems gel when a characteristic temperature is exceeded. Shear modulus independent of temperature - in agreement with the hard sphere model.	213
Viscometry, Ultrasonic Absorption, Light Scattering, Infrared + Raman Spectroscopy.	P178, POE MW 3000	*10 - 17% w/v in water*	Clouding phenomena connected with conformational changes of POE segments.	214
Viscometry, Dynamic light Scattering.	P184 and Meroxapol 17R4	*Water*	P184 forms micelles over a large temperature and concentration range. Meroxapol 17R4 only forms micelles at high concentration and at high temperatures. The entropy loss associated with the looping geometry of the central POE in micelle formation was determined to be largely responsible for the inability of 17R4 to form micelles.	215
Viscometry, Static + Dynamic Light Scattering, NMR, Vapour Pressure Osmometry.	P184	*o-Xylene, addition of water*	P184 was shown to not form polymolecular micelles in the absence of water. Micelles were formed when the water to EO ratio is greater than 0.2. Spherical micelles were observed with a hydrodynamic radius of 9.2nm.	216
Surface Tension, Static + Dynamic Light Scattering, DSC, NMR.	P407	*Fraction -ated samples in water*	Results similar for fractionated and unfractionated samples with the exception of surface tension. Thermal gelation resulted essentially from packing of spherical micelles.	217

Table 1.3.3 Summarised review of current literature. (continued)

Technique	Copolymer	Conditions	Conclusion	Ref
Dynamic Light Scattering, Surface Tension, Viscosity, Fluorescence (Pyrene), Oscillatory Shear Measurements.	P284	*Water*	Micelles, single chains + clusters present in solution with R_H ~9nm, ~2nm, +100nm respectively. cmc at 40°C ~0.002% w/w. Closest packing molecular area 1.28nm^2. Micelles were spherical . Thermorheological behaviour was reversible.	218
Viscosity, Ultrasound velocity, Static + Dynamic Light Scattering, Density.	Various Poloxa-mers	*Water*	Water solubility caused by binding of water to OE units. 2 water molecules per OE unit from sound and density measurements. Binding lost with increasing temperature (CP). Existence of polymeric associates from viscosity + DLS measurements.	219
Viscosity, Vapour Pressure Osmometry + sorption.	Various Poloxa-mers	*Water, Ethyl-benzene*	Hydrodynamic volume determined by POE shell. Theta temperature almost identical to pure POE. Incompatibility of POE and POP blocks causes intra- and inter- molecular phase separation in aqueous solution.	220
Dynamic Surface Tension (DST), Equilibrium Surface Tension (EST).	P237, P407, P338.	*Water (0.01-10% w/v)*	DST was shown to be associated to the POE chain length of the poloxamers. EST was related to the POP content of the polymer, and hence the cmc.	221
GPC, Surface Tension.	P407	*1% w/w in water*	Modelling of temperature dependent micellisation of Pluronics allowed prediction of radial distributions, decrease in cmc, increase in average aggregation number, micellar size and fraction of polymer molecules in micellar form - all with increasing temperature.	222
GPC.	P237	*0.21% w/v in water*	Presentation of a new method to study micellisation temperature of Pluronics represented by elution volume.	223
Densitometry	P055 and P064	*10-40% w/w in water*	Partial molar volumes and expansibility decrease with increasing content of POE indicating promotion of the supramolecular structure of water by apolar groups and its destruction by polar groups of the solute.	224

Table 1.3.3 Summarised review of current literature. (continued)

Technique	Copolymer	Conditions	Conclusion	Ref
Dilatometry	Various Poloxa-mers	*Water (dilute solution)*	Observed phase transitions in dilute aqueous solution indicating cooperativity were attributed to aggregation of the POP blocks as the change in apparent molar volume for the observed phase transition approach zero as the PO:EO ratio approach 0:1.	225
Flow Densimetry, Opacity, Viscosity, Differential Flow Microcalorimetry.	P402	*0 - 50% w/w in water*	Construction of a phase diagram for Poloxamer P402. Isotropic solution, liquid crystal, gel phase and anomalous regions observed.	208
Dynamic light Scattering, DSC, SANS, Electric Birefringence, Specific Conductivity.	P202	*Up to 50% (w/w) in water*	The formation of lyotropic liquid crystalline phases was determined, a lamellar phase (Lα) and a 'spongelike' phase (L3). The temperatures for the transitions were lowered with increasing NaCl concentration.	226
Static + Dynamic Light Scattering, NMR, Fluorescence (Pyrene).	P184	*0.2 - 25% w/w in water*	Single molecules observed at 21°C and micelles at higher temperatures. Micellisation temperature dependent on length of POP block. Light scattering measurements showed an increase in micellar size with increasing temperature.	227
Static Light Scattering, Ultrasonic Absorption, Viscosity.	P178	*17% w/w in water*	Temperature dependence of microphase separation due to critical behaviour.	228
Static + Dynamic Light Scattering, Refractive Index, Viscosity.	P184	*0 - 25% w/w in water + Addition of xylene*	Addition of xylene increases molar mass and hydrodynamic radius of micelles. Xylene solubilised in the micelle core and increases the aggregation tendency of the polymer.	229
Light Scattering, Ultrasonic Velocity.	P407	*0 - 1% w/w in water*	Micellar aggregation number varies with temperature from 0 - 44 at 10 and 40°C respectively. Aggregates are asymmetric at low temperatures but become spheroidal above 25°C.	230

Table 1.3.3 Summarised review of current literature. (continued)

Technique	Copolymer	Conditions	Conclusion	Ref
Static + Dynamic Light Scattering, Oscillatory Shear Measurements.	P235	*0 - 10% w/w in water*	At concentrations <10% co-existence of single chains and micelles observed with R_H = 1.8nm and 8.0nm respectively. Micelles form at 25°C when concentration = 5%, at 40 - 50°C only micelles observed.	231
Static + Dynamic Light Scattering, Surface Tension.	$E_{26}P_{29}$ $E_{14}P_{30}E_{14}$	*Water*	Micellisation and surface properties of the two polymers were not significantly affected by different block structures. Diblock more closely packed in surface monolayers.	232
Dynamic + Time Averaged Light Scattering, NMR.	P184	*2.04% w/v in water*	6-9 molecules observed per micelle after aggregation. Micellar molecular weight increases exponentially with temperature. Micelle size increases with temperature. Observed anomalous region removed after filtration of a 10% w/v solution of P184 at 25°C.	233
Time-correlated Fluorescence (Pyrene).	P235	*18.7% w/v in water*	With increasing temperature (10 - 50°C) the structure of the aggregated block copolymer changed from a micellar phase to a percolation cluster plus a second transition to a more ordered structure.	234
Fluorescence, Surface Tension, Density, Dynamic Light Scattering.	P335	*1-5% (w/v) in water and 1-4M Urea.*	Urea increased the cmc and cmt of the poloxamer. The enthalpy of micellisation decreased with increasing urea concentration using a closed association model, the hydrodynamic radii of the micelles was unaffected in 4M urea.	235
Fluorescence, DSC, Surface Tension, Density, Dynamic Light Scattering.	P334, P338.	*Water*	The effects of temperature on the micellisation of poloxamers was investigated, the polydispersity of micelle size decreased with increasing temperature, the core of the micelles comprised approximately 25% POE.	236

Table 1.3.3 Summarised review of current literature. (continued)

Technique	Copolymer	Conditions	Conclusion	Ref
Fluorescence, Dynamic Light Scattering.	P185, P235, P333, P335, P334, P338, P403.	*Water and various organic solvents*	The micellisation of the poloxamers showed an increase in aggregation number with temperature, the hydrodynamic radius remained constant and was interpreted in terms of dehydration of the POE block.	237
Fluorescence, NMR.	Various Poloxa-mers and Poloxa-mines	*Water*	The microviscosity was much larger than observed in conventional micelles and was dependent on the size of the POP block. With increasing temperature the micellar core became more compact.	238
Fluorescence.	P188	*Water 5 and 10% (w/v)*	A temperature dependent micellisation was observed, a drastic increase in micellar microviscosity from 20-40°C was attributed to a conformational change of the micelle from a loosely coiled aggregate to a compact structure.	239
Fluorescence, Light Scattering, Rheology, DSC, SANS, SAXS, Ultrasonic Velocity, NMR (Review).	Various poloxa-mers	*Water*	A review of the literature was presented. The phase behaviour of poloxamers is strongly dependent on temperature, the aggregation number increases with temperature, the core contains appreciable amounts of POE, and the POE mantle contracts with increasing temperature. Hexagonal, cubic and lamellar liquid crystalline phases are observed at high copolymer concentrations.	212
SAXS, ^{1}H-NMR.	Meroxapol 25R4	*Water/ p-xylene*	Lamellar, normal and reverse hexagonal and bicontinuous cubic liquid crystalline regions observed at 298K dependent on the composition of the ternary system.	240
Fluorescence (octadecylrhodamine-B).	P184	*Water*	A temperature induced micellisation was observed, and the local viscosity was determined by polarisation and lifetime measurements.	241
Fluorescence, Surface Tension, Light Scattering, Ultra-centrifugation.	P188, P235, P338	*Water*	The micelles formed had a hydrodynamic diameter ranging from 15-35nm dependent on the POP content.	126

Table 1.3.3 Summarised review of current literature. (continued)

Technique	Copolymer	Conditions	Conclusion	Ref
Fluorescence (Pyrene + ANS).	P407	*26 - 34% w/v in water*	Microviscosity of solutions decreases with increasing temperature. Addition of polyethylene glycols had little effect on polymer hydration despite producing changes in the gelation temperature.	242
Fluorescence.	P184, P188, P282, P407	*10% w/v in water Pressure 0 -2000 bar*	3 different fluorescent probes used. P184 - hydrophobic bonding is less than that observed for nonionic surfactants, $C_nPh(EO)_n$. Hydrophobic bonding weakened by increasing pressure (1000 - 1500 bar) but is strengthened above 1500 bar. More compact structure of poloxamer aggregates with increasing temperature. Effect of pressure more at higher temperatures. Pressure effects more significant with increasing POP MW.	243
Diode-array UV Spectrometry.	P237	*0.5% in Water*	The presence of a concentration dependent transition was determined, attributed to an aggregation of the copolymer, involving aggregation of the POP blocks, and was shown to be in agreement with HSDSC data previously obtained.	244
Diode-array UV Spectrometry.	P217, P237, P407.	*0.5% in Water*	Polymer mixtures aggregate independently or cooperatively dependent upon the molecular mass of the POP blocks. (P217/P237 - single transition, P237/P407 and P217/P407 two separate transitions.	245
^1H NMR relaxation.	P257 and POE (15k $gmol^{-1}$)	1-9% w/v in D_2O 280-345K	A temperature driven conformational change related to the formation of a water insoluble liquid core created by the POP block was attributed to micellisation. Concentration dependence on the cmt were described by a closed association model.	246
^{13}C NMR, Fluorescence (Pyrene).	P184, P188	*1% w/v in water SDS*	POP block strengthens interactions with SDS. P184 solution at 40°C, addition of SDS decreases micellar size until micellar size = 1 molecule. $-CH_2-$ resonance in POE are shifted downfield in the presence of SDS.	247

Table 1.3.3 Summarised review of current literature. (continued)

Technique	Copolymer	Conditions	Conclusion	Ref
^{13}C NMR, Ultrasonic Relaxation.	P407	*20% w/w in D_2O*	With increasing temperature changes in the orientation of the methyl groups is observed (POP) creating micellar core. These conformational changes are induced by extrusion of hydrated water with increasing temperature.	248
Water-self diffusion NMR.	P407	*10-40% w/w in D_2O*	Water self diffusion decreases monotonically with increasing polymer concentration explained by obstruction due to excluded volume and hydration of polymer molecules. 2.5 water molecules per EO are perturbed. With increasing temperature water diffusion increases. Dehydration was uncorrelated with the occurrence of the gel region.	249
Water-self diffusion NMR, GPC.	P407	*1% in water (GPC) 10-40% in D_2O (NMR)*	Micelle formation dependent on temperature. Micelles are small (R_H » 10nm). Gel region consists of discrete polymer aggregates. For gels to form the temperature > cmt.	250
Infrared + Raman Spectroscopy.	P178 POE MW 3000	*10% w/w in water 3% w/w in CCl_4*	Below the cloud point two water molecules per OE are bound by hydrogen bonds. At the CP the H-bonds partially break up increasing the hydrophobicity of the POE. Thus the predominantly dimeric micelles aggregate with a cooperativity number of ~ 100. Dehydration of POE chains does not occur at clouding.	251
SANS (Review)	Various poloxa-mers	*0-50% in water*	Thermodynamically stable micelles formed with increasing temperature and/or concentration. Micelles in the solid phase are organised on a body-centred cubic lattice. With increasing temperature, micelles undergo a sphere-rod transition. At elevated conc. lamellar phases are observed.	210
SANS and cryogenic transmission electron microscopy	P407	*water*	Formation of spherical micelles in solution. Under shear, the existence of lyotropic liquid crystalline phase transforms into a monodomain crystal with cubic symmetry	252

Table 1.3.3 Summarised review of current literature. (continued)

Technique	Copolymer	Conditions	Conclusion	Ref
SANS, DSC, electric birefringence, Dynamic light scattering, Specific conductivity.	P212	*0-50% w/w in water and NaCl solution*	Formation of a lamellar (Lα) and a 'spongelike' phase (L3) with increasing temperature. NaCl decreases the temperature at which these phases are observed. Conductivity of the added NaCl shows a bicontinuous structure of the L3 phase.	253
SANS.	P235	*0 - 25% w/w in D_2O*	The construction of a phase diagram for P235 using 3, 6 and 15Å neutrons with sample to detector distance of 1, 3 and 6m respectively. Many different phases identified as a function of concentration and temperature (6 different distinct phases).	209
SANS	P184	*D_2O*	The aggregation number decreased with decreasing temperature. The micellar molar mass increased with the addition of xylene reaching a maximum at about 0.3-0.4 molecules of xylene/OP unit. The volume fraction of the polymer segments in the micellar shell was less than 0.2.	254
SANS, Static Light Scattering, DSC.	P407	*Water/SDS*	The addition of sodium dodecyl sulphate (SDS) to solutions of P407 suppressed micellisation completely, the SDS was proposed to cooperatively bind to the copolymer causing the POP to become relatively hydrophilic.	255
SAXS, *NMR.*	P184	*Water / o-Xylene mixtures*	At low copolymer concentrations unimers and micelles co-existed, the micellar size increased with increasing amount of water in the mixture. The conformation of the copolymer and amount of solubilised water remained essentially the same before and after micellisation.	256
SAXS, *SANS,* *Light Scattering.*	P184	*Xylene /Water*	The micelles formed were shown to have a core-shell structure, the shell was heavily solvated. At high copolymer concentration large aggregates with a lamellar structure were formed.	257 - 260

Table 1.3.3 Summarised review of current literature. (continued)

Technique	Copolymer	Conditions	Conclusion	Ref
HSDSC.	P237	*0.5% w/v in water*	The observed phase transition was attributed to the temperature driven aggregation of the POP blocks.	261
HSDSC.	P184, 235, 207, 237, 407, 108, 188, 238, 308, 338	*0.5% w/v in water*	The observed temperature driven phase transitions are believed to result from changes in polymer solvation of the POP blocks. The transitions were completely reversible and attributed to aggregation.	262
^{13}C NMR, *HSDSC.*	P237	*0.5% w/v in D_2O*	T_1 relaxation measurements show a shift in the CH_3(PO) resonance with increasing temperature indicating increasing segmental motion up to the T_m (from HSDSC) and then resets subject to new steric requirements.	263
HSDSC.	P108, 188, 238, 308, 338, 207, 237, 407, 235, 184.	*0.5% w/v in water*	Theoretical analysis of the data predicts a lower and upper phase transition for the poloxamers and the model emphasised the dependence of POP on the observed phase transitions.	264
HSDSC	P122, 123, 124, 182, 184, 188, 215, 217, 234, 235, 237, 333, 335 407.	*0.05-2% P333, 0.1-5% P237, 0.5% P122-P407 in water*	A mass action model was employed to describe changes in heat capacity of the pre- and post-transitional states. Phase diagrams were constructed of the aggregation process as a function of c and T. From the calorimetric data, cmc and cmt data were obtained. Enthalpy-entropy plots indicate that the same solvent-solute interactions are responsible for the transitions for all polymers and concentrations studied.	265
HSDSC, *Differential Scanning Densitometry (DSD).*	P182, 184, 215, 235, 237, 238, 284, 333, 338, 407	*1.0%w/v in water*	The observed temperature driven phase transitions were attributed to the processes of aggregation, desolvation and a conformational change of the hydrophobic POP portion of the polymer.	266

Table 1.3.3 Summarised review of current literature. (continued)

Technique	Copolymer	Conditions	Conclusion	Ref
Isothermal Microcalorimetry.	P237, P238	*0.5% w/v in water*	The time driven phase transitions observed for aqueous solutions of poloxamers prepared at 298K with minimised mechanical agitation were attributed to an ageing process associated with the slow hydration of the poloxamer following the departure of a molecule from the solid phase to solution.	267
HSDSC.	Various poloxa-mers and POP	*Water*	The observed phase transition was attributed to physical changes of the POP portion of the copolymer, empirical multiple linear regression analysis allowed an aid in design of poloxamers with specific control of solution phase properties over the temperature range 273-373K.	268
HSDSC.	Various poloxa-mers	*Water*	Model fitting of data to experimental HSDSC scans was shown to be in good agreement. The thermodynamic model allowed estimates of the aggregation number and cooperativity to be made.	269 270
HSDSC	27 poloxa-mers	*0.5% (w/v) in water*	The observed phase transition was shown to be related to hydrophobic aggregation but independent of the cloud point, the coiled POP core associates to produce larger aggregates.	271
HSDSC	P188, 215, 217, 234, 235, 237, 238, 333, 335, 338, 407.	*0.5 + 1.0% (w/v) in water*	A method is presented for the determination of the concentration of poloxamer in thermodynamic equilibrium with micelles. HSDSC data was compared to previously published cmc data obtained using a dye solubilisation technique.	272
HSDSC	P237	*0.5% in water + MeOH, EtOH, PrOH, BuOH, formamide, urea and hydrazine*	Model fitting of the calorimetric output enabled determination of estimates for various thermodynamic parameters which characterise the process of micellisation. MeOH, EtOH, urea and formamide prevent the onset of micellisation. BuOH and hydrazine favour micelle formation.	273

1.4 References.

(1) Flory,P.J., *Principles of Polymer Chemistry*, Cornell University Press, Ithaca, N.Y., **1971**.
(2) Kobayashi,E.; Ohashi,T.; Furukawa,J. *Polym.J.*, **1989**, *21*, 111.
(3) Bassindale,A.R.; Gentle,T.E., *J.Mater.Chem.*, **1993**, *3(12)*, 1319.
(4) Vandijkwolthuis,W.N.E.; Franssen,O.; Talsma,H.; Vansteenbergen,M.J.; Vandenbosch,J.J.K.; Hennink,W.K., *Macromolecules*, **1995**, *28(18)*, 6317.
(5) Mori,S., *J.Appl.Polym.Sci.*, **1989**, *93*, 7262.
(6) Roush,P.B.; Hannah,R.W., Coates,J.P.; Bunn,A.; Willis,H.A., *Polym.Sci.Technol.*, **1987**, *36*, 261.
(7) Yang,Y.S.; Lee,L.J.; Lo,S.K.; Menardi,P.J., *J.Appl.Polym.Sci.*, **1989**, *37*, 2313.
(8) Kantcheva,M.; Dallalana,I.G.; Szymura,J.A., *J.Catalysts*, **1995**, *154(2)*, 329.
(9) So.S.; Rudin,A., *J.Appl.Polym.Sci.*, **1990**, *41*, 205.
(10) Druy,M.A.; Elandjian,L.; Stevenson,W.A.; Driver,R.D.; Leskowitz,G.M.; Curtiss,L.E., *Proc.SPIE-Int.Soc.Opt.Eng.*, **1989**, *1170*, 150.
(11) Gadoury,S.R.; Urban,M.W., *Polym.Mater.Sci.Eng.*, **1989**, *60*, 875.
(12) Kannan,S.; Nando,G.B.; Bhowmick,A.K.; Mathew,N.M., *J.Elastomers Plastics*, **1995**, *27(3)*, 268.
(13) Nyquist,R.A., *Appl.Spectrosc.*, **1989**, *43*, 440.
(14) Scherzer,T., *J.appl.Polym.Chem.*, **1995**, *58(3)*, 501.
(15) Reynolds,N.M.; Savage,J.D., Hsu,S.L., *Macromolecules*, **1989**, *22*, 2867.
(16) Siesler,H.W., *Makromol.Chem.*, **1989**, *190*, 2653.
(17) Marcos,J.I.; Orlandi,E.; Zerbi,G., *Polymer*, **1990**, *31*, 1899.
(18) Amram,B.; Bokobza,L.; Sergot,P.; Monnerie,L.; Queslel,J.P., *Macromolecules*, **1990**, *23*, 1212.
(19) Shen,D.Y.; Pollack,S.K.; Hsu,S.L., *Macromolecules*, **1989**, *22*, 2564.
(20) Higashi,N.; Matsumoto,T.; Niwa,M., *Langmuir*, **1994**, *10(12)*, 4651.
(21) Jo,W.H.; Cruz,C.A.; Paul,D.R., *J.Polym.Sci. Part B: Polym.Phys.*, **1989**, *27*, 1057.
(22) Kondo,T.; Sawatari,C.; Manley,R.S.; Gray,D.G., *Macromolecules*, **1994**, *27(1)*, 210.
(23) Pedrosa,P.; Pomposa,J.A.; Calahorra,E.; Cortazar,M., *Macromolecules*, **1994**, *27(1)*, 102.
(24) Harthcock,M.A., *Polymer*, **1989**, *30*, 1234.
(25) Musto,P.; Karaz,F.E.; MacKnight,W.J., *Polymer*, **1989**, *30*, 1012.
(26) Brudler,R.; Degroot,H.J.M.; Vanliemt,W.B.S.; Gast,P.; Hoff,A.J.; Lugtenburg,J.; Gerwert,K., *Febs.Lett.*, **1995**, *370(1-2)*, 88.
(27) Garcia,D.; Starkweather,H.W.Jr., *Polym.Sci.Technol.*, **1987**, *36*, 213.
(28) Shin,K.H.; Maeda,H., Fujiwara,T.; Akutsu,H., *Biochim.Biophys.Acta, Biomemb.*, **1995**, *1238*, 42.
(29) Feng,H.Q.; Ye,C.H.; Zhang,P.; Sun,Z.H.; Feng,Z.L., *Macromol.Chem.Phys.*, **1995**, *196(8)*, 2587.
(30) Swamy,M.J.; Wurz,U.; Marsh,D., *Biochemistry*, **1995**, *34(22)*, 7295.
(31) Grobelny,J.; Rice,D.M.; Karaz,F.E.; MacKnight,W.J., *Macromolecules*, **1990**, *23*, 2139.
(32) Grobelny,J.; Rice,D.M.; Karaz,F.E., MacKnight,W.J., *Polym.Commun.*, **1990**, *31*, 86.
(33) Parmer,J.F.; Dickinson,L.C.; Chien,J.C.W.; Porter,R.S., *Macromolecules*, **1989**, *22*, 1078.
(34) Pioteck,J.; Reid,V., Macknight,W.J., *Acta Polymerica*, **1995**, *46(2)*, 156.
(35) Dumais,J.J.; Jelinski,L.W.; Galvin,M.E.; Dybowski,C.; Brown,C.E.; Kovacic,P., *Macromolecules*, **1989**, *22*, 612.
(36) Zhang,K.W.; Khan,A., *Macromolecules*, **1995**, *28(11)*, 3807.
(37) Sugiura,Y.; Makimura,Y.; Kita,Y, Matsuo,M., *Coll.Polym.Sci.*, **1995**, *273(7)*, 633.
(38) Saito,S.; Moteki,Y.; Nakagawa,M.; Hori,F.; Kitamara,R., *Macromolecules*, **1990**, *23*, 3256.
(39) Hughes,C.D.; Sethi,N.K.; Baltisberger,J.H.; Grant,D.M., *Macromolecules*, **1989**, *22*, 2551.
(40) Kauffman,J.S., Dybowski,C.J., *J.Polym.Sci., Part B: Polym.Phys.*, **1989**, *27*, 2203.
(41) Mirau,P.A.; Heffner,S.A.; Bovey,F.A., *Macromolecules*, **1990**, *23*, 4482.
(42) Mohan,D.; Radhakrishnan,G.; Rajadurai,S.; Joseph,K.T., *Polym.Sci., Part C: Polym.Lett.*, **1990**, *28*, 307.
(43) Hill,D.J.; Lang,A.P.; O'Donnell,J.H.; O'Sullivan,P.W., *Eur.Polym.J.*, **1989**, *25*, 911.
(44) Duff,D.W.; Malciel,G.E., *Macromolecules*, **1990**, *23*, 3069.
(45) Gao,C.P.; Hay,A.S., *J.Polym.Sci., PartA: Polym.Chem.*, **1995**, *33(14)*, 2347.
(46) Andrieu,X., Fauvarque,J.F.; Goux,A.; Hamaide,T.; Mhamdi,R.; Vicedo,T., *Electrochim.Acta*, **1995**, *40(13-14)*, 2295.
(47) Echigo,Y.; Iwaya,Y.; Tomioka,I.; Yamada,H., *Macromolecules*, **1995**, *28(14)*, 4861.
(48) Hale,A.; Macosko,C.W.; Bair,H.E., *J.Appl.Polym.Sci.*, **1989**, *38*, 1253.
(49) Kowalczyk,B; Bragial,P.; Czerwinski,M., *Thermochim.Acta*, **1994**, *243(1)*, 35.
(50) Basu,S.; Chatterjee,N.; Maiti,M.M., *J.Appl.Polym.Sci.*, **1995**, *58(3)*, 523.

(51) Tsuji,T.; Wakasa,K.; Yamaki,M., *J.Mater.Sci., Mat.Med.*, **1995**, *7*, 396.
(52) Maeda,Y.; Watanabe,J., *Macromolecules*, *1995*, *28(5)*, 1661.
(53) Fu,Z.M.; Li,W.X., *Sci.China Series A : Math.Phys.Astr.Tech.Sci.*, **1995**, *38(8)*, 974.
(54) Wendlandt,W.W.; Gallagher,P.K., *Thermal Characterisation of Polymeric Materials*, Ed. Tsu, E.A., Academic Press, New York, **1981**, 1-90.
(55) Vassilev,S.V.; Kitano,K.; Takeda,S.; Tsurue,T., *Fuel Proc.Tech.*, **1995**, *45(1)*, 27.
(56) Khairou,K.S., *Polym.Degrad.Stab.*, **1994**, *46(3)*, 315.
(57) Peesapati,V.; Rao,U.N.; Pethrick,R.A., *Polym.Int.*, **1994**, *34(1)*, 35.
(58) DELTA Series Thermal Analysis System VP118610, *Perkin Elmer Technical Literature*, Perkin Elmer Corp., Norwalk, Connecticut, **1986.**
(59) Campbell,D.; Dix,L.R.; Roston,P., *Dyes and Pigments*, **1995**, *29(1)*, 77.
(60) Plummer,C.J.G.; Kausch,H.H., *Coll.Polym.Sci.*, **1995**, *273(8)*, 719.
(61) Klein,N.; Selivansky,D.; Marom.G., *Polym.Comp.*, **1995**, *16(3)*, 189.
(62) Sukhanova,T.E.; Lednicky,F.; Urban,J.; Baklagina,Y.G.; Mikhailov,G.M.; Kudryavstev,V.V., *J.Mater.Sci.*, **1995**, *30(9)*, 2201.
(63) Sarvaranta,L., *J.Appl.Polym.Sci.*, **1995**, *56(9)*, 1085.
(64) Hong,S.M.; Economy,J., *Macromolecules*, **1995**, *28(19)*, 6481.
(65) Khanna,Y.P.; Kuhn,W.P.; Macur,J.E.; Messa,A.F.; Murthy,N.S.; Reimschussel,A.C.; Schneider,R.L., Sibilia,J.P.; Signorelli,A.J., et al, *J.Polym.Sci., Part B: Polym.Phys.*, **1995**, *33(7)*, 1023.
(66) Opazo,A.; Gargallo,L.; Radic,D., *Int.J.Polym.Mater.*, **1994**, *27(1-2)*, 117.
(67) Tsukada,M.; Freddi,G.; Ishiguro,Y.; Shiozaki,H., *J.Appl.Polym.Sci.*, **1993**, *50(9)*, 1519.
(68) Arora,A.; Daniels,E.S.; Elaasser,M.S., *J.Appl.Polym.Sci.*, **1995**, *58(2)*, 301.
(69) Yao,K.D.; Cheng,G.X.; Lu,T.; Zhu,W.S.; Shun,Q.C.; Wang,T.Y.; Zhang,D.W., *J.Appl.Polym.Sci.*, **1995**, *58(3)*, 565.
(70) Miyashita,Y.; Kimura,N.; Nishio,Y.; Suzuki,H., *Kobunshi Ronbunshu*, **1994**, *51(7)*, 466.
(71) Vanhutten,P.F.; Mangnus,R.M.; Gaymans,R.J., *Polymer*, **1993**, *34(2)*, 4193.
(72) Hernandez,L.G.; Diaz,A.R.; Gonzalez,J.L.D., *Rubber Chem.Technol.*, **1992**, *65(5)*, 869.
(73) Gillham,J.K., *Amer.Inst.Chem.Eng.J.*, **1974**, *20*, 1066.
(74) Venditti,R.A.; Gillham,J.K., *J.Appl.Polym.Sci.*, **1995**, *56(13)*, 1687.
(75) Bahani,M.; Laupetre,F.; Monnerie,L., *J.Polym.Sci., Part B: Polym.Phys.*, **1995**, *33(2)*, 167.
(76) Zukas,W.X., *J.Appl.Polym.Sci.*, **1994**, *53(4)*, 429.
(77) Wang,X.R.; Gillham,J.K., *J.Appl.Polym.Sci.*, **1993**, *47(3)*, 447.
(78) Hacaloglu,J.; Yalcin,T.; Onal,A.M., *J.Macromol.Sci, Pure Appl.Chem.*, **1995**, *A32(6)*, 1167.
(79) Higgins,R.J.; Rhine,W.E.; Cima,M.J.; Bowen,H.K., Farneth,W.E., *J.Am.Ceramic Soc.*, **1994**, *77(9)*, 2243.
(80) Fares,M.M.; Hacaloglu,J.; Suzer,S., *Eur.Polym.J.*, **1994**, *30(7)*, 845.
(81) Tanaka,H.; Hall,H.K., *Macromol.Chem.Phys.*, **1994**, *195(6)*, 2073.
(82) Clark,G.M., *Proceedings of the 2nd European Symposium on Thermal Analysis.* Ed Dollimore,D., Heyden, London, **1981**, 255.
(83) Shimada,S., *Thermochim.Acta*, **1995**, *255*, 341.
(84) Lonvik,K., *Thermochim.Acta*, **1993**, *214(1)*, 51.
(85) Shimada,S, *Thermochim.Acta*, **1992**, *200*, 317.
(86) Vaugh,T.H.; Suter,H.R.; Lundsted,L.G.; Kramer,M.G., *J.Amer.Oil Chem.Soc.*, **1951**, 294.
(87) Gaylord,N.G.(ed), *'High Polymers', Vol 13, Polyethers, Part 1*, Interscience **1963.**
(88) Synperonic PE, T and LF Nonionic Surfactants, *ICI Technical literature*, **1991**.
(89) Schmolka,I.J., *J.Am.Oil Chem.Soc.*, **1977**, *54*, 110.
(90) Lunsted,L.G., **1961,***U.S.Patent 2,979,528.*
(91) Porter,C.J.H.; Moghimi,S.M.; Davies,M.C.; Davis,S.S.; Illum,L., *Int.J.Pharm.*, **1992**, *83*, 273.
(92) Ding,J.F.; Heatley,F., Price,C.; Booth,C., *Eur.Polym.J.*, **1991**, *27*, 895.
(93) Ding,J.F., Attwood,D.; Price,C.; BoothC., *Eur.Polym.J.*, **1991**, *27*, 901.
(94) Deng,Y.; Ding,J.; Yu,G.; Mobbs,R.H.; Heatley,F.; Price,C.; Booth,C., *Polymer*, **1992**, *33(9)*, 1959.
(95) Deng,Y., Ding,J.; Stubbersfield,R.B.; Heatley,F.; Attwood,D.; Price,C.; Both,C., *Polymer*, **1992**, *33(9)*, 1963.
(96) Lang,L.; Bedells,A.D.; Attwood,D.; Booth,C., *J.Chem.Soc.Faraday Trans.*, **1992**, *88(10)*, 1447.
(97) Wang,Q.; Price,C.; Booth,C., *J.Chem.Soc.Faraday Trans.*, **1992**, *88(10)*, 1437.
(98) Rassing,J.; Attwood,D., *Int.J.Pharm.*, **1983**, *13*, 47.
(99) Reddy,N.K.; Fordham,P.J.; Attwood,D.; Booth,C., *J.Chem.Soc.Faraday Trans.*, **1990**, *86*, 1569.
(100) Yu,G.E.; Deng,Y.; Dalton,S.; Wang,Q.E.; Attwood,D.; Price,C.; Booth,C., *J.Chem.Soc.Faraday Trans.*, **1992**, *88(17)*, 2537.

(101) Lawrence,M.J., *Chem.Soc.Rev.*, **1994**, *23(6)*, 417.
(102) Ulrich,C.E.; Geil,R.G.; Tyler,T.R.; Kennedy,G.L.Jr., *Drug Chem.Toxicol.*, **1992**, *15(1)*, 15.
(103) Kier,L.; Wagner,L.M.; Wilson,T.V.; Li,A.P.; Short,R.D.; Kennedy,G.L, *Drug Chem.Toxicol*, **1995**, *18(1)*, 29.
(104) Warheit,D.B.; Fogle,H.; Thomas,W.C.; Murphy,S.R., Tyler,T.R; Reinhold,R.W.; Kennedy,G.L., *Inhalation Toxicol.*, **1995**, *7(3)*, 377.
(105) Zeevi,A.; Klang,S.; Alard,V.; Brossard,F.; Benita,S., *Int.J.Pharm.*, **1994**, *108(1)*, 57.
(106) Das,S.K.; Tucker,I.G.; Hill,D.J.T.; Ganguly,N., *Pharm.Res.*, **1995**, *12(4)*, 534.
(107) Myrtil,E.; Zarif,L.; Greiner,J.; Riess,J.G.; Pucci,B.; Pavia,A.A., *J.Fluorine Chem.*, **1995**, *71(1)*, 101.
(108) Levy,M.Y.; Polacheck,I.; Barenholz,Y.; Benita,S., *Pharm.Res.*, **1995**, *12(2)*, 223.
(109) Klang,S.H.; Fruchtpery,J.; Hoffman,A.; Benita,S., *J.Pharm.Parmacol.*, **1994**, *46(12)*, 986.
(110) Fresta,M.; Puglisi,G., *Drug Development Ind.Pharm.*, **1994**, *20(14)*, 2227.
(111) Lee,M.J.; Lee,M.H.; Shim,C.K., *Int.J.Pharm.*, **1995**, *113(2)*, 175.
(112) Illum,L.; Hunneyball,I.M.; Davis,S.S., *Int.J.Pharm.*, **1986**, *29*, 53.
(113) Moghimi,S.M.; Porter,C.J.H.; Illum,L.; Davis,S.S., *Int.J.Pharm.*, **1991**, *68*, 121.
(114) Douglas,S.J.; Davis,S.S.; Illum,L., *Int.J.Pharm.*, **1986**, *34*, 145.
(115) Watrouspeltier,N.; Uhl,J.; Steel,V.; Brophy,L.; Meriskoliversidge,E., *Pharm.Res.*, **1992**, *9(9)*, 1177.
(116) Lee,H.J.; Ahn,B.N.; Paik,W.H.; Shim,C.K.; Lee,M.G., *Int.J.Pharm.*, **1996**, *131(1)*, 91.
(117) Lee,J.; Martic,P.A.; Tan,J.S., *J.Coll.Int.Sci.*, **1989**, *131(1)*, 252.
(118) Tan,J.S.; Martic,P.A., *J.Coll.Int.Sci.*, **1990**, *136(2)*, 415.
(119) Seijo,B.; Fattal,E.; Roblot-Treupel,L.; Courvreur,P., *Int.J.Pharm.*, **1990**, *62*, 1.
(120) Pimienta,C.; Choinard,F.; Labib,A.; Lenaerts,V., *Int.J.Pharm.*, **1992**, *80*, 1.
(121) Paradis,R.; Noel,C.; Page,M., *Int.J.Oncology*, **1994**, *5(6)*, 1305.
(122) Alakhov,V.Y.; Moskaleva,E.Y.; Batrakova,E.V.; Kabanov,A.V., *Bioconjugate Chem.*, **1996**, *7(2)*, 209.
(123) March,K.L.; Madison,J.E.; Trapnell,B.C., *Human Gene Therapy*, **1995**, *6(1)*, 41.
(124) Pec,E.A.; Wout,Z.G.; Johnston,T.P., *J.Pharm.Sci.*, **1992**, *81(7)*, 626.
(125) Bhatnagar,S.; Nakhare,S.; Vyas,S.P., *J.Microencap.*, **1995**, *12(1)*, 13.
(126) Kabanov,A.V.; Nazarova,I.R.; Astafieva,I.V.; Batrakova,E.V.; Alakhov,V.Y.; Yaroslavov,A.A.; Kabanov,V.A., *Macromolecules*, **1995**, *28(7)*, 2303.
(127) Kabanov,A.V.; Batrakova, E.V.; Meliknubarov,N.S., Fedoseev,N.A.; Dorodnich,T.Y.; Alakhov,V.Y.; Chekhonin,V.P.; Nazarova,I.R., Kabanov,V.A., *J.Contr.Rel.*, **1992**, *22(2)*, 141.
(128) Miyazaki,S.; Oda,M.; Takada,M.; Attwood,D., *Biol.Pharm.Bull.*, **1995**, *18(8)*, 1151.
(129) Miyazaki,S.; Tobiyama,T.; Takada,M., Attwood,D., *J.Pharm.Parmacol.*, **1995**, *47(6)*, 455.
(130) Xu,X.; Lee,P.I., *Pharm.Res.*, **1993**, *10(8)*, 1144.
(131) Guzman,M.; García,F.F.; Molpeceres,J.; Arberturas,M.R., *Int.J.Pharm.*, **1992**, *80*, 119.
(132) Gates,K.A.; Grad,H.; Birek,P.; Lee,P.I., *Pharm.Res.*, **1994**, *11(11)*, 1605.
(133) Wu,H-L.S.; Miller,S.C., *Int.J.Pharm.*, **1990**, *66*,213.
(134) Johnston,T.P.; Punjabi,M.A.; Froelich,C.J., *Pharm.Res.*, **1992**, *9(3)*, 425.
(135) Wang,P.L.; Johnston,T.P., *Int.J.Pharm.*, **1995**, *113(1)*, 73.
(136) Park,T.G.; Cohen,S.; Langer,R., *Pharm.Res.*, **1992**, *9(1)*, 37.
(137) Park,T.G.; Cohen,S.; Langer,R., *Macromolecules*, **1992**, *25*, 116.
(138) Cappel,M.J.; Kreuter,J., *Int.J.Pharm.*, **1991**, *69*, 155.
(139) Waddell,W.R.; Geyer,R.P.; Olsen,F.R.; Stare,F.J., *Metabolism*, **1957**, *6*, 815.
(140) Geyer,R.P.; Olsen,F.R.; Andrus,S.B.; Waddell,W.R.; Stare,F.J., *J.Am.Oil Chem.Soc.*, **1955**, *32*, 365.
(141) Wells,R.; Bygdeman,M.S.; Shahriari,A.A.; Matloff,J.M.; Harken,D.W., *Circulation*, **1968**, *37-38 (Suppl.II)*, II-168.
(142) Vasko,K.A.; Riley,A.M.; DeWall,R.A., *Trans.Amer.Soc.Artif.Int.Organs*, **1972**, *28*, 526.
(143) Danielson,G.K.; Dubilier,L.D., Bryant,L.S., *J.Thoracic Cardiovasc.Surg.*, **1970**, *59(2)*, 179.
(144) Wells,R.; Bygdeman,M.S.; Shahriari,A.A.; Matloff,J.M., *Circulation*, **1968**, *37*, 638.
(145) Hymes,A.C.; Safavian,M.H.; Gunther,T., *J.Surg.Res.*, **1971**, *11(4)*, 191.
(146) Grover,F.L., Newman,M.M.; Paton,B.C., *Surg.Forum*, **1970**, *21*, 30.
(147) Grover,F.L.; Amundsen,D.; Warden,J.L.; Fosburg,R.G.; Paton,B.C., *J.Surg.Res.*, **1974**, *17(1)*, 30.
(148) Mayer,D.C.; Strada,S.J.; Hoff,C.; Hunter,R.L.; Artman,M., *Ann.Lin.Lab.Sci.*, **1994**,*24(4)*, 302.
(148) Weatherley-White,R.C.A.; Knize,D.M.; Geisterfer,D.J.; Paton,B.C.' *Surgery*, **1969**, *66(1)*, 208.
(150) Knize,D.M.; Weatherley-White,R.C.A., *Surg.Gynec.Obstet.*, **1969**, *129*, 1019.
(151) Lowe,K.C., *Clin.Hemorheol.*, **1992**, *12(1)*, 141.
(152) Zuck,T.F.; Riess,J.G., *Crit.Rev.Clin.Lab.Sci.*, **1994**, *31(4)*, 295.

(153) Spence,R.K.; Norcross,E.D.; Costabile,J.; McCoy,S.; Cernaianu,A.C.; Alexander,J.B.; Pello,M.J.; Atabek,U.; Camishion,R.C., *Artificial Blood Subst.Immob.Tech.*, **1994**, *22(4)*, 955.
(154) Schaer,G.L.; Spaccavento,L.J.; Browne,K.F.; Krueger,K.A.; Gibbons,R.J., *J.Am.Coll.Cardiol.*, **1994**, *Suppl.1A*, 344A.
(155) Schaer,G.L.; Hursey,T.L.; Abrahams,S.L.; Buddemeier,K.; Ennis,B.; Rodriguez,E.R.; Hubbell,J.P.; Moy,J.; Parrillo,J.E., *Circulation*, **1994**, *90(6)*, 2964.
(156) Schaer, G.L.; Spaccavento,L.J.; Browne,K.F.; Krueger,K.A.; Krichbaum,D.; Phelan,J.M.; Fletcher,W.O.; Grines,C.L.; Edwards,S.; Jolly,M.K.; Gibbons,R.J., *Circulation*, **1996**, *94(3)*, 298.
(157) Adams-Graves,P., *Blood*, **1994**, *84*, 410a.
(158) Carter,C.; Fisher,T.C.; Hamai,H.; Johnson,C.S.; Meiselman,H.J.; Nash,G.B.; Stuart,J., *Clin.Hemorheol.*, **1992**, *12(1)*, 109.
(159) Danielson,G.K.; Dubilier,L.D.; Bryant,L.R., *J.Thoracic Cardiovasc.Surg.*, **1970**, *59*, 178.
(160) Grover,F.L.; Heron,M.W.; Mewman.M.M.; Paton,B.C., *Circulation*, **1969**, *39 and 40 (Suppl.)*, I249.
(161) Armstrong,J.K.; Meiselman,H.J.; Fisher,T.C., *Thromb.Res.*, **1995**, *79(5/6)*, 437.
(162) Edwards,C.M.; May,J.A.; Heptinstall,S.; Lowe,K.C., *Thromb.Res.*,**1996**, *81(4)*, 511.
(163) Edwards,C.M.; Heptinstall,S.; Lowe,K.C., *Brit.J.Pharmacol.*, **1996**, *118(suppl.S)*, P98.
(164) Kolodgie,F.D.; Farb,A.; Carlson,G.C.; Wilson,P.S.; Virmani,R., *J.Am.Coll.Cardiol.*, **1994**, *24(4)*, 1098.
(165) Mezrow,C.K.; Mazzoni,M.; Wolfe,D.; Shiang,H.H.; Litwak,R.S.; Griepp,R.B., *J.Thor.Cardiovasc.Surg.*, **1992**, *103(6)*, 1143.
(166) Steinleitner,A.; Lopez,G.; Suarez,M.; Lambert,H., *Fertility and Sterility*, **1992**, *57(2)*, 305.
(167) Rice,V.M.; Shanti,A.; Moghissi,K.S.; Leach,R.E., *Fertility and Sterility*, 1993, 59(4), 901.
(168) Reigel,D.H.; Bazmi,B.; Shih,S.R.; Marquardt,M.D., *Ped.Neurosurg.*, **1993**, *19(5)*, 250.
(169) Follis,F.; Jenson,B.; Blisard,K.; Hall,E.; Wong,R.; Kessler,R.; Temes,T.; Wernly,J., *J.Invest.Surg.*, **1996**, *9(2)*, 149.
(170) Solberg,G.S.; Larsen,T.; Smabrekke,A.; Brox,J.H.; Bertheussen,K.; Sorlie,D.; Osterud,B.; Jorgensen,L., *Scand.J.Clin.Lab.Invest.*, **1992**, *52(2)*, 73.
(171) Tolson,G.E.; Singh,B.B.; Billman,M.A.; McPherson,J.C.; McPherson,J.C., *J.Dental Res.*, **1995**, *74*, 173.
(172) Paustian,P.W.; McPherson,J.C.; Haase,R.R.; Runner,R.R.; Plowman,K.M.; Ward,D.F.; Nguyen,T.H.; McPherson,J.C., *Burns*, **1993**, *19(3)*, 187.
(173) Paustian,P.W.; Chuang,A.H.; Runner,R.R.; McPherson,J.C.; McPherson,J.C, *FASEB J.*, **1993**, *7(3) suppl.1*, A139.
(174) Bridgett,M.J.; Davies,M.C.; Denyer,S.P., *Biomaterials*, **1992**, *13(7)*, 411.
(175) Portoles,M.; Refojo,M.F.; Leong,F.L., *J.Biomed.Mat.Res.*, **1994**, *28(3)*, 303.
(176) Wang,P.L.; Udeani,G.O.; Johnston,T.P., *Int.J.Pharm.*, **1995**, *114(2)*, 177.
(177) Levy,M.L.; Anderson,K.; Armstrong,J.K.; McComb,J.G., "*A Pilot Study to Evaluate the Bacteriocidal Efficacy of Pluronic Surfactants In Pediatric Patients Undergoing Ventriculo-Peritoneal Shunt Replacement or Revision*", Childrens' Hospital Los Angeles, CA, **October 1995.**
(178) Amiji,M.; Park,K., *Biomaterials*, **1992**, *13(10)*, 682.
(179) Ng,C.L.; Lee,H.K.; Li,S.F.Y., *J.Chromatog.A*, **1994**, *659(2)*, 427.
(180) Swim,H.E.; Parker,R.F., *Proc.Soc.Exp.Biol.Med.*, **1960**, *103*, 252.
(181) Slepnev,V.I.; Kuznetsova,L.E.; Gubin,A.N.; Batrakova,E.V.; Alakhov,V.Y.; Kabanov,A.V., *Biochem.Int.*, **1992**, *26(4)*, 587.
(182) Astafieva,I.; Maskimova,I., Lukanidin,E., Alakhov,V.; Kabanov,A., *Febs Lett.*, **1996**, *389(3)*, 278.
(183) Al-Rubeai,M.; Emery,A.N.; Chalder,S., *Appl.Microbiol.Biotech.*, **1992**, *37*, 44.
(184) Bentley,P.K.; Gates,R.; Lowe,K., *Biotechnol.Lett.*, **1989**, *11*, 111.
(185) Mizrahi,A., *J.Clin.Microbiol.*, **1975**, *2*, 11.
(186) Hua,J.M.; Erickson,L.E.; Yiin,T.Y.; Glasgow,L.A., *Crit.Rev.Biotech.*, **1993**, *13(4)*, 305.
(187) Oh,S.K.W.; Nienow,A.W.; Alrubeai,M.; Emery,A.N., *J.Biotech.*, **1992**, *22(3)*, 245.
(188) Zhang,S.; Handacorrigan,A.; Spier,R.E., *J.Biotech.*, **1992**, *25(3)*, 289.
(189) Zhang,J., Kalogerakis,N.; Behie,L.A., *J.Biotech.*, **1994**, *33(3)*, 249.
(190) Elibol,M.; Mavituna,F., *Process Biochem.*, **1996**, *31(5)*, 507.
(191) Kumar,K.; Laouar,L., Davey,M.R.; Mulligan,B.J., Lowe,K.C., *J.Exp.Bot.*, **1992**, *43(249)*, 487.
(192) Khehra,M.; Lowe,K.C.; Davey,M.R.; Power,J.B., *Plant Cell Tiss.Org.Cult.*, **1995**, *41(1)*, 87.
(193) Brutovska,R.; Cellarova,E.; Davey,M.R.; Power,J.B.; Lowe,K.C., *Acta Biotech.*, **1994**, *14(4)*, 347.
(194) Khatun,A.; Davey,M.R.; Power,J.B.; Lowe,K.C., *Plant Cell Rep.*, **1993**, *13(1)*, 49.
(195) Khatun,A.; Laouar,L.; Davey,M.R.; Power,J.B.; Mulligan,B.J.; Lowe,K.C., *Plant Cell Tiss.Org.Cult.*, **1993**, *34(2)*, 133.

(196) Anthony,P.; Davey,M.R.; Power,J.B.; Washington,C.; Lowe,K.C., *Plant Cell Reprod.*, **1994**, *13(5)*, 251.
(197) Bassetti,L.; Hagendoorn,M.; Tramper,J., *J.Biotech.*, **1995**, *39(2)*, 149.
(198) Bassetti,L., Tramper,J., *Enzyme Microbial Tech.*, **1995**, *17(4)*, 353.
(199) Subbaraj,K.; Jayaraman,S.; Gunasekaran,M., *J.Ind.Microbiol.*, **1992**, *9(3-4)*, 225.
(200) Kumar,S.; Laouar,L.; Pritchard,D.I.; Lowe,K.C., *J.Parasitol.*, **1992**, *78(3)*, 550.
(201) Hurter,P.N.; Hatton,T.A. *Langmuir*, **1992**, *8*, 1291.
(202) Jafvert,C.T.; Vanhoof,P.L.; Chu,W., *Water Res.*, **1995**, *29(10)*, 2387.
(203) Hall,J.W.; Walker,I.; Majak,W., *Canad.Vet.J.-Rev.Vet.Canad.*, **1994**, *35(11)*, 702. and Wigman,L.S.; Abdelkader,H.; Menon,G.K., *J.Pharm.Biomed.Anal.*, **1994**, *12(5)*, 719.
(204) Schmolka,I.R.; Raymond,A.J., *J.Am.Oil Chem.Soc.*, **1965**, *42*, 1088.
(205) Schmolka,I.R.; Raymond,A.J., *Soap Chem.Specialities*, **1965**, *41(8)*, 60.
(206) Becker,P., *J.Phys.Chem.*, **1959**, *63*, 1675.
(207) Cowie,J.M.G.; Sirianni,A.F., *J.Am.Oil Chem.Soc.*, **1966**, *43*, 572.
(208) Camiré,C.; Meilleur,L.; Quirion,F., *J.Phys.Chem.*, **1992**, *96*, 2360.
(209) Mørtensen,K., *Europhys.Lett.*, **1992**, *19(7)*, 599.
(210) Mørtensen,K, *J.Phys.Cond.Matter*, **1996**, *8(25A)*, A103.
(211) Alexandridis,P.; Hatton,T.A., *Colloids and Surfaces A: Physicochem.Eng. Aspects*,**1995**, *96*, 1.
(212) Almgren,M.; Brown,W.; Hvidt,S., *Colloid Polymer Sci.*, **1995**, *273(1)*, 2.
(213) Wanka,G.; Hoffman,H.; Ulbricht,W., *Colloid Polym. Sci.*, **1990**, *268*, 101.
(214) Hergeth,W.D.; Alig,I.; Lange,J.; Lochmann,J.R.; Scherzer,T.; Waterwig,S., *Macromol.Chem., Macromol.Symp.*, **1991**, *52*, 289.
(215) Zhou,Z.; Chu,B., *Macromolecules*, **1994**, *27(8)*, 2025.
(216) Wu,G.W.; Zhou,Z.; Chu,B., *Macromolecules*, **1993**, *26(8)*, 2117.
(217) Yu,G-E., Deng,Y.; Dalton,S.; Wang,Q-G.; Attwood,D.; Price,C.; Booth,C., *J.Chem.Soc. Faraday Trans.*, **1992**, *88(17)*, 2537.
(218) Bahadur,P.; Pandya,K., *Langmuir*, **1992**, *8*, 2666.
(219) Bloss,P.; Hergeth,W-D.; Döring,E.; Witkowski,K.; Waterwig,S., *Acta Polymerica*, **1989**, *40(4)*, 260.
(220) Bloss,P.; Hergeth,W-D.; Wohlforth,C.; Waterwig,S., *Makromol.Chem.*, **1992**, *193*, 957.
(221) Buckton,G.; Machiste,E.O., *J.Pharm.Sci.*, **1997**, *86(2)*, 163.
(222) Linse,P.; Malmsten,M., *Macromolecules*, **1992**, *25*, 5434.
(223) Wang,Q.; Price,C.; Booth,C., *J.Chem.Soc.Faraday Trans.*, **1992**, *88(10)*, 1437.
(224) Šimek,L.; Bohdanecký,M., *Eur.Polym.J.*, **1996**, *32(1)*, 129.
(225) Williams,R.K.; Simard,M.A.; Jolicoeur,C., *J.Phys.Chem.*, **1985**, *89*, 178.
(226) Hecht,E.; Mortensen,K.; Hoffmann,H., *Macromolecules*, **1995**, *28(16)*, 5465.
(227) Almgren,M.; Bahadur,P.; Jansson,M.; Li,P; Brown,W; Bahadur,A., *J.Colloid Int.Sci.*, **1992**, *151(1)*, 157.
(228) Alig,I.; Ebert,R.U.; Hergeth,W-D.; Waterwig, S., *Polymer Comm.*, **1990**, *31*, 314.
(229) Tontisakis,A.; Hilfiker,R.; Chu,B., *J.Colloid Polym.Sci.*, **1990**, *135(2)*, 427.
(230) Rassing,J.; Attwood,D., *Int.J.Pharm.*, **1983**, *13*, 47.
(231) Brown,W.; Schillen,K.; Almgren,M.; Hvidt,S.; Bahadur,P., *J.Phys.Chem.*, **1991**, *95*, 1850.
(232) Yang,L.; Bedells,A.D.; Attwood,D.; Booth,C., *J.Chem.Soc.Faraday Trans.*, **1992**, *88(10)*, 1447.
(233) Zhou,Z.; Chu,B., *Macromolecules*, **1988**, *21*, 2548.
(234) Lianos,P.; Brown,W., *J.Phys.Chem.*, **1992**, *96*, 6439.
(235) Alexandridis,P.; Athanassiou,V.; Hatton,T.A., *Langmuir*, **1995**, *11(7)*, 2442.
(236) Alexandridis,P.; Nivaggioli,T.; Hatton,T.A., *Langmuir*, **1995**, *11(5)*, 1468.
(237) Nivaggioli,T.; Alexandridis,P.; Hatton,T.A.; Yekta,A.; Winnik,M.A., *Langmuir*, **1995**, *11(3)*, 730.
(238) Nivaggioli,T.; Tsao,B., Alexandridis,P.; Hatton,T.A., *Langmuir*, **1995**, *11(1)*, 119.
(239) Nakashima,K.; Anzai,T.; Fujimoto,Y., *Langmuir*, **1994**, *10(3)*, 658.
(240) Alexandridis,P.; Olsson,U.; Lindman,B., *J.Phys.Chem.*, **1996**, *100(1)*, 280.
(241) Nakashima,K.; Fujimoto,Y.; Anzai,T., *Photochem.Photobiol.*, **1995**, *61(6)*, 592.
(242) Gilbert,J.C.; Washington,C; Davies,M.C.; Hadgraft,J., *Int.J.Pharm.*, **1987**, *40*, 93.
(243) Turro,N.J; Kuo,P.L., *J.Phys.Chem.*, **1986**, *90*, 4205.
(244) Gaisford,S.; Beezer,A.E.; Mitchell,J.C.; Loh,W.; Finnie,J.K.; Williams,S.J., *J.Chem.Soc.Chem.Comm.*, **1995**, *18*, 1843.
(245) Gaisford,S.; Beezer,A.E.; Mitchell,J.C., *Langmuir*, **1997**, *13*, 2606.
(246) Cau,F., Lacelle,S., *Macromolecules*, **1995**, *29(1)*, 170.
(247) Almgren,M.; vanStam,J.; Lindblad,C.; Li,P.; Stilbs,P.; Bahadur,P., *J.Phys.Chem.*, **1991**, *95*, 5677.
(248) Rassing,J.; McKenna,W.P.; Bandyopadhyay,S.; Eyring,E-M., *J.Mol. Liq.*, **1984**, *27*, 165.

(249) Malmsten,M.; Lindman,B., *Macromolecules*, **1992**, *25*, 5446.
(250) Malmsten,M.; Lindman,B., *Macromolecules*, **1992**, *25*, 5440.
(251) Waterwig,S.; Alig,I.; Hergeth,W-D.; Lange,J.; Lochmann,R., Scherzer,T., *J.Mol.Struc.*, **1990**, *219*, 365.
(252) Mørtensen,K.; Talmon,Y., *Macromolecules*, **1995**, *28(26)*, 8829.
(253) Hecht,E.; Mørtensen,K.; Hoffmann,H., *Macromolecules*, **1995**, *28(16)*, 5465.
(254) Wu,G.W.; Chu,B.; Schneider,D.K., *J.Phys.Chem.*, **1995**, *99(14)*, 5094.
(255) Hecht,E.; Mørtensen,K.; Gradzielski,M.; Hoffmann,H., *J.Phys.Chem.*, **1995**, *99(13)*, 4866.
(256) Chu,B.; Wu,G.W., *Macromolecular Symp.*, **1995**, *90*, 251.
(257) Chu,B.; Wu,G.W., *Macromolecular Symp.*, **1994**, *87*, 55.
(258) Chu,B.; Wu,G.W.; Schneider,D.K., *J.Polymer Sci. PartB: Polymer Phys.*, **1994**, *32(16)*, 2605.
(259) Wu,G.W.; Ying,Q.C.; Chu,B., *Macromolecules*, **1994**, *27(20)*, 5758.
(260) Wu,G.W.; Zhou,Z.K.; Chu,B., *J.Polymer Sci. Part B: Polymer Phys.*, **1993**, *31(13)*, 2035.
(261) Mitchard,N.; Beezer,A.E.; Rees,N.; Mitchell,J.C.; Leharne,S.; Chowdhry,B.Z.; Buckton,G., *J.Chem.Soc.Chem.Comm.*, **1990**, *13*, 900.
(262) Beezer,A.E.; Mitchard,N.; Mitchell,J.C.; Armstrong,J.K.; Chowdhry,B.Z.; Leharne,S., Buckton,G., *J.Chem.Res.(S)*, **1992**, 236.
(263) Beezer,A.E.; Mitchell,J.C.; Rees,N.H.; Armstrong,J.K.; Chowdhry,B.Z.; Leharne,S.; Buckton,G., *J.Chem.Res.(S)*, **1991**, 254.
(264) Mitchard,N., Beezer,A.E.; Mitchell,J.C.; Armstrong,J.K.; Leharne,S.; Chowdhry,B.Z.; Buckton,G., *J.Phys.Chem.*, **1992**, *96*, 9507.
(265) Paterson,I.; Armstrong,J.; Chowdhry,B.; Leharne,S., *Langmuir*, **1997**, *13*, 2219.
(266) Armstrong,J.K.; Parsonage,J.; Chowdhry,B.Z.; Leharne,S.; Mitchell,J.; Beezer,A.; Löhner,K.; Laggner,P., *J.Phys.Chem.*, **1993**, *97*, 3904.
(267) Irwin,J.J., Beezer,A.E.; Mitchell,J.C.; Buckton,G.; Chowdhry,B.Z.; Eagland,D.; Crowther,N.J., *J.Phys.Chem.*, **1993**, *97*, 2034.
(268) Armstrong,J.K.; Leharne,S.A.; Mitchell,J.C.; Beezer,A.E.; Chowdhry,B.Z., *Macromolecular Reports*, **1994**, *A31(Suppl.6/7)*, 1299.
(269) Armstrong,J.K.; Chowdhry,B.Z.; Beezer,A.E.; Mitchell,J.C.; Leharne,S.A., *J.Chem.Res.(S)*, **1994**, *9*, 364.
(270) Armstrong,J.; Chowdhry,B.; O'Brien,R.; Beezer,A.; Mitchell,J.; Leharne,S., *J.Phys.Chem.*, **1995**, *99(13)*, 4590.
(271) Beezer,A.E.; Loh,W.; Mitchell,J.C.; Royall,P.G.; Smith,D.O.; Tute,M.S.; Armstrong,J.K.; Chowdhry,B.Z.; Leharne,S.A.; Eagland,D.; Crowther,N.J., *Langmuir*, **1994**, *10(11)* , 4001.
(272) Patterson,I.; Chowdhry,B.Z.; Leharne,S., *Colloids and Surfaces A - Physicochem.Eng. Aspects*, **1996**, *111(3)*, 213.
(273) Armstrong,J.; Chowdhry,B.; Mitchell,J.; Beezer,A.; Leharne,S., *J.Phys.Chem.*, **1996**, *100(5)*, 1738.

CHAPTER 2 THEORETICAL BASIS OF TECHNIQUES

2. Theoretical Basis of Techniques

2.1 Calorimetry

Any change within a system, whether that change constitutes a reaction between species, change of state, a physical change involving the formation of a new macromolecular conformation or alterations in solvent structure, involves the absorption or evolution of heat. Thus calorimetry (the study of heat) is a technique that can, theoretically, be applied to study the changes within any system. The main restrictions for the study of a system using the technique of calorimetry being the magnitude, in thermodynamic terms, of the change and efficient control of the environment temperature of the system under study.

One of the first examples in the development of experimental thermochemistry was the description, in 1780, by Lavoisier and Laplace[(1)] of the use of an ice calorimeter in which the heat liberated in a reaction was measured by the mass of ice melted. They measured the heat of combustion of carbon, finding that "*one ounce of carbon in burning melts six pounds and two ounces of ice*". This result corresponds to a heat of combustion of -413.6kJmol^{-1}, as compared to the most accurate present day value of -393.5kJmol^{-1}.[(2)]

Calorimetry has always been one of the most exacting techniques of physical chemistry, and a prodigious amount of experimental ingenuity has been devoted to the design of calorimeters.[(3)] Before the 1960's, any scientist interested in the measurement of heat had to build a calorimeter of their own, today a large variety of instruments are commercially available. Owing to new production techniques and particularly the introduction of modern electronics and computer control, these calorimeters permit accurate and reliable measurements within short periods of time. It is not surprising, therefore, that calorimetry is becoming a standard procedure in many branches of science. A classification of calorimeters is shown in figure 2.1, and it is quite obvious that commercially available calorimeters are very specific for the type of system under analysis, although many calorimeters are multifunctional, e.g., operating in adiabatic scanning or isothermal mode.

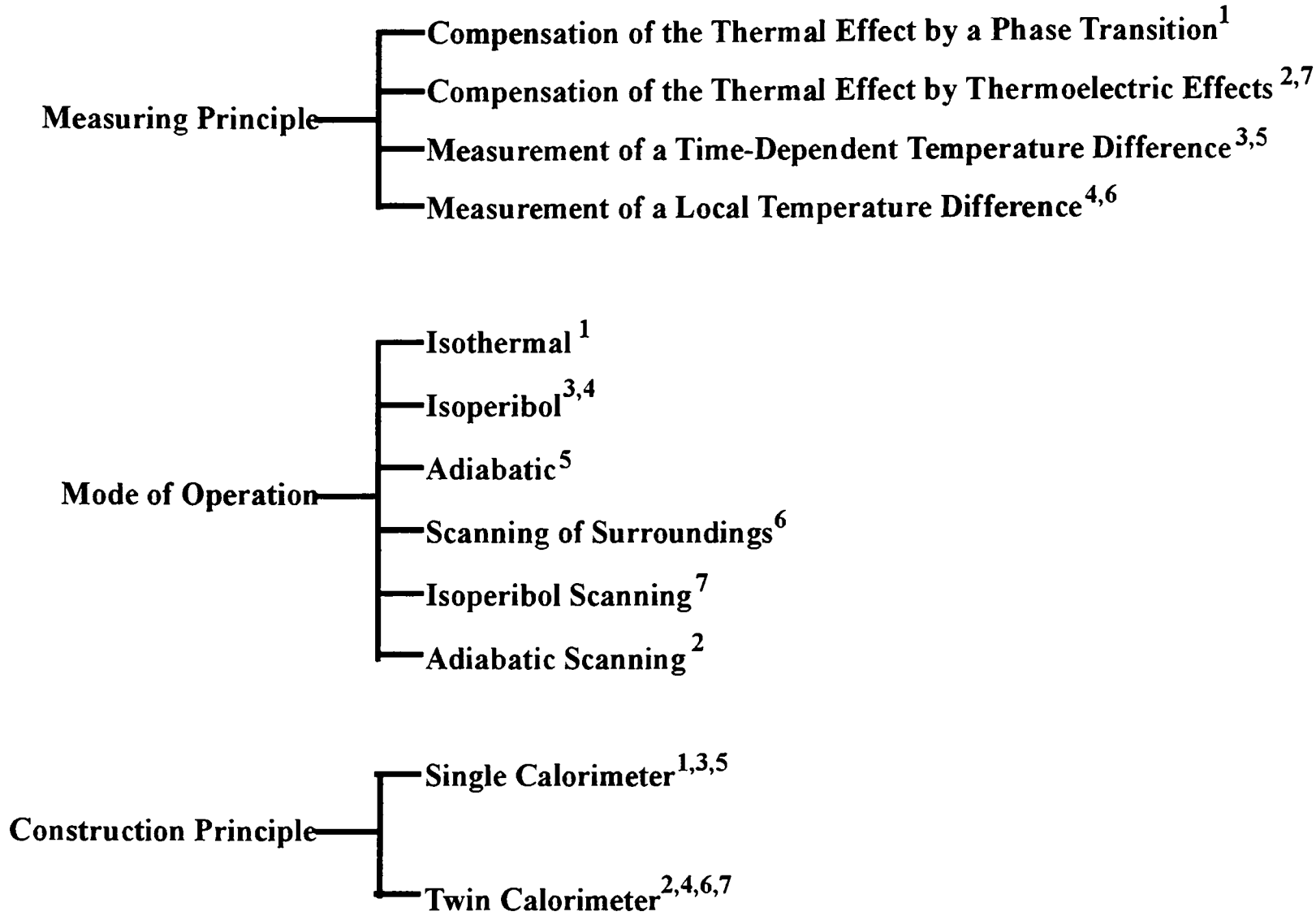

[1] Ice Calorimeter (Black 1760)

[2] High Sensitivity Differential Scanning Calorimeters e.g. MC-2, DASM-4

[3] Mixing Calorimeters Wilke (1781)

[4] Heats of Combustion Müller (1971)

[5] Drop Calorimeter Levinson (1962)

[6] Heat Flux Calorimeter Calvet (1948)

[7] DSC-7 Perkin Elmer

Figure 2.1 Classification of Calorimeters.

2.1.1 **High Sensitivity Differential Scanning Calorimetry (HSDSC).**

All temperature-induced changes in macroscopic systems always proceed with a corresponding change in enthalpy i.e., they are accompanied by heat absorption if the process is induced by a temperature increase, or by the evolution of heat if the process is caused by a temperature decrease.

The temperature dependence of the enthalpy can be determined experimentally by calorimetric measurements of the heat capacity of the sample over the temperature range of interest. Since the heat capacity determined at constant pressure is a temperature derivative of the enthalpy function:

$$C_p = \left(\frac{\partial H}{\partial T}\right)_p \qquad (1)$$

An estimate of the enthalpy function is achieved by integration of the heat capacity:

$$H(T) = \int_{T_0}^{T} C_p(T)dT + H(T_0) \qquad (2)$$

The important feature in calorimetric studies is that the physical behaviour of macromolecules in solution e.g., polymers, proteins is particularly important at low concentrations i.e., at a concentration at which the interaction between macromolecules is sufficiently small to be neglected. For average proteins, the concentration at which proteins can be regarded as individual macroscopic systems surrounded by solvent is of the order of 10^{-4} M i.e., the order of 0.1% w/w. In such dilute solutions, however, the macromolecular contribution to the thermal properties of the entire sample should also be small: the macromolecule heat capacity does not exceed 0.03%, while the excess heat capacity for proteins at the peak of unfolding is less than 1% of the solution heat capacity.[4] The creation of a qualitatively new technique, heat capacity microcalorimetry, has been driven, in part, by such parameters as the availability and high cost of isolation and purification of biological molecules. Thus the amount of material available to be used in experiments does not exceed a few milligrams, even dilute solutions of biological materials are quite viscous so that they cannot be stirred to achieve rapid thermal equilibrium during heating, as is usually done in studies of liquids. Calorimetric studies of very small heat effects which occur in a few millilitres of a viscous solution heated over a broad temperature range cannot be performed in any of the available heat capacity calorimeters used for the physicochemical studies of nonbiological materials.

All heat capacity microcalorimeters have a number of features in common. First, they do not possess a mechanical stirrer as the stirring of a liquid with a high and variable viscosity produces uncontrollable Joule heat in an amount much greater than the measured heat effect. The elimination of the mechanical stirrer was made possible by decreasing the operational volume of the calorimetric cells. Therefore, a small volume of the calorimetric cell is a key requirement in the construction of heat capacity microcalorimeters. All microcalorimeters measure heat capacity continuously with continuous heating or cooling of the sample at a

constant rate i.e., they scan along the temperature scale by continuously measuring small changes in the heat capacity of the samples. As a result, these instruments are usually called scanning microcalorimeters.

Continuous heating facilitates complete automation of all the measurement processes, the disadvantage being that the studied sample is never in complete thermal equilibrium within the experimental environment. This sets certain requirements for the samples and for instrument construction: the temperature-induced changes in the samples should not be too sharp and the relaxation processes at these changes should be sufficiently fast, while the construction of the calorimetric cell should provide minimal thermal gradients which do not change with temperature or heating rate.

Almost all scanning calorimeters measure the difference in heat capacity i.e., they are all differential instruments with two identical calorimetric cells. One of the cells is loaded with the solution to be studied and the other one with solvent, thus the measured difference heat capacity will correspond directly to the heat capacity contribution of the molecules dissolved in solution. The cells are heated by electric heaters in good thermal contact with them, the power to the heaters is adjusted by means of a control circuit, activated by the output of a 200-junction thermopile between the cells (in the case of the DASM-4 instrument (Biopribor, Puschino, Russia[4]) which maintains them at closely equal temperatures. Thermopiles between the cells and adiabatic shields activate control circuits, which hold the shield temperatures close to that of the cells; the signals may be registered on an X-Y recorder or the instrument may be interfaced with a computer for subsequent analysis.

One of the most difficult problems encountered is the loading of the cells with equal and definite amounts of the studied and standard materials. When measuring heat capacity with an error of less than 10^{-5} JK^{-1} the error in loading the cells with the sample should not exceed 10^{-6} g. A calorimeter with extractable cells never gives reproducible results; each replacement of the cells results in a different slope and position of the baseline of the instrument. The problem of loading a scanning microcalorimeter with equal and reproducible volumes was resolved by replacing heat capacity measurements of a sample of definite volume.[4,5] The volume of the studied sample can be fixed by the fixed operational volume of the calorimetric cells. A thin capillary tube is connected to the cell, so that the cell can be filled without removing it from the adiabatization system of thermal shells. This permits the

liquid expended on heating to flow from the cell. The application of excess pressure to the external ends of the capillary tubes by a manostat prevents bubble formation in the cells, and all the measurements are performed under this constant pressure.

2.1.2.1 **Analysis of HSDSC Data.**

For the systems under investigation, the overall chemical processes can be considered as complete dissociation or complete aggregation involving an aggregate in one state and a unimer in the other:-

$$nA \overset{K_1}{\Leftrightarrow} B_n$$

$$\text{where} \quad K_1 = \frac{[B_n]}{[A]^n} \qquad (3)$$

The extent of the reaction, α, may be defined as the fraction of the monomer present in aggregates. Considering that $[B_n] = \alpha C / n$ and $[A] = (1-\alpha)C$ where C is the total concentration of material initially added. The equilibrium expression thus becomes:

$$K_1 = \frac{\alpha C}{n(1-\alpha)^n C^n} \qquad (4)$$

an expression for lnK is:

$$\ln K = \ln(\alpha) + \ln(C) - \ln(n) - n(\ln(1-\alpha) - n\ln(C)) \qquad (5)$$

differentiating with respect to α at constant n and C the following expression is obtained:

$$\left(\frac{\partial \ln K}{\partial \alpha}\right)_{n,C} = \frac{1}{\alpha} - \frac{n}{(1-\alpha)} \qquad (6)$$

An HSDSC instrument measures the power required to maintain the sample and reference cell temperatures equal whilst the temperature of the system (T) is raised as a linear function of time, t, i.e., the scan rate dT/dt is constant. The output of the instrument $(dq/dt)_p$ versus t is readily converted to a plot of apparent excess heat capacity ($C_{p,xs}$) versus temperature by multiplying the X-axis by the scan rate and the Y-axis by it's reciprocal.[7] This process is referred to as scan rate normalisation. $C_{p,xs}$ at any point in the scan is related to the measured instrumental enthalpy (ΔH_{cal}) by the equation:

$$C_{p,xs} = \Delta H_{cal} d\alpha / dT \qquad (7)$$

Combining equations 6 and 7 allows the van't Hoff isochore to be written in the form:

$$\frac{\partial \ln K}{\partial \alpha}\frac{d\alpha}{dt} = \frac{\partial \ln K}{\partial T} = \left(\frac{1}{\alpha} + \frac{n}{1-\alpha}\right)\frac{C_{p,xs}}{\Delta H_{cal}} = \frac{\Delta H_{vH}}{RT^2} \qquad (8)$$

For data analysis, evaluation of the van't Hoff enthalpy, ΔH_{vH} is important. This may be obtained by setting α to 0.5 (the point at which the reaction is half completed in equation 8). The equation rearrangement thus becomes:

$$\Delta H_{vH} = 2(n+1)C_{p,1/2}RT_{1/2}^2 / \Delta H_{cal} \qquad (9)$$

$C_{p,1/2}$ and $T_{1/2}$ are the values of $C_{p,xs}$ and T when $\alpha = 0.5$.

If, in place of $T_{1/2}$, the temperature (T_m) at which $C_{p,xs}$ has a maximal value in equation 9 and $C_{\mathbf{max}}^{\mathbf{p}}$ in place of $C_{p,1/2}$, for an essentially two state process n = 1 (A $\Leftrightarrow$ B) the expression becomes:

$$\Delta H_{vH} = 4C_p^{max}RT_m^2 / \Delta H_{cal} \qquad (10)$$

For a two state process carried out under essentially equilibrium conditions $\Delta H_{vH}/\Delta H_{cal}$ = 1. If $\Delta H_{vH} < \Delta H_{cal}$ it can be concluded that one or more intermediate states are of significance in the overall process, whereas if $\Delta H_{vH} > \Delta H_{cal}$ intermolecular cooperation is clearly indicated. HSDSC is the only experimental technique that gives such positive indications concerning these characteristics of a process that are only subject to kinetic limitations.

2.1.2.2 **Two State Processes.**

The value of $T_{1/2}$ or T_m in equation 9 should be independent of concentration for essentially two-state processes. On the other hand, an increase in T_m with an increase in concentration is a clear indication of a decrease in the degree of oligomerisation during the reaction[6], and conversely a decrease in T_m with an increase in concentration shows that the degree of oligomerisation increases. If the reacting species is known to be oligomeric at ordinary temperature and T_m is found to be independent of concentration, it may be concluded either that the reacting species has become monomeric by the time the reaction temperature is reached or that no dissociation or association accompanies the reaction. When an oligomer is incompletely dissociated in either the initial or final states, the equilibrium is as follows:

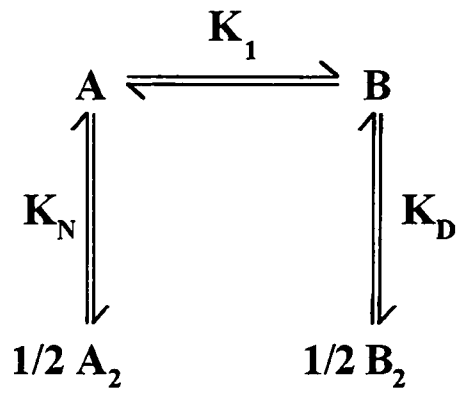

(11)

If K_N and K_D do not vary significantly with temperature over the range of the reaction controlled by K_1 then the equilibrium constant K_1 is given by:

$$K_1 = \frac{1-(1+8\alpha K_D^2(A)_0)^{1/2}}{1-(1+8(1-\alpha)K_N^2(A)_0)^{1/2}} \bullet \frac{K_N^2}{K_D^2} \qquad (12)$$

Where $(A)_0$ is the total concentration expressed in monomer units. For the process observed by HSDSC, the value of T_m should vary with concentration, when $\alpha = 0.5$ for the process:

$$A_n \Leftrightarrow nB \qquad (13)$$

then,

$$\ln K_{1/2} = c + (n-1)\ln(A)_0 = \frac{-\Delta H_{vH}}{RT_{1/2}} + c \qquad (14)$$

where c = constant.

A van't Hoff plot of $\ln(A)_0$ versus $(1/T_{1/2})$ will have a slope:

$$\text{slope} = \frac{-\Delta H_{vH}}{(n-1)R} \qquad (15)$$

ΔH_{vH} calculated in this way for a two-state process should agree with the calculated value given in equation 9.

Simulations in which $1/T_{1/2}$ is calculated as a function of $\ln(A)_0$ where K_N and K_D are in the range 0.01 to $10\mu M^{1/2}$, $(A)_0$ is in the range 50-100μM, and ΔH_{vH} is independent of temperature, a plot of $\ln(A)_0$ versus $1/T_{1/2}$ is linear. Therefore this can indicate the multiplication factor necessary to arrive at ΔH_{vH} from the slope of this plot.

Calculation of the ratio of ΔH_{vH} (obtained via the appropriate method described above) to the ΔH_{cal} obtained from the instrument is therefore possible. As mentioned, for a strictly two-state process the ratio is approximately one, however, when one or more intermediate steps are significant the ratio is less than one, whereas for intermolecular cooperation the ratio

is greater than one. HSDSC is the only experimental technique allows direct calculation of both enthalpy values at the same time, so that the nature of the process can be identified.

The symmetry of the reaction process is affected by the nature of the states involved. For the process in equation (13), where n = 1 the HSDSC curve is very nearly symmetric about $T_{1/2}$, but if n = 4 it is very asymmetric with a sharper decrease in $C_{p,xs}$ beyond $T_{1/2}$; for association instead of dissociation the asymmetry is the other way around.

2.1.2.3 **Non Two-State Processes.**

(a) $\Delta H_{vH} < \Delta H_{cal}$.

This situation is most prevalent for large molecular weight polymers e.g., proteins with several domains where a significant contribution to the thermodynamics of denaturation is made by intermediate states between the native and denatured states. Analysis of such transitions is routinely achieved by deconvolution of the HSDSC data such that the individual two-state transitions, corresponding to the two-state unfolding of each domain, can be characterised as above. However, it is extremely difficult to assign changes in $\Delta C_{p,d}$ (the difference between the pre- and post-transitional baselines) to each domain in this way, which means that the post-transitional baselines of each domain cannot be accurately calculated and therefore nor can their ΔH_{cal}.

Sturtevant[7] has attempted to do this by an arbitrary procedure of partitioning the overall change in specific heat between the steps in the process at each temperature in proportion to their individual enthalpies at that temperature. Application of the appropriate algebra to each component transition allows calculation of the total excess heat capacity which can be compared to the overall process to determine the validity of the assumed model (i.e., that the total process involves, as an approximation, the sum of the two-state processes).

Examples of the fitting of several two-state processes to an observed HSDSC scan are the HSDSC curve obtained for the melting of transfer RNAase which has been accurately represented as the sum of several two-state curves, which were attributed to the melting of substructures of the overall molecule.[8,9] A recursive method was developed to evaluate the thermodynamic parameters of each step in a multistate transition, and such quantities as the

fractional occupancy of each state were calculated as functions of temperature. The analysis was applied in general form to cooperative phenomena,[10] including the helix-coil transition of nucleic acids[11] and phase transitions of phospholipid bilayers.[12]

(b) $\Delta H_{vH} > \Delta H_{cal}$.

This result is obtained when intermolecular cooperation occurs during the phase transition. Phase transitions of hydrated phospholipids offer the most common example of this situation, since the melting of a perfectly pure crystalline substance is an isothermal process, ΔH_{vH} approaches infinity. For example dipalmitoylphosphatidylcholine (DPPC) in water has a ratio of $\Delta H_{vH}/\Delta H_{cal}$ of 1400 when scanned at $0.023 K min^{-1}$ [13] The ratio which is usually limited by the instrumental lag can be taken as the lower limit for the size, in monomer molecules, of the average "cooperative unit" for the process: This interpretation can apply to lipid phase transitions or to nucleotide polymerisation in helix-coil transitions equally well.[7]

(c) Irreversible Processes.

In the case of irreversible processes, the above analysis cannot be used to fit the data and to describe the process under examination: This situation is often encountered for many of the high molecular weight complex multimeric proteins which are irreversibly denatured as judged by HSDSC. However, in some such cases there is possible justification of application of the above analysis to the irreversible process. Furthermore, reasonable van't Hoff plots based on equation 12 to irreversible protein denaturations nave been observed[7] indicating that the T_m of the regulatory subunits of aspartyl transcarbamylase increases with ATP concentration.[14] Similar results for the *lac* repressor of *E.coli* have been observed[15] for $T_{1/2}$, ΔH_{cal} and ΔH_{vH} to those calculated using n = 4 in equation 9.

2.1.3 **Microcal MC-2 HSDSC.**

The Microcal MC-2 HSDSC consists of twin symmetric cells 1.2mL in total volume and are constructed of a niobium-tantalum alloy. Tantalum is one of the most corrosion resistant materials available. While its resistance to acid attack is comparable to that of glass and platinum, it is far less susceptible to breakage than glass and is much less expensive than platinum. Niobium is more resistant to corrosion than most common metals, but is considerably poorer than tantalum. Niobium has the advantages of lower density and a low thermal neutron cross-section.

Each cell has two sets of heaters on its outer surface i.e., the main and auxilliary heaters (figure 2.2). The main heaters on each cell are in series and are powered by a 15V power supply, with a resistance cascade to control the scan rate. The main heaters are pretrimmed so that the sample cell receives slightly less power than the reference cell thus its temperature rises slightly less rapidly when current passes through the main heaters. There is a 100-junction thermopile between the sample and reference cells, which senses the off-balance temperature ΔT and produces a corresponding voltage. This small voltage (0-5μV) is amplified and used to drive (0.5mA) the auxilliary heater on the sample cell, which then acts to keep the off-balance signal close to zero. The signal driving the auxilliary heater is also passed through a squaring amplifier which then gives a signal proportional to the differential power, which is then displayed on the Y-axis of a recorder after processing for zero-suppression and full-scale sensitivity. The X-axis of the recorder receives a signal from a temperature transducer activated by a thermistor located in the adiabatic shield.

The high sensitivity of the instrument is achieved by having the cells located in an adiabatic chamber. This consists of an aluminium jacket which surrounds the cells and which always has the same temperature as the cells. This jacket is also powered by a main heater and an auxilliary heater. The latter is driven by a feedback circuit very similar to the one described above for the sample cell i.e., there is a 20-junction thermopile between the cells and the jacket whose signal (0-100μV) is amplified and fed back into the jacket auxilliary heater. This provides the feedback control necessary to assure that the temperature of the jacket increases at the same rate as the temperature of the cells.

2.1.3.1 **Cell Feedback.**

For all scan rates used (10,20,30,45,60 and 90Kh^{-1}) the inherent response time of the HSDSC depends upon the cell feedback (CFB):

$$CFB = \frac{450}{T_R} \qquad (16)$$

where T_R = response time. After an initial equilibration period of approximately 60 minutes the CFB reading is adjusted using the manual baseline shift control prior to data accumulation to read between 30 and 50. The CFB reading is adjusted to 30-35 for all scans giving an optimum response time of approximately 13 seconds. A higher CFB value i.e., a short response time, is required for phase transitions with a large $dC_{p.xs}/dT$, (e.g. for phase

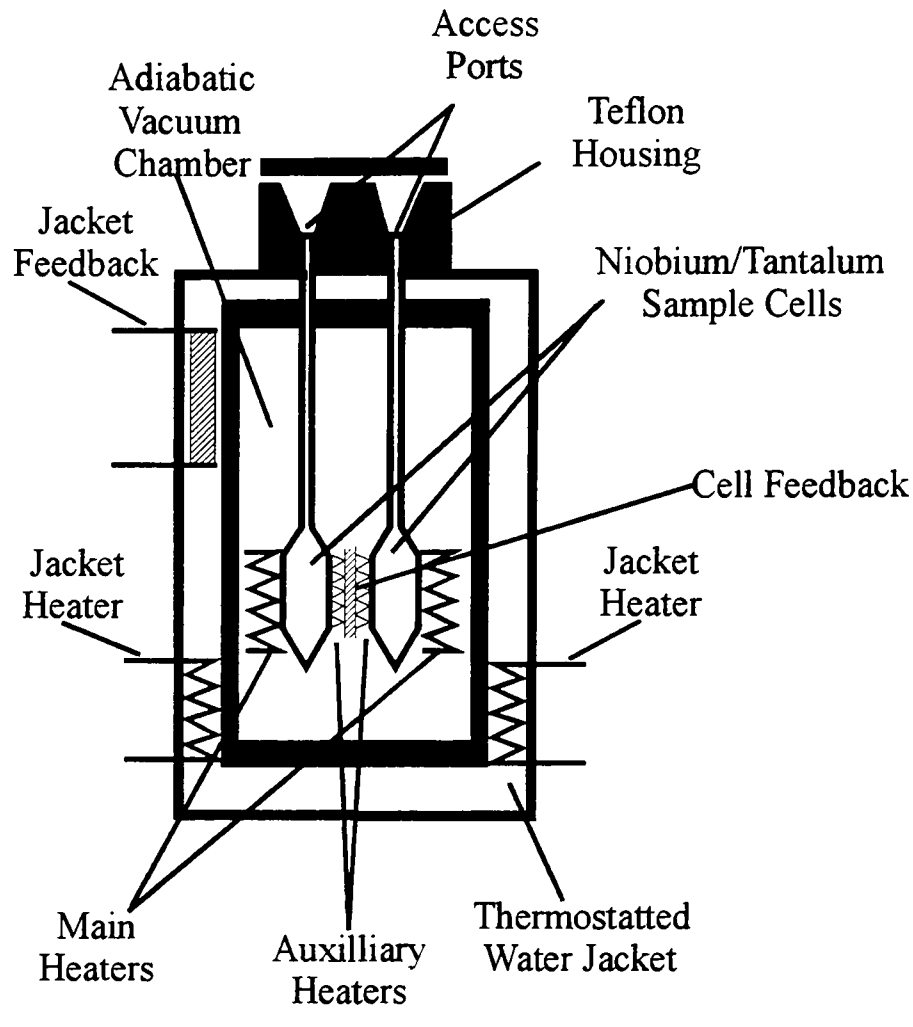

Figure 2.2 Schematic representation of the Microcal MC-2 Calorimetric Unit.

transitions of phospholipid bilayers), and a lower CFB value is required for phase transitions with a low $dC_{p,xs}/dT$ (e.g. for the denaturation phase transition of proteins). The selected CFB value is a balance between sensitivity and over-compensation of the calorimeter for any thermally driven event that occurs in the sample cell. The time-filter used for each scan (i.e., the sampling time interval for which the response from the calorimeter is averaged for each data point) was 15 seconds and is consistent with achieving the shortest possible response time i.e., the baseline shift would first have to be adjusted to a give a higher CFB value in order to benefit from lowering the time-filter value.

2.1.3.2 **Data Accumulation and Analysis.**

The Microcal MC-2 HSDSC is interfaced with a PC using the DA-2 dedicated software package for calorimeter control and data accumulation and analysis. Upscans are controlled by the main and auxilliary heaters within the calorimeter and the scan rate controlled by the manual setting on the calorimeter (10-90Kh^{-1}). Downscans are controlled externally using the DA-2 dedicated software interfaced with a Haake F3-C waterbath, and is only effective for scan rates of $< 30Kh^{-1}$ due to the waterjacket surrounding the adiabatic

chamber not being in direct contact with the sample and reference cells, and therefore cooling is achieved by convection between the cooling jacket and cells for temperature and scan rate control (figure 2.2).

The data stored from a scan (up to 4000 data points per file) is stored as temperature (°C), $C_{p,xs}$ ($mcalmin^{-1}$) and Time (sec) and is displayed as $C_{p,xs}$ ($mcalmin^{-1}$) versus T(°C) during a scan. For data analysis, the $C_{p,xs}$ data is first converted from units of $mcalmin^{-1}$ to $mcalK^{-1}$ by division of the 'raw' $C_{p,xs}$ by the scan rate i.e., scan rate normalisation. The data is then converted to molar units by dividing the normalised data by a constant equivalent to the number of moles of solute in the sample cell:

$$C = \frac{cV}{m} \qquad (17)$$

Where C = constant, c = concentration of solute (gL^{-1}), V= cell volume (1.1902mL), and m = molecular weight ($gmol^{-1}$). The factor of $1x10^3$ for conversion of the cell volume to units of L is omitted in order for conversion of the $C_{p,xs}$ units from $mcalK^{-1}$ to $calmol^{-1}K^{-1}$. The data can be further converted to $kJmol^{-1}K^{-1}$ by division of the data by the constant 239.006 ($=(4.184x10^{-3})^{-1}$).

The thermodynamic parameters that can be obtained directly from a HSDSC scan are shown in figure 2.3.

Firstly a baseline is constructed, as invariably the pre- and post-transitional baselines have different $C_{p,xs}$ values due to the change in heat capacity of the solute. The baseline is determined using a splines function which involves the selection of two reference temperatures T_1 and T_2 corresponding to the start and end of the observed phase transition. The data points below and above T_1 and T_2 respectively are then extrapolated to form a theoretical baseline between points T_1 and T_2 and a curve fitted using a splines function which represents an average between the two extrapolated baselines. The baseline is then subtracted from the calorimetric scan and this allows integration of the area below the phase transition and determination of the ΔH_{cal}, ΔS and C_p^{max}.

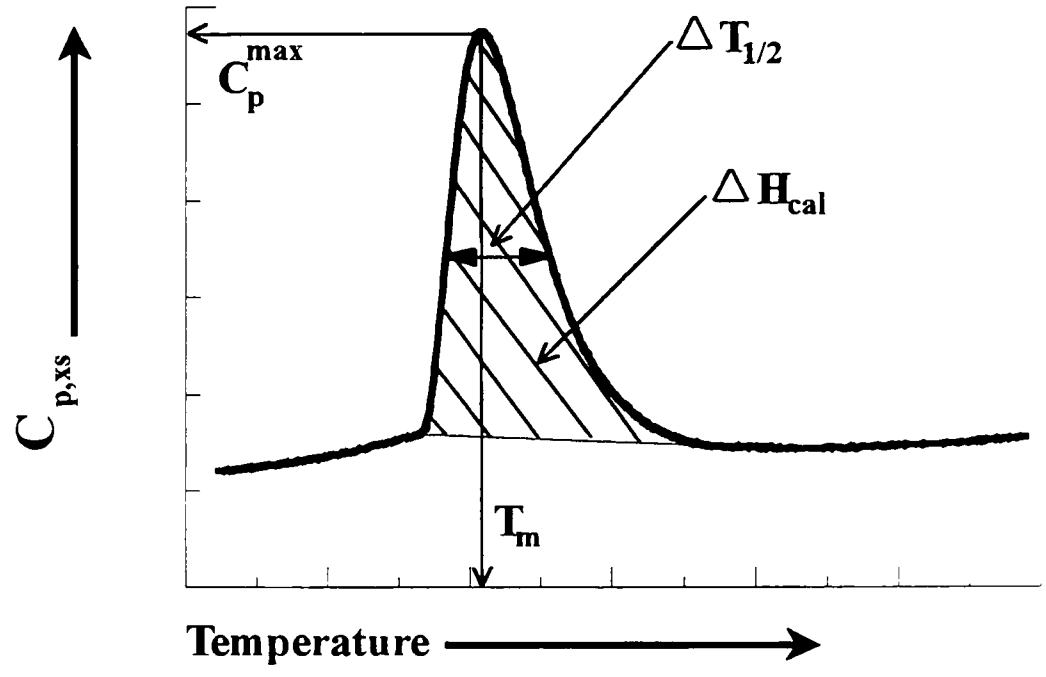

Figure 2.3 Idealised HSDSC Output.

2.1.4 **Applications and Uses of HSDSC.**

HSDSC is a technique that has been widely employed to study the thermodynamics of reversible and irreversible denaturation of proteins in dilute aqueous solution and the effects of cosolutes on these processes.[16-19] The HSDSC curves are generally complex for protein unfolding and the temperature dependence of denaturation enthalpy is partly determined by the number of non-polar groups exposed to the bulk phase during the transition from the native to the denatured state. Studies of globular proteins support the idea of applying equilibrium thermodynamics to approximate apparently irreversible processes. The study of denaturation of proteins containing site- and group-specific amino acids replacements has attracted much attention in relation to protein engineering because they enable such macromolecules to be (a) made reversibly denaturable, (b) made (for industrial enzymes) more thermo- and pH-stable in the presence and absence of relevant ligand and co-enzyme molecules and (c) better understood physicochemically, potentially with a view to designing tailor-made enzymes.

Studies of proteins by HSDSC include the elucidation of the kinetics of thermal denaturation e.g., pepsin and pepsinogen,[20] thermolysin,[21] the interactions between proteins/solutes and membranes e.g., the interaction between human defensin and liposomes,[22] and lipid polymorphism in the presence of squalene.[23] The dependence of the nature and size of micelle clusters and the concentration and nature of added alkyl ureas for solutions of hexadecyltrimethylammonium chloride and bromide was shown by HSDSC

studies[24]. Evidence of a sphere to rod transition was shown by HSDSC for solutions of hexa- and tetra-decyltrimethylammonium bromide in the 10^{-2} moldm^{-3} region.[25] Two processes were observed, one assigned to changes in counterion binding and the other to the change in the extent of exposure of the hydrocarbon core of the micelle solvent and/or extent of penetration of water into the micelles.

2.2 Densitometric Analysis

2.2.1 General Considerations.

Any system under investigation undergoes changes in density as a function of increasing temperature due to increased molecular motion. Macromolecules dissolved in aqueous systems may undergo rapid changes in conformation with increasing temperature due to changes in polymer-solvent and polymer-polymer interactions (hydrogen bonding, dipole-dipole interactions and van der Waals dispersion forces) and/or exposure of hydrophobic moieties to the bulk solvent, and associated with these changes there must be alterations in the overall density of the system.

An important parameter characterising such systems is the partial specific volume of the solute. This parameter assists in the interpretation of other physical information regarding the state of the system resulting from complex conformational changes and molecular associations. It is also an important function relating sedimentation rates and small-angle X-ray scattering intensity data with the molecular weight of the macromolecule. In order to reduce the error in such molecular weight determinations to the order of $\pm$ 1%, the partial specific volume must be measured with an uncertainty of less than $\pm$ 0.15%, which in turn requires accurate and differential density measurements with a precision of $\pm 4 \times 10^{-6}$ gcm^{-3}. For the design of a differential scanning instrument the primary requirement is the ability to measure fluid density differentials with a maximum error of $\pm 2 \times 10^{-6}$ gcm^{-3}. The most significant point to be considered in developing any method and procedure is the criticality of temperature control. This can be calculated from a consideration of the fluid thermal expansion coefficient, γ :

$$\frac{d\rho}{dT} = -\gamma \qquad (18)$$

where ρ = density. For aqueous solutions $\gamma \approx 10^{-3}\ cm^3K^{-1}$; an absolute density error of 10^{-6} gcm^{-3} requires temperature control to within $10^{-2}K$. Such precise temperature control immediately indicates that the sample volume should be small and that the experimental measurement should be completed within a short time period, of the order, 1-2 minutes.

2.2.2 **Principle of the Mechanical Oscillator Technique.**

In any general coordinate system, if a point mass **m** is attracted toward an origin by a force proportional to it's distance **x** from the origin, then in the absence of any external restraint, the Hooke's law force is exactly compensated by Newton's second law force, and the motion is thus described:

$$mx' + Cx = 0 \qquad (19)$$

where **C** is the elastic modulus. At any time **t** the location of the point mass is given by the real part of equation (20):

$$x = a\exp(i\omega_0 t) \qquad (20)$$

The motion is said to be harmonic, with a complex amplitude **a** and an angular velocity $\omega_0 = (C/m)^{1/2}$. In a real system, the motion will decay to zero due to the restraining action of a frictional force **f** proportional to and acting in opposition to the natural inertia of the system. The motion is now described by the equation:

$$mx' + Cx = -fx' \qquad (21)$$

and the position of the moving mass is given by the real part of equation (22):

$$x = a\exp(i\omega_1 - \lambda)t \qquad (22)$$

Equation 22 describes damped harmonic motion, which is simple harmonic motion with an exponentially decreasing amplitude. The angular velocity $\omega_1 = (\omega_0^2 - \lambda^2)^{1/2}$, is reduced by the damping coefficient $\lambda = f/2m$. If an external force is to be applied to counterbalance the damping effects of friction, then it must have the form $b\exp(i\omega_0 t)$ where **b** is a complex amplitude. Figure 2.4a is a simple vector diagram of the balanced forced harmonic motion system. If, for any reason, there is a phase shift in the external force, the system is out of balance (figure 2.4b) and a component of the external force acts in the direction of the dynamic force, thereby altering the effective mass of the oscillating system. It is important, therefore, in a real system to monitor continually the forced motion and thereby control the phase and magnitude of the external force. Furthermore, it is important that this rigorous control be maintained for an oscillator of varying frequency. It is the measurement of the

change in the resonant frequency of a hollow, vibrating tube, when filled with fluids of varying density, which is the principle of the mechanical oscillator technique. The relationships discussed apply to any real situation provided certain limits are not exceeded. Thus, a hollow U-shaped tube excited into a bending-type vibration orthogonal to its plane about a nodal axis

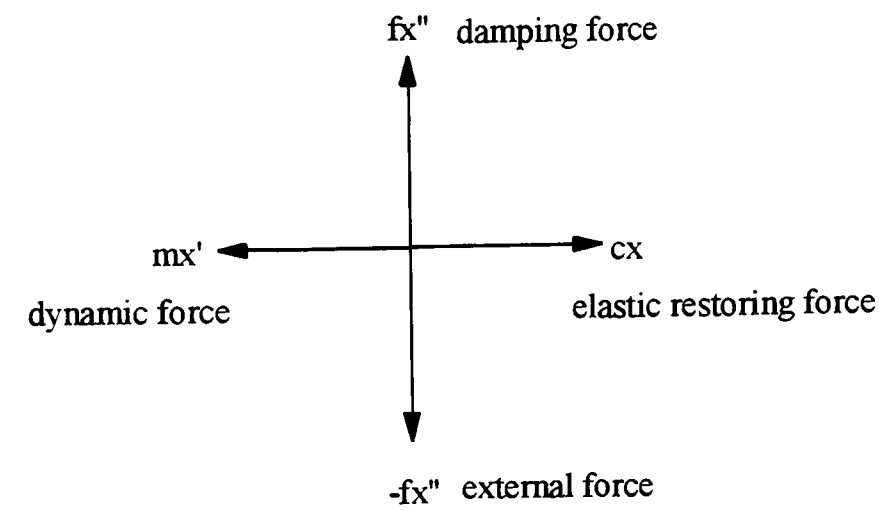

Figure 2.4 Vector diagram of force harmonic oscillation (a) a balanced system, and (b) an unbalanced system.

will exhibit forced harmonic motion, provided that the material remains in the elastic region of deformation. The amplitude must be limited such that the elastic modulus **C** remains constant, and Hooke's law applies. In equation 19, **m** now represents the total mass of the system (comprising the tube body), **M**, of volume **V** and its contents of density ρ:

$$m = M + V \tag{23}$$

The resonance period **t** is:

$$t = \frac{1}{\nu} = \frac{2\pi}{\omega_0} = 2\pi\left(\frac{M + V\rho}{C}\right)^{1/2} \tag{24}$$

From equation (24):

$$t^2 = A\rho + B \tag{25}$$

where $A = 4\pi^2\ V/C$ and $B = t_{M^2} = 4\pi^2\ M/C$. t_M is the resonance period of the tube alone, which may be calculated from calibration data or measured directly. The density differential between two fluids is therefore:

$$\Delta\rho = \rho_1 - \rho_2 = \frac{1}{A}\left(t_1^2 - t_2^2\right) = K\left(\Delta t^2\right) \qquad (26)$$

The procedure for measuring density differentials is therefore reduced to developing a method for measuring a time period accurately and precisely.

2.2.3 **Experimental Procedure.**

The experimental partial specific volume, $\bar{v}$, at a given concentration, c, is the apparent partial specific volume, $\bar{v}(c)$, which can be determined from density measurements according to the following relationship:

$$\bar{v}(c) = \frac{1}{\rho_0}\left[1 - \left(\frac{\rho_s - \rho_0}{c_s}\right)\right] \qquad (27)$$

and the cubic expansion coefficient:

$$\alpha = \frac{1}{\bar{v}(c)} \bullet \frac{d\bar{v}(c)}{dt} \qquad (28)$$

where the subscripts "0" and "s" refer to the solvent and sample respectively, and values of ρ and **c** are expressed in gcm^{-3}. A modified version of the hollow-oscillator Precision Density Meter DMA 60 (Anton Paar, Graz, Austria) introduced by Laggner and Stabinger,[26] consists of two hollow oscillator cells instead of one, as normally used, which are thermally parallel coupled in a thermostat circuit (F3 and K Haake, Berlin, Germany). One cell contains the solvent and the other sample, each with a volume of approximately $1cm^3$. By using the solvent cell as the reference in the determination of the oscillation period of the sample cell, the intrinsic, high temperature coefficients are minimised such that the sample density can be determined in a temperature scanning experiment. Calibration is performed by measuring the pairs water-water and water-air respectively, in the reference and sample cells, over the temperature range of interest for which precise density values are available in the literature.[27] Temperature is measured by a calibrated Pt-100 sensor connected to an electronic millikelvin-thermometer (Systemteknik, Bromma, Sweden). The precision achieved in the determination of density differences is better than $\pm 2x10^{-6}\ gcm^{-3}$. Heating and cooling rates between 0.01 and 0.5 $Kmin^{-1}$ can be selected. The reference cell is filled with the solvent used to dissolve the solute in the sample cell. Density scans are performed under microprocessor control

(TEDI-33) using a dedicated software package (Program DENSITY) written in Turbo Pascal 3.0, which allows repeated scans with variable equilibration periods at the end of each run.

The raw data is converted to partial specific volume (cm^3g^{-1}) of solute using the dedicated software package program DENSCALC by inputting the solute concentration, and isothermal calibration values for water and air performed prior to starting a run. The program corrects for the baseline by deducting a stored calibration curve over the temperature range of interest after inputting the initial isothermal calibration values. The partial specific volume change ($\Delta\bar{v}$), transition temperature (T_m) and half width of the transition ($\Delta T_{1/2}$) are calculated manually by extrapolation of the pre- and post-transition (figure 2.5).

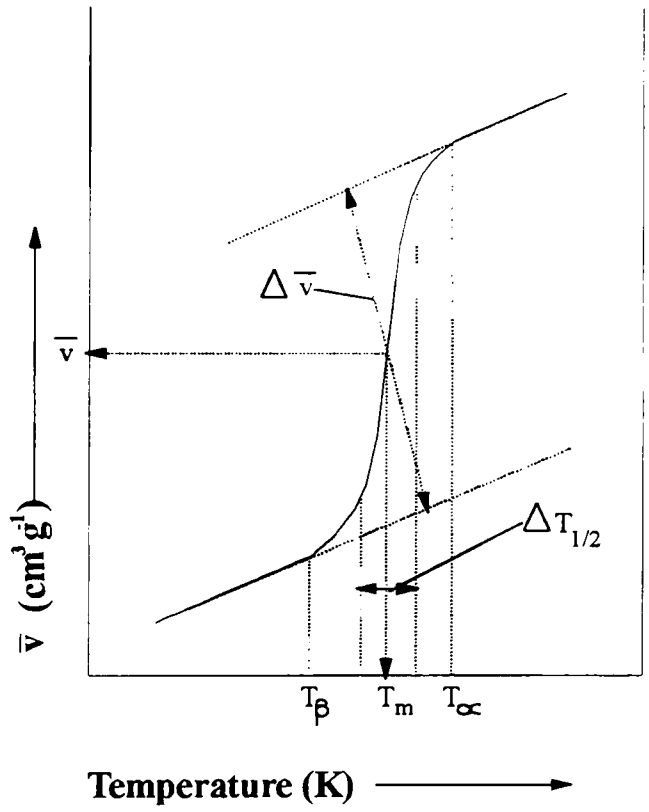

Figure 2.5 Idealised Differential Scanning Densitometric scan, where T_β and T_α denote the start and end of the observed phase transition, the half width $\Delta T_{1/2} = T_{\left(\bar{v}+\frac{\Delta\bar{v}}{4}\right)} - T_{\left(\bar{v}-\frac{\Delta\bar{v}}{4}\right)}$ and the transition temperature $T_m = T$ at $\alpha^{max}(\alpha = \frac{1}{\bar{v}} \bullet \frac{d\bar{v}}{dT})$

2.2.4 **Applications and Uses of Differential Scanning Densitometry.**

In molecular biophysics, the following are the most important areas of applications:

(a) determination of partial specific volumes and preferential interaction parameters of biological molecules in solution

(b) determination of transition volumes in thermal transitions (e.g., lipid phase transitions,[28,29] protein denaturation; studies of ligand effects on thermal behaviour).

This method can also be used in isothermal mode to determine compressibilities of solutions of biological interest ($(P/V)_T$ effects). Differential scanning densitometry has been used to study the interactions between Mellitin and phosphatidylcholine model membranes[30] and the effects of delta-lysin on the phase transitions of lipid assemblies.[31] The binding of a tyrosine-rich protein and collagen have been studied by DSD and it was shown that the binding reached saturation at a molar ratio of approximately 1:2 respectively.[32] DSD has been used to characterise the phase transition behaviour of synthetic and novel glycolipids,[33] substituted phospholipids,[34] and mixtures of alkylresorcinol analogues and DPPC.[35] DSD has also been employed to study the phase transition behaviour of block copolymers in dilute aqueous solution (poloxamers).[36]

2.3 Nuclear Magnetic Resonance (NMR).

2.3.1 **Principles of NMR.**

Nuclear magnetic resonance can be carried out on nuclei that possess a magnetic moment. As a basic example, using the hydrogen nucleus, a proton may be regarded as a spinning positively charged unit. Like any rotating electric charge, it generates a tiny magnetic field **H'** along its spinning axis. If this nucleus is placed in an external magnetic field $\mathbf{H_0}$, it will line up parallel (A) or antiparallel (B) to the direction of the applied field (figure 2.6).

The parallel arrangement (A) is of lower energy, although the difference between the orientations is very small. Only an excess of about 10 out of 10^6 nuclei are in the low energy spin state at 298K.

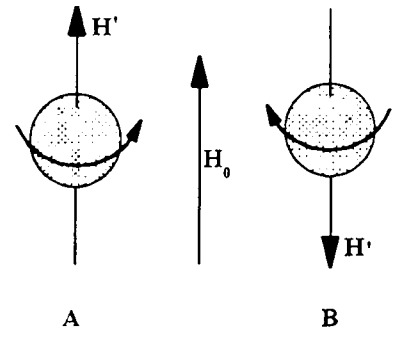

Figure 2.6 Spin-state orientations of the hydrogen nucleus in a magnetic field, H_0.

.Nuclei are energetically perturbed during NMR analysis by a combination of the applied magnetic field and radio frequency radiation. Most routine NMR spectrometers operate at a fixed radiofrequency and make small variations in the magnetic field as the

spectrum is scanned. When the energy exerted on a nucleus equals the energy difference between spin states, resonance is attained. Energy is absorbed as the nucleus 'flips' between the two spin states. The absorption and subsequent emission of energy is detected by the radiofrequency receiver and ultimately recorded as a peak on the NMR spectrum.

The energy difference between spin states is characteristic of the particular type of nucleus and the strength of the magnetic field experienced by that nucleus. A proton in a field of 14100 gauss the value is 23.8×10^{-6} kJmol^{-1}. The relationship is expressed in the following equation:

$$\Delta E = h\upsilon = \frac{\gamma h H}{2\pi} \qquad (29)$$

where ΔE = the energy difference between the two spin states, h = Planck's constant, ν = the frequency of resonance, γ = the gyromagnetic ratio, a characteristic of that particular nucleus, and H = the magnetic field of the nucleus.

Equation 29 shows that the frequency at which resonance occurs is proportional to the magnetic field experienced by the nucleus. The chemical shift is the position along the NMR spectrum at which resonance occurs for a particular nucleus in a specific molecular environment, and is always recorded relative to a standard resonance peak. For a proton NMR spectrum the single resonance peak of the methyl groups in tetramethylsilane is normally used as the reference and set as zero.

Frequency units in Hertz are used to record chemical shifts whether the spectrometer is operated at fixed frequency with variable field or fixed field with variable frequency. Instruments typically function at 60-600MHz. Since the energy required for resonance of a particular nucleus depends on the instrument frequency and field strength, chemical shifts recorded in hertz may vary with the spectrometer. To simplify comparison of spectra from one instrument to another, the delta scale (δ) is used. Chemical shifts in the delta scale are expressed in parts per million (ppm):

$$\delta_A = \frac{\Delta\upsilon}{\upsilon} X10^6 \text{ppm} \qquad (30)$$

where δ_A = chemical shift of nucleus A (ppm), $\Delta\nu$ = difference in resonance frequency, Hz, between the standard and peak being measured, ν = spectrometer frequency (Hz).

In general, chemical shifts are observed downfield from the reference standard and are shifted further downfield by the deshielding effect of neighbouring atoms, either from electronegative groups or unsaturated groups (figure 2.7).

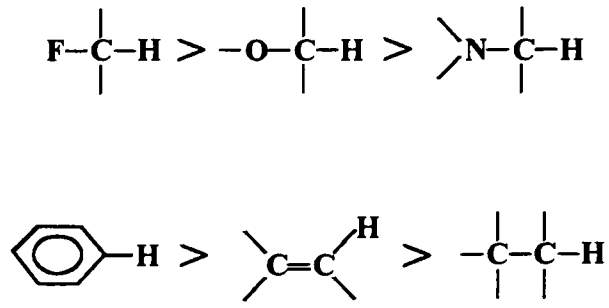

Figure 2.7 Deshielding effects of neighbouring groups on the downfield shift for proton NMR.

The areas of the peaks are directly proportional to the number of atoms in a particular environment and can yield important information to elucidate molecular structure.

Multiplets arise from small magnetic interactions that occur between the nuclei of neighbouring atoms, the resulting NMR spectral patterns are referred to as spin-spin splitting. The effects that give rise to spin-spin splitting are much smaller than those which result in chemical shift differences as a nucleus experiences a change in molecular environment. Several rules characterise spin-spin splitting of resonance peaks (using the proton as an example):

(1) the simple first order splitting occurs between protons or adjacent atoms.

(2) splitting only occurs between nuclei with different shifts, i.e., between magnetically non-equivalent atoms.

(3) the number of peaks, **N**, into which a proton signal is split equals the number of equivalent neighbouring protons plus one (**N** = n+1), e.g., a doublet results from one adjacent proton.

(4) peak area ratios within a multiplet are:

doublet 1:1

triplet 1:2:1

quartet 1:3:3:1

(5) the chemical shift of a multiplet is at the centre of the particular groups of lines.

The coupling constant, J, is the distance, expressed in hertz, between adjacent peaks of a multiplet. Coupling constants are independent of the magnetic field strength, whereas the chemical shift (Hz) is proportional to the field strength. Spin-spin splitting is normally not observed for a proton attached to an oxygen or nitrogen atom as they rapidly interchange between molecules. Longer range coupling is often observed between non-adjacent nuclei in compounds with multiple bonds or ordered macromolecular structures.

T_2 relaxation time is defined as the time constant of the decay of the M_{xy} components (vectors at right angles to the applied field, B_0). It is also related to the linewidth:

$$\Delta\upsilon_{1/2} = \frac{1}{\pi T_2} \qquad (31)$$

Field inhomogeneity affects the observed linewidth and transient decay because a spread of fields produces a spread of frequencies. There are, however, methods for reducing the effect of such inhomogeneities and thus obtaining T_2. For example, a 90°-τ - 180° -τ pulse sequence generates an echo at time 2τ and the decay of this echo is relatively insensitive to field inhomogeneity effects.

The T_1 relaxation time is defined to be the time constant that describes the recovery of M_z component (vectors in the direction of the applied field) after a peturbation. The component M_z can be perturbed in several ways. If B_1 is applied for a long time, for example, then saturation takes place - that is, the population difference between the levels is destroyed and $M_z = 0$. The recovery to equilibrium can then be monitored. A more practical way of carrying out the experiment involves the use of 90° and 180° B_1 pulses (rotating the field at right angles to B_0). The 180° pulse inverts the populations, so the magnetisation component along the z-axis, M_0, becomes $-M_0$. This recovers along the z-axis with a first-order rate constant $1/T_1$. Thus M_z, as a function of time is given by:

$$M_z(t) = M_0\left(1 - 2e^{\frac{-t}{T_1}}\right) \qquad (32)$$

Since this recovery takes place along the z-axis, it cannot be observed directly because there are no M_{xy} components (no phase coherence). The recovery is therefore monitored by applying a 90° pulse at intervals, thus tipping the resultant z-magnetisation into the xy plane.

The rate at which a Boltzmann distribution of populations is set up among the energy levels is $1/T_1$. All NMR transitions are caused by magnetic fields fluctuating at frequencies

related to resonant frequency (ω_0). Thermal motion of molecules in the sample causes small fluctuating local fields in the nuclei of interest. Since these motions also have an energy distribution, the probabilities of inducing upward and downward NMR transitions are not equal, so a slight excess population is set up in the lower energy level. Fluctuating magnetic fields caused by motion , can arise from a variety of sources, but for I = 1/2 nuclei, the most important one is usually the dipole-dipole interaction. The field exerted by one nuclear magnetic moment on another is given by $(3\cos^2\theta - 1)/r^3$. If the moments μ_1 and μ_2 are on the same molecule, then the separation between them, r_1 , is fixed (figure 2.8). As the molecule tumbles the spins will stay oriented in the field. Thus, θ will vary in a random way as the molecule undergoes Brownian motion, and μ_1 will produce a fluctuating field at μ_2 and vice versa.

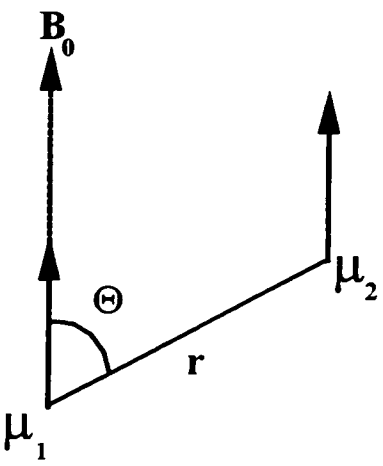

Figure 2.8 The interaction between two dipoles in field B_0 .

The time scale of the random motion is defined by some function $g(\tau)$. In many cases this function is exponential and can be expressed as $\exp(-t/\tau_c)$, where τ_c is a correlation time. This simply means that the probability of finding a correlation between the orientation of the vector r and some defined direction decreases exponentially with time constant τ_c.

The frequency content of a function that varies with time can be analysed by Fourier transformation. In the case of an exponential $g(\tau)$, this transformation is given by:

$$J(\omega) = \tau_c / (1 + \omega^2 \tau_c^2) \qquad (33)$$

The function $J(\omega)$ expresses the probability of finding a fluctuation with frequency ω for a particular correlation time τ_c. For a macromolecule of radius **a** in a solution of viscosity η, the rotational correlation time τ_c is given approximately by:

$$\tau_c \cong \frac{4\pi\eta a^3}{3kT} \qquad (34)$$

The probability that field fluctuations will induce a transition between energy levels will depend not only on the existence of a component at the correct frequency but also on the amplitude of the fluctuation. The amplitude of the dipole-dipole interaction is $\mu_0\ \mu_1\ \mu_2 / 4\pi r^3$. The nuclear magnetic moments have magnitude γhI and the transition probability depends on the amplitude squared. For two spins with the same T_1 and with $\gamma_1 = \gamma_2$ the full expression for T_1 is given by:

$$\frac{1}{T_1} = \frac{3\mu_0^2\gamma_1^4h^2}{160\pi^2r^6}\left\{\frac{\tau_c}{1+\omega^2\tau_c^2} + \frac{4\tau_c}{1+4\omega^2\tau_c^2}\right\} \qquad (35)$$

Fluctuations at both ω and 2ω cause transitions, thus there are terms for both $J(\omega)$ and $J(2\omega)$. From T_1 processes, M_z will recover to the equilibrium M_0 value, but this will also cause M_{xy} to disappear. From this, T_1 is often observed to equal T_2. There are, however, additional ways in which M_{xy} components can be destroyed. If there is a spread of ω_0 values because of local fields produced in the sample, or if there is an exchange between different environments with different values of ω_0, then T_2 can be decreased. Thus, in general, $T_2 < T_1$

For dipole-dipole interactions, the T_2 equation, which corresponds to the one for T_1 is:

$$\frac{1}{T_2} = \frac{3\mu_0^2\gamma^4h^2}{320\pi^2r^6}\left\{3\tau_c + \frac{5\tau_c}{1+\omega^2\tau_c^2} + \frac{2\tau_c}{1+4\omega^2\tau_c^2}\right\} \qquad (36)$$

2.3.2 **Applications and Uses of NMR.**

Applications of NMR can be categorised under the following headings:

(1) analytical uses: compounds can be identified, concentrations can be measured, including that of the proton (pH); and biosynthetic pathways can be elucidated using the isotopes ^{13}C, ^{15}N, ^{2}H or ^{3}H.

(2) ligand binding and ionisation states: K_d can be measured for a wide variety of ligands, including metal ions, anions and small organic molecules; pK_a values of ligands and individual groups on macromolecules can be measured.

(3) kinetics: the rates of processes can be determined over a wide range by analysing chemical exchange effects ($1\text{-}10^5\ s^{-1}$) and by monitoring concentration changes ($10^{-1}\ s^{-1}$ - $10^{-3}\ s^{-1}$).

(4) structural information can be obtained from the r^6 dependence of dipolar relaxation, which can influence T_1 and T_2 respectively. Shifts depend on $1/r^3$.

(5) molecular motion: the terms T_1 and T_2 depend on molecular motion. In addition, information about motion can sometimes be obtained from partially averaged spectra.

(6) spatial distribution: information on the spatial distribution of molecules can be obtained. In some cases, it is possible to distinguish whether a molecule is inside or outside a cell, and a method known are NMR imaging can be used to give good images of various objects, including the human body.

2.4 Overview.

The increasing applications and potential applications of poloxamers and poloxamines in the pharmaceutical and related industries (Section 1.3) has led to an increase in the amount of fundamental research in this area over the past decade in order to elucidate the solution behaviour of this group of water soluble copolymers. However, in general, these fundamental studies have been concerned with investigations of poloxamer solutions at high concentrations (>10% w/v) and there is a paucity of data relating to the dilute aqueous solution behaviour of these water soluble copolymers. It is also of paramount importance to investigate the dilute aqueous solution behaviour (<1% w/v) of poloxamers and poloxamines, firstly, to aid in the interpretation of the observed applications of poloxamers and poloxamines e.g., drug delivery, control of blood rheology, stimulation of plant growth (Section 1.3) for which the block copolymers are utilised at low concentration; Secondly, to aid in the interpretation of the observed oxyalkylene block copolymers at higher concentrations, the behaviour of which is complicated due to observations of many distinct phases dependent on temperature, concentration, cosolute concentration, copolymer composition and molecular weight.

The understanding of the dilute aqueous solution behaviour of oxyalkylene block copolymers has presented a great challenge to polymer scientists for several reasons:

(1) the absence of chromophores

(2) the similarity in structure and solution behaviour of polyoxypropylene (POP) and polyoxyethylene (POE), i.e., the blocks are relatively hydrophobic and hydrophilic respectively, therefore the ability to conclusively differentiate the observed effects

between POP or POE has complicated interpretations. It is also apparent that in the aggregated form of poloxamers and poloxamines in dilute aqueous solution, the hydrophobic POP remains partially hydrated, and thus the relative densities of POP and POE remain similar posing problems for scattering techniques (especially light scattering, small angle X-ray scattering).

(3) the aqueous solution behaviour of poloxamers and poloxamines varies greatly dependent on composition and molecular weight.

(4) this oxyalkylene family of surface active agents cannot be classified as classical micelle forming surfactants (e.g., sodium dodecyl sulphate) as they do not form inverted micelles in organic solvents, it is possible that the observed aggregation of the hydrophobic POP can be monomolecular, and in aqueous solution the observed "critical micelle temperature" is due to the processes of dehydration, aggregation and a conformational change, the latter two processes are only observed for surfactants with insoluble hydrophobic moieties (e.g. C_nEO_x type surfactants).

HSDSC is a noninvasive technique, therefore it is possible to directly derive thermodynamic parameters (such as calorimetric enthalpy, ΔH_{cal}, phase transition temperature, T_m) for the phase behaviour of oxyalkylene block copolymers in dilute aqueous solution, which cannot be derived directly by any other ultrasensitive technique. By studying a range of copolymers of varying composition and molecular weight it is therefore possible to derive trends for the aqueous solution behaviour of oxyalkylene block copolymers as a function of temperature and copolymer concentration leading to an interpretation of the observed phase behaviour on a microscopic basis. Also, by comparison to homopolymers, and diblock copolymers it is possible to create an overall view of the dilute solution behaviour.

2.4.1 **Objectives of Research.**

In the literature there is a lack of thermodynamic data relating to the phase behaviour of oxyalkylene block copolymers in dilute aqueous solution. The objectives of the research presented in this thesis are as follows:

(1) to determine the nature of the dilute aqueous solution behaviour of oxyethylene-oxypropylene block copolymers using macroscopic (HSDSC,DSD) and microscopic (NMR) noninvasive techniques.

(2) to derive trends relating the oxypropylene and oxyethylene contents and molecular weight in order to predict the solution behaviour of theoretical copolymers of this type (e.g., to aid in the design of block copolymers to perform specific functions such as drug delivery).

(3) to study the effects of pH and cosolutes on the phase behaviour of oxyethylene-oxypropylene block copolymers e.g., sodium chloride, and cosolutes such as urea and phosphate buffer that strongly affect the structure of water.

(4) to study the effects of copolymer mixtures on the thermodynamic parameters of the observed phase transitions of poloxamers in dilute aqueous solution.

2.5 References

(1) Lavoisier,A.; Laplace,P.S.de, *Sur La Chaleur*, **1780**.
(2) "*Chemistry Data Book*", Stark,J.G.; Wallace,H.G. (Eds.), John Murray Publishers, London, **1975**, 54.
(3) Armstrong,G.T., *J.Chem.Ed.*, **1964**, *41*, 297.
(4) Privalov,P.L.; Plotnikov,V.V.; Filimonov,V.V., *J.Chem.Thermodyn.*, **1975**, *7*, 41
(5) Privalov,P.L., *Pure Appl.Chem.*, **1980**, *52*, 479.
(6) Chang,L-H.; Li,S-J.; Ricca,T.L.; Marshall,A.G., *Anal.Chem.*, **1984**, *56*, 1502.
(7) Sturtevant,J.M., *Ann.Rev.Phys.Chem.*, **1987**, *38*, 463.
(8) Filimonov,V.V.; Privalov,P.L.; Hinz,H-J.; van der Haar,F.; Cramer,F., *Eur.J.Biochem.*, **1976**, *70*, 25.
(9) Privalov,P.L.; Filimonov,V.V., *J.Mol.Biol.*, **1978**, *122*, 447.
(10) Freire,E.; Biltonen,R.L., *Biopolymers*, **1978**, *17*, 481.
(11) Freire,E., Biltonen,R.L., *Biopolymers*, **1978**, *17*, 497.
(12) Freire,E.; Biltonen,R.L., *Biochim.Biophys.Acta*, **1978**, *514*, 54.
(13) Albon,N.; Sturtevant,J.M., *Proc.Nat.Acad.Sci., USA*, **1978**, *75*, 2258.
(14) Edge,V.; Allwell,N.M.; Sturtevant,J.M., *Biochemistry*, **1985**, *24*, 5899.
(15) Manly,S.P.; Matthews,K.S.; Sturtevant,J.M., *Biochemistry*, **1985**, *24*, 3842.
(16) Privalov,P.L., *Adv.Protein Chem.*, **1982**, *35*, 1.
(17) Privalov,P.L., *Adv.Protein Chem.*, **1979**, *33*, 167.
(18) Fukada,H.; Sturtevant,J.M.; Quiocho,F.A., *J.Biol.Chem.*, **1983**, *258*, 13193.
(19) Novokhatny,V.V.; Stanislav,A.K.; Privalov,P.L., *J.Mol.Biol.*, **1984**, *179*, 215.
(20) Privalov,P.L.; Mateo,P.L.; Khechinashvili,N.N., *J.Mol.Biol.*, **1989**, *152*, 445.
(21) Sánchez-Ruiz,J.M.; López-Lacomba,J.L.; Cortijo,M.; Mateo,P.L., *Biochemistry*, **1988**, *27*, 1648.
(22) Lohner,K.; Latal,A.; Lehrer,R.; Ganz,T., *Biochemistry*, **1997**, *36*, 1525.
(23) Lohner,K.; Degovics,G.; Laggner,P.; Gnamusch,E.; Paltauf,F., *Biochim.Biophys.Acta*, **1993**, *1152*, 69.
(24) Blandamer,M.J.; Briggs,B.; Butt,M.D.; Cullis,P.M.; Gorse,L.; Engberts,J.B.F.N., *J.Chem.Soc.Faraday Trans.*, **1992**, *88(19)*, 2871.
(25) Blandamer,M.J.; Briggs,B.; Burgess,J.; Cullis,P.M.; Eaton,G., *J.Chem.Soc.Faraday Trans.*, **1991**, *87(8)*, 1167.
(26) Laggner,P.; Stabinger,H., *Colloid Int.Sci.*, Kerker,M. (Ed), Academic Press Inc., **1976**, *Vol.V*, 91.
(27) Kohlrausch, *Practische Physik Bd.3*, **1968**, *40*, 12.
(28) Laggner,P.; Stabinger,H., Colloid Int.Sci., 1976, 5, 91.
(29) Laggner,P.; Löhner,K.; Degovics,G.; Müller,K.; Schüster,A., *Chem.Phys.Lipids*, **1987**, *44*, 31.
(30) Posch,M., Rakusch,U., Mollay,C.; Laggner,P., *J.Biol.Chem.*, **1983**, *258(3)*, 1761.
(31) Neitchev,V.; Löhner,K.; Collotto,A.; Laggner,P., *Mol.Biol.Reports*, **1992**, *16(4)*, 249.
(32) Macbeath,J.R.E.; Shackleton,D.R.; Hulmes,D.J.S., *J.Biol.Chem.*, **1993**, *268(26)*, 19826.
(33) Koynova,R.D.; Tenchov,B.G., Kuttenreich,H.; Hinz,H.J., *Biochemistry*, **1993**, *32(46)*, 12437.
(34) Pax,H., Blume,A., *Chem.Phys.Lipids*, **1993**, *66(1-2)*, 63.

(35) Gerdon,S.; Hoffmann,S.; Blume,A., *Chem.Phys.Lipids*, **1994**, *71(2)*, 229.
(36) Armstrong,J.K.; Parsonage,J.; Chowdhry,B.Z.; Leharne,S.; Mitchell,J.; Beezer,A.; Löhner,K.; Laggner,P., *J.Phys.Chem.*, **1993**, *97(15)*, 3904.

CHAPTER 3 - GENERAL EXPERIMENTAL SECTION

3.1 Materials.

3.1.1 **Polymers.**

The poloxamers and poloxamines studied were a gift from ICI Chemicals Ltd. (Middlesbrough, Cleveland, U.K.) under the tradenames of Synperonic PE and T nonionic surfactants respectively. The molecular mass, POP and POE contents of the copolymers are shown in Table 3.1 (poloxamers) and Table 3.2 (poloxamines). The diblock copolymers studied were purchased from Polysciences, the POP and POE homopolymers were purchased from the Aldrich Chemical Co. (Poole, Dorset, U.K.). Poly(ethylene oxide) (MW = $1x10^6$ $gmol^{-1}$, Polyox WSR-301) was a gift from Union Carbide. The molecular masses of the homopolymers and diblock copolymers are shown in Table 3.3.

3.1.2 **Cosolutes and Cosolvents.**

Sodium chloride, sodium dihydrogen phosphate, disodium hydrogen orthophosphate, urea and guanidinium chloride were of Analar grade and purchased from the Aldrich Chemical Co. (Poole, Dorset, U.K.). Methanol, ethanol, propan-1-ol, butan-1-ol and formamide were of HPLC grade and purchased from the Aldrich Chemical Co. (Poole, Dorset, U.K.).

3.1.3 **Molecular Mass Distribution.**

The molecular mass distribution of the polymers was determined by gel permeation chromatography using the following conditions:

Columns	:	PL-gel, 2x mixed bed B, 30cm, 10 microns.
Solvent	:	tetrahydrofuran with antioxidant.
Flow Rate	:	$1mLmin^{-1}$.
Temperature	:	ambient.
Detector	:	refractive index
Calibrants	:	polystyrene standards.

Approximately 20mg of sample was dissolved in approximately 10mL of solvent (dimethylformamide for poly(ethylene oxide) MW $1x10^6$ $gmol^{-1}$) and a small amount of 1,2-dichlorobenzene was added as a marker. Run times were 25-30 minutes and each run was performed in duplicate. The molecular mass values (M_w, M_n) were expressed as polystyrene equivalents, the values agreed reasonably well with the molecular mass values quoted by the manufacturer. Polymers with a molecular mass < 10 000 $gmol^{-1}$ all gave a single elution peak, and polymers with a molecular mass > 10 000 $gmol^{-1}$ all showed the presence of a low molecular mass impurity, the amount of which appeared to increase proportionally with increasing molecular mass of the sample. The low molecular mass impurity was attributed to the presence of a diblock copolymer[1,2] (for the poloxamers and poloxamines).

The poloxamers and poloxamines were used without further purification as these copolymers are used industrially as commercial products.

Table 3.1 Coding and Molecular Masses of the Poloxamers.

Poloxamer Industrial Pluronic Code[a]	Poloxamer Generic Code	Molecular Mass[b] ($gmol^{-1}$)	POP Content ($gmol^{-1}$)	POE Content ($gmol^{-1}$)	HLB Value[b]	Polydispersity[c]
L31	P101	1100	950	150	-	-
L35	P105	1900	950	950	18.5	-
F38	P108	4800	950	3850	30.5	-
L42	P122	1650	1200	450	8.0	-
L43	P123	1925	1200	725	-	-
L44	P124	2200	1200	1000	16.0	-
L61	P181	2090	1750	340	3.0	-
L62	P182	2400	1750	650	7.0	1.2
L64	P184	2900	1750	1150	15.0	-
F68	P188	8350	1750	6600	29.0	-
P75	P215	4150	2050	2100	16.5	-
F77	P217	6600	2050	4550	-	-
L81	P231	2750	2250	500	2.0	-
P84	P234	3750	2250	1500	-	-
P85	P235	4650	2250	2400	16.0	1.2
F87	P237	7700	2250	5450	24.0	1.2
F88	P238	11800	2250	9550	28.0	1.3
L92	P282	3450	2750	700	5.5	-
P94	P284	4600	2750	1850	13.5	-
L101	P331	3800	3250	550	1.0	-
P103	P333	4950	3250	1700	9.0	1.4
P105	P335	6500	3250	3250	-	-
F108	P338	14000	3250	10750	27.0	1.4
L121	P401	4400	4000	400	0.5	-
F127	P407	12000	4000	12000	22.0	1.5

[a] Pluronic Code: L = Liquid P = Paste F = Flake, [b] Data supplied by ICI "*Synperonic PE, T, LF and Ukanil Range of Nonionic Surfactants*" 1991, [c] M_n / M_z values determined by GPC, RAPRA Technology Ltd., Shawbury, Shropshire.

Table 3.2 Coding and Molecular Masses of the Poloxamines.

Poloxamine	Molecular Mass[a] ($gmol^{-1}$)	POP Content ($gmol^{-1}$)	POE Content ($gmol^{-1}$)	HLB Value[a]	Polydispersity[b]
T304	1650	1000	650	12-18	1.25
T701	3700	3000	700	1-7	1.45
T707	12500	3000	9500	>24	1.60
T803	5500	3500	2000	-	1.40
T904	8200	4000	4200	12-18	2.00
T908	26000	4000	22000	>24	1.50
T1301	6900	6000	900	1-7	2.45
T1302	7400	6000	1400	1-7	1.95

[a] Data supplied by ICI "*Synperonic PE, T, LF and Ukanil Range of Nonionic Surfactants*" 1991, [b] M_n / M_z values determined by GPC, RAPRA Technology Ltd., Shawbury, Shropshire.

Table 3.3 Molecular Masses and Suppliers of Homopolymers and Diblock Copolymers.

Polymer	Molecular Mass[a] ($gmol^{-1}$)	POP Content ($gmol^{-1}$)	POE Content ($gmol^{-1}$)	Physical State at Room Temperature[a]	Supplier
Diblock	3438	2585	853	L	Polysciences
Diblock	8750	1458	7292	F	Polysciences
Diblock	13333	3333	10000	F	Polysciences
POP	725	725	0	L	Aldrich
POP	1000	1000	0	L	Aldrich
POP	2000	2000	0	L	Aldrich
POP	4000	4000	0	L	Aldrich
POE	1000	0	1000	F	Aldrich
POE	2000	0	2000	F	Aldrich
POE	3000	0	3000	F	Aldrich
Polyox WSR-301	$1x10^6$	0	$1x10^6$	F	Union Carbide

[a] L = Liquid, F = Flake

3.2 Experimental

3.2.1 **General.**

Polymer solutions were, unless otherwise stated, prepared at a concentration of 5mgmL^{-1} in double distilled water or relevant buffer. Approximately 100mg of polymer (accurately weighed to ±0.2mg, minimising errors to ±0.1%) was dissolved in 20mL of solvent. The solvent was deaerated prior to use, as deaeration of the polymer solution resulted in foaming. Dissolution of the polymer samples was aided by chilling the polymer + solvent to 277K, and for POP homopolymer samples of MW > 1000gmol^{-1}, dissolution was only achieved by chilling the solvent + homopolymer to 277K approximately 1-2h prior to use. POE (MW ≅ 1x10^{6}gmol^{-1}) solutions were prepared at a concentration of 2.5mgmL^{-1} in double distilled water or relevant buffer unless otherwise stated, as higher concentrations produced solutions of high viscosity which could not be accurately studied by HSDSC due to poor thermal mixing during a scan. Complete dissolution and solution equilibrium of high molecular mass POE solutions was achieved by chilling the mixture to 277K for 1 week prior to use and with agitation at 24h intervals.

Approximately 1mL of polymer solution was required for each experiment and due to the sensitivity of the techniques employed, sample volumes were prepared in excess to minimise errors in the resultant polymer concentration, as the polymer concentration could not be readily confirmed spectroscopically due to the absence of functional groups or chromophores, as in the case for proteins where concentrations are routinely confirmed by use a characteristic extinction coefficient for the absorption value at 280nm.

Urea and guanidinium chloride solutions were prepared 24h prior to use and the molar concentration was determined on a mass basis and after 24h by refractive index measurements using the following formulae[2a] (solutions of urea and guanidinium chloride can not be prepared volumetrically due to the effect of the solute on water structure):

(a) Molarity of urea solutions (by mass).

(1) weight fraction of urea (**W**) = (mass of urea) / (mass of solution)

(2) $\mathbf{d/d_0} = 1 + 0.2658\mathbf{W} + 0.0330\mathbf{W}^2$

(3) volume = [mass of solution (g)] / ($\mathbf{d/d_0}$)

(4) Molarity = [mass of urea (g)] / {[RMM urea (g)] x [volume (L)]}

(b) Molarity of urea solutions (by refractive index) at 298K.

$$\text{Molarity} = 117.660\ \Delta\mathbf{N} + 29.753(\Delta\mathbf{N})^2 + 185.560(\Delta\mathbf{N})^3$$

where $\Delta\mathbf{N}$ = (refractive index of solution) - (refractive index of water)

(c) Molarity of guanidinium chloride (GdCl) solutions (by mass).

(1) weight fraction (**W**) = (mass of GdCl) / (mass of solution)

(2) $\mathbf{d}/\mathbf{d}_0 = 1 + 0.271\mathbf{W} + 0.033\mathbf{W}^2$

(3) volume = [mass of solution(g)] / ($\mathbf{d}/\mathbf{d}_0$)

(4) Molarity = [mass of GdCl (g)] / {[RMM GdCl (g)] x [volume (L)]}

(d) Molarity of GdCl solutions (by refractive index).

$$\text{Molarity} = 57.147\ \Delta\mathbf{N} + 38.680(\Delta\mathbf{N})^2 - 91.600(\Delta\mathbf{N})^3$$

where $\Delta\mathbf{N}$ = (refractive index of solution) - (refractive index of water)

For both methods of molarity determination the solutions were only used if the values were within 1% agreement.

3.2.2 **High sensitivity differential scanning calorimetry (HSDSC).**

Calorimetric measurements were carried out using a Microcal MC-2 instrument (Microcal Inc., Amherst, Mass., USA) and the DA-2 dedicated software package (provided by Microcal Inc.) for data accumulation and analysis.[3,4] A 2.5mL Hamilton syringe, fitted with a steel 6" narrow bore flat ended needle was filled with the reference buffer, and then the reference cell was filled by carefully inserting the syringe vertically via the access port of the to about ca. 2-3mm from the bottom of the cell. The plunger on the syringe was then slowly

depressed until an excess of buffer was observed at the top of the access port. The plunger was then depressed and raised quickly over a range of ca. 0.2mL for about 5 repetitions in order to displace any bubbles that may have been present inside the cell. The sample cell was filled in the same manner. The reference cell was always loaded first in order to avoid contamination of the reference cell with the sample. Excess fluid from the access ports of the cells was removed via a vacuum line, such that both cells contained equal volumes. The cells were sealed and placed under a pressure of 1 atmosphere of nitrogen to prevent bubble formation during a scan. Samples were equilibrated for a minimum of 60 minutes prior to the start of each upscan and scans were performed at a scan rate of $60Kh^{-1}$ unless otherwise stated. The effects of scan rate were examined at scan rates of 10, 30 and $60Kh^{-1}$ and for POP (MW = $1000gmol^{-1}$) scan rates of 10, 20, 30, 45, 60 and $90Kh^{-1}$ were examined. Reversibility scans were performed at $\pm 30Kh^{-1}$ allowing an equilibration period of 90 minutes prior to the downscan. Upscans were controlled by the calorimeter and downscans controlled by a computer interfaced with a Haake F-3 circulating waterbath. The calorimetric cells were cleaned between each sample by flushing 500mL of double distilled water through the cells and residual solvent was removed by means of a vacuum line. General experimental considerations for the Microcal MC-2 are discussed in Section 2.1.4

3.2.3 **Differential scanning densitometry (DSD).**

Copolymer samples were prepared at a concentration of $10mgmL^{-1}$, which was observed to be the minimum concentration at which the phase transition could be clearly observed for all samples. The reference cell was filled with double quartz distilled water for all experiments, for both cells the exit port of the glass capillary was plugged after filling, the entrance port was left open to allow for thermal expansion during a scan. All experiments were performed at atmospheric pressure and at a scan rate of $\pm 30Kh^{-1}$. A modified version of the hollow oscillator Precision Density Meter DMA 60 (Anton Paar, Graz, Austria) was used for DSD experiments. Temperature was measured using a calibrated Pt-100 sensor connected to an electronic millikelvin thermometer (Systemteknik, Bromma, Sweden), the DSD system was operated under microprocessor control and raw data was converted into partial specific volume and expansivity data using a dedicated software package (DENSCALC). The reference and sample cells were cleaned by flushing each cell with water and then methanol, filtered air dried (via a vacuum line) and recalibrated with the pairs water-water and air-water

between each experiment. General experimental considerations for the Precision Density Meter DMA 60 are discussed in Section 2.2.

3.2.4 **Nuclear magnetic resonance (NMR).**

^{1}H and ^{13}C NMR spectra were recorded at 500MHz and 125MHz respectively using a Varian VXR 500S spectrometer at copolymer concentrations of 10mgmL^{-1} in D_2O. All chemical shift values were referenced against an aqueous solution of 2,2-dimethyl-2-silapentane sulphate held in an inner capillary of a 5mm coaxial tube. Temperature measurements were accurate to ±0.2K.

3.2.5 **Fractionation of Poloxamer 407.**

A two phase solvent extraction technique was employed to fractionate P407 into diblock- and triblock-rich fractions based on the preferential solubility of diblocks in hexane.[1] P407 was selected, as this polymer was observed from GPC data to give a broad molecular mass distribution with two distinct polymer populations. The lower molecular mass peak was assumed to be mainly diblock copolymer.

Poloxamer 407 (35.0g) was dissolved in 250mL of CH_2Cl_2 in a 2L conical flask. Hexane was then added while stirring until a slight precipitate was observed (750mL). The mixture was then heated to 40°C with continuous stirring for 2h. Dichloromethane was then added dropwise until a clear solution was obtained. The mixture was cooled to room temperature and then transferred to a 2L separating funnel and allowed to stand for 24h. The layers were separated and rotary evaporated to dryness. The upper layer fraction (hexane, diblock rich, 2.6g) was dried under vacuum at room temperature with a liquid nitrogen trap for 24h. The CH_2Cl_2 fraction (27.6g) was redissolved in CH_2Cl_2 and the fractionation with hexane repeated. The polymer sample recovered from the hexane layer from the second fractionation was weighed (2.7g), vacuum dried and pooled with the first fraction recovered from the hexane layer. The lower layer fraction (CH_2Cl_2, triblock rich, 22.8g) was rotary evaporated, and the polymer sample finally dried under vacuum at room temperature with a liquid nitrogen trap for 24h. The total yield of polymer was 80%, of which 81% (triblock rich, 22.8g) was recovered from the CH_2Cl_2 layer, and 19% (diblock rich, 5.3g) was recovered

from the hexane layer. Samples of P407 and the two fractionated samples (hexane layer, CH_2Cl_2 layer) were analysed for molecular mass distribution by GPC as described previously (Section 3.1.3). Calorimetric scans were performed for the unfractioned and fractioned samples of P407 at a concentration of $5mgmL^{-1}$ in double distilled water at a scan rate of $60Kh^{-1}$.

3.3 References

(1) Dr.C.Booth, *Personal communication*, **1992**.
(2) Dr.I.R.Schmolka, *Personal communication*, **1995**.
(2a) Pace,C.N.; Shirley,B.A.; Thompson,J.A., *"Protein Structure: A Practical Approach"*, Creighton,T.E. (Ed), IRL Press, Oxford, U.K., **1989**, Chapter 13, 316.
(3) Sturtevant,J.M., *Ann.Rev.Phys.Chem.*, **1987**, *38*, 463.
(4) Chowdhry,B.Z.; Cole,S.C., *TIBTECH*, **1989**, *7*, 11.

CHAPTER 4 - POLYOXYETHYLENE AND POLYOXYPROPYLENE HOMOPOLYMERS

4.1 General

Polyoxyethylene (POE) is a nonionic neutral polyether and is soluble in water and most organic solvents (Table 4.1). POE is commercially available over a wide range of molecular masses and as a linear or branched polymer. Despite the apparent simplicity of POE structure, this molecule and ethoxylated adducts have been the focus of much research[1-20] especially in the biotechnical and biomedical fields,[2] and is probably the most widely investigated water soluble polymer. POE of molecular mass of less than 1000 $gmol^{-1}$ are colourless, odourless viscous liquids and above a molecular mass of 1000 $gmol^{-1}$ these polymers are waxy, colourless solids or amorphous powders. POE is also termed poly(ethylene glycol) (PEG), poly(ethylene oxide) (PEO) or polyoxirane. In general terms poly(ethylene glycol) refers to polyethers of molecular masses below 20000 $gmol^{-1}$, poly(ethylene oxide) refers to higher molecular mass polymers, polyoxyethylene and polyoxirane are not specific regarding molecular mass.

Polyoxypropylene (POP), in contrast to POE, is observed to be insoluble in water[21] above a molecular mass of 750 $gmol^{-1}$ despite the apparent similarity in structure to POE (Table 4.1). POP is soluble in most organic solvents but is insoluble in such solvents as diethyl ether and glycols (e.g., ethylene glycol, glycerol). POP is commercially available over a narrow range of molecular masses (generally < 10000 $gmol^{-1}$), are colourless, odourless viscous liquids, increasing in viscosity with increasing molecular mass.

The water solubility of POE is due to some specific hydrogen bonding and at temperatures >370K the POE-water system phase separates for all molecular masses of POE. It is interesting to note that polymers of a similar nature are all insoluble in water with the exception of a few low molecular mass oligomers (Table 4.1), and this effect is believed to be due to water-structure and the related conformation of the polymer in aqueous solution.[22] POE is insoluble in hexane (and similar aliphatic hydrocarbons), ethyl ether and ethylene glycol, molecules that closely resemble POE. This solubility pattern is useful in the synthesis of POE derivatives[2] since reactions can be conducted in an organic solvent, such as toluene,

and the product isolated by addition of a non-solvent such as hexane or ethyl ether. Since POE is soluble in both organic and aqueous media, it is apparent that the polymer will be present to some extent in both phases of an organic-water two-phase system. In biological systems, it appears that POE partitions between aqueous media and cell membranes. Evidence for this lies in the observation that POE induces cell fusion, a property used to great benefit in the production of hybridomas and monoclonal antibodies.[23-25]

Table 4.1 Solubility of some Polyethers in Water.

Polymer	Generalised Formula	Solubility in Water
Polyoxymethylene	$HO\text{-}(CH_2O)_n\text{-}H$	Insoluble
Polyoxyethylene	$HO\text{-}(CH_2CH_2O)_n\text{-}H$	Soluble
Polyoxytrimethylene	$HO\text{-}(CH_2CH_2CH_2O)_n\text{-}H$	Insoluble
Polyoxypropylene	$HO\text{-}(\underset{\displaystyle CH_3}{\underset{\vert}{CH}}\,CH_2O)_n\text{-}H$	Insoluble

The commercial production of ultra-high molecular mass POE (MW > $1x10^6$) was first introduced in 1958 by Union Carbide[3-5] under the tradename Polyox resins. In aqueous solution, these high molecular mass polymers form thermoreversible gels above a concentration of 20% w/v,[4] and at higher concentrations the solution plasticizes. Solutions of high molecular mass POE are non-Newtonian, and show a dramatic increase in viscosity with decreasing shear rate.[4,5] The non-Newtonian behaviour of POE in aqueous solution becomes less pronounced with decreasing molecular mass and concentration.[4,6] In the crystalline state, the POE chain has a helical conformation with a distance between the hetero-oxygens of 2.88Å, very close to that of the O-O distance in liquid water (2.85Å).[7] The high solubility of POE in water is believed to be a reflection of this similiarity in structure between the polymer and a tetrahedral water lattice.[8] POE in aqueous solution acts as a highly mobile molecule with a large exclusion volume. Relaxation-time studies show rapid motion of the polymer chain[26] and GPC shows that POE chains are much larger in solution than many other molecules (e.g., proteins) of comparable molecular mass.[27,28] Interesting consequences of

this property are that POE excludes other polymers, and if the concentration of POE is high enough, will form two-phase systems with other polymers (e.g., dextran). Applications that result from this property include protein and nucleic acid precipitation and two-phase partitioning and, when the POE is covalently bound, protein-rejecting molecules and surfaces. Incorporation of hydrophobic end-groups, inclusion of hydrophobic propylene oxide as comonomer,[29] and addition of salts lead to the lowering of the lower cosolute temperature or cloud point;[30] this phenomenon has been utilised to produce two-phase systems for partitioning purifications.[31] POE forms complexes with metal cations,[29] this property is demonstrated by the application of POE as a phase transfer agent, a process of much importance in organic chemistry.[32-34] In this application POE transfers a salt from a solid phase or aqueous phase by complexing or co-ordinating with a metal cation and partitioning into an organic phase with the corresponding anion, and in the process the anion becomes more reactive due to its poor solvation; hence this process is frequently referred to as phase transfer catalysis,[32-34] similar to the process of phase transfer observed for crown ethers.[35] Crown ethers show selectivity in metal binding related to the size of the cavity in the centre of the crown; interestingly POE also shows selectivity in metal binding, apparently because POE adopts a helical conformation with cavities of preferred sizes.[33,36]

4.2 Experimental

POP samples of molecular mass 725, 1000, 2000 and 4000 $gmol^{-1}$ were dissolved in doubly distilled water at a concentration of 5 $mgmL^{-1}$, dissolution was attained by cooling the samples to 277K. POE samples of molecular mass 1000, 3000 and $1x10^6$ $gmol^{-1}$ were dissolved in doubly distilled water or sodium chloride solution at concentrations of 5 and 2.5 $mgmL^{-1}$ respectively. Calorimetric traces were recorded as described in Section 3 at a scan rate of 60 Kh^{-1}. The effect of scan rate (10, 20, 30, 45, 60 and 90 Kh^{-1}) was studied for POP 1000 $gmol^{-1}$ and reversibility ($\pm$30 Kh^{-1}) was studied for POP 1000 and 2000 $gmol^{-1}$. The effects of polymer concentration (2.5 - 50 $mgmL^{-1}$) was studied for POP 1000 $gmol^{-1}$. Mixtures of POPs were also investigated at a polymer concentration of 5 $mgmL^{-1}$ in double distilled water and at a scan rate of $60Kh^{-1}$.

4.3 Results and Discussion.

4.3.1 Polyoxypropylenes and polyoxyethylenes in water

The calorimetric traces obtained for the POP samples at a concentration of 5 $mgmL^{-1}$ in double distilled water and at a scan rate of 60 Kh^{-1} are shown in figure 4.1. The thermodynamic parameters associated with the observed phase transitions are shown in Table 4.2. The phase transition temperature (T_m), transition half-width ($\Delta T_{1/2}$) decrease with increasing molecular mass. The calorimetric enthalpy (ΔH_{cal}) and maximum excess heat capacity (C_p^{max}) increase with increasing molecular mass. The solutions were all observed to be transparent below the phase transition temperature and became turbid at the onset of the phase transition (from qualitative experiments using a waterbath). The phase transitions were reversible and not kinetically limited, as shown by identical transitions observed for the downscans for POP 1000 $gmol^{-1}$ and POP 2000 $gmol^{-1}$ at a scan rate of ± 30 Kh^{-1} (figure 4.2), the observation that the phase transition for POP 1000 $gmol^{-1}$ was unaffected by scan rate (10-90 Kh^{-1}, Table 4.3) within experimental error, and the reproducibility of the phase transition upon repeated upscans (data not shown). The effect of polymer concentration (2.5-51.5$mgmL^{-1}$, Table 4.4) show a decrease in T_m and an increase in ΔH_{cal} with increasing temperature, this merely reflects the temperature dependence of the aggregation process with polymer concentration. The HSDSC scans obtained are asymmetric with a pronounced leading edge. The leading edges do not however show any sudden changes and therefore indicate that the calorimeter is detecting an aggregation process. The HSDSC data also include a gently sloping negative curve on the post-transitional side of the phase transition which may be associated with the phase separation process. The observed decrease in T_m with increasing molecular mass is a trend also encountered in the clouding phenomenon of POE systems.[22] It may be explained by the fact that the decrease in entropy associated with the structured water surrounding the chains is offset by a gain in combinatorial entropy of mixing, given by the Flory Huggins theory.[1] This is largest for small polymer chains. Small POE chains therefore have relatively smaller negative entropies of mixing with water compared to larger molecules. The entropy gain arising from hydrophobic interaction during aggregation and eventually phase separation thus tends to be smaller for small molecules compared to larger molecules and is thus offset to higher temperatures.

Thermodynamic parameters normally associated with descriptions of transition co-operativity, C_p^{max} and $\Delta T_{1/2}$ indicate that as molecular weight increases cooperativity of the transition increases. This is demonstrated by increasing values for C_p^{max} and decreasing values for

$\Delta T_{1/2}$ as molecular mass increases. For studies on thermodynamically reversible phase transitions of proteins, Sturtevant[37] points out that this is indicative of intermolecular cooperation; and in such a case the calculated ratio of $\Delta H_{vH}/\Delta H_{cal}$ is a reflection of the number[38] of molecules which cooperate in the transition. The ratio is an indication of the base molar mass referred to in the enthalpy units.[38] Determination of the ΔH_{vH} for the studies presented here and modelling of the observed temperature driven phase transition of POP's in aqueous solution are discussed in Chapter 8.

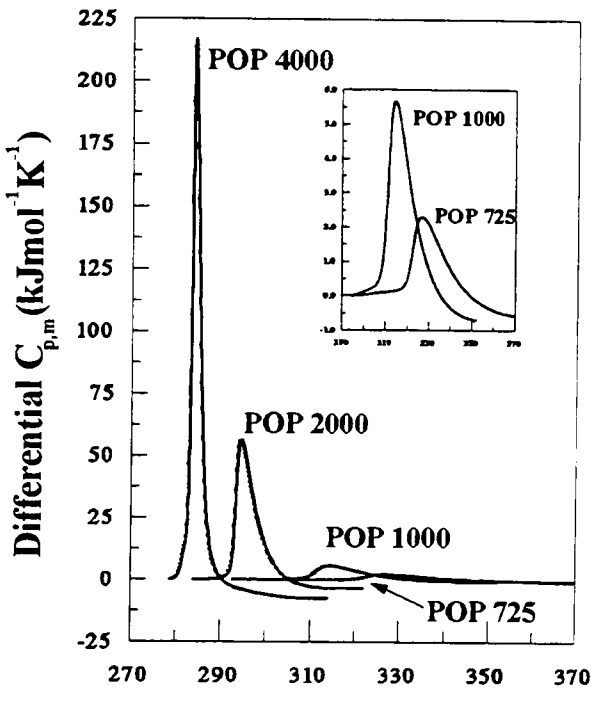

Figure 4.1 HSDSC scans of POP in double distilled water at a concentration of 5 mgmL^{-1}, at a scan rate of 60Kh^{-1}.

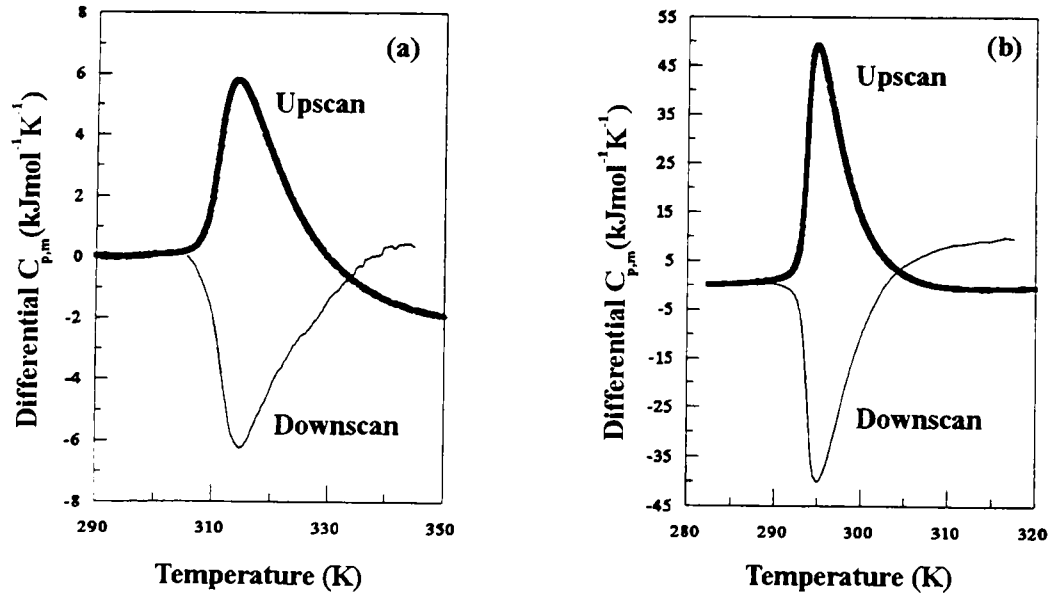

Figure 4.2 Reversibility of the phase transitions of (a) POP 1000 gmol^{-1} and (b) POP 2000 gmol^{-1}, at a concentration of 5 mgmL^{-1} in double distilled water, scanned at ±30Kh^{-1}.

For the POE's of low molecular mass, no phase transition was observed over the temperature range of study (275-370K). There is, however, a gradual increase in $C_{p,xs}$ with increasing temperature, which was observed for all POE homopolymers studied. Densitometric studies of low molecular mass POE (200-1000 $gmol^{-1}$) also showed no indication of a thermal phase transition or a conformational change,[39] but the hydration properties of POE altered depending on the degree of polymerisation. The gradual increase in $C_{p,xs}$ as a function of increasing temperature is in contrast to the negative change in $C_{p,xs}$ for the POP homopolymers at temperatures above the phase transition compared to the pre-transitional baseline. Literature evidence suggests that a positive increase in $C_{p,xs}$ is usually interpreted as being due to an increase in water structure,[40,41] which is often observed for the unfolding of proteins where the exposure of hydrophobic residues to the solvent results in an increase in water structure as compared with the pre-transitional state. A gradual increase in $C_{p,xs}$ may therefore reflect a gradual decrease in the hydrophilic nature of POE with increasing temperature due to increased molecular motion and disruption of the hydrogen bonds associated with the ether oxygens, precipitation then occurs at elevated temperatures (>370K) when the POE phase separates. At the point of complete phase separation, a negative change in $C_{p,xs}$ would therefore be expected, as the POE would partition into a polymer-rich phase as no further interactions would occur between the polymer and solvent. This observation may indeed be true for POP homopolymers, as the negative change in $C_{p,xs}$ from the pre- to post-transitional state may be interpreted as the formation of a separate polymer-rich phase resulting from hydrophobic dehydration of the POP. The CP of both POE and POP may not reflect complete phase separation, as from qualitative observations from waterbath experiments, POP of molecular mass 4000 $gmol^{-1}$ at a concentration of 5 $mgmL^{-1}$ in double distilled water forms two distinct phases at approximately 320K, an "oil phase" and a water phase, the "oil phase" being the polymer plus water. The turbidity of the water phase reflects the molecular mass distribution of the sample, as POP solubility decreases with increasing molecular mass. Also, the observation, that complete phase separation does not occur at the observed phase transition of POP, suggests that a number of monomer units at each end of the polymer chain remain hydrated and hence maintain a colloidal suspension of the precipitated polymer, and that this supramolecular structure only undergoes complete phase separation into the native form of the polymer (viscous oil) at temperatures in excess of the observed phase transition. For the POP samples, the qualitative observation from waterbath experiments could not be identified from the calorimetric output, and therefore, it is possible that the process is either of very low enthalpy and beyond the limits of detection of the calorimeter, or the process is a gradual

process that occurs over a broad temperature range.

4.3.2 **The effects of sodium chloride on high molecular mass polyoxyethylene.**

Calorimetric studies of POE of molecular mass $1x10^6$ $gmol^{-1}$ revealed a phase transition upon addition of sodium chloride, which was observed to decrease in temperature with increasing concentration of sodium chloride. The calorimetric scans of POE of molecular mass $1x\ 10^6$ $gmol^{-1}$ (Polyox-WSR 301) at a concentration of 2.5 $mgmL^{-1}$ are shown in Figure 4.4. The lower concentration was selected due to the high viscosity of samples at higher concentrations which would result in poor thermal mixing within the calorimetric cell during a scan. The observed phase transition corresponded to the CP of the polymer from qualitative experiments using a waterbath. The observed phase transitions were of low enthalpy, (the exact enthalpy values could not be determined due to a large $\Delta C_{p,d}$ or large change in the post-transitional baseline). The phase separation of POE is characterised by a very small enthalpy, a relatively large positive increment in apparent $C_{p,xs}$ and a long gently sloping "tail" which is a manifestation of the temperature dependence of the excess heat capacity[37] and may represent, mechanistically, the changing composition of the dilute and polymer-rich phases. A decrease in the transition temperature with increasing molecular mass has been encountered in POE systems.[22] It may be explained by the fact that the decrease in entropy associated with the structured water surrounding the chains is offset by a gain in combinatorial entropy of mixing, given by the Flory-Huggins theory.[1] This is largest for small polymer chains. Small POE chains therefore have relatively smaller negative entropies of mixing with water compared to larger molecules. The entropy gain arising from hydrophobic interaction during aggregation and eventually phase separation thus tends to be smaller for small molecules compared to larger molecules and is thus offset to higher temperatures. The Lund group[42,43] have interpreted the thermal behaviour of POE in terms of conformational adaptation. They argue that at low temperatures polar conformers of the polymer chains are favoured. At higher temperatures, however, non-polar conformers predominate. Conformational changes also occur in the absence of water[43] which precludes any suggestion that changing interaction

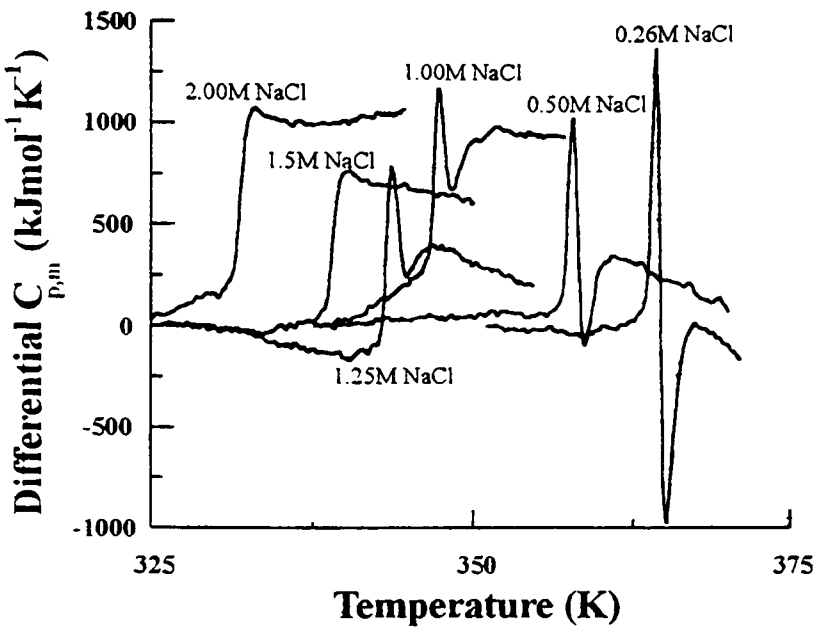

Figure 4.4 Calorimetric traces obtained for POE of molecular mass $1x10^6$ gmol^{-1} at a concentration of 2.5 mgmL^{-1} in aqueous sodium chloride solution, at a scan rate of 60 Kh^{-1}.

with water is the driving force for conformational change. However, it is likely that the decrease in polarity associated with the thermally induced change in conformation will affect interaction with water. Similar arguments have been presented by Hergeth *et.al.* for phase separation observed for poloxamers.[44] The effect of depression of the cloud point temperature by added cosolutes was observed by Karlström *et.al.*[45] The effect of adding a cosolute more polar than water (e.g. NaCl) will preferentially interact with water and thereby make the solvent more polar. This interaction increases the polarity difference between the polymer and water and hence the cloud point temperature is observed to be lowered.[45] It was also shown that compounds that decrease the polarity of water (e.g. salts with large negative ions I^-, SCN^-) would increase the CP temperature. The effect of cosolutes on the clouding of POE can be described by partitioning, that cosolutes depleted at the polymer (e.g. NaCl) will decrease the CP while those enriched will increase the CP. Large monovalent ions bind to the polymer which causes an effective polymer-polymer repulsion and an increase in CP. The effects of salts on the CP of high molecular mass POE has been shown to be comparable to the Hofmeister series for proteins[9] and follows the order for solutes at constant ionic strength:

Anions: $OH^- > F^- > CO_3^{2-} = SO_4^{2-} > Cl^- > PO_4^{3-} > Br^- = ClO_3^-$

Cations: $K^+ = Na^+ > Li^+ > Ca^{2+} = Mg^{2+} > Zn^{2+} > H^+$

For any given cation, the effectiveness of the salt in lowering the cloud point temperature increases as the ionic radius of the anion increases.[9] The electrostatic theories of Debye and McAulay and Debye[46,47] describe the salting in and out effects in terms of dielectric effects. They predict that a given nonelectrolyte is salted in by all electrolytes if it raises the dielectric constant of the solvent. If it lowers the dielectric constant, it is salted out by all elecrolytes. However, the electrostatic theories do not account for the observations by Schott[16] that some electrolytes raised the CP of OE-surfactants, whereas other electrolytes of the same valency lowered the CP. The complex formation between cations and POE increase the solubility of the polymeric chain and hence raise the CP.[16,17] Only Na^+, K^+, NH_4^+, and Cs^+, which do not

form complexes with model ethers, lower the CP[48]. Anions that enhance the structure of water compete with the POE for water of hydration (F^-, Cl^-, SO_4^{2-}, PO_4^{3-}, OH^-) lower the CP, and water structure breakers (I^-, SCN^-, ClO_4^-) promote hydrogen bonding between POE-water and thereby increase the solubility of the POE and raises the CP.[16,17,48,49] The observation that NaCl lowers the CP of POE is merely a manifestation of the competition between ether oxygens and Cl^- and Na^+ ions for available water of hydration, these ions decrease hydrogen bonding between POE and water, and hence decrease the solubility of POE.

4.3.3 **Polyoxypropylene Mixtures.**

Mixtures of POP's of molecular mass 725, 1000, 2000 and 4000 $gmol^{-1}$ and poloxamer P237 were mixed in pairs at a concentration of 5 $mgmL^{-1}$ and HSDSC scans were performed at a scan rate of 60 Kh^{-1}. The phase transition temperatures for each mixture are shown in Table 4.5. For each pair, two phase transitions were observed, showing that the formation of mixed aggregates did **not** occur, but the polymer chains aggregate and phase separate independently of one another. The phase transition temperature for the polymer with the higher molecular mass in each pair was unaffected, but the lower molecular mass copolymer showed a slight decrease in T_m when the co-polymer solute was close in molecular mass. Poloxamer 237 had no effect on the T_m of the POP's studied. The observation that only copolymers with closely related molecular masses slightly depressed the T_m of the lower molecular mass polymer may be due to the changes associated with the solvent following partial dehydration of the POP. It is possible that prior to complete phase separation, the partially hydrated POP polymer increases the order of the solvent and hence a less polar conformation of the hydrated POP chain is favoured. As a consequence, the phase transition temperature of the lower molecular mass POP is depressed. In the case of a large difference in molecular mass (e.g. POP 725 and POP 4000 $gmol^{-1}$), the observation that the T_m is unchanged for both polymer samples is indicative that the larger molecular mass POP has completely phase separated and no longer interacts with the solvent, the only solvent-polymer interactions are between the lower molecular mass POP and solvent, and hence the phase behaviour of the polymer mixture behaves as independent polymer-water mixtures.

4.4 Tables

Table 4.2 Thermodynamic parameters for the solution-phase transitions of POP at a concentration of 5 $mgmL^{-1}$ in double distilled water, at a scan rate of $60Kh^{-1}$.

POP ($gmol^{-1}$)	T_m (K)	ΔH_{cal} ($kJmol^{-1}$)	C_p^{max} ($kJmol^{-1}K^{-1}$)	$\Delta T_{1/2}$ (K)	ΔS_{cal} ($Jmol^{-1}$)
725	327.0	30	2.1	13.8	94
1000	314.0	65	5.6	10.7	209
2000	294.5	268	54.2	4.3	912
4000	284.1	520	215.9	2.0	1833

Table 4.3 The effects of scan rate on the thermodynamic parameters for the solution-phase transition of polyoxypropylene (1000 $gmol^{-1}$) in double distilled water at a concentration of 5 $mgmL^{-1}$.

Scan Rate (Kh^{-1})	T_m (K)	ΔH_{cal} ($kJmol^{-1}$)	C_p^{max} ($kJmol^{-1}K^{-1}$)	$\Delta T_{1/2}$ (K)	ΔS_{cal} ($Jmol^{-1}$)
10	314.0	69	5.6	11.0	218
20	314.2	69	5.7	10.9	219
30	314.2	68	5.6	10.9	217
45	314.2	68	5.6	11.2	218
60	314.0	66	5.6	10.7	209
90	314.3	61	5.4	10.3	193

Table 4.4 The effects of polymer concentration on the thermodynamic parameters for the solution-phase transition of polyoxypropylene (1000 $gmol^{-1}$) at a scan rate of 60 Kh^{-1}.

Conc. ($mgmL^{-1}$)	T_m (K)	ΔH_{cal} ($kJmol^{-1}$)	C_p^{max} ($kJmol^{-1}K^{-1}$)	$\Delta T_{1/2}$ (K)	ΔS_{cal} ($Jmol^{-1}$)
2.5	318.2	66	4.7	12.3	206
5.0	314.0	66	5.6	10.7	209
10.0	310.6	85	7.1	10.4	274
20.0	307.1	86	8.4	8.9	279
30.6	304.9	97	10.2	8.3	319
51.5[(1)]	302.3	99	11.0	7.8	327

[(1)] Scan Rate = 45 Kh^{-1}

Table 4.5 The effects of polymer mixtures on the solution-phase transition temperature of POP at a concentration of 5 $mgmL^{-1}$ in double distilled water, and at a scan rate of 60 Kh^{-1}.

T_m of with ↓ → (K)	POP 725	POP 1000	POP 2000	POP 4000	P237
POP 725	327.2	314.1	320.4	322.7	326.9
POP 1000	314.1	314.0	(310.2)	312.0	313.8
POP 2000	294.9	294.8	294.5	294.1	294.8
POP 4000	284.0	284.0	283.9	284.1	-
P237	315.1	313.8	314.7	-	314.9

4.5 References

(1) Flory,P.J., *"Statistical Mechanics of Chain Molecules"*, Hanser Publishers, New York, **1989**, 165.
(2) *"Poly(Ethylene Glycol) Chemistry: Biotechnical and Biomedical Applications"*, Milton Harris (Ed.), Plenum Press, New York, **1992**.
(3) Hill,F.N.; Bailey,F.E.(Jr.); Fitzpatrick,J.T., *Ind.Chem.Eng.*, **1958**, *50(1)*, 5.
(4) Bailey,F.E.(Jr.); Powell,G.M.; Smith,K.L., *Ind.Chem.Eng.*, **1958**, *50(1)*, 8.
(5) Smith,K.L.; Van Cleve,R., *Ind.Chem.Eng.*, **1958**, *50(1)*, 12.
(6) *"Nonionic Surfactants"*, Schick,M.J. (Ed.), Marcel Dekker, New York, **1967**, 801.
(7) Donato,I.D.; Magazu,S.; Maisano,G.; Majolino,D.; Migiliardos,P.; Pollicino,A., *Mol.Phys.*, **1996**, *87(6)*, 1463.
(8) Bieze,T.W.N.; Barnes,A.C.; Huige,C.J.M.; Enderby,J.E.; Leyte,J.C., *J.Phys.Chem.*, **1994**, *98*, 6568.
(9) Bailey,F.E.(Jr.); Callard,R.W., *J.Appl.Polymer Sci.*, **1959**, *1(1)*, 56.
(10) Bailey,F.E.(Jr.); Callard,R.W., *J.Appl.Polymer Sci.*, **1959**, *1(3)*, 373.
(11) Bailey,F.E.(Jr.); Kucera,J.L.; Imhof,L.G.; *J.Polymer Sci.*, **1958**, *32(125)*, 517.
(12) Flory,P.J., *JACS*, **1940**, *62*, 1561.
(13) Rogers,J.A.; Tam,T., *Can.J.Pharm.Sci.*, **1977**, *12(3)*, 65.
(14) Hammes,G.G.; Schimmel,P.R., *JACS*, **1967**, *89(2)*, 442.
(15) Annable,T.; Ettelaie,R., *Macromolecules*, **1994**, *27*, 5616.
(16) Schott,H.; Han,S.K., *J.Pharm.Sci.*, **1975**, *64(4)*, 658.
(17) Schott,H.; Royce,A.E., *J.Pharm.Sci.*, **1984**, *73(6)*, 793.
(18) Schott,H., *J.Coll.Int.Sci.*, **1995**, *173*, 265.
(19) Florence,A.T., *J.Pharm.Pharmac.*, **1966**, *18*, 384.
(20) Malcolm,G.N.; Rowlinson,J.S., *Trans.Faraday Soc.*, **1957**, *53*, 92.
(21) Schmolka,I.J., *J.Am.Oil Chem.Soc.*, **1977**, *54*, 110.
(22) Kjellander,R.; Florin,E., *J.Chem.Soc.Faraday Trans.*, **1981**, *77*, 2053.
(23) Kao,K.N.; Constabel,F.; Michayluck,R.; Gamborg,O.L., *Planta*, **1974**, *120*, 215.
(24) Ahkong,Q.F.; Fisher,D.; Tampion,W.; Lucy,J.A., *Nature*, **1975**, *253*, 194.
(25) Pontecorvo,G., *Somat.Cell.Genet.*, **1975**, *1*, 397.
(26) Nagaoka,S.; Mori,Y.; Takiuchi,H.; Yakota,K.; Tazawa,H., Nishiumi,S., in *"Polymers as Biomaterials"*(Shalaby,S.W.; Hoffmann,A.S.; Ratner,B.D.; Horbett,T.A. Eds.), Plenum Press, New York, **1985**, 361.
(27) Hellsing,K., *J.Chromatogr.*, **1968**, *36*, 270.
(28) Ryle,A.P., *Nature*, **1965**, *206*, 1256.
(29) Bailey,F.E.(Jr.); Koleske,J.V., *"Poly(Ethylene Oxide)"*, Academic Press, New York, **1976**.
(30) Florin,E.; Kjellander,R.; Eriksson,J.C., *J.Chem.Soc.Faraday Trans.*, **1984**, *80*, 2889.
(31) Tjerneld,F., in *"Poly(Ethylene Glycol) Chemistry: Biotechnical and Biochemical Applications"* (Harris,M. Ed.), Plenum Press, New York, **1992**, 85.
(32) Harris,J.M.; Case,M.G., *J.Org.Chem.*, **1983**, *48*, 5390.
(33) Harris,J.M.; Hundley,N.H.; Shannon,T.G.; Struck,E.C., *J.Org.Chem.*, **1982**, *47*, 4789.
(34) Harris,J.M.; Hundley,N.H.; Shannon,T.G.; Struck,E.C., in *"Crown Ethers and Phase Transfer Catalysis in Polymer Science"*, (Mathias,L.; Carreher,C.E., Eds.), Plenum Press, New York, **1984**, 371.
(35) Storks,C.; Liotta,C., *"Phase Transfer Catalysis"*, Academic Press, New York, **1978**.
(36) Bailey,F.E.(Jr.); Koleske,J.V., *"Alkylene Oxides and Their Polymers"*, Marcel Dekker, New York, **1991**.
(37) Sturtevant,J.M., *Ann.Rev.Phys.Chem.*, **1987**, *38*, 463.
(38) Blandamer,M.J.; Briggs,B., Brown,H.R.; Burgess,J.; Butt,M.D., Cullis,P.M.; Engberts,J.B.F.N., *J.Chem.Soc.Faraday Trans.*, **1992**, *88*, 979.
(39) Lorinczi,D., Tigyi,J.; Laggner,P., *"Water and Ions in Biological Systems"*, Birkhauser Verlag: Basel, **1988**, p387.
(40) Privalov,P.L., Gill,S.J., *Adv.Protein Chem.*, **1989**, *39*, 191.
(41) Privalov,P.L., *Annu.Rev.Biophys.Chem.*, **1989**, *18*, 47.
(42) Karlström,G., *J.Phys.Chem.*, **1985**, *89*, 4962.
(43) Björing,M.; Karlström,G.; Linse,P., *J.Phys.Chem.*, **1991**, *95*, 6706.

(44) Hergeth,W.-D.; Alig,I.; Lange,J.; Lochmann,J.R.; Scherzer,T.; Waterwig,S., *Makromol.Chem.Macromol.Symp.*, **1991**, *52*, 289.
(45) Karlström,G.; Carlsson,A.; Lindman,B., *J.Phys.Chem.*, **1990**, *94*, 5005.
(46) Harned,H.S.; Owen,B.B., "*The Physical Chemistry of Electrolytic Solutions*", Reinhold,New York, N.Y., **1958**. Chapters 3 and 12.
(47) Edsall,J.T.; Wyman,J., "*Biophysical Chemistry*", Academic Press, New York, N.Y., **1958**, Chapters 5 and 6.
(48) Schott,H., *J.Coll.Int.Sci.*, **1973**, *43*, 150.
(49) Schick,M.J., *J.Coll.Int.Sci.*, **1962**, *17*, 801.

CHAPTER 5 - POLYOXYETHYLENE-POLYOXYPROPYLENE DIBLOCK COPOLYMERS

5.1 Results and Discussion.

5.1.1 Diblock copolymers in water.

The phase behaviour of the 3 diblock copolymers was studied at a concentration of 5 $mgmL^{-1}$ in double distilled water at a scan rate of 60 Kh^{-1}. The calorimetric scans are shown in figure 5.1, and the thermodynamic parameters are shown in Table 5.1. The effect of scan rate (10, 30 and 60 Kh^{-1}) and reversibility (±30 Kh^{-1}) was studied for the diblock of molecular mass 13333 $gmol^{-1}$, the observed phase transition was unaffected by scan rate and was completely reversible on the downscan (Table 5.2) indicative that the phase behaviour of the diblock copolymer was not kinetically limited. The T_m and $\Delta T_{1/2}$ was observed to decrease with increasing molecular mass of the POP block. The ΔH_{cal} and C_p^{max} increased with increasing mass of the POP block. The observed phase transitions all show a steep leading edge and a gentle slope back to the baseline above the T_m indicative of an aggregation process.[1] The observed phase transitions differ from those observed for POP homopolymers in that clouding is not observed for the diblocks 8750 and 13333 $gmol^{-1}$, and is only observed for diblock 3438 $gmol^{-1}$. The higher molecular mass copolymers both possess a high percentage POE content (83 and 75% respectively). Based on the observation that the phase transition is consequent upon the processes of dehydration, aggregation and a conformational change of the POP moiety, by comparison with homopolymers, it is reasonable to assume that the solubility of the copolymer is maintained above the T_m by the POE blocks, the structures formed in solution are probably similar to those for poloxamers. A direct comparison of the aqueous solution phase behaviour of a triblock and diblock copolymer of near identical molecular mass and OE/OP ratio by light scattering and surface tension techniques showed that both the diblock and triblock copolymer behaved identically [2] The composition of the copolymers were $OE_{26}OP_{29}$ and $OE_{14}OP_{30}OE_{14}$ from GPC and NMR analyses. Both copolymers were observed to undergo a temperature driven micellisation between 298-308K at a concentration of 15 and 18 $mgmL^{-1}$ for the diblock and triblock copolymer respectively. The only major difference between the micellisation behaviour of the two copolymers was that

the diblock copolymer formed more closely packed aggregates than the triblock copolymer, determined from the average area per molecule from surface tension measurements.

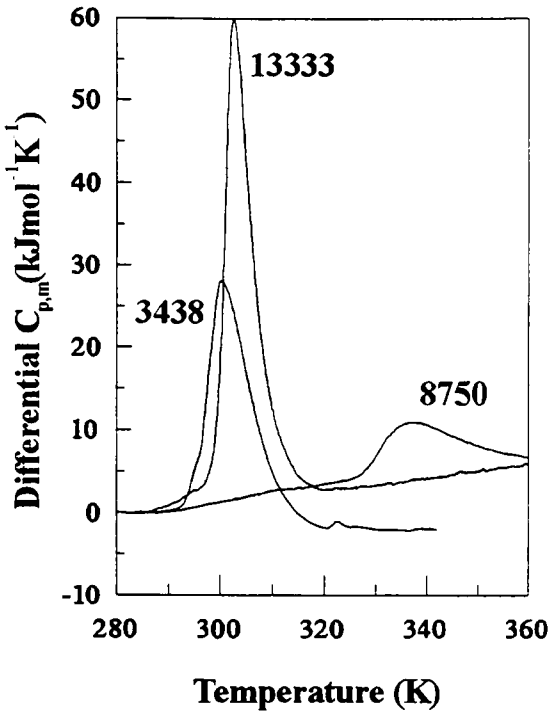

Figure 5.1 Calorimetric scans of diblock copolymers in double distilled water at a concentration of 5 mgmL^{-1} and at a scan rate of 60 Kh^{-1}. (Each scan is identified by the molecular mass of the copolymer)

Comparison of the solution behaviour of oxybutylene(OB)-POE triblock and diblock copolymers showed that the micellisation behaviour of the two copolymers was near identical, but the diblock copolymer for much larger micelles than the triblock copolymer.[3] Cyclisation of the central core of OB for the triblock copolymer did not alter the cmc but increased the micellar volume compared to the linear triblock copolymer,[4] this effect was probably due to less efficient packing of the micellar core of the cyclic OB as anticipated, but the cmc was about 10 times larger than the diblock OB-OE.[4] Modelling of the aqueous solution behaviour of diblock and triblock OP-OE copolymers of a comparable group of copolymers of fixed OP/OE ratio and molar mass (diblock, poloxamer and a reverse poloxamer - meroxapol) was investigated.[5] These three copolymers possess the same solubility in the Flory-Huggins model, however, there was a 5 fold increase in the cmc between the diblock and meroxapol, and the cmc of the poloxamer was 2 fold lower than the meroxapol. The diblock was shown to have a much greater aggregation number than the triblock copolymers (80 compared to 20-40) at 320K, the aggregation number of the two triblock copolymers were comparable but were greater for the meroxapol.[5] The diblock copolymer was predicted to possess a more compact core than the triblock copolymer, and this was also reflected in the higher aggregation numbers of the diblock copolymers, this was concluded to be due to the loss of free energy and a doubling of the chain flux across the OP-OE interface region when compared to the triblock copolymers. The experimental studies comparing a diblock and poloxamer of equal molar mass and OP/OE ratio did not confirm the calculated difference in

cmc, although the increased aggregation number and a more compact micellar core were observed for the diblock copolymer.[3]

5.2 Tables

Table 5.1 Thermodynamic parameters for the solution-phase transitions of POP-POE diblock copolymers in double distilled water at a concentration of 5 $mgmL^{-1}$, at a scan rate of 60 Kh^{-1}.

Molecular Mass ($gmol^{-1}$)	OE:OP Ratio	T_m (K)	CP (K)	ΔH_{cal} ($kJmol^{-1}$)	C_p^{max} ($kJmol^{-1}K^{-1}$)	$\Delta T_{1/2}$ (K)	ΔS_{cal} ($Jmol^{-1}K^{-1}$)
3438	0.33:1	300.2	294.2	244	26.6	8.3	812
8750	5:1	336.5	>370	90	5.5	15.6	268
13333	3:1	302.5	>370	347	55.5	5.4	1146

Table 5.2 The effects of scan rate and reversibility of the solution-phase transition of POP-POE diblock copolymer (13333 $gmol^{-1}$) in double distilled water at a concentration of 5 $mgmL^{-1}$.

Diblock Copolymer	Scan Rate (Kh^{-1})	T_m (K)	ΔH_{cal} ($kJmol^{-1}$)	C_p^{max} ($kJmol^{-1}K^{-1}$)	$\Delta T_{1/2}$ (K)	ΔS_{cal} ($Jmol^{-1}K^{-1}$)
13333	+10	302.4	331	55.5	5.2	1092
13333	+30	302.6	347	56.2	5.4	1146
13333	-30	302.7	350	48.8	6.0	1159

5.3 References.

(1) Sturtevant,J.M., *Ann.Rev.Phys.Chem.*, **1987**, *38*, 463.
(2) Yang,L.; Bedells,A.D.; Attwood,D.; Booth,C., *J.Chem.Soc.Faraday Trans.*, **1992**, *88(10)*, 1447.
(3) Yang,Z.; Pickard,S.; Deng,N.J., Barlow,R.J.; Attwood,D., Booth,C., *Macromolecules*, **1994**, *27(9)*, 2371.
(4) Yu,G,E.; Yang,Z.; Attwood,D.; Price,C.; Booth,C., *Macromolecules*, **1996**, *29(26)*, 8479.
(5) Linse,P., *Macromolecules*, **1993**, *26*, 4437.

CHAPTER 6 - POLYOXYETHYLENE-POLYOXYPROPYLENE-POLYOXYETHYLENE TRIBLOCK COPOLYMERS (POLOXAMERS)

6.1 Calorimetric Studies

6.1.1 Results and Discussion.

6.1.1.1 Poloxamers at 5mgmL^{-1} and Constant Oxypropylene Concentration

The HSDSC outputs for the poloxamers in double distilled water at a concentration of 5 mgmL^{-1} are shown in figure 6.1 and the thermodynamic parameters associated with the phase transitions are shown in Table 6.1, and at constant oxypropylene concentration in Table 6.2. The observed transitions are asymmetric with a steep leading edge and a gentle slope back to the baseline above the T_m indicative of an aggregation process.[1-3] The observed phase transitions were reversible and unaffected by scan rate (10, 30 and 60 Kh^{-1}) indicative that the phase transitions are not kinetically limited (Figure 6.3).[1-3] From the data in Table 6.1, the T_m and $\Delta T_{1/2}$ decrease while the ΔH_{cal} and C_p^{max} increase with increasing molecular mass of the hydrophobic POP block. The phase transitions for the poloxamers with a POP content of 1200 gmol^{-1} show an increase in T_m with increasing mass of the POP block, which is an opposite trend for all other homo- and co-polymer samples studied, and no explanation is offered for this observation. The dependence of the phase transition on the POP content of the poloxamers can be shown from a plot of T_m versus POP or POE content (figure 6.2), the figure clearly shows that there is a strong dependence of T_m on the POP content with a r^2 value of 0.98. The plot of T_m versus POE content gives a scatter with no apparent relationship. A plot of ΔH_{cal} per average monomer unit versus oxypropylene/oxyethylene ratio (Figure 6.4) shows a log-linear relationship which approaches zero as the ratio approaches 0:1 i.e., POE homopolymer, indicative that the observed phase transition is consequent upon changes associated with the hydrophobic POP block only. The changes in pre- and post-transitional baselines ($\Delta C_{p,d}$)appear to be dependent on the percentage content of POE (figure 6.1), the values are not presented as the post-transitional baseline varies as a function of temperature. The $\Delta C_{p,d}$ values change from a negative value to a positive value as the percentage POE increases. The literature suggests that a positive $\Delta C_{p,d}$ value is usually interpreted as being due to an increase in water structure,[1-3] which is observed when

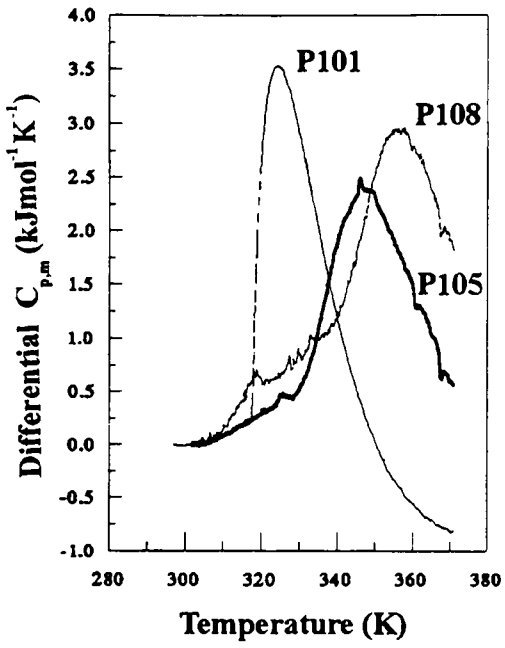

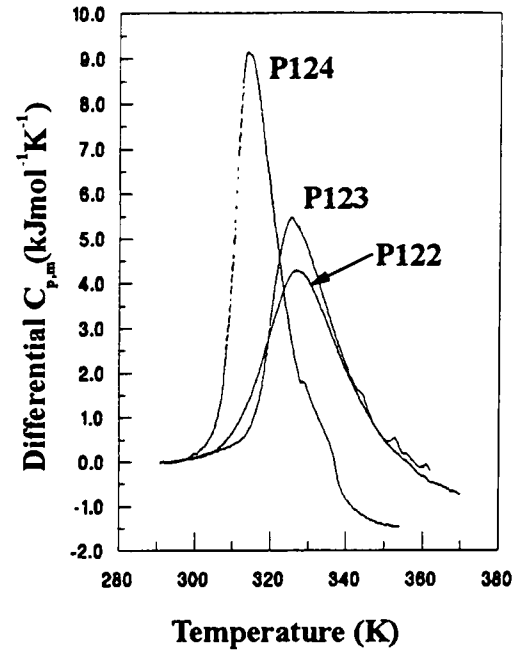

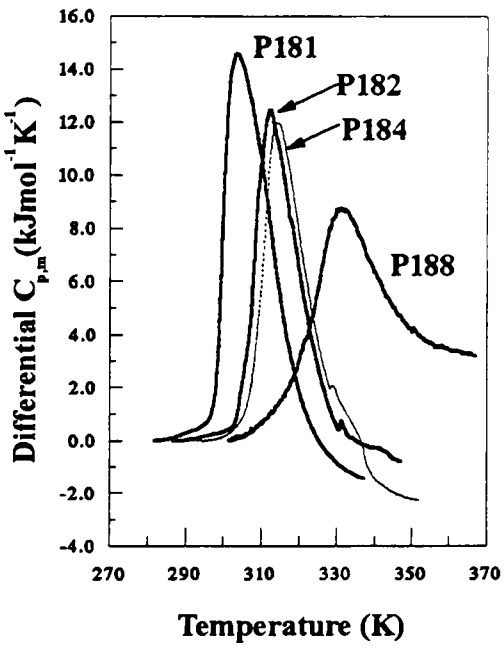

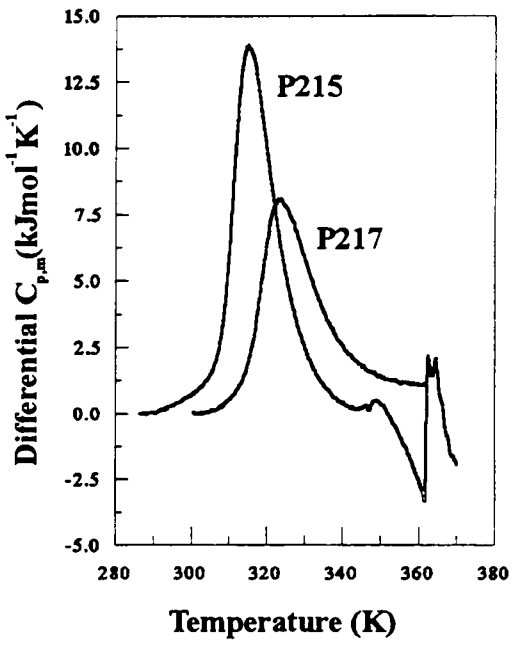

Figure 6.1a Calorimetric traces of poloxamers in double distilled water at a concentration of 5 mgmL^{-1}, scanned at 60Kh^{-1}.

hydrophobic residues are exposed to water. In the case of POP homopolymers a large negative $\Delta C_{p,d}$ is observed which is consequent upon desolvation of the relatively hydrophobic POP block, and for low POE homopolymers a gradual increase in $C_{p,xs}$ is observed with increasing temperature (figure 4.3). Thus for the poloxamers a combination of an increasing negative $\Delta C_{p,d}$ due to desolvation of the POP block and an increasing $C_{p,xs}$ due to increasing order of the water structure surrounding the POE block is observed. The resultant calorimetric traces for poloxamers are observed to yield both positive and negative values of

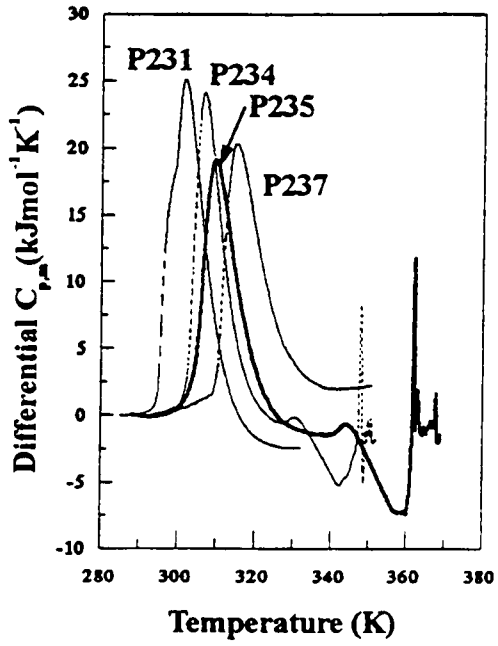

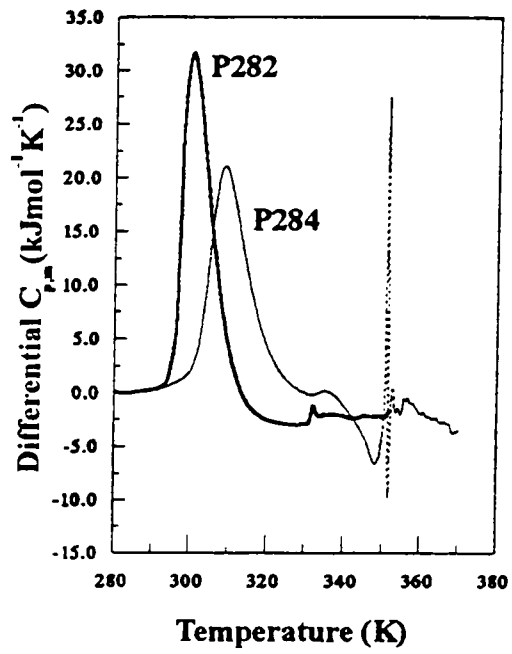

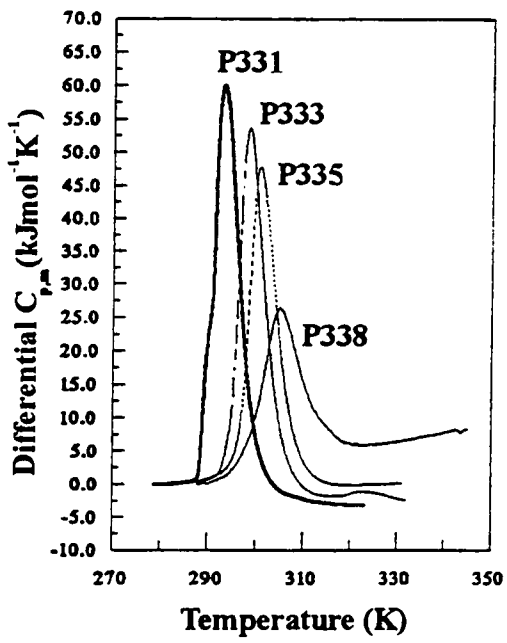

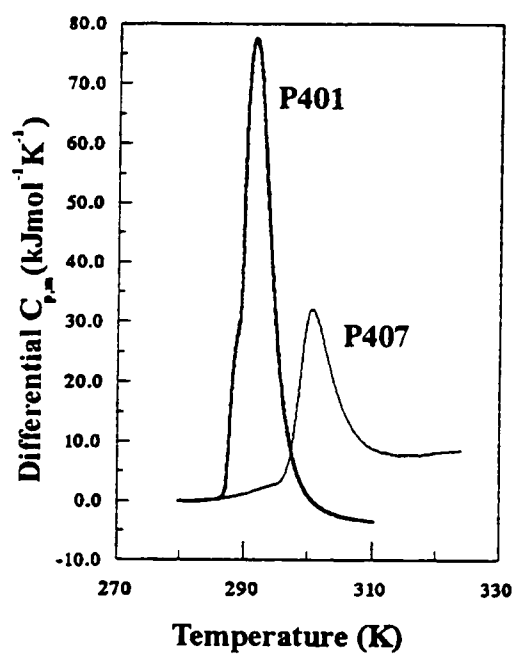

Figure 6.1b Calorimetric traces of poloxamers in double distilled water at a concentration of 5 mgmL^{-1}, scanned at 60Kh^{-1}.

$\Delta C_{p,d}$ for the poloxamers with a high and low percentage POE content respectively. The data in Figure 6.5 have been produced by calculating the average calorimetric enthalpy associated with a OP unit for each of the differing series of polymers. The series members are identified as those polymers containing the same fraction of OE but which have varying total molar masses. This calculation effectively assigns the total calorimetric enthalpy to the OP portion of the polymers. The excellent linearity (regression coefficient -0.992) suggests that indeed there is a unifying behaviour which aligns the HSDSC data for these twenty five polymers in a systematic fashion. Of course the slope of this plot is, then, the average enthalpy per OP unit per fraction of OE content. Thus the **magnitude** of this enthalpy depends upon the OE fraction but the **change** in enthalpy is dependent upon the OP content.

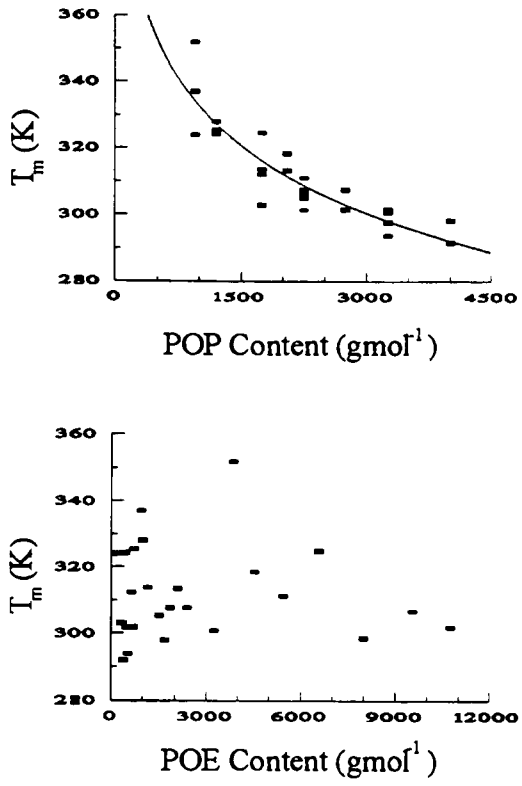

Figure 6.2 The relationship between the phase transition temperature and POE or POP content of the poloxamers for the phase transitions obtained at a concentration of 5 mgmL^{-1} in double distilled water and at a scan rate of 60 Kh^{-1}.

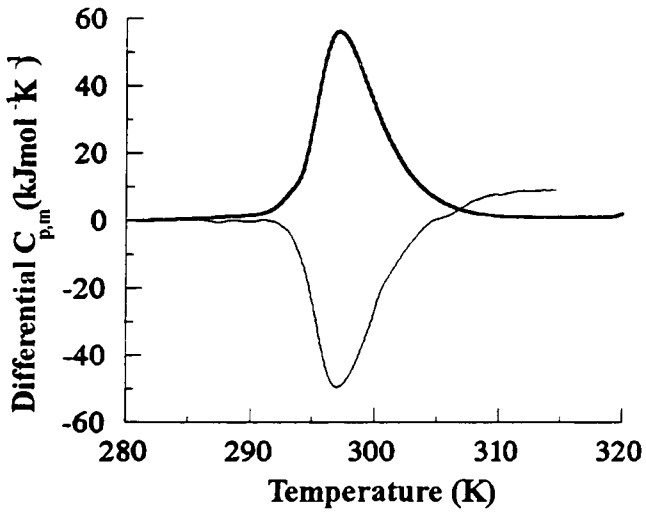

Figure 6.3 Calorimetric scan to show the reversibility of the phase transition of poloxamer P333 in double distilled water at a scan rate of ±30 Kh^{-1}.

The intercept value of approximately 5 kJ (unit of OP)$^{-1}$ may, therefore, be regarded as the calorimetric enthalpy per OP in the absence of **any** OE. It appears, therefore, that the relationship displayed in Figure 6.5 does indeed provide a means of systematising the behaviour of all the pluronics and that it offers some means of predicting properties of POP based polymers.

For the 25 poloxamers examined, the analysis of their solution behaviour on the basis of a fixed physical concentration (5 mgmL^{-1} , Table 6.1) and at a fixed OP monomer unit concentration (5 mgmL^{-1} , Table 6.2) has allowed an insight into their phase behaviour from the following groupings:

(i) Constant POP molecular mass e.g., P231, P234, P235, P237 and P238.

(ii) Constant POE percentage content e.g., P101, P181, P231, P331 and P401.

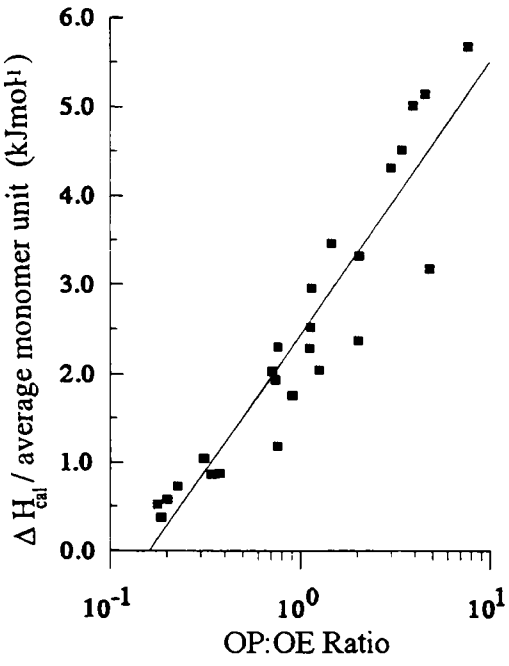

Figure 6.4 A plot to show the relationship between the calorimetric enthalpy per average monomer unit versus oxypropylene/oxyethylene ratio.

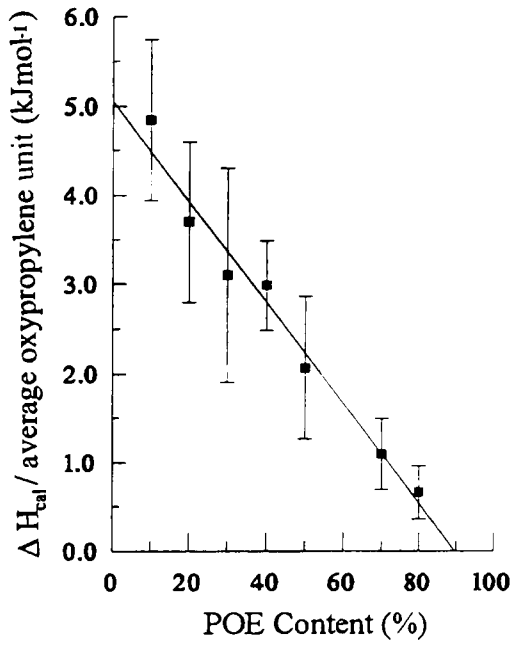

Figure 6.5 A plot to show the relationship between the calorimetric enthalpy per average oxypropylene unit, averaged for each series of poloxamer, plotted against the percentage POE content.

The first grouping allows an insight into the contribution from the OE content of the poloxamers to the phase transition. The second grouping allows an insight into the effect of molecular mass on the observed phase transition, as the OE/OP ratios are directly comparable. The data is again analysed in terms of thermodynamic parameter e.g., ΔH_{cal} versus POP content, OP/OE mass or number ratio. Overall, the comparison between the thermodynamic parameters at constant physical concentration (5 mgmL^{-1}) and constant OP concentration, show that the trends are the same for each experimental condition. For example, the relationship for ΔH_{cal} per average monomer unit versus OE/OP ratio (Figure 6.4) is the same for both experimental conditions. The lower values of T_m and higher values of ΔH_{cal} at constant OP concentration compared to the values at 5 mgmL^{-1} are explained by the equilibrium $nX \leftrightarrow X_n$ (where X = copolymer chain). The effect of concentration on T_m being an effect of an increase in the concentration of the starting species (single, hydrated copolymer chains) forces the equilibrium in the direction of producing more aggregates. Since the aggregation process is endothermic this must result in a decrease in temperature at which the

transition occurs. The corresponding increase in ΔH_{cal} with increasing concentration is merely a manifestation of the temperature dependence on this enthalpy value.

The contribution from the POE content of the poloxamers to the observed phase transition can be analysed from grouping (i) above. From Figure 6.1, it can be seen that with increasing POE content, T_m increases slightly, $\Delta T_{1/2}$ increases and ΔH_{cal} decreases. However the effects are of a far smaller magnitude than of the dependence of the phase transition on the POP content. The POE has an apparent minor contribution to the overall phase transition although the hydrophilic POE allows the copolymer aggregate to remain in solution when the POE content is greater than 20%. It is apparent, however, that the temperature difference between the cloud point and T_m (ΔT) is dependent on the POE content **only** (Figure 6.6). This observation may reflect the fact that the limit on solubility of the aggregated molecular clusters is dependent on the relative length of the hydrated POE chains. Thus as the molecular aggregates increase in size, with increasing temperature, there must be a limiting size of aggregate dependent on the relative length of the POE block, before the dehydrated POP blocks are exposed to the bulk phase resulting in the observed cloud point. Above the cloud point temperature, the POE blocks remain in solution until a temperature is reached which corresponds to the cloud point of the POE blocks and therefore complete phase separation occurs.

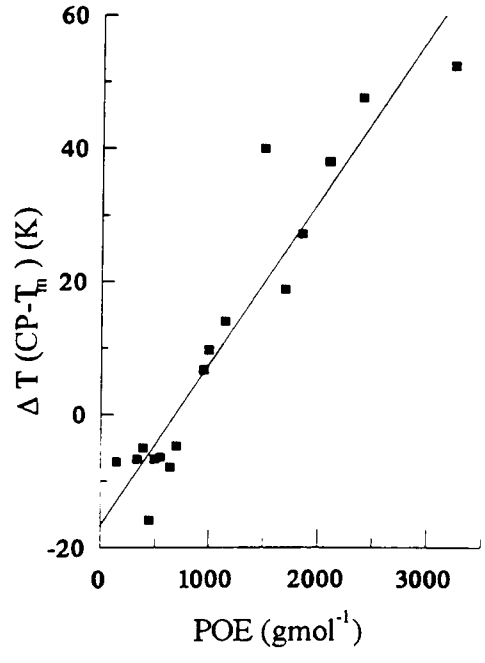

Figure 6.6 A plot to show the dependence of the difference between the cloud point and phase transition temperature on the POE content of the poloxamers.

The observation that the temperature driven phase transition of poloxamers in aqueous solution occurs as a consequence of changes with the POP moiety has been confirmed using a variety of techniques (summarised in Table 1.3.3 and in several reviews[4-6]). The phase change associated with increasing temperature occurs over a wide temperature range for all of the poloxamers studied, and this has been attributed to the polydispersity of the copolymer sample[4] as low molecular mass surfactants (e.g., SDS) tend to display a sharp cmc or cmt. However, for other surfactants where the hydrophobic moiety posses no water solubility (e.g., alkane chain), one would expect an aggregation process to be rapid, highly cooperative, and occur over a narrow concentration/temperature range. For poloxamers, the hydrophobic POP moiety does possess limited water solubility, and for aggregation of the POP chains to occur, the weakly hydrated POP chains must also dehydrate to facilitate micelle formation. Also, as the hydrophilic POE chains are large relative to the ionic groups for other surfactant systems (e.g., SO_4^{2-}) then steric reasons may also interfere with the rate of aggregation. Therefore, the nature of the hydrophobic moiety rather than the polydispersity of the sample may reflect the broad temperature range over which the phase change is observed in dilute aqueous solution, although the polydispersity may be a small contributing factor to a widening of the temperature range of the phase transition.

Light scattering studies have shown that the phase change for poloxamers in aqueous solution consists of an equilibrium between several species in solution, reflecting a gradual change in equilibrium with a change in temperature/concentration.[5,7-31] Brown et al[19] showed for P235 at a concentration of 4.8% (w/v) in aqueous solution that at low temperature (< 288K) only one species existed with a hydrodynamic radius of approximately 18Å corresponding to monomers. With increasing temperature, two distinct populations were observed with hydrodynamic radii of 18Å and 80Å corresponding to monomers and micelles. The concentration of micelles increased with increasing temperature, and at 313K only micelles were observed. The authors noted that at infinite concentration, the hydrodynamic radii for micelles remained constant over the temperature range studied (up to 323K), but at higher concentrations a gradual increase in micellar size was observed with increasing temperature. Similar observations have been made using light scattering for P184,[15,21] but both groups observe an exponential increase in micellar size with increasing temperature as opposed to the linear increase observed for P284[12] P235[19] and P188[32]. The hydrodynamic radius was observed to remain relatively constant with increasing temperature, but the aggregation number increased significantly.[7,32] The calorimetric studies presented here show

that the increase in micellar size with increasing temperature is calorimetrically silent, this is indicative that the increase in micellar size represents the aggregation of micelles, with the POP portions of the polymer in the aggregated form, with no further dramatic phase change occurring up to the cloud point. The phase transition observed by HSDSC must therefore represent the initial formation of micellar aggregates, and also from ^{13}C-NMR data the initial phase transition is reflected in a sharp change in T1 relaxation times for the OP(Me) group, but at elevated temperatures, no further dramatic change is observed for the POP block.[33] The observed trend of decreasing transition temperature with increasing molecular mass of the POP block has been confirmed by others using the techniques of light and neutron scattering.[34]

Various fluorescent probes have been used to study the solution behaviour of poloxamers,[5,12,15,23,24,35-42] (pyrene,[12, 15, 39, 40, 41] 8-anilino-1-naphthalene sulphonic acid,[40] octadecylrhodamine-B,[25] KI-I_2,[42] bis(1-pyrenylmethyl)ether,[36] octadecyl rhodamine-B [37]]. However, as fluorescence techniques are invasive, the nature of the fluorescent probe must be considered as the aggregation behaviour of the poloxamers is sensitive to co-solutes. It may be anticipated that a very hydrophobic fluorescent probe may nucleate aggregation of the poloxamer and thus may yield results that do not accurately reflect the behaviour of the poloxamer due to the formation of mixed aggregates. This has been pointed out using the technique of diode array UV spectroscopy with an I_2 probe to study the aggregation behaviour of P237,[42] and it was concluded that the inclusion of I_2 produced no observable differences in the phase transition temperature to those observed by the non-invasive technique of HSDSC. The aggregation behaviour of a range of poloxamers (P185, P235, P333, P334, P335, P338 and P403) in aqueous solution were studied using the fluorescent probe pyrene.[24] In the absence of polymer, the eximer fluorescence decreases linearly with increasing temperature, but in the presence of poloxamer, a rapid change in fluorescence was observed over a narrow temperature range indicative of micelle formation. The midpoint of the phase transition observed for 0.5 and 1% solutions of P235, P333, P335 and P338 (302, 291, 293 and 302K respectively) are approximately 5-10K lower than the T_m values obtained by HSDSC (Tables 6.1, 6.2 and 6.5). The differences in the transition mid-point observed between the two techniques may be a reflection of differences between the polymer samples (from BASF and ICI), differences in the fraction of the sample that is being observed, and also that the process reflected by HSDSC may differ from that observed by the solubilisation of pyrene. HSDSC is a macroscopic technique and therefore detects any thermal event that occurs in the sample,

fluorescence spectroscopy reflects changes in the microenvironment surrounding the fluorescent probe. One would expect that the fraction within a copolymer with a higher molecular mass of the POP block sample would tend to aggregate prior to lower molecular mass POP blocks, and hence the changes in fluorescence may reflect the onset of aggregation of the fraction of the sample with a longer POP block rather than reflecting micellisation of the whole of the copolymer sample. This may partially reflect the difference observed between fluorescence and HSDSC data as well as the possible effect that hydrophobic molecules like pyrene would tend to nucleate micellisation in this system. For the poloxamers in micellar form, the intensity of the fluorescence of pyrene decreased in the order of P335>P235>P185 which reflected that the higher molecular mass copolymers exhibited more hydrophobic microdomains.[24] Other studies using fluorescent probes reflect changes in the microviscosity within the core of the copolymer micelle,[36,37] and show that with increasing temperature the microviscosity for P338 is comparable to that observed for POP homopolymers.[36] At 308K the microviscosity is comparable to that observed for POP 725 and at 323K exceeds the observed viscosity for POP 2000. This observation indicates that the micellar core of poloxamers becomes more compact with increasing temperature, this effect was confirmed by light scattering studies.[15,19,21] The increase in microviscosity due to the formation of a more compact structure within the copolymer micelle is calorimetrically silent as no significant change in the post-transitional baseline between the main phase transition and the cloud point is observed for the HSDSC or densitometric studies presented here.

Gel permeation chromatography has been used to study the aggregation behaviour of poloxamers in aqueous solution as a function of temperature.[43,44] For P237 at a concentration of 2.1mgmL^{-1} a single elution peak at different elution volumes was detected at 300 and 332K which was characteristic of single polymer chains and micelles respectively.[44] At 315K two elution volume peaks were detected characteristic of a mixture of unimers and micelles. The observations by GPC for P237 are comparable to the results obtained by HSDSC (Table 6.3). However, as the aggregation temperature of poloxamers in aqueous solution increases dramatically at concentrations <5mgmL^{-1} (Table 6.3), the comparison between GPC and other techniques for analysing the aggregation behaviour of poloxamers would prove difficult as the concentration of poloxamer will decrease as the copolymer passes through the column. Thus the concentration of copolymer loaded on the column or the eluent concentration may not reflect the relative amounts of unimer/micelle determined by other techniques (especially light scattering), but as a general comparison, the technique does

demonstrate the temperature dependence of the aggregation behaviour of poloxamers in aqueous solution. GPC studies for P407 at a loading concentration of 10mgmL^{-1} showed that the micelle form of the polymer was detected at 303K, below this temperature a single peak characteristic of unimers was detected. At 313K the elution profile indicated that the polymer was mostly composed of micellar aggregates.[43] The results for the aggregation behaviour of P407 are in contrast to the comparable results obtained for P237,[44] and occur at a higher temperature than observed by HSDSC over a concentration range of 2-20mgmL^{-1}. This may merely be a reflection of a more dramatic decrease in copolymer concentration as the sample passes down the column.

There are few calorimetric studies by other groups on the phase behaviour of poloxamers.[7, 45, 46] Wanka *et al.*[7] used several techniques to study the solution behaviour of P407, P403 and P334. Low sensitivity DSC detected an endothermic transition for the poloxamers in water at a concentration of 10-250mgmL^{-1}. The transition temperature decreased with increasing copolymer concentration in a linear manner and the shape of the endotherm was indicative of a first-order transformation. The enthalpy value reported[7] of 487kJmol^{-1} for P407 is considerably higher than enthalpy values determined by HSDSC (Table 6.3, 129-190 kJmol^{-1}). However, the enthalpy determined by HSDSC for P407, by comparison with other poloxamers, is lower than anticipated. This may be a reflection of the polydisperisty of the sample. There was no relationship observed between the enthalpy and POE content of the copolymers and was concluded to be due to a dehydration or "melting" of the OP groups.[7] Similar enthalpic values were obtained by Hecht and Hoffmann[45,46] for P407 and P403 (459 and 376kJmol^{-1}) and are comparable to HSDSC values for P401 (Table 6.1, 400kJmol^{-1}). The enthalpy determined for P238 (182kJmol^{-1})[45] is comparable to the enthalpy obtained by HSDSC (Table 6.1, 166kJmol^{-1}) and demonstrates that the thermal process detected by low sensitivity DSC at higher concentrations is essentially the same as the aggregation behaviour observed by HSDSC for poloxamers in dilute aqueous solution.

6.1.1.2 **Empirical Relationships.**

In order to demonstrate the contribution of the POP and POE blocks to the observed phase transition, multiple linear regression analysis has been performed of the form:

$$\text{Parameter} = a(\text{POP}) + b(\text{POE}) + c$$

where POP = molecular mass of the POP block ($gmol^{-1}$), POE = molecular mass of the POE block ($gmol^{-1}$), a,b and c = constants. This qualitative treatment of the data enables a prediction of the T_m and ΔH_{cal} for a theoretical poloxamer. However, it is immediately apparent that this treatment of the data has no real physical meaning, as the constants a,b and c are dimensionless and the POP and POE values are in terms of $gmol^{-1}$, also any parameter would have a value when the POP and POE values are zero, which is obviously meaningless. Despite this treatment being purely empirical and qualitative, r^2 values, the coefficient of determination and correlation of fit for ΔH_{cal} and $1/T_m$ are 0.986 and 0.999 respectively. For poloxamers, at a concentration of 5 $mgmL^{-1}$ in double distilled water, and scanned at a scan rate of 60 Kh^{-1} the following relationships hold:

$$\Delta H_{cal} = 0.117\,(POP) - 7.31x10^{-3}(POE) - 52.27 \qquad r^2 = 0.986$$

$$1/T_m = 3.54x10^{-4}\ln(POP) - 5.43x10^{-5}\ln(POE) + 9.07x10^{-4} \qquad r^2 = 0.999$$

The high r^2 values warrant these relationships being presented here. The contribution of POP and POE to both parameters is clearly demonstrated. ΔH_{cal} is dependent on the molecular mass of the POP block and increases relative to the molecular mass of POP block. ΔH_{cal} is slightly reduced in magnitude with increasing POE content, although the contribution is minimal relative to the hydrophobic POP. It is also clear that increasing POE content increases the T_m and this parameter is significantly lowered with increasing POP content.

6.1.1.3 **Effects of Copolymer Concentration.**

The effects of copolymer concentration were studied for poloxamer P237 over a concentration range of 1.0 to 50.0 $mgmL^{-1}$ and for poloxamers P333 and P407 over a concentration range of 0.1 to 20 $mgmL^{-1}$ in double distilled water, at a scan rate of $60Kh^{-1}$ The calorimetric traces observed for poloxamer P237 are shown in Figure 6.7 and the thermodynamic parameters for P237, P333 and P407 are shown in Table 6.3 The shape of the observed phase transition is the same for all concentrations examined, indicating that the underlying molecular process is the same for all concentrations studied. The phase transitions were reproducible, unaffected by scan rate and gave identical scans on the downscan, indicative that the transitions are reversible and not kinetically limited. The observed phase

transitions all have a steep leading edge and above the T_m a gentle slope back to the baseline indicative of an aggregation process.[1-3] The T_m decreases with increasing copolymer concentration (Figure 6.8), the log-linear relationship may reflect that at low copolymer concentrations (< 10 $mgmL^{-1}$) there may be a mixture of single copolymer chains and loosely associated copolymer clusters below the phase transition temperature, and at higher concentrations the copolymer may exist predominantly in the form of clusters. In both situations the POP block is in the hydrated form, as the ΔH_{cal} increases slightly and cooperativity remains virtually unchanged as a function of concentration. The decrease in T_m and increase in ΔH_{cal} merely reflects an effect of increasing the concentration of starting species (hydrated POP blocks) and thus forces the equilibrium in the direction of producing more aggregates (dehydrated POP blocks). Since the aggregation process is endothermic this must result in a decrease in temperature at which the transition occurs. The corresponding decrease in ΔH_{cal} is merely a manifestation of the temperature dependence of this enthalpy value.

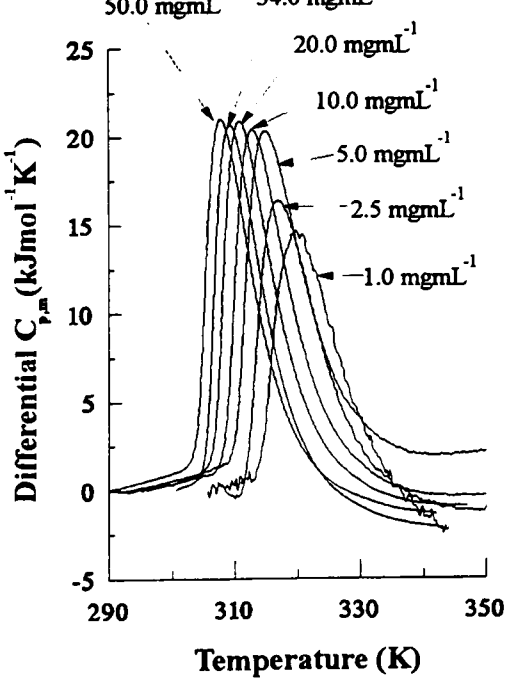

Figure 6.7 Calorimetric scans of poloxamer P237 at various copolymer concentrations (1.0 - 50.0 $mgmL^{-1}$) in double distilled water.

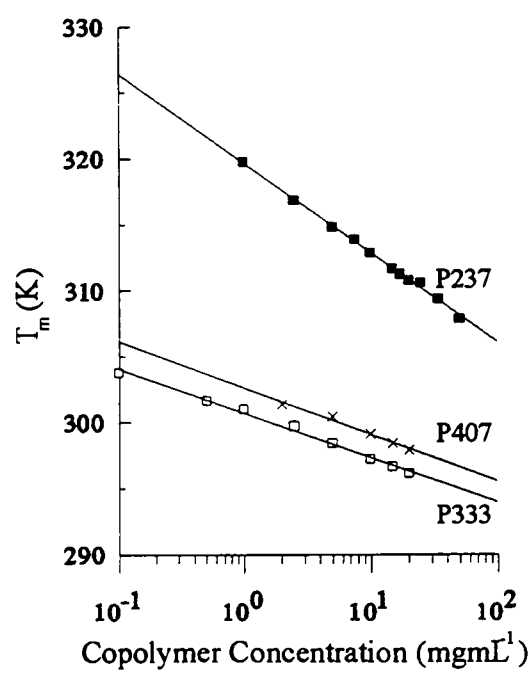

Figure 6.8 The effect of copolymer concentration on the phase transition temperature in double distilled water.

6.1.1.4 **Effects of Fractionation on Poloxamer 407**

Fractionation of P407 was attempted using a two phase separation technique (*Personal communication*, Booth,C., Manchester Polymer Centre) The method was based on the relative solubilities of the diblock and triblock copolymer in the immiscible solvents hexane and dichloromethane. The extraction was repeated twice, and the diblock-rich sample from the hexane layer was pooled and constituted 21% of the final yield. From GPC analysis (Figure 6.9), it can be seen that a lower molecular mass fraction is concentrated in the hexane fraction. From triangulation of the GPC outputs, the lower molecular mass product constitutes approximately 46% of the hexane fraction and 34% of the dichloromethane fraction, compared to 38% for the original unfractionated sample of P407. The calorimetric outputs and corresponding data (Figure 6.10 and Table 6.4) show that there is little difference between the unfractioned and fractioned samples of P407. The diblock rich fraction recovered from hexane showed a slightly lowered T_m , ΔH_{cal}, $\Delta T_{1/2}$ and ΔS. The observed reduction of these parameters of approximately 9% compared to the dichloromethane fraction and unfractioned P407 may be explained by an increase in a lower molecular mass triblock sample contained in the hexane partitioned fraction.

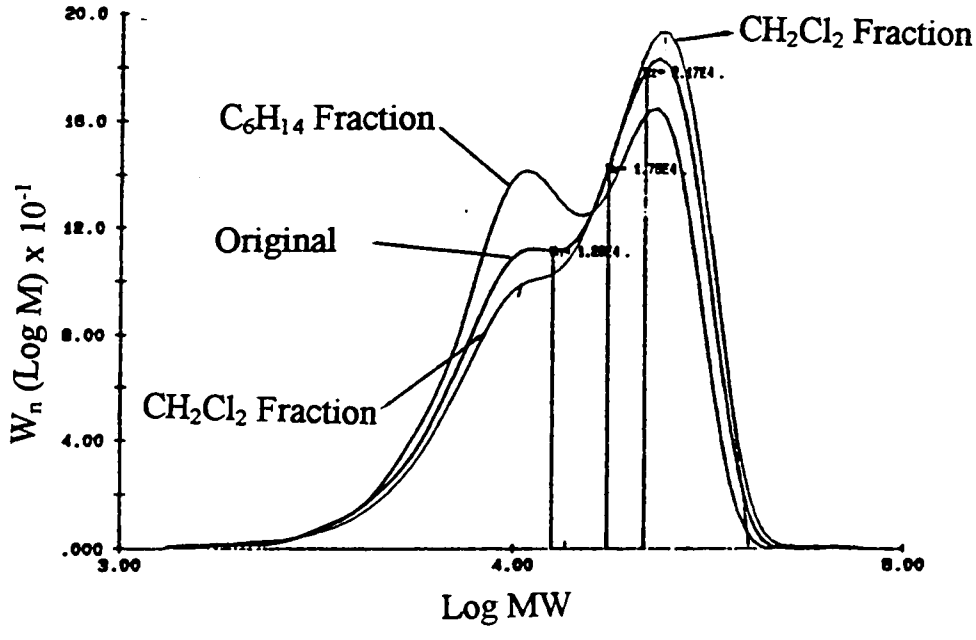

Figure 6.9 GPC output of the molecular mass distribution of P407 following fractionation from hexane/dichloromethane.

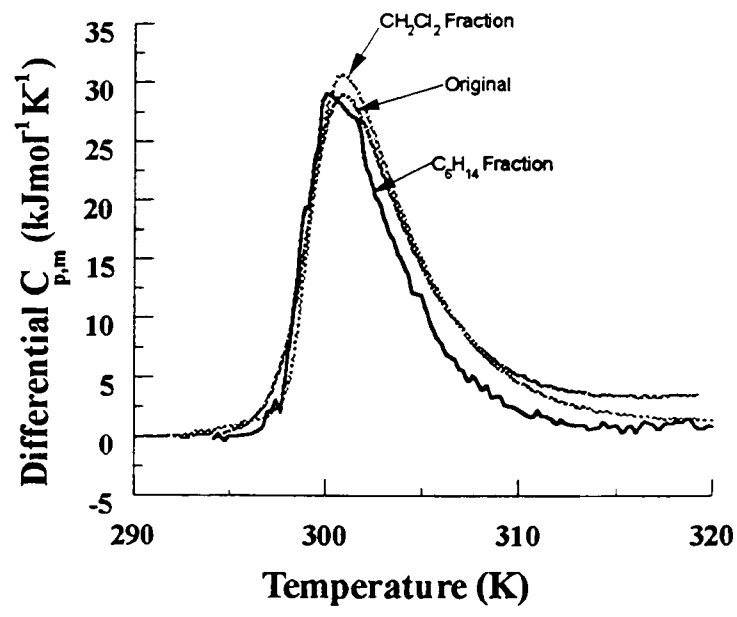

Figure 6.10 Calorimetric scans of P407, and fractioned P407 recovered from hexane and dichloromethane

One may expect a similar increase in these thermodynamic parameters for the dichloromethane fraction, however, as 81% of the recovered copolymer partitioned into the

dichloromethane layer, then the effect of increasing the concentration of the higher molecular mass triblock fraction would not be as marked. For the dichloromethane fraction, the ΔH_{cal} is observed to slightly increase versus the unfractioned P407, but the increase is within the experimental error of the HSDSC and therefore not significant.

6.2 NMR Studies.

The methyl carbon atoms in the POP block of the poloxamers is a reasonable ^{13}C probe of the hydrophobicity of the POP region. Poloxamer P237 was analysed by ^{13}C NMR as a function of temperature at a copolymer concentration of 10 $mgmL^{-1}$ in D_2O and all shift values were calibrated against an aqueous solution of sodium 2,2-dimethyl-2-silapentane-5-sulphonate held in an inner capillary of a 5mm coaxial tube. Relaxation studies measurements (T_1) were performed on nitrogen purged samples using a 180-τ -90 sequence (inversion-recovery), and analysed using standard JEOL software. Figure 6.11 shows the trend in for the ^{13}C shift of the methyl group resonance versus temperature.

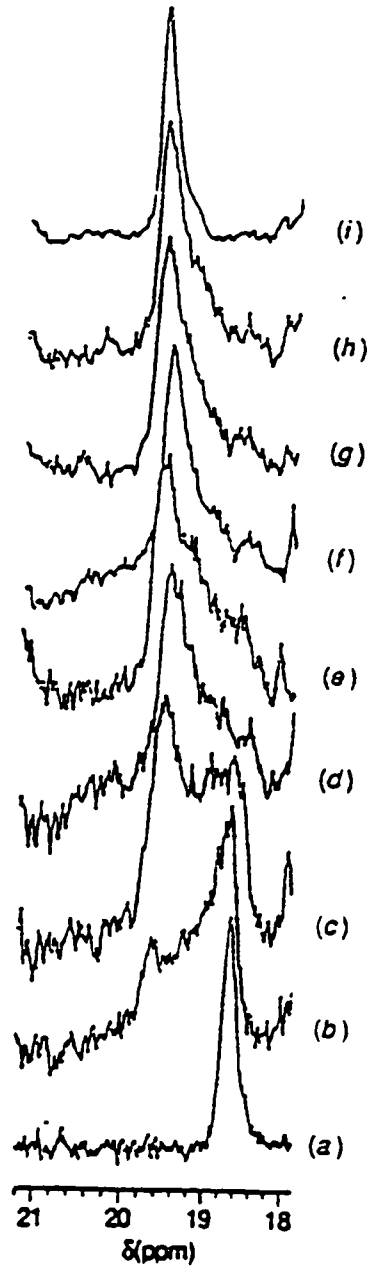

Figure 6.11 OP methyl ^{13}C NMR shift positions (ppm) from 293K to 333K for P237 at a concentration of 10$mgmL^{-1}$ in D_2O. Shifts relative to DSS. Temperatures (K): (a) 293, (b) 303K, (c) 305K, (d) 307K, (e) 308K, (f) 309K, (g) 311K, (h) 313K and (i) 333K.

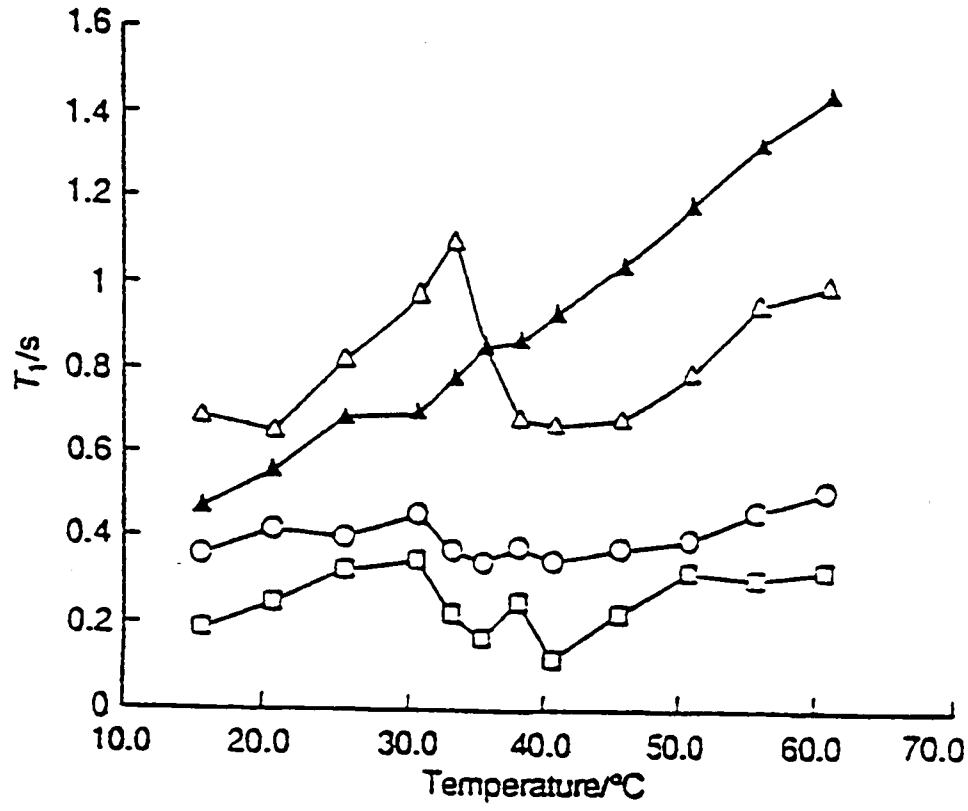

Figure 6.12 T_1 relaxation measurements for P237 from 288K to 333K. O, CH_2 (OP), □, -CH(Me)- (OP), ▲ CH_2 (OE), Δ,-CH_3 (OP).

A shift of the OP methyl resonance to a higher frequency with respect to increased temperature is seen for P237 in dilute D_2O solution, while the EO resonance is, within experimental error, unaffected. This could be due to greater interaction of OP groups within a single copolymer chain. The other OP resonances (CH and CH_2) exhibit similar ^{13}C shift changes to a lesser degree than the methyl resonance. This shift in resonance position for the methyl singlet of the isopropyl block reflects the phase transition as observed by HSDSC. The smooth temperature-induced transition of this ^{13}C resonance is centred about the observed T_m and is reversible on cooling. Changes in ^{13}C NMR shifts of this order (18.6 ppm at 293K to 19.4 ppm at 313K) can be caused by steric effects due to conformational changes or to local solvent effects. In order to assess the mobility of the OP and OE regions as a function of increasing temperature, spin lattice (T_1) measurements were performed from 288 to 333K (Figure 6.12).

In general, given that relaxation is dominated by dipole-dipole interactions, longer T_1 values can give an indication of an increase in segmental motion. It is interesting to note the smooth increase of T_1 with temperature for the CH_2 (OE) resonance; perhaps an indication of weakening hydrogen bonding and greater mobility of the POE chain with increased temperature. The CH (OP) and CH_2 (OP) resonances show little change with temperature, while the relationship between the CH_3 (OP) resonance and temperature appears discontinuous at the phase transition temperature. That segmental motion appears to increase up to the transition temperature and then "resets" to new steric requirements is unique to the CH_3 (OP) resonance. This discontinuity at the T_m for P237 provides a direct probe of conformational change at the phase transition.

The transition detected by NMR and HSDSC is a solution phase transition. For some water-soluble block copolymers this transition occurs close in temperature to, or simultaneously with, the cloud point transition.[48] However, in the case of P237 at the concentration of the copolymer used in this study, the cloud point is separated by a large temperature increment of >40K from the solution phase transition. There is, therefore, no cloud point for P237 in the 278-353K temperature range examined using HSDSC and NMR in this study. This is also demonstrated by the observation that there is no change in the percentage optical transmission of the sample as measured at 540nm in the temperature range 278-353K.

Relaxation measurements through the copolymer T_m appear to give an insight into the molecular processes during the phase transition of dilute copolymer solutions. In this case, these are centred around the POP block. Both ^{13}C shift positions and T_1 relaxation measurements indicate that substantial reorganisation occurs at this specific site for poloxamer-type surfactants. This reorganisation is not associated with the formation of classical-type micelles of the type studied by Lenaerts *et.al.*, (which are also temperature and concentration dependent),[49] as the concentrations studied here are much lower (<1% w/v versus 15-30% w/v) than those CMC values.

A variety of NMR techniques has been used to study the solution behaviour of poloxamers in dilute and concentrated aqueous solutions.[5, 10, 11, 15, 33, 36, 38, 41, 50-54] For dilute aqueous solutions of poloxamers, ^1H-NMR has been employed to study the microviscosity of the micellar core of P338 and P334[36] at a concentration of 10mgmL^{-1} in D_2O. The NMR data showed that upon micellisation, a broadening of the OP(Me) shift was observed with increasing temperature, this was interpreted as an increase in viscosity of the POP blocks, the -CH_2- shifts remained unchanged with increasing temperature, this effect was also observed for P407 in D_2O at a concentration of 10mgmL^{-1}.[7] T_1 relaxation for P334 showed that the values for POE segment increase exponentially with temperature, and those for the POP segment remained relatively constant. With increasing temperature, the increase in molecular motion (vibrational, rotational and translational) of the polymer chains decrease the viscosity and thus a decrease in spin-lattice relaxation, hence an increase in T_1 relaxation. For the POP core, a more viscous environment slows down chain movements and increased interactions between the POP with the rest of the molecule facilitate faster relaxation, and therefore lower T_1 values. These opposing effects of temperature and viscosity resulted in the observation that

the T_1 relaxation values for the POP chain remaining relatively constant with increasing temperature. Below the micellisation temperature the T_1 relaxation values for the POP and POE chains of the poloxamer were similar, indicative that both blocks were in a similar environment. ^{13}C-NMR of P407 at high concentration (25-200mgmL^{-1}) in D_2O shows a distinct downfield shift in the methyl resonance of 18.5-20.2 ppm between 293-298K (25mgmL^{-1}) and 285-290K (200mgmL^{-1}), the observations were proposed to be due to steric effects caused by conformational changes or intermolecular interactions such as methyl overcrowding.[50] From the NMR data presented here, the similar change in shift values for the OP(Me) groups of P237 indicate that the processes observed are comparable to those observed for P407 at higher concentrations.

6.3 Densitometric Studies.

6.3.1 **Experimental.**

The experimental conditions for DSD studies are discussed in Chapter 3. The lowest concentration attained to clearly differentiate the phase transition by DSD for all of the copolymers studied was found to be 10 mgmL^{-1}. Therefore, HSDSC data is also presented here in order to accurately compare to the DSD studies. All scans, unless otherwise stated, were performed at 30 Kh^{-1} and at a concentration of 10 mgmL^{-1}. The poloxamers used for DSD analysis were selected on the basis that the observed phase transition was completed at temperatures below approximately 333K (the DSD system is at atmospheric pressure, and air bubbles may form at elevated temperatures in excess of 333K).

6.3.2 **High Sensitivity DSC.**

The phase transitions for the poloxamers at a concentration of 10 mgmL^{-1} and at a scan rate of 30 Kh^{-1} all show a slightly asymmetric transition with a steep leading edge and a gentle slope back to the baseline above the T_m. The T_m of the observed phase transitions for the poloxamers studied range from 297.2K to 312.7K, and decreases with increasing POP content. The calorimetric enthalpy (ΔH_{cal}) increases with increasing POP content whilst $\Delta T_{1/2}$ decreases with increasing POP content (Table 6.5). The observed T_m has been shown to

decrease with increasing polymer concentration.[55] Brown *et al.*[56] have studied P235 in dilute aqueous solutions by dynamic and static light scattering techniques and showed that at low temperatures a mixture of monomer and micelles coexisted and at elevated temperatures (313K) only the micellar form existed for a 5% aqueous solution. The mid-point for both forms occurred at about 294K which compares to the T_m of the observed phase transition of a 1% solution by HSDSC of 307.6K, the difference being explained by the higher concentration used for the light scattering technique. The observations made by HSDSC are indicative of an aggregation process. The observed phase transition properties of the poloxamers (Table 6.5) show that many of the thermodynamic parameters (e.g. ΔH_{cal}, $\Delta T_{1/2}$) are of similar order of magnitude to those found in the native $\rightarrow$ denatured (folded $\rightarrow$ unfolded) transitions of globular proteins.[1-3] The HSDSC observed T_m for the phase transitions of the poloxamers agree reasonably well with the T_m values derived by differential scanning densitometry (DSD). The effects of scan rate (10,30 and 60 Kh^{-1}) on T_m and the complete reversibility of the phase transition at 30 Kh^{-1} indicate that the phase transition of the poloxamers show no kinetic limitations as shown previously for P237.[57]

6.3.3 **Differential Scanning Densitometry (DSD).**

The phase transitions for the poloxamers observed by DSD show a sharp increase in partial specific volume ($\bar{v}$) (Figure 6.13 and Table 6.5) around the T_m which then gradually decreases in gradient above the T_m. The phase transitions observed by HSDSC and DSD are superimposed for P215 and P333 in order to demonstrate that the observations using the two techniques correlate (Figure 6.14). It is interesting to note that the cloud point transition for P215 is virtually calorimetrically silent, whereas a rapid increase in $\bar{v}$ is observed (Figure 6.14). The observed mid-point of the transitions (T_m) are in good agreement with the observed T_m of the phase transitions from the HSDSC study. Analysis of the partial specific volume change ($\Delta\bar{v}$) shows a volume change of 5.13 to 10.06 $Å^3$ per oxypropylene monomeric unit (PO) giving an average value of 7.4 $Å^3$ per PO, which is comparable to an average value of 6.7 $Å^3$ per PO calculated from the data presented by Williams *et.al.*[55] for a range of poloxamers in aqueous solution, studied using the technique of dilatometry. The present analysis was limited to those poloxamers that gave only one elution peak from the gel permeation analysis. The volume of a water molecule is approximately 30 $Å^3$ which then suggests that one

molecule of water per 4 PO units is lost as the temperature is increased over the observed phase transition. However, the process of dehydration must be accompanied by a conformational change of the hydrophobe, which would account for the value of 7.4 $Å^3$ per PO unit.

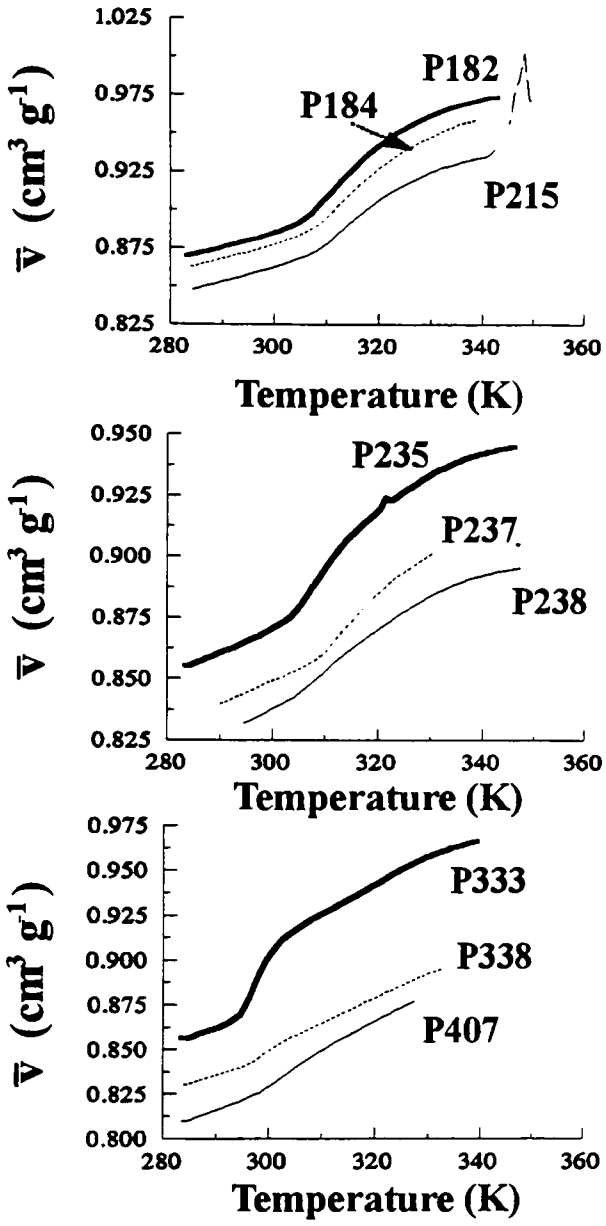

Figure 6.13 Partial specific volume ($\bar{v}$) of the poloxamers in double quartz distilled water at a concentration of 10 mgmL^{-1} at a scan rate of 30 Kh^{-1}.

T_1 relaxation nuclear magnetic resonance (NMR) measurements[33] have shown that there is a sharp increase in rotation of the methyl groups of the POP portion of the polymer and no sharp change for the POE portion of the polymer over the transition temperature for P237. The processes of dehydration and aggregation are thermally driven and are constituents of the same process. However, the methods used in this study are macroscopic techniques and cannot prove in which order the two processes occur. Williams *et al.*[55] examined dilute aqueous solutions of poloxamers using the technique of dilatometry and concluded that the observed temperature driven transition was dependent upon the POP portion of the polymer, and that the phase transition involved cooperative association of many molecules or large segments of individual polymer molecules and a large number of water molecules. The observations reported by Williams *et.al.*[55] are therefore in general agreement with those reported here. The 8 poloxamers studied by Williams *et.al.*[55] are different to the poloxamers examined in this study and the T_m values reported there are lower than would be expected due to the higher concentrations used (1.1 to 9.8% w/w), however, the general trend of decreasing T_m with increasing POP content is observed .

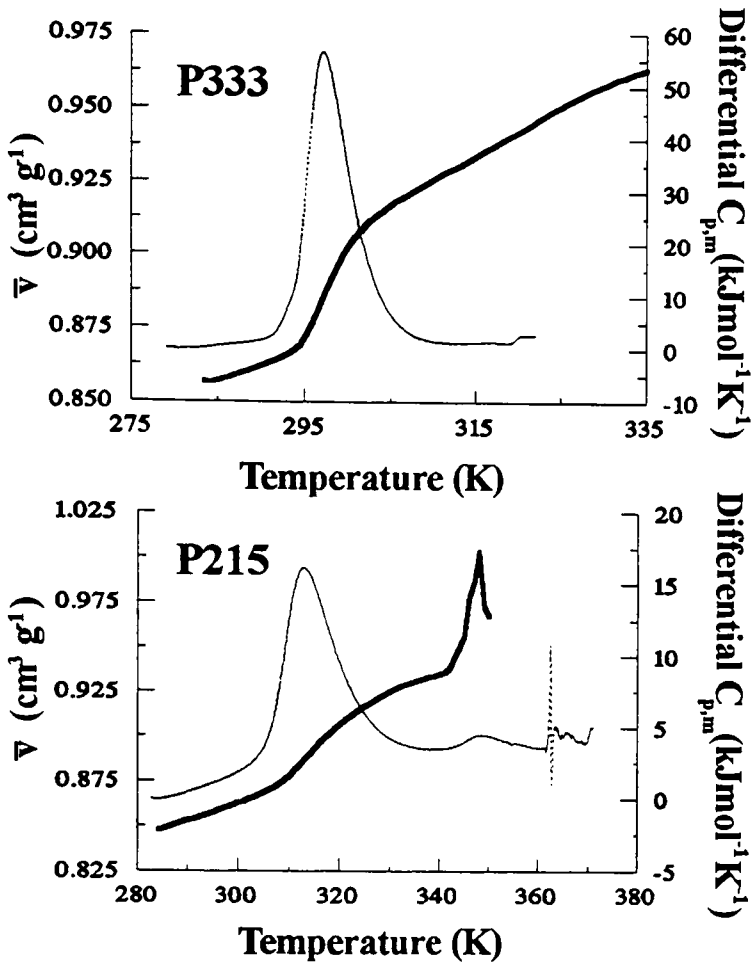

Figure 6.14 Calorimetric traces and partial specific volume ($\bar{v}$) of poloxamers P215 and P333 at a concentration of 10 mgmL^{-1}, in pure water, at a scan rate of 30 Kh^{-1}.

Theoretical partial specific volumes based on van der Waals radii, α-hexagonally packed chains (based on alkanols) and β and γ forms - orthorhombic perpendicular or monoclinic lattice were calculated (Table 6.6). The experimental partial specific volumes ($\bar{v}$) at a temperature of 293K correspond more closely to the β and γ forms (orthorhombic perpendicular or monoclinic lattice respectively). As the temperature is increased above the T_m, the experimental $\bar{v}$ values agree more closely to the α-form, which is as expected. The α-form is the most expanded form which would correspond theoretically to a more hydrophobic environment. That is, as the temperature is increased, the more hydrophobic POP portion of the polymer dehydrates and aggregates almost simultaneously forming a hydrophobic core surrounded by the hydrated polyoxyethylene hydrophilic chains. The dehydrated core of the aggregate would theoretically be less dense and hence more expanded than that of a hydrated polyoxypropylene chain.

From the values for the partial specific volume ($\bar{v}$), it is possible to derive the apparent molal volume (φ_v) from the relationship:

$$\varphi_v = \frac{\rho_0 - \rho}{m(\rho\rho_0)} + \frac{M_2}{\rho} \qquad (1)$$

where M_2 is the molecular mass of the copolymer (kg), ρ the solution density (kgm^{-3}), ρ_0 the density of the solvent (kgm^{-3}) and m the molality of the solution. The partial molal volume ($\bar{V}_2$) is related to φ_v by the equation:

$$\overline{V}_2 = \varphi_v + \frac{m\delta\varphi_v}{\delta m} \qquad (2)$$

However, at vanishing molality:

$$\overline{V}_2^0 = \varphi_v^0 \qquad (3)$$

which by definition holds true for systems at infinite dilution.

These data suggest that the poloxamers undergo a gradual change in molecular size and a rapid change in conformation around the observed T_m. With these molecular changes, large changes in the degree of solute-solvent interaction will occur. Partial molal expansibility ($\overline{E}_2$) is a thermodynamic parameter sensitive to hydrophobic and hydrophilic interactions involving solute and solvent; values of $\overline{E}_2^0$ were obtained via the relationship:

$$\overline{E}_2^0 = \left(\frac{\delta\overline{V}_2^0}{\delta T}\right)_p \qquad (4)$$

and are shown in Figure 6.15. Eagland and Crowther [58] showed that an increasingly positive values of $\overline{E}_2^0$ is indicative of a decrease in hydration of the hydrophobe and that negative values of $\overline{E}_2^0$ are indicative of an increase in hydration of the hydrophobe. The $\overline{E}_2^0$ values for the poloxamers in dilute aqueous solution are all positive with a rapid increase in $\overline{E}_2^0$ over the phase transition temperature indicative of a decrease in hydration of the POP block of the copolymer with increasing temperature and a rapid decrease in hydration of the POP around the T_m. Positive values for $\overline{E}_2^0$ have also been reported for meroxapols (POP-POE-POP triblock copolymers) in aqueous solution.[14] However, linear relationships were observed over the temperature range studied indicative of no change in phase. This may be attributed to the possibility that the copolymers studied were in the aggregated form only as the concentrations examined were 100-390mgmL^{-1} [14] Eagland and Crowther[58] attributed a rapid change in the solvated state of poly(vinyl alcohol) to a conformational change, similar to native structure formation of a globular protein, whereby dehydration of the hydrophobic residues resulted in a macroscopic structure with a greater degree of hydration of the hydrophilic residues at the surface of the structure. In the case of poly(vinyl alcohol), at elevated temperatures, the increasing thermal agitation of the system appeared to produce a decrease in hydration of the hydrophilic portion of the polymer. The $\overline{E}_2^0$ values for the poloxamers in dilute aqueous solution, by comparison with the observations made by Eagland and Crowther[58] for the dilute aqueous solution behaviour of poly(vinyl alcohol), suggest that the process of dehydration accompanied by a conformational change of the hydrophobic POP occurs in the temperature range of the observed phase transition. At elevated temperatures, a

gradual dehydration of the hydrophilic POE is indicated and is related to an increase in molecular motion of the copolymer chain.

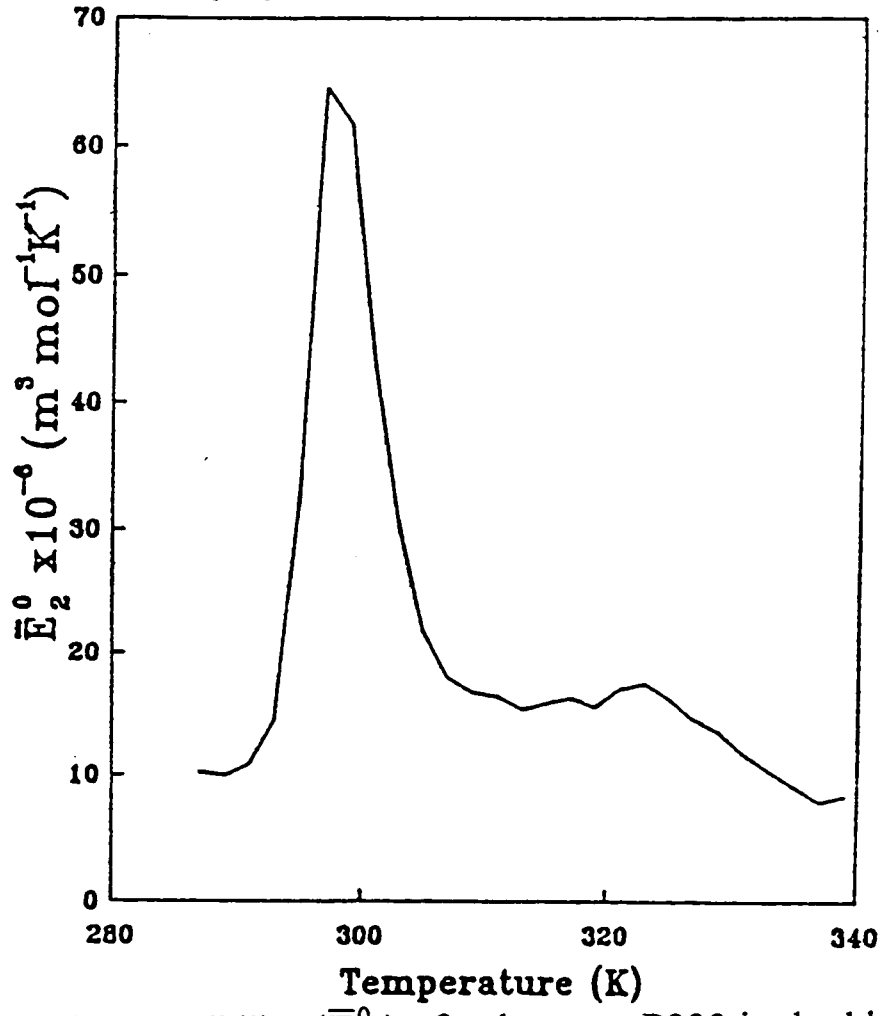

Figure 6.15 Molal expansibility ($\bar{E}_2^0$) of poloxamer P333 in double quartz distilled water (10 $mgmL^{-1}$) as a function of temperature.

6.4 Cosolute Effects.

6.4.1 Effects of Sodium Chloride and Phosphate Buffer.

The effect of sodium chloride on the phase behaviour of poloxamers in dilute aqueous solution was investigated as a function of increasing NaCl concentration (0-3.08M) at a fixed copolymer concentration (5 $mgmL^{-1}$) for P237, P235 and P407. Also, the effect of copolymer concentration (1-20 $mgmL^{-1}$) was investigated for P237 in 1.03M NaCl. The effect of increasing concentration of phosphate buffer at pH7.20 (0.03-0.50M) was also investigated for P237 at a copolymer concentration of 5 $mgmL^{-1}$. All calorimetric scans were performed at a scan rate of 60 Kh^{-1}. The phase transitions observed for P237 at a concentration of 5 $mgmL^{-1}$ are shown in Figure 6.16. The corresponding thermodynamic parameters for poloxamers P237, P235 and P407 are shown in Table 6.7.

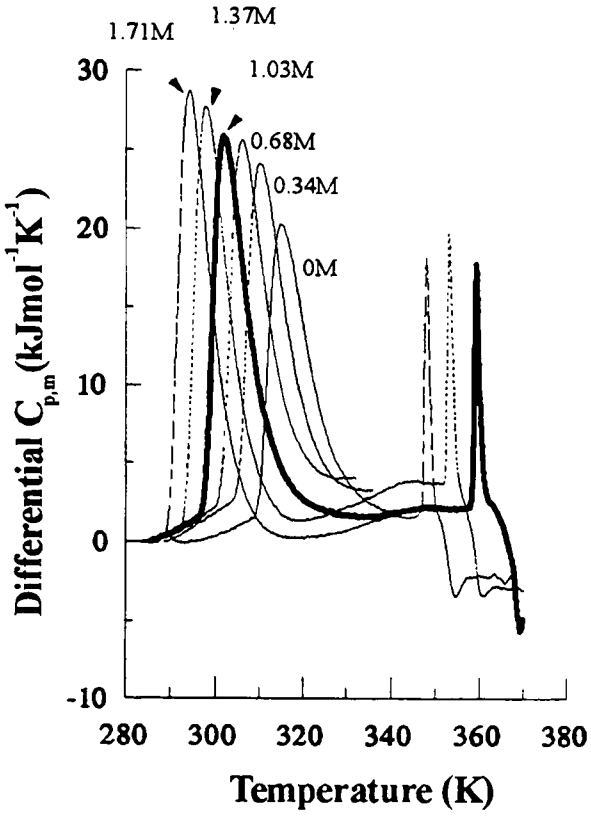

Figure 6.16 Calorimetric scans of P237 in sodium chloride solutions (0 - 1.71M) at a copolymer concentration of 5 mgmL^{-1}, at a scan rate of 60Kh^{-1}.

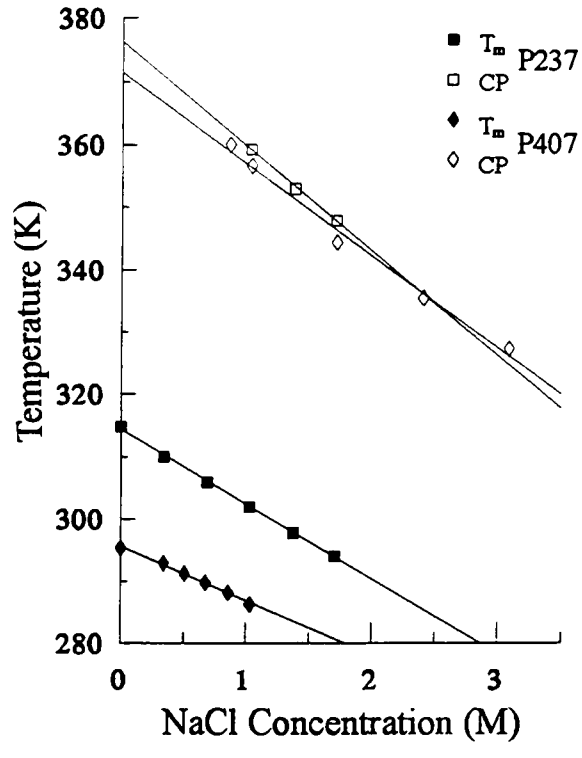

Figure 6.17 The effect of sodium chloride concentration on the phase transition temperature and cloud point of P237 and P407 at a copolymer concentration of 5 mgmL^{-1}.

With increasing concentration of sodium chloride the observed T_m and $\Delta T_{1/2}$ decrease and ΔH_{cal} and C_p^{max} increase. Also, the temperature at which clouding is observed was decreased with increasing sodium chloride concentration. The depression of the T_m and CP for P237 and P407 was observed to occur in a linear manner with increasing sodium chloride concentration, and the magnitude of the depression in temperature was observed to yield almost parallel lines for the T_m and CP versus salt concentration (Figure 6.17, Table 6.7).

The effects of phosphate buffer on the phase transition properties of poloxamer P237 are comparable to those effects shown for sodium chloride. The T_m was sharply depressed with increasing concentration of phosphate buffer (Figure 6.21, Table 6.8), however the ΔH_{cal} was not increased by the same magnitude as observed for increasing sodium chloride concentration, which is not as expected. Both phosphate buffer and sodium chloride increase water structure, and hence increase the order of the system under study, therefore, as the phase transition observed for poloxamers is due to an aggregation of monomeric and loosely associated copolymer clusters resulting in a more ordered state (dehydrated and aggregated

POP), it is possible to conclude that the effect of cosolutes that increase the structure of water, shift the equilibrium towards the aggregated and more ordered form of the copolymer. The CP transition corresponding to phase separation has been investigated for POE[59] and for poloxamers.[47] In Kjellander and Florin's statistical mechanical treatment, model building provides evidence that POE is capable of fitting into an ice-like lattice in which hydrogen bonds are readily established between water and the ether oxygens. At 308K the interaction between polymer chains is low as revealed by low negative values for *w*, a correction term for polymer-polymer interaction. As the temperature is raised *w* becomes more negative indicating greater polymer chain interaction. Experimental evidence[59] suggests that both the enthalpic and entropic contributions to *w* are large and positive. The coming together and interaction of two polymer chains results in the transfer of water molecules from hydration shells surrounding the polymer to the bulk. Thus transfer increases entropy since the restrictions on thermal motion of water molecules in the shell is, to a certain extent lifted, in the bulk. However the loss of thermal stabilisation energy associated with the hydrogen bonded structure results in a positive enthalpy change. If the nature of the solvent is changed, e.g., by the addition of salts, the transfer of weakly hydrogen-bonded water molecules from copolymer chains to the hydration sphere of dissolved ions in the bulk phase is increased compared to systems containing copolymer and water only. Therefore, the observation of a decrease in the temperature at which the observed phase transition occurs is merely a manifestation of this effect. The observed increase in calorimetric enthalpy associated with increasing salt concentration is merely a reflection of the temperature dependence of the observed endothermic transition. The effects of sodium chloride on the diffusion of atrial natriuretic factor (ANF) in a 5-25% (w/v) aqueous solution of P407 was investigated using ^{13}C NMR.[60] The NMR spectra for all concentrations studied were practically identical, with slight broadening of the signals at elevated copolymer concentrations, which was attributed to an increase in viscosity. A significant reduction in phase transition temperature was observed upon addition of NaCl to the copolymer solutions. ANF diffusion was greatly affected by the addition of NaCl and this was attributed to modification of the protein due to the elevated ionic strength. The effect of NaCl on P407 was attributed to a decrease in free water.[60]

The effect of potassium fluoride on the clouding behaviour of P188 was studied using the techniques of light scattering and NMR self-diffusion measurements,[61] the authors showed that increasing KF concentration in a 1% (w/v) aqueous solution of P188 lowered the temperature at which "micellisation" began to occur, although the size of the molecular

aggregates was the same in the presence and the absence of KF. The decrease in temperature of the cloud point was observed to be linear with respect to KF concentration. The effect of NaCl on both the T_m and CP transition of P237 and P407 is also observed to be linear with respect to increasing NaCl concentration.

The effects of cosolutes on the phase behaviour of POE homopolymers and copolymers in aqueous solution have been studied by several investigators.[5,45, 52, 62-70] The gelation behaviour of P407 was dramatically affected by NaCl, $CaCl_2$, $MgSO_4$, $Al_2(SO_4)_3$, Na_2SO_4 , Na_3PO_4 [67] a slight reduction of the lower gelation temperature and a dramatic decrease in the upper gelation and cloud point temperature was observed with increasing salt concentration. The effect on the upper gelation temperature and CP paralleled phase separation for POE, and the effectiveness of "salting out" followed the Hofmeister series and appeared to be unrelated to ionic strength. The effects were observed to be associated with the nature of the anion, the cation having little effect. The effect on the lower gelation temperature was attributed to lowering of the CMC, the presence of salts facilitating closer packing of the micelles due to a reduction in the water activity.[67] Malmsten and Lindman[52] investigated the effects of various cosolutes on the gelation and aggregation behaviour of P407 in aqueous solution. The effects were interpreted in terms of the distribution of ions in solution. Large polarisable ions, such as SCN^-, tend to accumulate close to the polymer, increasing the solubility of the polymer and hence raising the CP and gelation temperature. The lowering of the gelation and clouding behaviour of the polymer by salts, such as Na_2SO_4, was attributed to a depletion of the ions close to the polymer, which effectively increased the interfacial tension between the polymer and water.[52] This interpretation of the effect on the clouding behaviour of POE chains has also been shown by Karlström[68,69] and Kjellander and Florin.[59, 70] Florin *et al.*[70] explained the lowering of the CP of POE chains in aqueous solution as primarily due to the existence of a salt-deficient zone surrounding POE chains: small ions with little polarisability would be repelled by the poorly polarisable polymer chain and there would also be a repulsive contribution from the change in the water coordination of the ion on approach to the polymer.

The effect of increasing NaCl concentration on the aggregation and clouding behaviour of poloxamers is apparent from Figures 6.16 and 6.17 in that the addition of NaCl changes the solvent from a good to a poor solvent for both POE and POP blocks of the copolymer, as the depression of the cloud point and phase transition temperature is observed to be reduced at a

comparable rate for both transitions. As shown for the poloxamers in water (Section 6.1), the T_m is dependent on the POP content and the CP is dependent on the POE content.

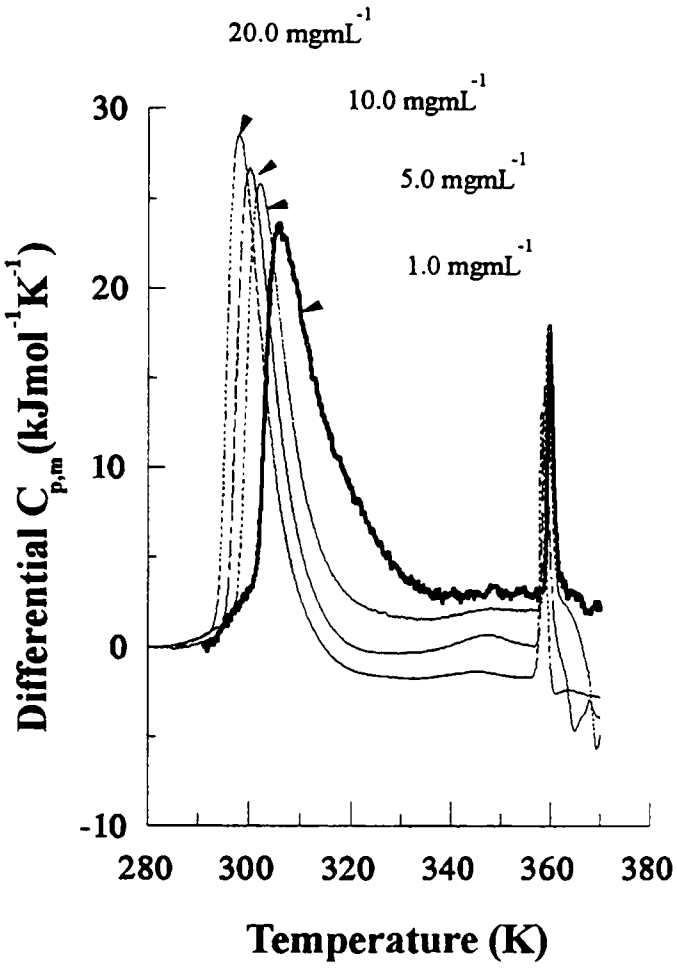

Figure 6.18 Calorimetric scans of P237 at various copolymer concentrations (1.0 to 20.0 $mgmL^{-1}$) in 1.03M NaCl at a scan rate of 60 Kh^{-1}.

The effect of increasing copolymer concentration in a fixed concentration of sodium chloride (1.03M) was studied for P237 over the concentration range of 1-20 $mgmL^{-1}$ at a scan rate of 60 Kh^{-1}. The calorimetric traces obtained are displayed in Figure 6.18 and the thermodynamic parameters associated with the phase transitions are shown in Table 6.9. Two transitions are observed, the lower temperature transition corresponds to aggregation and dehydration of the POP block as previously observed for poloxamers in double distilled water (Figure 6.7 and Table 6.3). The lower phase transition has a steep leading edge and a gentle slope above the T_m back to the baseline, indicative of an aggregation process. The upper transition corresponds to complete phase separation of POE and POP(cloud point). The CP transition is of low enthalpy, highly cooperative and occurs over a narrow temperature range, the post-transitional baselines are all negative, and decrease sharply with increasing temperature. This is indicative of complete phase separation, which is probably as a result of gradual complete phase separation of the copolymer due to increasing molecular motion of the POE blocks, and reflects an increase in the hydrophobic nature of the POE blocks with increasing temperature. Interestingly, increasing copolymer concentration significantly decreases the T_m of the main phase transition but has little effect on the CP temperature (Figure 6.19). The effect on the T_m is presumably a manifestation of Le Chatelier's principle

in that an increase in the concentration of starting species forces the equilibrium from single and loosely associated copolymer clusters (hydrated POP blocks) in the direction of producing more aggregates (dehydrated and aggregated POP). The small effect on lowering the CP temperature with increasing concentration may be due to the fact that POE chains do not aggregate in the same manner as POP chains, but act as single chains and that the dehydration process is monomeric in nature.

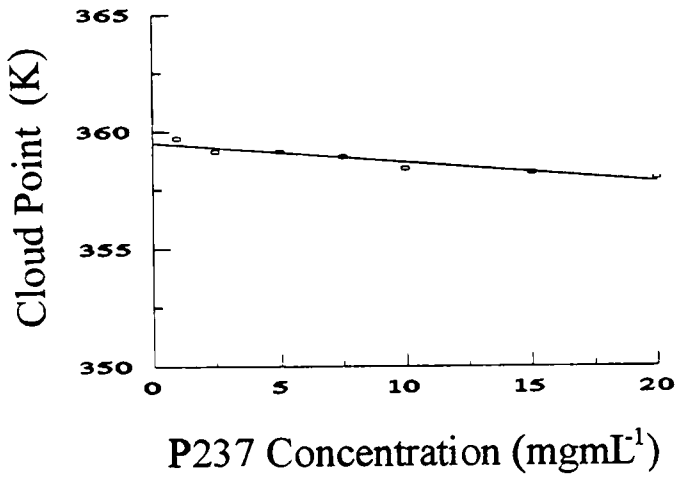

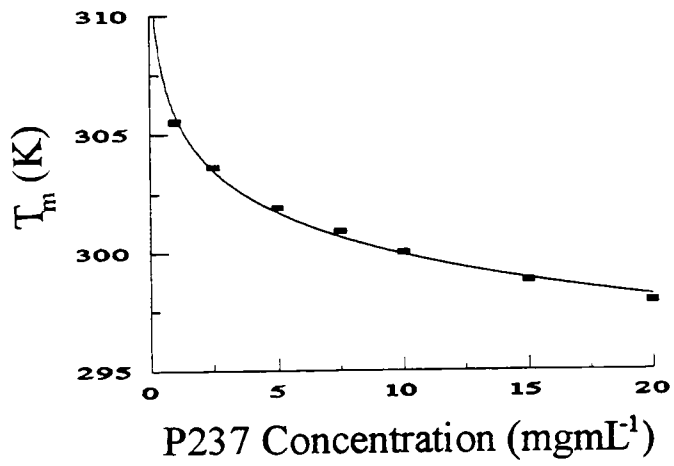

Figure 6.19 The effect of concentration of P237 (1.0 to 20.0 $mgmL^{-1}$) on the phase transition temperature and cloud point in 1.03M sodium chloride.

Aggregation only occurs as a **consequence** of dehydration and phase separation, reflected by the decrease in the post-transitional baseline. The CP temperature is only reported here due to the nature of the post-transitional baseline and therefore the enthalpy associated with complete phase separation could not be determined. However, the sharp transition associated with the cloud point would reflect a highly cooperative process, but the observation of a small decrease in CP with increasing copolymer concentration is indicative that clouding is independent of concentration and may essentially reflect a process involving single chains only. The processes of dehydration and aggregation of the POE blocks may occur simultaneously, and thus the observation of a highly cooperative transition for a process that is initiated by a unimolecular process may be purely a manifestation of superimposition of these two processes.

6.4.2 **Effects of Urea and Guanidinium Chloride.**

The effects of urea and guanidinium chloride on the phase transition behaviour of P237 at a copolymer concentration of 5 $mgmL^{-1}$ as a function of cosolute concentration (0 - 7.83M) was investigated. The urea and guanidinium solutions were prepared on a w/w basis as described in Chapter 3, and concentrations confirmed by refractive index measurements. The calorimetric traces obtained for P237 in urea solution are shown in Figure 6.20, and the thermodynamic parameters associated with the observed phase transition in both urea and guanidinium solutions are presented in Table 6.10.

An increase in T_m and $\Delta T_{1/2}$ and a decrease in ΔH_{cal} and C_p^{max} is observed with increasing urea or guanidinium chloride concentration. The increase in T_m is linear and curvilinear with respect to cosolute concentration for guanidinium chloride and urea respectively (Figure 6.21). The effects of cosolutes on the solubility of proteins and copolymers has been examined by Fields *et al.*[70] Using a theoretical model, it was proposed that a copolymer in a poor solvent will expand with increasing polymer concentration because of "screening" of the solvent interactions by the other chains; the chain ultimately reaches a theta-like structure in the absence of solvent. Urea and guanidinium chloride are common denaturants used to solubilise proteins in inclusion bodies.[72-74] Two mechanisms explaining the effects of organic denaturants in aqueous systems have been proposed. Firstly, an indirect mechanism where urea acts as a structure breaker and facilitates the hydration of hydrophobic moieties[75, 76] and secondly, a direct mechanism, whereby urea replaces some of the water molecules in the hydration shell of the solute[77-80] The indirect mechanism has been widely accepted.[81] However, recent studies using FTIR,[82] electron spin-echo[83] and fluorescence[84, 85] spectroscopy have demonstrated that the direct mechanism occurs, by showing that urea replaces some of the water molecules around the hydration shell of the solute.

With increasing concentration of urea or alkylureas (ethylurea and diethylurea), an increase in aggregation number and a decrease in the micellisation temperature was observed for hexadecyltrimethylammonium bromide (an ionic surfactant).[86] Alkylureas shift from being water-structure breakers to formers with increasing alkyl substitution[87] and therefore an increase in CMT would be anticipated with increasing alkyl substitution based on the indirect model. The decrease in CMT with increasing urea concentration was best explained by direct interactions between the solute and solvent.

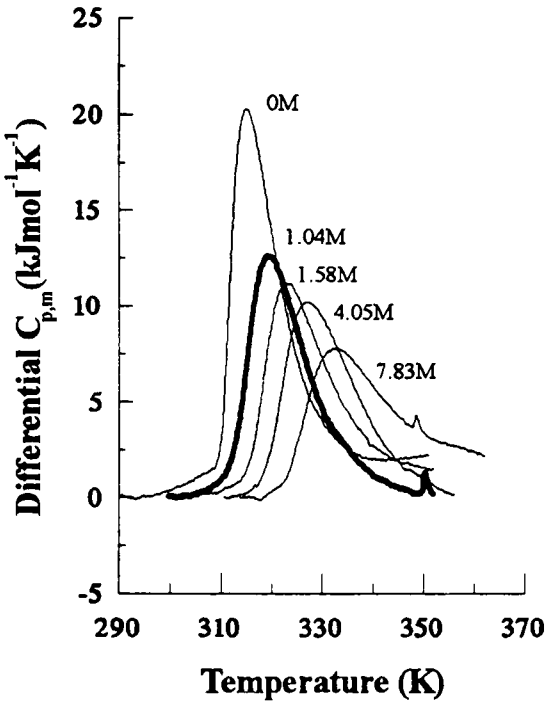

Figure 6.20 Calorimetric scans of poloxamer P237 in urea solutions (0 - 7.83M) at a copolymer concentration of 5mgmL^{-1}, at a scan rate of 60Kh^{-1}.

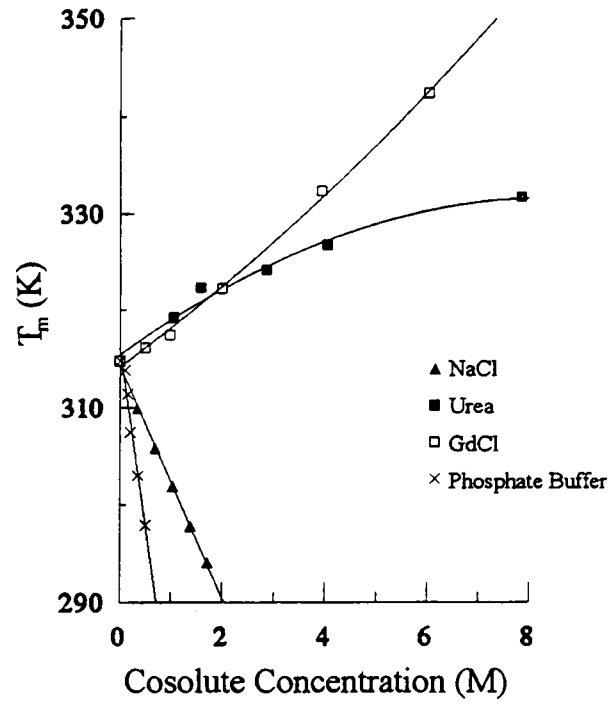

Figure 6.21 The effects of sodium chloride, phosphate buffer (pH 7.2), urea and guanidinium chloride concentration on the phase transition temperature of poloxamer P237 (5 mgmL^{-1}) in aqueous solution.

The effect of urea and guanidinium chloride concentration on the phase behaviour of P237 is opposite to that observed for proteins. For proteins, the effect of lowering the denaturation temperature with increasing urea concentration in aqueous solution is due to disruption of water structure and hydration sphere which favours "hydrophobic hydration" and the equilibrium process for protein denaturation is an effect of exposure and subsequent "hydration" of the hydrophobic residues of a protein with increasing temperature. However, the process of aggregation of the poloxamer with increasing temperature is due to dehydration of the hydrophobic POP blocks. Therefore, a cosolute that favours hydration of hydrophobic moieties by direct interaction with the polymer chain as well as altering the nature of the bulk solvent, will increase the stability of a hydrated copolymer chain and hence offset the aggregation and dehydration of the copolymer to higher temperatures. The effect of a decrease in enthalpy with increasing denaturant concentration is a manifestation of the temperature dependence of this process as observed for poloxamers in sodium chloride and phosphate buffer solution. The effects of urea on the solution behaviour of POE-alkanols has

been shown by Schick[88] to increase the CMC, and was suggested to be due to an increase in the hydration of the POE chain by reducing the cooperative structure of water. Alexandridis *et al.*[22] concluded that urea increased the CMC of P335 indirectly by breaking the "water structure" and directly by replacing water molecules and hydrogen bonding to water molecules. The increase in CMC with increasing urea concentration was greater than observed for POE-alkanols[22, 88] and was indicative that POP exhibits a greatly increased solubility in the presence of urea. The presence of urea on P335 and P338 was observed to have no effect on the structure of the copolymer, reflected by the size of aggregate from light scattering studies (R_H = 8 and 10.5nm for P335 and P338 respectively both in the absence and presence of 4M urea)

Figure 6.21 summarises the effects of cosolute concentration on the observed T_m of poloxamer P237 in aqueous solution, and it is apparent from this figure and from the data in Tables 6.7-6.10 that the phase behaviour of poloxamers in water is extremely sensitive to changes in water structure and interactions between cosolutes and the hydration sphere surrounding the copolymer chain. Cosolutes that increase water structure ("water stucture formers" e.g. NaCl) decrease the solubility of the poloxamer and the solvent becomes a poor solvent with increasing salt concentration. The effect is more profound for the POP portion of the copolymer as the solvation sphere is weakly hydrated compared to the POE block. Cosolutes that disrupt water structure ("water structure breakers" e.g. urea) increase the solubility of the poloxamer and the solvent approaches a theta-solvent with increasing denaturant concentration. Hence the observations of increasing or decreasing T_m with increasing denaturant or salt concentration repectively, reflects changes in water structure and hydration sphere surrounding the copolymer chain. The POP block has a comparatively weak hydration sphere and changes in the nature of the solvent have a more pronounced effect on the solvation and aggregation status of the POP block compared to the POE block.

6.5 Effects of Cosolvents.

The effects of methanol, ethanol, n-propanol and n-butanol on the phase transition of P237 in aqueous solution at a polymer concentration of 5mgmL^{-1} were investigated. The calorimetric outputs for P237 in various concentrations of alcohol in water (% w/v) are shown in Figures 6.22-27.

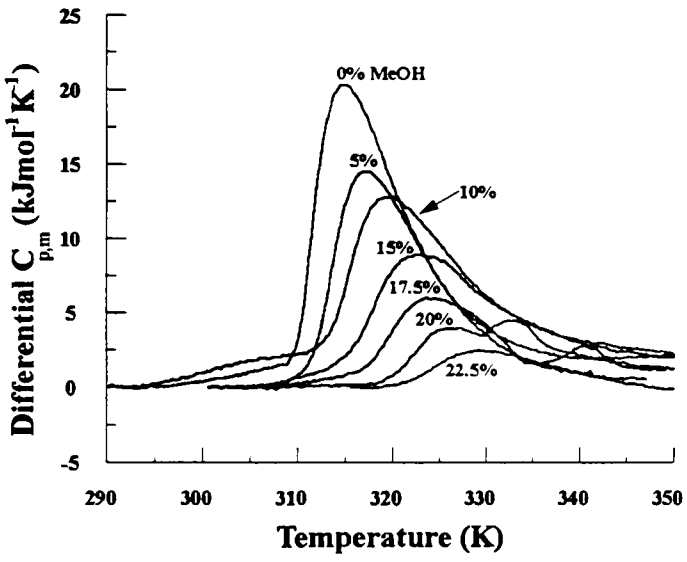

Figure 6.22 The effect of methanol on the observed phase transition of P237 at a copolymer concentration of 5mgmL^{-1}.

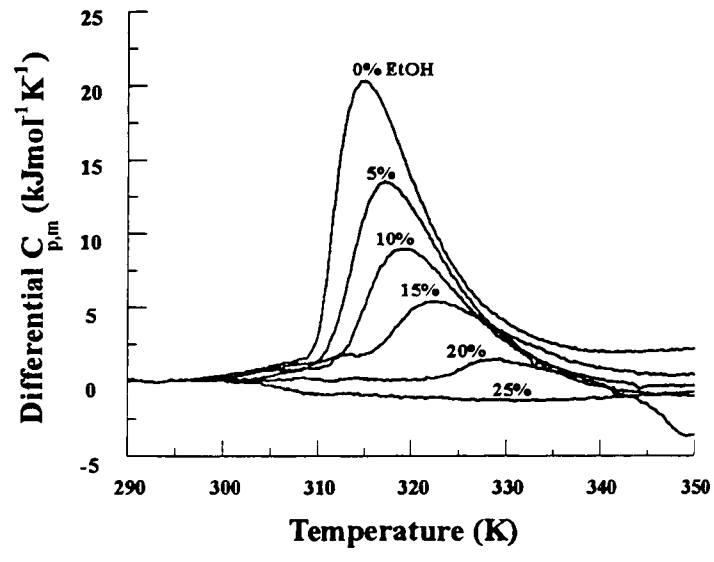

Figure 6.23 The effect of ethanol on the observed phase transition of P237 at a copolymer concentration of 5mgmL^{-1}.

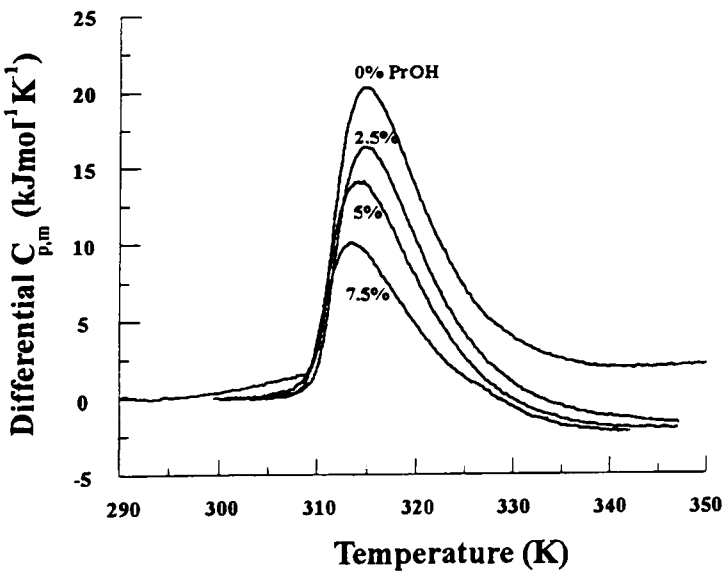

Figure 6.24 The effect of propanol on the observed phase transition of P237 at a copolymer concentration of 5mgmL^{-1}.

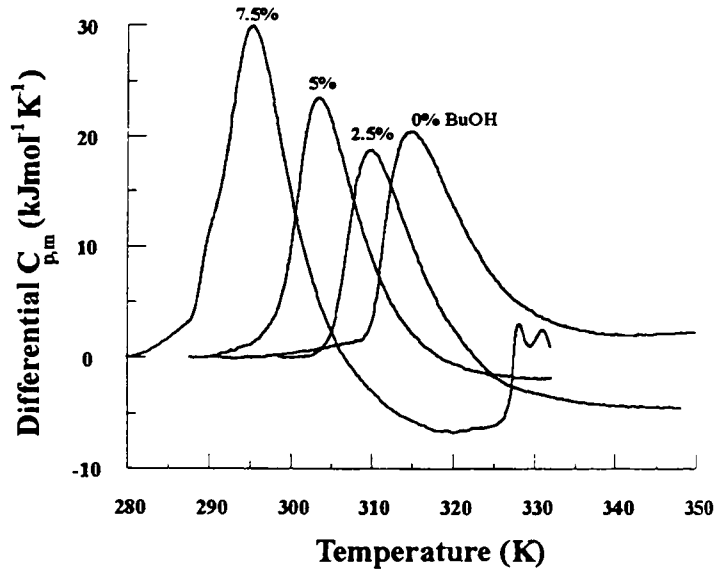

Figure 6.25 The effect of butanol on the observed phase transition of P237 at a copolymer concentration of 5mgmL^{-1}.

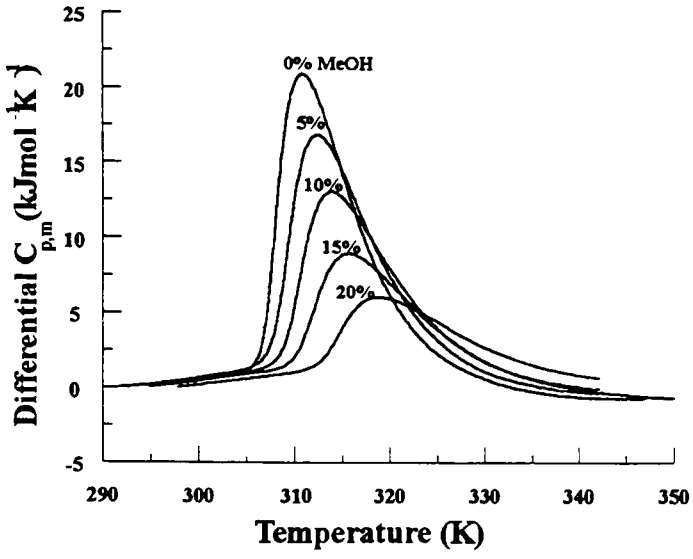

Figure 6.26 The effect of methanol on the observed phase transition of P237 at a copolymer concentration of 20mgmL^{-1}.

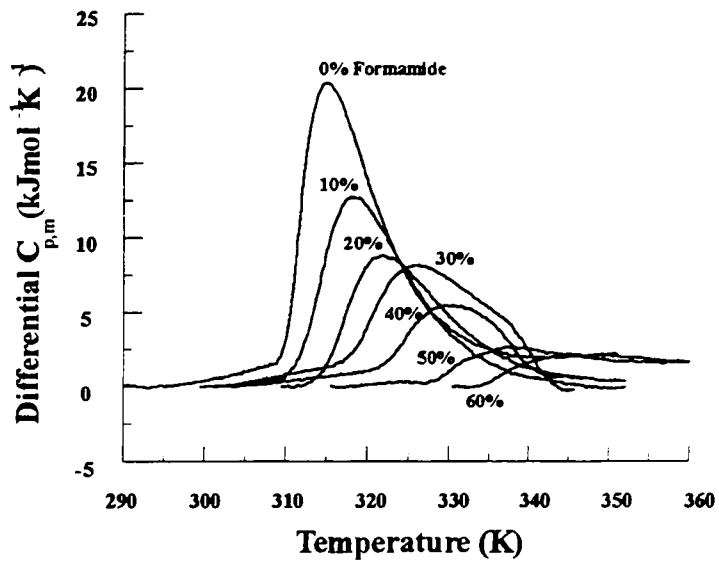

Figure 6.27 The effect of formamide on the observed phase transition of P237 at a copolymer concentration of 5mgmL^{-1}.

The phase transition for P237 in the solvents studied display a steep leading edge with a gentle slope back to the baseline, indicative of an aggregation process. The observed phase transitions were fully reversible and the thermodynamic parameters independent of scan rate (10-90Kh^{-1}). It is apparent that with increasing concentrations of methanol, ethanol and formamide the T_m is elevated and the ΔH_{cal} decreases dramatically (Figures 6.28 and 6.29). With increasing propanol concentration, there is a slight decrease in T_m and a large decrease in ΔH_{cal}, and with increasing butanol concentration a large decrease in T_m and increase in ΔH_{cal} is observed (Figures 6.28 and 6.29). The shifts observed for the T_m of P237 in these solvents reflect the nature of the solvent for the POP moiety, a good solvent for the POP moiety raises the T_m and vice versa, and the change in ΔH_{cal} reflects the decrease or increase in hydrogen bonding between the solvent and POP block dependent on the nature of the solvent. Aggregation arises from a reversal of the process of hydrophobic hydration.[89] Thus, T_m can be linked to the stability of the solvation sphere. Changes in the stability of the solvation sphere brought about by the incorporation of a cosolvent/cosolute can thus be demonstrated by changes in T_m. Under these circumstances changes in ΔH_{cal} may be linked to the changes in T_m and reflect that the aggregation process is accompanied by a permanent change in heat capacityΔC_p. The data obtained for ΔH_{cal} have been plotted with the corresponding T_m values and are shown in Figure 6.30, the correlation of fit for the straight line (r^2) is 73%. The heat capacity change obtained from the plot is -5.06 kJmol^{-1}K^{-1}.

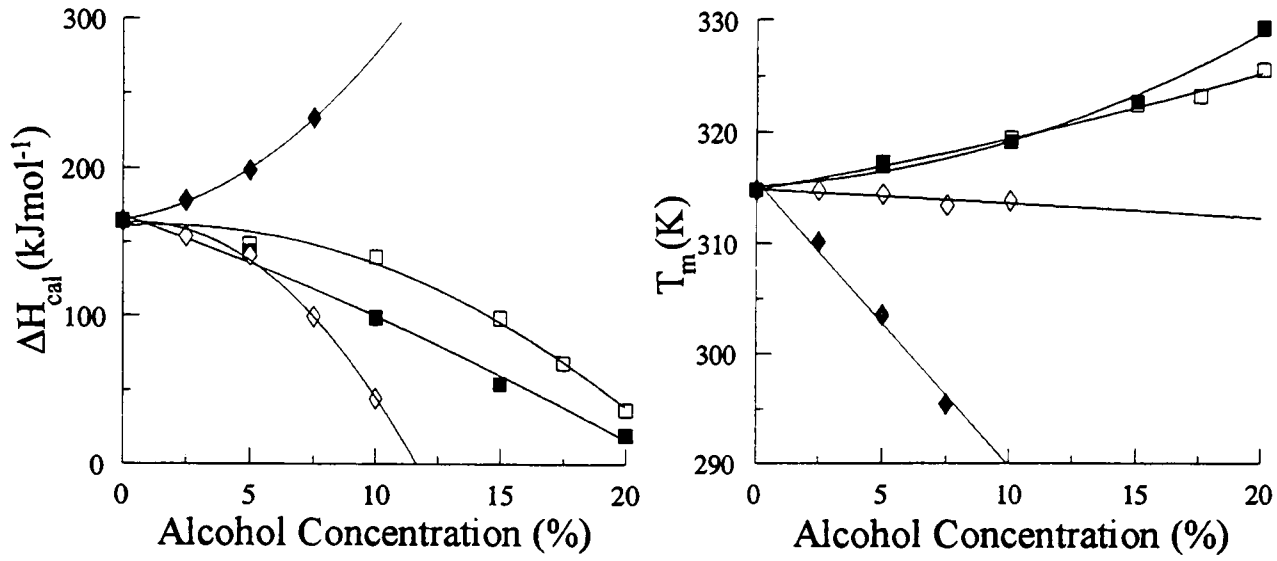

Figure 6.28 The effects of alcohol concentration on the calorimetric enthalpy and phase transition temperature of P237 at a concentration 5mgmL^{-1}, scanned at 60Kh^{-1}. (□ MeOH, ■ EtOH, ◊ PrOH, ◆BuOH)

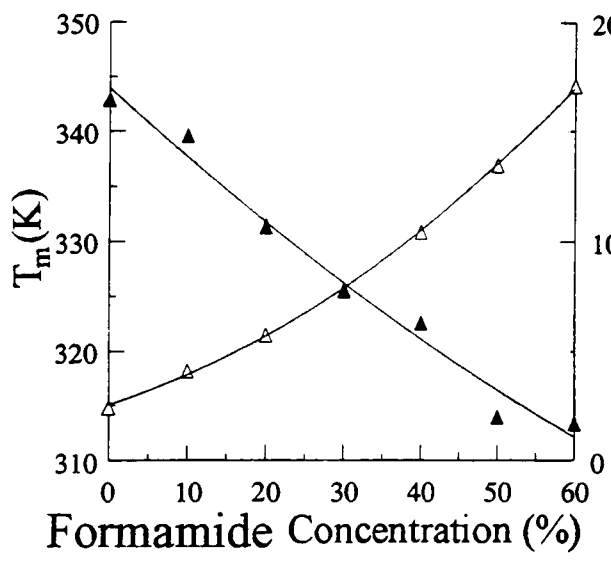

Figure 6.29 The effects of formamide on the phase transition temperature and calorimetric enthalpy of P237 in aqueous solution at a concentration of 5mgmL^{-1}. (△ = T_m, ▲ = ΔH_{cal})

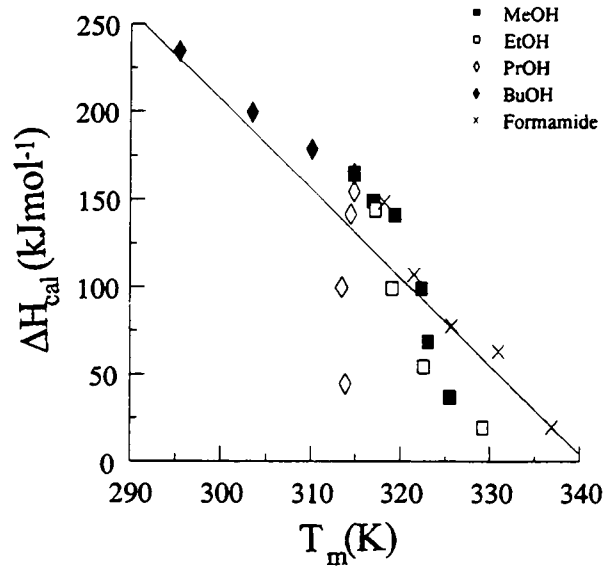

Figure 6.30 Plot of the calorimetric enthalpy as a function of T_m.

Changes in heat capacity are indicative of changes in structure which is related to changes in cohesion.[90] It is therefore concluded that the changes in T_m occur because the cosolvents produce cohesional changes. The shift of the transition to different temperatures and the permanent change in heat capacity result in changes in ΔH_{cal} in agreement with Kirchoff's law.[91] The modelling of the phase transitions will be discussed in chapter 8.

The effects of formamide on the phase behaviour of P237 show similar effects to those observed for the addition of urea and guanidinium chloride (chapter 6.4.2), MeOH and EtOH, this is indicative that formamide preferentially interacts with the POP chain, and hence shifting the desolvation of the POP block to elevated temperatures. Schott reported the effects of many cosolutes and cosolvents on the clouding behaviour of POE-containing surfactants.[62-64] The addition of trolamine (2,2',2"-nitrilotriethanol) to an aqueous solution of a nonionic ethoxylated surfactant (octoxynol 9)dramatically increased the CP and he concluded that the observations of increasing the CP were due to the effect of increasing hydrogen bonding between ether groups and unassociated water molecules while reducing water-water interactions.[63]

The effects of alcohols on the clouding behaviour of ethyl(hydroxyethyl)cellulose (EHEC) was investigated by Karlström *et al.*[69] Methanol and ethanol slightly increased the CP, propanol had little effect, butanol, pentanol, hexanol and heptanol decreased the CP, the effect correlating with increasing alkyl chain length (a longer chain length requiring a lower concentration for phase separation). The effects were discussed in terms of preferential interactions between the cosolvent and polymer, addition of a less polar compound (e.g. pentanol) will increase interactions between the added cosolvent and polymer and decrease the CP The authors tended towards partitioning of the cosolvent between the polymer and bulk aqueous medium. Cosolvents depleted at the polymer (strongly solvated ions e.g. NaCl) would decrease the CP, while those enriched will increase the CP.[69] The effects observed here for the phase behaviour of P237 in the presence of alcohols are very comparable to those observed for EHEC.[69]

6.6 Summary.

The aggregation behaviour of poloxamers in aqueous solution observed using the technique of HSDSC are associated with changes in the solvation state of the POP block. The asymmetry of the phase transition with a steep leading edge and a gentle slope back to the baseline is indicative of a cooperative process, and appears to be due to the processes of dehydration, a conformational change and aggregation of the POP block, the POE blocks allow the aggregated form of the polymer to remain in solution. The ΔH_{cal} increases and T_m decreases with increasing molecular mass of the POP block. Changes in ΔH_{cal} with cosolutes, cosolvents and polymer concentration are merely a reflection of the temperature dependence

of the phase transition, an increase in T_m decreases the ΔH_{cal} and a decrease in T_m results in an increase in ΔH_{cal}. Cosolutes that increase water structure (NaCl, phosphate) favour polymer-polymer interactions and shift the equilibrium between single copolymer chains/weakly associated clusters to the aggregated form which results in a decrease in the T_m . Cosolutes that decrease water structure (urea, guanidinium chloride) have the opposite effect and stabilise the disaggregated from of the copolymer, and raises the T_m . The effects of cosolvents on the phase behaviour of poloxamers show that the addition of fairly large quantities of cosolvent are required before changes in the thermodynamic parameters become apparent. The effects of cosolvents are similar to those observed for cosolutes and may be rationalised in terms of invoking changes in the water structure or by direct interaction with the POP polymer block. Methanol, ethanol and formamide raise the T_m either by behaving as water structure breakers or by replacing water molecules in the solvation sphere of the POP block. Propanol and butanol lower the T_m either because they behave as water structure promoters or because they partition into the POP block forming a cosolvent-rich phase and hence favour aggregation.

6.7 Tables.

Table 6.1 Thermodynamic parameters for the solution-phase transitions of poloxamers in double distilled water at a concentration of 5 $mgmL^{-1}$, at a scan rate of $60Kh^{-1}$.

Poloxamer	T_m (K)	ΔH_{cal} ($kJmol^{-1}$)	C_p^{max} ($kJmol^{-1}K^{-1}$)	$\Delta T_{1/2}$ (K)	ΔS_{cal} ($Jmol^{-1}K^{-1}$)
P101	324.2	60.6	3.3	17.6	187
P105	346.2	32.4	1.6	20.6	94
P108	354.8	20.6	1.2	16.9	58
P122	326.6	87.2	3.9	20.8	267
P123	325.3	75.8	4.6	15.8	233
P124	313.7	107.3	8.3	11.2	342
P181	303.5	183.1	13.6	13.0	603
P182	312.1	138.4	11.4	11.6	444
P184	314.0	184.9	12.3	12.6	589
P188	330.5	91.6	5.5	14.8	277
P215	315.0	143.4	11.9	11.1	455
P217	323.2	113.0	7.1	14.4	350
P231[(1)]	301.5	226.7	21.8	10.4	749
P234	306.6	178.7	22.5	7.4	583
P235	309.4	193.5	18.7	9.2	626
P237	314.8	197.7	18.2	9.9	628
P238	310.1	166.1	14.8	9.9	536
P282	300.3	278.1	31.1	8.2	926
P284	308.8	210.0	19.1	10.1	680
P331	293.1	379.6	59.4	5.5	1297
P333	298.1	334.6	52.2	5.7	1121
P335	300.7	313.1	45.8	6.1	1041
P338	304.9	226.3	22.6	8.6	742
P401	291.5	400.8	74.9	4.6	1372
P407	300.6	160.8	26.4	5.4	535

[(1)] Concentration of P231 = 5.6 $mgmL^{-1}$

Table 6.2 Thermodynamic parameters for the solution-phase transitions of poloxamers in double distilled water at a constant oxypropylene concentration of 5 $mgmL^{-1}$, at a scan rate of $60Kh^{-1}$.

Poloxamer	Conc. ($mgmL^{-1}$)	CP (K)	T_m (K)	ΔH_{cal} ($kJmol^{-1}$)	C_p^{max} ($kJmol^{-1}K^{-1}$)	$\Delta T_{1/2}$ (K)	ΔS_{cal} ($Jmol^{-1}K^{-1}$)
P101	5.8	316.7	323.9	62.9	3.5	17.5	193
P105	10.0	343.7	337.0	44.8	2.4	19.8	134
P108	25.3	>370	351.9	38.2	2.0	18.8	109
P122	6.9	308.2	324.2	73.4	3.7	18.6	226
P123	8.0	-	-	-	-	-	-
P124	9.2	337.7	328.0	76.3	4.3	17.0	234
P181	6.0	296.2	303.0	190.3	14.0	13.2	628
P182	6.9	304.2	312.2	149.3	12.0	11.7	481
P184	8.3	327.7	313.7	166.9	11.9	12.0	531
P188	23.9	>370	324.7	102.9	7.0	13.6	318
P215	10.1	351.2	313.3	160.3	14.4	10.2	510
P217	16.1	>370	318.5	118.5	8.9	12.2	372
P231	5.6	294.7	301.5	226.7	21.8	10.4	749
P234	8.3	345.2	305.2	183.7	23.3	7.1	602
P235	10.3	355.2	307.6	189.2	20.0	8.5	615
P237	17.1	>370	311.2	169.4	18.0	8.3	544
P238	26.2	>370	306.6	132.4	12.7	9.1	427
P282	6.3	296.7	301.6	273.8	30.5	8.4	908
P284	8.4	334.7	307.5	204.5	20.7	9.0	665
P331	5.9	287.2	293.7	352.9	50.5	6.5	1201
P333	7.6	316.7	297.9	328.2	54.1	5.5	1100
P335	10.0	353.2	300.8	300.0	44.4	5.8	996
P338	21.5	>370	301.8	218.9	18.6	10.9	724
P401	5.5	286.7	291.8	443.7	83.2	4.7	1519
P407	15.0	>370	298.4	217.7	44.0	4.5	728

Table 6.3 Thermodynamic parameters for the solution-phase transitions of poloxamers in double distilled water at varying copolymer concentrations(1-50 $mgmL^{-1}$), at a scan rate of $60Kh^{-1}$.

Poloxamer	Conc. ($mgmL^{-1}$)	T_m (K)	ΔH_{cal} ($kJmol^{-1}$)	C_p^{max} ($kJmol^{-1}K^{-1}$)	$\Delta T_{1/2}$ (K)	ΔS_{cal} ($Jmol^{-1}K^{-1}$)
P237	1.0	319.7	142.0	13.0	10.4	444
	2.5	316.8	156.0	15.4	9.6	492
	5.0	314.8	197.7	18.2	9.9	628
	7.5	313.8	177.1	17.9	9.2	564
	10.0	312.8	180.6	18.5	8.9	577
	15.0	311.6	183.6	19.4	8.7	589
	17.1	311.2	169.4	18.6	8.3	544
	20.0	310.7	178.7	19.2	8.5	575
	25.0	310.5	171.7	17.6	8.8	553
	34.1	309.3	179.9	19.9	8.2	582
	50.0	307.8	169.5	19.3	8.0	551
P333	0.1	303.8	*97.0*[1]	*24.0*[1]	*3.8*[1]	*319*[1]
	0.5	301.6	314.2	44.1	6.6	1042
	1.0	301.0	298.5	41.7	6.5	992
	2.5	299.7	316.5	46.4	6.2	1056
	5.0	298.4	334.6	52.2	5.7	1121
	10.0	297.2	318.0	53.0	5.4	1070
	15.0	296.6	315.6	54.0	5.2	1064
	20.0	296.1	342.1	57.2	5.3	1155
P407	2.0	301.4	129.4	22.5	5.5	429
	5.0	300.4	165.7	27.1	5.3	552
	10.0	299.1	178.1	29.4	5.2	596
	15.0	298.4	181.0	30.4	5.2	607
	20.0	297.9	190.0	31.4	5.2	638

[1]Extrapolated data

Table 6.4 Thermodynamic parameters of fractioned samples of P407. Fractionation achieved by partitioning of P407 between hexane and dichloromethane, and subsequent separation and drying. Calorimetric data for unfractioned and fractioned samples were obtained from scans at a copolymer concentration of 5mgmL^{-1} in double distilled water and at a scan rate of 60Kh^{-1}.

Poloxamer	Fraction	T_m (K)	ΔH_{cal} (kJmol^{-1})	C_p^{max} (kJmol^{-1}K^{-1})	$\Delta T_{1/2}$ (K)	ΔS_{cal} (Jmol^{-1}K^{-1})
P407	Original Sample	300.9	158.6	26.1	5.4	528
	CH_2Cl_2 (Triblock rich)	300.8	162.5	28.1	5.3	541
	Hexane (Diblock rich)	300.0	140.4	26.7	4.9	467

Table 6.5 Thermodynamic parameters derived by HSDSC and DSD for the solution-phase transitions of poloxamers in double distilled water at a concentration of 10 mgml^{-1} and at a scan rate of 30 Kh^{-1}.

Calorimetric Data

Poloxamer	T_m (K)	ΔH_{cal} (kJmol^{-1})	C_p^{max} (kJmol^{-1}K^{-1})	$\Delta T_{1/2}$ (K)	ΔS_{cal} (Jmol^{-1}K^{-1})
P182	309.0	163	13.0	11.7	527
P184	311.6	133	11.6	10.6	427
P215	312.6	153	13.0	10.8	490
P235	307.6	202	20.5	8.7	657
P237	312.7	188	19.4	9.0	602
P238	308.2	153	15.7	8.8	494
P284	307.0	236	20.8	10.1	770
P333	297.2	337	54.1	5.4	1134
P338	303.4	235	24.7	8.2	774
P407	299.1	178	29.4	5.2	594

Densitometric Data

Poloxamer	T_m (K)	$\Delta T_{1/2}$ (K)	$\overline{V}$ (cm^{3}g^{-1})	$\Delta\overline{V}$ (cm^{3}g^{-1})	$\Delta\overline{V}$ (x10^{-4} m^{3}mol^{-1})	$\Delta\overline{V}$ per avg monomer unit (x10^{-6}m^{3}mol^{-1})
P182	314.6	8.9	0.9164	0.062	1.49	3.31
P184	316.5	6.8	0.9164	0.042	1.21	2.15
P215	315.8	6.7	0.8952	0.037	1.55	1.87
P235	313.0	10.1	0.9038	0.051	2.36	2.54
P237	314.7	3.2	0.8717	0.017	1.29	0.80
P238	317.6	8.7	0.8660	0.027	3.19	1.25
P284	311.8	9.7	09024	0.056	2.57	2.89
P333	298.0	2.8	0.8915	0.035	1.73	1.86
P338	305.7	3.0	0.8404	0.011	1.55	0.52
P407	299.5	1.3	0.8482	0.006	0.67	0.27

Table 6.6 Theoretical and experimental partial specific volumes of the poloxamers (cm^3g^{-1}) at a concentration of 10 $mgmL^{-1}$ in water.

Poloxamer	van der Waals	α^a	β^b	γ^b	Experimental	
					293 K	T_m
P182	0.8195	0.9372	0.8318	0.7980	0.8778	0.9164
P184	0.8127	0.9227	0.8233	0.7865	0.8711	0.9164
P215	0.8130	0.9174	0.8153	0.7827	0.8556	0.8952
P235	0.8122	0.9166	0.8146	0.7820	0.8633	0.9038
P237	0.8113	0.9061	0.8062	0.7745	0.8409	0.8717
P238	0.8099	0.8969	07985	0.7674	0.8313	0.8660
P284	0.8110	0.9221	0.8190	0.7859	0.5898	09024
P333	0.8268	0.9440	0.8381	0.8042	0.8663	0.8915
P338	0.8086	0.8983	0.7995	0.7682	0.8193	0.8404
P407	0.8115	0.9078	0.8075	0.7757	0.8385	0.8482

[a] Hexagonally packed chains (based on alkanols). [b]Orthorhombic perpendicular or monoclinic lattice.

Theoretical partial specific volumes calculated from precise density an volume values (Kohlraush, *Praktische Physik*, Bd 3, **1968**, *40* and *Handbook of Chemistry and Physics*, CRC Press, Cleveland, Ohio, 55th Edition, **1975**.)

Table 6.7 Thermodynamic parameters derived by HSDSC solution-phase transitions of poloxamers in sodium chloride at a copolymer concentration of 5 $mgml^{-1}$ and at a scan rate of 60 Kh^{-1}.

Poloxamer	[NaCl] (M)	T_m (K)	CP (K)	ΔH_{cal} ($kJmol^{-1}$)	C_p^{max} ($kJmol^{-1}K^{-1}$)	$\Delta T_{1/2}$ (K)	ΔS_{cal} ($Jmol^{-1}K^{-1}$)
P237	0	314.8	-	197.7	18.2	9.9	628
	0.34	309.9	-	193.9	20.3	8.9	626
	0.69	305.8	-	200.9	22.1	8.4	657
	1.03	301.9	359.1	209.1	23.4	8.1	693
	1.38	297.8	352.8	230.3	26.1	8.1	773
	1.71	294.1	347.7	242.7	27.9	8.0	825
P235	0	309.1	-	199.7	19.1	9.2	646
	0.34	304.3	-	256.1	26.1	8.7	842
	0.69	299.8	-	334.8	36.1	8.2	1117
	1.03	296.1	-	309.4	34.8	7.8	1045
	1.38	291.9	-	342.9	41.8	7.3	1175
P407	0	295.4	-	148.7	21.3	6.6	503
	0.34	293.0	-	184.5	26.0	6.2	630
	0.51	291.3	-	170.7	24.0	6.1	586
	0.68	289.8	-	216.0	29.4	6.0	745
	0.86	288.2	359.9	243.5	30.9	5.7	845
	1.03	286.4	356.5	189.0	28.3	5.5	660
	1.71	-	344.3	-	-	-	-
	2.40	-	335.4	-	-	-	
	3.08	-	327.2	-	-	-	

Table 6.8 Thermodynamic parameters derived by HSDSC solution-phase transitions of poloxamer P237 in phosphate buffer (pH 7.2) at a copolymer concentration of 5 $mgmL^{-1}$ and at a scan rate of 60 Kh^{-1}.

Poloxamer	Phosphate Conc. (M)	T_m (K)	ΔH_{cal} ($kJmol^{-1}$)	C_p^{max} ($kJmol^{-1}K^{-1}$)	$\Delta T_{1/2}$ (K)	ΔS_{cal} ($Jmol^{-1}K^{-1}$)
P237	0.10	313.8	160.2	13.1	11.2	510
	0.15	311.4	166.3	14.5	10.5	536
	0.20	307.5	153.1	15.4	9.2	498
	0.35	303.0	160.7	17.4	8.5	531
	0.50	297.9	145.0	17.7	7.7	485

Table 6.9 Thermodynamic parameters derived by HSDSC for the solution-phase transitions of poloxamer P237 in 1.03M sodium chloride at copolymer concentrations of 1 to 20 $mgmL^{-1}$ at a scan rate of 60 Kh^{-1}.

Poloxamer	Conc. ($mgmL^{-1}$)	T_m (K)	CP (K)	ΔH_{cal} ($kJmol^{-1}$)	C_p^{max} ($kJmol^{-1}K^{-1}$)	$\Delta T_{1/2}$ (K)	ΔS_{cal} ($Jmol^{-1}K^{-1}$)
P237	1.0	305.5	359.7	178.1	17.8	8.8	583
	2.5	303.6	359.1	214.7	20.9	9.4	707
	5.0	301.9	359.1	209.1	23.4	8.1	693
	7.5	300.9	358.9	227.4	25.0	8.2	756
	10.0	300.0	358.4	230.4	25.7	8.1	768
	15.0	298.8	358.2	234.7	26.7	7.9	786
	20.0	297.9	358.0	243.0	27.9	7.8	816

Table 6.10 Thermodynamic parameters derived by HSDSC solution-phase transitions of poloxamer P237 in urea and guanidinium chloride solutions at a copolymer concentration of 5 $mgml^{-1}$ and at a scan rate of 60 Kh^{-1}.

Poloxamer	[Urea] (M)	T_m (K)	ΔH_{cal} ($kJmol^{-1}$)	C_p^{max} ($kJmol^{-1}K^{-1}$)	$\Delta T_{1/2}$ (K)	ΔS_{cal} ($Jmol^{-1}K^{-1}$)
P237	1.04	319.2	167.1	13.0	11.7	523
	1.58	322.3	145.7	11.3	12.2	452
	2.86	324.1	173.4	13.7	12.0	536
	4.05	326.7	136.2	10.0	13.2	418
	7.83	331.7	97.8	6.7	13.9	293
	[GdCl] (M)					
P237	0	314.8	197.7	18.2	9.9	628
	0.50	316.1	167.7	14.4	11.1	531
	0.98	317.4	158.7	13.5	11.5	498
	1.99	322.2	157.3	13.0	11.7	490
	3.92	332.3	158.0	10.7	14.2	477
	6.02	342.3	129.2	8.4	14.6	377

Table 6.11 Thermodynamic parameters derived by HSDSC solution-phase transitions of poloxamer P237 in methanol, ethanol, propanol, butanol and formamide solutions at a copolymer concentration of 5 $mgml^{-1}$ and at a scan rate of 60 Kh^{-1}.

Alcohol	Cosolvent Concentration (%)	T_m (K)	ΔH_{cal} ($kJmol^{-1}$)	C_p^{max} ($kJmol^{-1}K^{-1}$)	$\Delta T_{1/2}$ (K)	ΔS_{cal} ($Jmol^{-1}K^{-1}$)
MeOH	0	314.8	197.7	18.2	9.9	628
	5	317.0	148.9	13.2	10.6	470
	10	319.4	140.5	10.4	12.2	440
	15	322.4	99.0	7.1	12.4	307
	17.5	323.1	68.5	5.1	12.5	212
	20	325.5	36.7	3.0	12.3	113
EtOH	5	317.2	143.6	12.3	10.7	453
	10	319.1	99.1	7.9	11.5	311
	15	322.6	54.3	4.2	12.2	168
	20	329.2	19.2	1.6	13.2	58
PrOH	2.5	314.8	154.3	15.1	9.4	490
	5	314.4	141.3	13.5	9.7	449
	7.5	313.4	100.0	9.8	9.2	319
	10	313.8	44.6	6.0	7.3	142
BuOH	2.5	310.1	178.4	18.5	8.8	575
	5	303.5	199.4	21.9	8.1	657
	7.5	295.4	234.4	26.1	8.0	794
Formamide	10	318.2	148.1	11.7	11.5	465
	20	321.5	106.9	8.1	12.5	333
	30	325.7	77.7	5.5	13.5	239
	40	330.9	62.1	3.9	15.4	188
	50	336.9	19.7	1.6	12.7	59
	60	344.2	16.8	1.2	14.0	49

6.6 References

(1) Privalov,P.L.; Gill,S.J., *Adv.Protein Chem.*, **1989**, *39*, 191.
(2) Privalov,P.L., *Ann.Rev.biophys.Chem.*, **1989**, *18*, 47.
(3) Sturtevant,J.M., *Ann.Rev.Phys.Chem.*, **1987**, *38*, 463.
(4) Alexandridis,P.; Hatton,T.A., *Colloids and Surfaces A: Physicocem. Eng. Aspects*, **1995**, *96*, 1.
(5) Almgren,M.; Brown,W.; Hvidt,S., *Colloid Polymer Sci.*, **1995**, *273(1)*, 2.
(6) Mortensen,K., *J.Phys.:Condens. Matter*, **1996**, *8*, A103.
(7) Wanka,G.; Hoffman,H.; Ulbricht,W., *Colloid Polym. Sci.*, **1990**, *268*, 101.
(8) Hergeth,W.D.; Alig,I.; Lange,J.; Lochmann,J.R., Scherzer,T.; Waterwig,S., *Macromol.Chem., Macromol.Symp.*, **1991**, *52*, 289.
(9) Zhou,Z.; Chu,B., *Macromolecules*, **1994**, *27(8)*, 2025.
(10) Wu,G.W.; Zhou,Z.; Chu,B., *Macromolecules*, **1993**, *26(8)*, 2117.
(11) Yu,G-E.; Deng,Y.; Dalton,S.; Wang,Q-G.; Attwood,D.; Price,C.; Booth,C., *J.Chem.Soc. Faraday Trans.*, **1992**, *88(17)*, 2537.
(12) Bahadur,P.; Pandya,K., *Langmuir*, **1992**, *8*, 2666.
(13) Bloss,P.; Hergeth,W-D.; Döring,E.; Witkowski,K.; Waterwig,S., *Acta Polymerica*, **1989**, *40(4)*, 260.
(14) Šimek,L.; Bohdanecký,M., *Eur.Polym.J.*, **1996**, *32(1)*, 129.
(15) Almgren,M.; Bahadur,P.; Jansson,M.; Li,P; Brown,W; Bahadur,A., *J.Colloid Interface Sci.*, **1992**, *151(1)*, 157.
(16) Alig,I.; Ebert,R.U.; Hergeth,W-D.; Waterwig, S., *Polymer Comm.*, **1990**, *31*, 314.
(17) Tontisakis,A.; Hilfiker,R.; Chu,B., *J.Colloid Polym.Sci.*, **1990**, *135(2)*, 427.
(18) Rassing,J., Attwood,D., *Int.J.Pharm.*, **1983**, *13*, 47.
(19) Brown,W.; Schillén,K.; Almgren,M.; Hvidt,S.; Bahadur,P., *J.Phys.Chem.*, **1991**, *95*, 1850.
(20) Yang,L.; Bedells,A.D.; Attwood,D.; Booth,C., *J.Chem.Soc.Faraday Trans.*, **1992**, *88(10)*, 1447.
(21) Zhou,Z.; Chu,B., *Macromolecules*, **1988**, *21*, 2548.
(22) Alexandridis,P.; Athanassiou,V.; Hatton,T.A., *Langmuir*, **1995**, *11(7)*, 2442.
(23) Alexandridis,P.; Nivaggioli,T.; Hatton,T.A., *Langmuir*, **1995**, *11(5)*, 1468.
(24) Nivaggioli,T.; Alexandridis,P.; Hatton,T.A.; Yekta,A., Winnik,M.A., *Langmuir*, **1995**, *11(3)*, 730.
(25) Nakashima,K.; Fujimoto,Y.; Anzai,T., *Photochem.Photobiol.*, **1995**, *61(6)*, 592.
(26) Hecht,E.; Mørtensen,K.; Hoffmann,H., *Macromolecules*, **1995**, *28(16)*, 5465.
(27) Hecht,E.; Mørtensen,K.; Gradzielski,M.; Hoffmann,H., *J.Phys.Chem.*, **1995**, *99(13)*, 4866.
(28) Chu,B.; Wu,G.W., *Macromolecular Symp.*, **1994**, *87*, 55.
(29) Chu,B.; Wu,G.W.; Schneider,D.K., *J.Polymer Sci. PartB: Polymer Phys.*, **1994**, *32(16)*, 2605.
(30) Wu,G.W.; Ying,Q.C.; Chu,B., *Macromolecules*, **1994**, *27(20)*, 5758.
(31) Wu,G.W.; Zhou,Z.K.; Chu,B., *J.Polymer Sci. Part B: Polymer Phys.*, **1993**, *31(13)*, 2035.
(32) Zhou,Z.; Chu,B., *J.Colloid Interface Sci.*, **1988**, *126*, 171.
(33) Beezer,A.E.; Mitchell,J.C.; Rees,N.H.; Armstrong,J.K.; Chowdhry,B.Z.; Leharne,S.; Buckton,G., *J.Chem.Res.(S)* , **1991**,254.
(34) Mortensen,K.; Brown,W., *Macromolecules*, **1993**, *26*, 4128.
(35) Kabanov,A.V.; Nazarova,I.R.; Astafieva,I.V.; Batrakova,E.V.; Alakhov,V.Y.; Yaroslavov,A.A.; Kabanov,V.A., *Macromolecules*, **1995**, *28(7)*, 2303.
(36) Nivaggioli,T.; Tsao,B.; Alexandridis,P.; Hatton,T.A., *Langmuir*, **1995**, *11(1)*, 119.
(37) Nakashima,K.; Anzai,T.; Fujimoto,Y., *Langmuir*, **1994**, *10(3)*, 658.
(38) Turro,N.J; Kuo,P.L., *J.Phys.Chem.*, **1986**, *90*, 4205.
(39) Lianos,P.; Brown,W., *J.Phys.Chem.*, **1992**, *96*, 6439.
(40) Gilbert,J.C.; Washington,C; Davies,M.C.; Hadgraft,J., *Int.J.Pharm.*, **1987**, *40*, 93.
(41) Almgren,M.; vanStam,J.; Lindblad,C.; Li,P.; Stilbs,P.; Bahadur,P., *J.Phys.Chem.*, **1991**, *95*, 5677.
(42) Gaisford,S.; Beezer,A.E.; Mitchell,J.C.; Loh,W.; Finnie,J.K.; Williams,S.J., *J.Chem.Soc.Chem.Comm.*, **1995**, *18*, 1843.
(43) Linse,P., Malmsten,M., *Macromolecules*, **1992**, *25*, 5434.
(44) Wang,Q.; Price,C.; Booth,C., *J.Chem.Soc.Faraday Trans.*, **1992**, *88(10)*, 1437.
(45) Hecht,E.; Hoffmann,H., *Colloids Surfaces: A Physicochem.Eng.Aspects*, **1995**, *96*, 181.
(46) Hecht,E., Hoffmann,H., *Langmuir*, **1994**, *10*, 86.
(47) Hergeth,W.D.; Alig,I.; Lange,J.; Lochmann,J.R., Scherzer,T.; Waterwig,S., *Makromol.Chem.Macromol.Symp.*, **1991**, *52*, 289.
(48) Schild,H.G.; Tirrell,D.A., *J.Phys.Chem.*, **1990**, *94*, 4352.
(49) Lenaerts,V.; Triqueneaux,M.; Quarton,M.; Rieg-Falson,F.; Couvreur,P., *Int.J.Pharm.*, **1987**, *39*, 121.
(50) Rassing,J.; McKenna,W.P.; Bandyopadhyay,S.; Eyring,E-M., *J.Mol. Liq.*, **1984**, *27*, 165.

(51) Malmsten,M.; Lindman,B., *Macromolecules*, **1992**, *25*, 5446.
(52) Malmsten,M.; Lindman,B., *Macromolecules*, **1992**, *25*, 5440.
(53) Chu,B.; Wu,G.W., *Macromolecular Symp.*, **1995**, *90*, 251.
(54) Walderhaug,H.; Nyström,B., J.Phys.Chem., 1997, 101, 1524.
(55) Williams,R.K.; Simard,M.A.; Jolicoeur,C., *J.Phys.Chem.*, **1985**, *89*, 178.
(56) Brown,W.; Schillen,K.; Almgren,M.; Hvidt,S.; Bahadur,P., *J.Phys.Chem.*, **1991**, *95*, 1852.
(57) Mitchard,N.M.; Beezer,A.E.; Rees,N.; Mitchell,J.C.; Leharne,S.A.; Chowdhry,B.Z.; Buckton,G., *J.Chem.Soc.Chem.Comm.*, **1990**, *13*, 900.
(58) Eagland,D; Crowther,N., *J.Faraday Symp.Chem.Soc.*, **1983**, *17*, 141.
(59) Kjellander,R.; Florin,E., *J.Chem.Soc.Faraday Trans.*, **1981**, *77*, 2053.
(60) Juhasz, J.; Lenaerts,V.; Tan,P.V.M.; Ong,H., *J.Colloid Interface Sci.*, **1990**, *136*(1), 168.
(61) Bahadur,P.; Li,P.; Almgren,M.; Brown,W., *Langmuir*, **1992**, *8* ,1903.
(62) Schott,H.; Han,S.K., *J.Pharm.Sci.*, **1975**, *64(4)*, 658.
(63) Schott,H.; Royce,A.E., *J.Pharm.Sci.*, **1984**, *73(6)*, 793.
(64) Schott,H., *J.Colloid Interface Sci.*, **1994**, *173*, 265.
(65) Gu,T.; Qin,S.; Ma,C., *J.Colloid Interface Sci.*, **1989**, *127(2)*, 586.
(66) Almgren,M.; van Stam,J.; Lindbald,C.; Li,P.; Stilbs,P.; Bahadur,P., *J.Phys.Chem.*, **1991**, *95*, 5677.
(67) Pandit,N.; Kisaka,J., *Int.J.Pharm.*, **1996**, *145*, 129.
(68) Samieh,A.A.; Karlström,G.; Lindman,B., *Langmuir*, **1991**, *7*, 1067.
(69) Karlström,G.; Carlsson,A.; Lindman,B., *J.Phys.Chem.*, **1990**, *94*, 5005.
(70) Florin,E.; Kjellander,R.; Eriksson,J.C., *J.Chem.Soc.Faraday Trans.I*, **1984**, *80*, 2889.
(71) Fields,G.B.; Alonso,D.O.V.; Stigter,D.; Gill,K.A., *J.Phys.Chem.*, **1992**, *96*, 3974.
(72) Marston,F.A.O., *Biochem.J.*, **1986**, *240*, 1.
(73) Weir,M.P.; Sparks,J., *Biochem.J.*, **1987**, *245*, 85
(74) Mitraki,A.; King,J., *Bio.Technology*, **1989**, *7*, 690.
(75) Wetlaufer,D.B.; Malik,S.K.; Stoller,L.; Coffin,R.L., *J.Am.Chem.Soc.*, **1964**, *86*, 508.
(76) Frank,H.S.; Franks,F., *J.Chem.Phys.*, **1968**, *48*, 4746.
(77) Nozaki,Y.; Tanford.C., *J.Biol.Chem.*, **1964**, *238*, 4074.
(78) Stokes,R.H., *Aust.J.Chem.*, **1967**, *20*, 2087.
(79) Roseman,M.; Jencks,W.P., *J.Am.Chem.Soc.*, **1975**, *97*, 631.
(80) Muller,N., *J.Phys.Chem.*, **1990**, *94*, 3856.
(81) Kresheck,G.C., In *"Water - A Comprehensive Treatise,* Vol. 4, *Aqueous Solutions of Amphiphiles and Macromolecules"*, Franks,F. (Ed), Plenum Press, New York, **1975**.
(82) Fukushima,K.; He,H.C., *Bull.Chem.Soc.Jpn.*, **1993**, *66*, 1820.
(83) Baglioni,P.; Ferroni,E.; Kevan,L., *J.Phys.Chem.*, **1990**, *94*, 4296.
(84) Ruiz,C.C.; Sanchez,F.G., *J.Colloid Interface Sci.*, **1994**, *165*, 110.
(85) Sarkar,N.; Bhattacharyya,K., *Chem.Phys.Lett.*, **1991**, *180*, 283
(86) Blandamer,M.J.; Briggs,B.; Butt,M.D.; Cullis,P.M.; Gorse,L.; Engberts,J.B.F.N., *J.Chem.Soc.Faraday Trans.*, **1992**, *88(19)*, 2871
(87) Blandamer,M.J., *Adv.Phys.Org.* , **1977**, *14*, 203.
(88) Schick,M.J., *J.Phys.Chem.*, **1964**, *68*, 3585.
(89) Sobisch,T.; Wüstnick,R., *Colloids Surf.*, **1992**, *62*, 187.
(90) Andreoli-Ball,L.; Sun,S.J.; Trejo,L.M.; Costas,M.; Patterson,D., *Pure Appl.Chem.*, **1990**, *62*, 2097.
(91) Atkins,P.W., *Physical Chemistry*, 5th ed.; Oxford University Press: Oxford, U.K., **1994**.

CHAPTER 7 - ETHYLENE DIAMINE ALKOXYLATES (POLOXAMINES)

7.1 Introduction.

Poloxamines are AB block copolymers of poly(oxyethylene) (A) and poly(oxypropylene) (B) bonded to an ethylene diamine central group via the poly(oxypropylene) moiety resulting in four AB blocks per ethylene diamine molecule.[1] Poloxamines are also termed ethylene diamine alkoxylates, N,N',N",N"'- tetra[(oxyethylene)-(oxypropylene)] diaminoethylenes, Tetronics or Synperonic T nonionic surfactants. The molecular weight of the poloxamines examined in this study range from 1650 to 26000. The low molecular weight poloxamines are viscous oils or pastes and the high molecular weight poloxamines are amorphous solids. Their uses in industry are numerous because of the ability to alter the POE to POP ratio giving rise to variations in hydrophilic/hydrophobic balance and total molecular weight of the polymers. Poloxamines can be used as demulsifiers or emulsifiers, anti-foaming agents, and corrosion inhibitors.[2] However, general industrial use of the poloxamines is at high polymer concentrations and, as a result, most research regarding the poloxamines has been performed at high concentrations (>>10% w/v). Investigations of the poloxamines at low concentrations has generally been concerned with drug delivery systems.[3-9] There is a paucity of physico-chemical data for poloxamines. Aqueous solutions of POE are probably the most widely investigated polymeric systems; POE solubility decreases with increasing temperature. POP has been observed to become insoluble in water above a molecular weight of 750.[1] The solubility of POE in water has been suggested to be due to hydrogen bond formation between the ether oxygens of POE and water; at elevated temperatures the POE-water system phase separates.[10] Similarly the effect of decreased solubility in water, upon heating, is observed for several other nonionic polymers.[11] The decrease in solubility may be explained by changes in solute-solute, solute-solvent as well as solvent-solvent interactions. The phase separation of POE with increasing temperature from an aqueous system is explained as a consequence of a change in conformational equilibrium of the polymer chain between polar and less polar conformations.[11]

7.2 Experimental Section.

The poloxamines examined (T304, T701, T707, T803, T904, T908, T1301, T1302) were a gift from ICI Chemicals Ltd. (Middlesbrough, Cleveland, UK.) under the tradename of Synperonic T nonionic surfactants. As these polymers are commercial products, the poloxamines were used as received, without any further purification. The declared molecular weights, POP and POE contents are shown in Table 3.2 (Chapter 3). The molecular weight distribution of the poloxamines were determined by gel permeation chromatography (GPC) using mixed PL gel columns, a mobile phase of tetrahydrofuran (with antioxidant), ambient temperature, a flow rate of $1mLmin^{-1}$ and a refractive index detector. GPC analysis showed that all but two of the poloxamines (T707, T908) gave a single elution peak and as a result the thermodynamic parameters derived by HSDSC for poloxamines T707 and T908 can only be quoted on a qualitative basis. Buffers (0.03M), although not at controlled ionic strength, were used for pH experiments and 0.51 to 3.08M Analar sodium chloride was used for the study of salt effects on the lower main phase transition (LMPT) of a 0.5% (w/v) aqueous solution of poloxamine T304.

7.2.1 **High Sensitivity Differential Scanning Calorimetry (HSDSC).**

Further to the HSDSC experimental procedure in Chapter 3 the effects of pH were studied for poloxamine T701 over a pH range of pH 2.5 to pH 11.1 using dilute buffer systems (0.03M) and a scan rate of $60Kh^{-1}$. The concentration of poloxamine T701 was varied from 0.1% to 2.0% (w/v) in double distilled water and HSDSC scans examined at a scan rate of $60Kh^{-1}$.

7.2.2 **Turbidimetric Analysis.**

Turbidity measurements were carried out at 540nm for the poloxamines at a concentration of 0.5% (w/v) in quartz cells with double distilled water as a reference using a Perkin-Elmer Lambda II spectrophotometer over a temperature range of 278 to 370K at a scan rate of $60Kh^{-1}$. The waterbath was parallel coupled to the reference and sample cell and was accurate to ±0.2K. The cloud point temperature (CP) was recorded as the temperature at which the percentage of transmitted light at 540nm began to decrease below that of the reference cell.

7.2.3 **Titrimetric Analysis.**

Grade A burettes were used for all titrations and each experiment was run in triplicate at 293K. An approximate 0.01M NaOH solution was standardised with 0.01M potassium hydrogen phthalate using phenolphthalein indicator according to the method described in Vogel.[12] The standardised NaOH solution was then titrated against an approximate 0.01M HCl solution. Conductimetric measurements were recorded using Pt electrodes and pH measurements were carried out using a glass electrode after calibration with pH 4, 7 and 9 standard buffer solutions. 25mL of 0.01M poloxamine T701 was added to 25mL of standardised 0.01M HCl and made up to 100mL with double distilled water. This solution was then titrated against standardised 0.01M NaOH. Conductivity and pH values were recorded after every 0.5mL addition, and after every 0.1mL addition 2mLs below and above the equivalence points.

7.2.4 **Nuclear Magnetic Resonance (NMR).**

^{1}H and ^{13}C NMR spectra were recorded at 500MHz and 125MHz respectively on a Varian VXR500S spectrometer using 1.0% (w/v) solutions of poloxamines T701 and T904 in D_2O. All chemical shift values were referenced against an aqueous solution of sodium 2,2-dimethyl-2-silapentane sulphate held in the inner capilliary of a 5mm coaxial tube. Temperature measurements were accurate to ±0.2K.

7.3 Results and Discussion.

7.3.1 **Background.**

Phase transitions, with no turbidity change, of poly(vinyl alcohol) in dilute aqueous solution (0.02 to 0.17% w/w) over the temperature range of 283 to 293K, observed by densitometric analysis, indicated that with increasing temperature the hydrophobic portions of the polymer partially desolvated resulting in self-association of the hydrophobic portions of the polymer.[13] At higher temperatures, a gradual desolvation of the hydrophilic portions of the polymer was observed. HSDSC has been employed to study the micellar reorganisation of aqueous solutions of hexadecyltrimethylammonium bromide and tetradecyltrimethylammonium bromide over a small concentration range in the 10^{-2} moldm^{-3} region.[14] The lower critical solution temperatures of poly(N-isopropylacrylamide), poly(vinylmethylether), POP and

hydroxypropylcellulose have also been examined by HSDSC.[15] It was concluded that, for each of the polymers studied, the transition enthalpies were consistent with the loss of one hydrogen bond per repeating monomeric unit on phase separation. Poloxamers being ABA block copolymers of POE (A) and POP (B) are similar in structure and surfactant properties to those observed for poloxamines.[1] Poloxamers are finding increasing applications in the pharmaceutical and related industries ranging from drug delivery[16-19] and haemorheology,[20] to stimulating plant growth.[21] In dilute aqueous solution (0.5% w/v) poloxamers have been observed by HSDSC to undergo a phase change with increasing temperature[22] similar in nature to the phase transitions of poloxamines in dilute aqueous solution reported in this paper. The observed transition for P237 showed no turbidity and it was hypothesised that desolvation of the POP portion of the polymer as well as a conformational change occurred during the transition. The phase transition for P237 has been shown by T_1 relaxation NMR measurements[23] to be associated with rotation of the methyl groups of the POP portion of the polymer, and no sharp change in NMR parameters for the POE portion of the polymer was observed over the transition temperature range observed by HSDSC. Brown *et.al.*,[24] studied P235 using light scattering techniques and showed that for a 5% (w/v) aqueous solution below 294K both monomer and an aggregated form existed, and above 294K only the aggregated form was observed. Zhou and Chu[25] examined a 2% (w/v) aqueous solution of poloxamer P184 using light scattering and NMR techniques. They observed only the monomeric form at temperatures below 307K and at elevated temperatures aggregates were formed that were observed to increase exponentially in hydrodynamic radius with increasing temperature. Wang *et.al.*[26] reported an aggregation of P237 using gel permeation chromatography over a temperature range of 299 to 332K and showed that for a 0.2% (w/w) aqueous solution below 306K only one peak was observed at an elution volume characteristic of single molecules and on raising the temperature, a second peak at a lower elution volume was detected which became more predominant at higher temperatures and was assigned to micelles. It has also been shown that the size of the micellar core is dependent upon the POP content and it has been proposed that the aggregation number of the micelles increases strongly with rising temperature.[27] The phase behaviour of AB block copolymers of POE and POP in various solvents by observation of the cloud point (CP), has been investigated by Samii *et.al.*[28,29] The block copolymers showed non-monotonic behaviour in a mixed system of water and N-methylacetamide (NMA), the CP temperature decreased as the percentage of NMA was increased, and at concentrations above 70% NMA the CP temperature increased. Samii *et.al.*[29] also showed that at low polymer concentrations (1% w/v) in water, the addition of

sodium chloride decreased the CP temperature whereas sodium iodide increased the CP. Gu *et.al.*[30] studied the effects of electrolytes on the CP's of mixed aqueous solutions of ionic and nonionic surfactants. They showed that the addition of sodium, calcium or lanthanum chloride to a 1% (w/v) aqueous solution of Triton X-100 decreased the CP temperature. It was also reported that the addition of an ionic surfactant (cetyltrimethylammonium bromide) to a 1% (w/v) solution of Triton X-100 drastically increased the CP temperature.

7.3.2 **Thermal Analysis**.

The phase transitions for the poloxamines (Figure 7.1) all show slightly asymmetric endotherms with a steep leading edge to the transition below the T_m and a gentle slope back to the baseline above the T_m , indicative of aggregation.[31,32] With the exception of T1301 and T701 the T1302, T904 and T803 exhibit a further asymmetric low enthalpy transition above the main transition (LMPT). This low enthalpy transition corresponds to the cloud point (CP) of the poloxamine, i.e. the temperature at which phase separation of the polymer begins to occur. For T701 and T1301 the CP is observed within the envelope of the LMPT, as confirmed by qualitative experiments using a waterbath and turbidimetric analysis at 540nm. The reason for the close proximity of both transitions for T701 and T1301 is probably due to the low percentage of POE content of the polymer. The T_m range for the observed LMPT's for the poloxamines is from 291.3 to 368.2K for T1301 and T304 respectively (Table 7.1 and 7.2). Many of the thermodynamic parameters (e.g. ΔH_{cal} , $\Delta T_{1/2}$) are of similar order of magnitude to those found in native→ denatured (folded→unfolded) transitions of proteins.[31-33] The ΔH_{cal} , C_p^{max} and ΔS increase with increasing POP content. T_m and $\Delta T_{1/2}$ values decrease with increasing POP content. The observed trends in thermodynamic parameters are comparable at $5mgmL^{-1}$ and constant oxypropylene concentration (Tables 7.1 and 7.2 respectively) and therefore the underlying molecular processes must be the same in both situations. The thermodynamic parameters for T707 and T908 are not reported here because GPC analysis shows that they are relatively impure and very polydisperse and

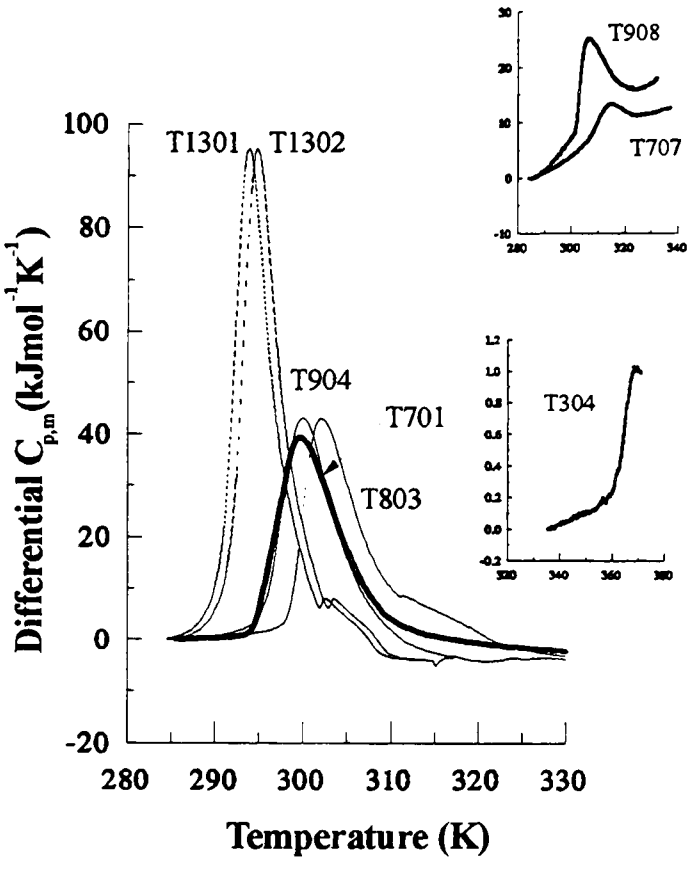

Figure 7.1 Calorimetric scans of poloxamines in double distilled water at a concentration of 5 mgmL^{-1} and at a scan rate of 60Kh^{-1}.

therefore only qualitative values such as T_m are quoted. A plot of ΔH_{cal} per average monomer unit versus POP/POE ratio (Figure 7.2) shows that ΔH_{cal} approaches zero as the POP/POE ratio approaches 0:1 (i.e., polyoxyethylene homopolymer). This relationship suggests that the observed phase transitions of poloxamines are associated with changes in the hydrophobic POP portion of the polymer, and are similar to those relationships reported for the phase transitions of poloxamers in dilute aqueous solution using the techniques of HSDSC,[35] differential scanning densitometry[35] and dilatometry.[36] The POE content of the poloxamines must play an important role in effecting the conformational changes associated with the LMPT as well as giving solubility to the hydrophobic POP, as observed for T701 and T1301 where aggregation is observed at the onset of hydrophobic interactions associated with the low POE content. The CP corresponds to conditions under which POE/H_2O interaction is less favoured than POE/polymer interaction i.e., the POE loses water and the polymer precipitates as a result of conformational change(s) and aggregation. For the relationship between the CP and T_m of the LMPT, a plot of ΔT (where $\Delta T = CP - T_m$) versus POE content (in units of gmol^{-1}) shows a linear plot with the following relationship (Figure 7.3):

$$\Delta T = 8.87 \times 10^{-3} (POE) - 8.57 \qquad r^2 = 0.93$$

However the same plot for ΔT versus POP content shows no obvious relationship. It appears, therefore, that the difference between the CP and T_m is determined by the POE content whereas the temperature at which the LMPT occurs is determined more by the POP content of the poloxamine. The relationship given in the above equation, between ΔT and [POE], is

purely empirical and the exact physico-chemical meaning of the equation is not immediately obvious.

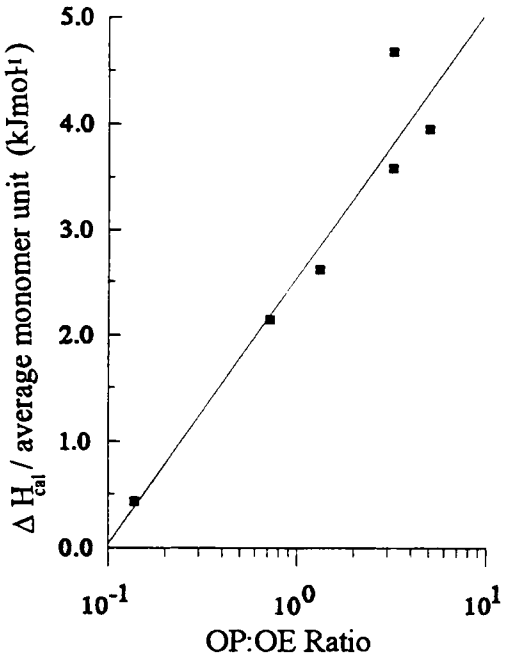

Figure 7.2 The relationship between the calorimetric enthalpy and oxypropylene/oxyethylene ratio of the poloxamines.

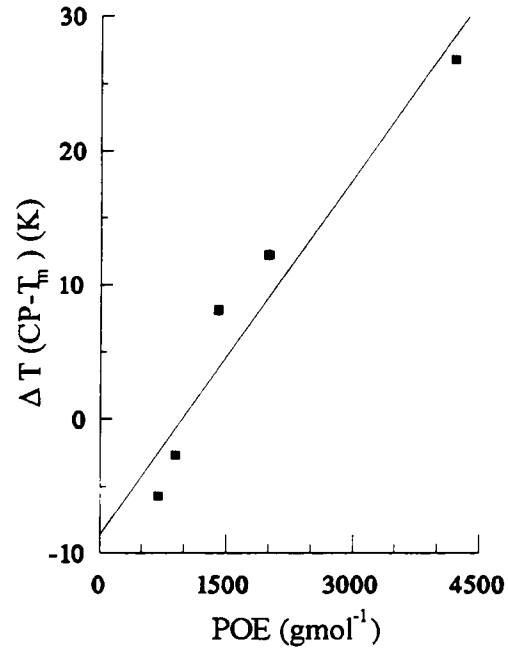

Figure 7.3 A plot to show the dependence of the difference between the main phase transition and cloud point to the oxyethylene content of the poloxamines.

7.3.2.1 **Scan Rate Effects for T701.**

The effects of scan rate (10, 30 and 60Kh^{-1}) for T701 are shown in Table 7.3. It can be seen that there is a slight increase in T_m and a decrease in ΔH_{cal} and C_p^{max} because of broadening of the transition as scan rate decreases ($\Delta T_{1/2}$ increases).

7.3.2.2 **Reversibility.**

The reversibility of the transitions observed for T904 was examined at a concentration of 0.5% (w/v) in double distilled water at a scan rate of 30Kh^{-1} for the upscan and for the downscan. The reversibility HSDSC scans for T904 are shown in Figure 7.4. The calorimetrically derived thermodynamic parameters for T904 (T_m , ΔH_{cal}, C_p^{max}, $\Delta T_{1/2}$, ΔS) for both the upscan and downscan show marginal differences and these are within the limits of detection for the HSDSC (Table 7.4) showing that the LMPT is not, observably, kinetically

limited. T904 when scanned for a third time after the downscan, gave an identical HSDSC scan to the original upscan showing that the observed phase transition is reversible.

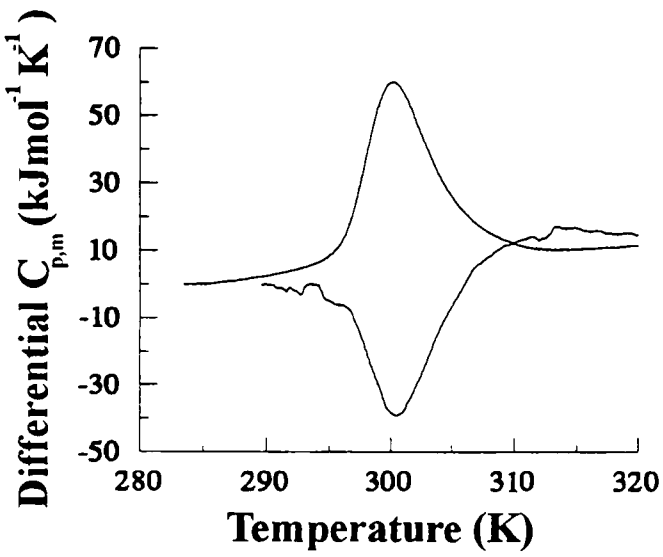

Figure 7.4 Calorimetric scan to show the reversibility of T904 in double distilled water at a concentration of 5mgmL^{-1}, at a scan rate of ±30 Kh^{-1}

7.3.2.3 **Concentration Effects.**

The effect of varying the concentration of T701 from 0.1 to 2.0% (w/v) in double distilled water was studied at a scan rate of 60Kh^{-1} (Table 7.5). With increasing polymer concentration there is a gradual decrease in T_m and $\Delta T_{1/2}$, and a gradual increase in ΔH_{cal}, C_p^{max} and ΔS. Brown *et.al.*[24] concluded that the observed phase transition of a 5% (w/v) aqueous solution of P235 studied by light scattering techniques, corresponded to a (monomer + aggregate) to aggregate transition. The observations for T701 over the lower concentration range of 0.1 - 2.0% (w/v) may correspond to a monomer to aggregate transition, in agreement with the observations made by Zhou and Chu[25] for a 2% (w/v) solution of P184.

7.3.2.4 **pH Effects.**

The pH of the poloxamine solutions in double distilled water range from pH 7.6 - 8.8 because of a residue of OH^- ions from the polymerisation process of the poloxamines to prevent acid hydrolysis of the polymers over prolonged periods of storage.

The effects of varying pH from pH 2.5 to 11.1 were examined for poloxamine T701 at a concentration of 0.5% (w/v) in relevant dilute buffer (0.03M) at a scan rate of 60Kh^{-1} (Figure 7.5). The observed phase transition becomes broader with decreasing pH ($\Delta T_{1/2}$ increases, C_p^{max} decreases). The ΔH_{cal} increases with increasing pH and the transition is

observed to become more symmetric (Table 7.5). The T_m of the LMPT decreases with increasing pH up to pH 8.1 and is observed to increase at pH 11.1. The values for the thermodynamic parameters at pH 11.1 show an opposing trend to those observed at lower pH values. As the pH increases, the amine groups become progressively deprotonated, facilitating desolvation of the POP hydrophobe up to the pH at which the ethylene diamine moiety becomes completely deprotonated. At higher pH values, the observed effects may be due to changes in the ionic strength of the bulk phase. The conclusion that the observed pH effects are associated with the ethylene diamine moiety is supported by the observation that the phase transitions for poloxamers in dilute aqueous solutions are unaffected by variations in pH.[22]

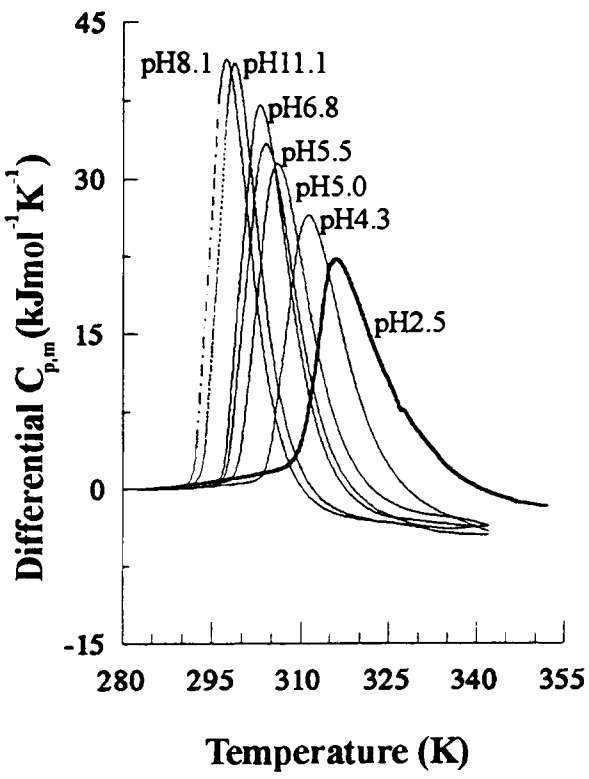

Figure 7.5 The effects of pH on the observed phase transition of T701 in dilute aqueous solution (5mgmL^{-1}), scanned at 60Kh^{-1}.

7.4 Titrimetric Analysis.

The pH curve for the titration of 25mL of 9.75×10^{-3} M T701 + 25mL of 1.05×10^{-2} M HCl titrated against 8.43×10^{-3} M NaOH with a plot of T_m versus pH are shown in Figure 7.6. The first equivalence point corresponds to neutralisation of the excess acid added initially and the second equivalence point corresponds to deprotonation of the ethylene diamine moiety of the poloxamine. Approximately one proton per poloxamine molecule was calculated to have been removed at the second equivalence point. The pK_a of T701 was determined to be 7.6 which is comparable to pK_a values observed for simple secondary and tertiary amines.[37] The deprotonation effect observed for the LMPT of T701 in dilute aqueous solution (0.5%

w/v) at various pH by HSDSC is confirmed by the titrimetric analysis. Below pH 9, T701 exists as a protonated form and above pH 10 the poloxamine becomes deprotonated.

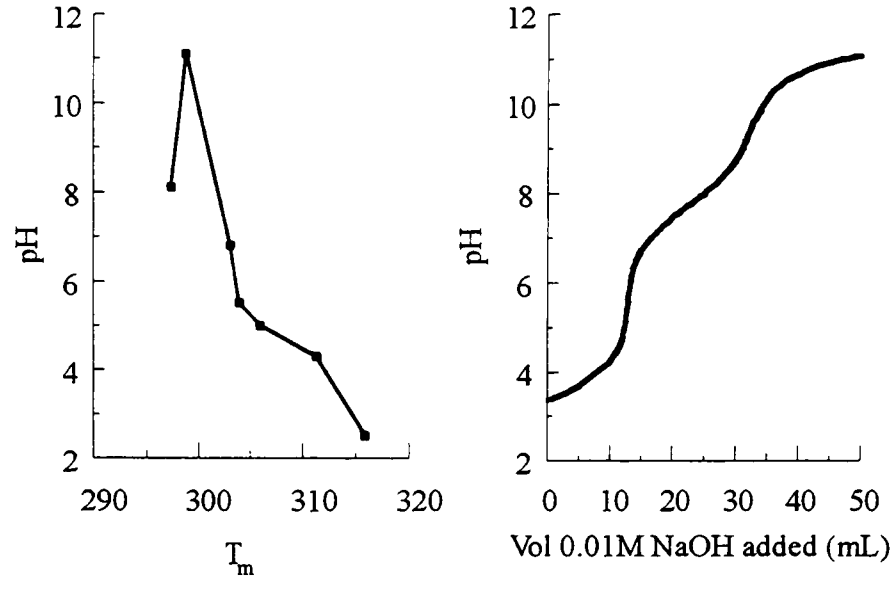

Figure 7.6 Graphs to show the effect of pH on the phase transition temperature of T701 and the corresponding back-titration of an acidified solution of T701 with 0.01M NaOH.

7.5 Turbidimetric Analysis.

The CP of a 0.5% (w/v) aqueous solution of a poloxamine was defined as the temperature at which the percentage of transmitted light of wavelength 540nm was less than 100% of that of the reference cell. Figure 7.7 shows the turbidimetric runs for T701 and T904 superimposed over the corresponding calorimetric scan and for T701 the increase in turbidity is observed to correspond with the onset of the main phase transition, and for T904 it is clear that the cloud point is not associated with the main phase transition, but is observed to correspond with a low enthalpy transition that is almost calorimetrically silent. The CP is observed to increase with increasing POE content. The LMPT of the poloxamines probably corresponds to a dehydration of the POP portion of the polymer and so the polymer remains in solution due to the effect of the hydrophile when the POE content is greater than 10% of the overall molecular weight.

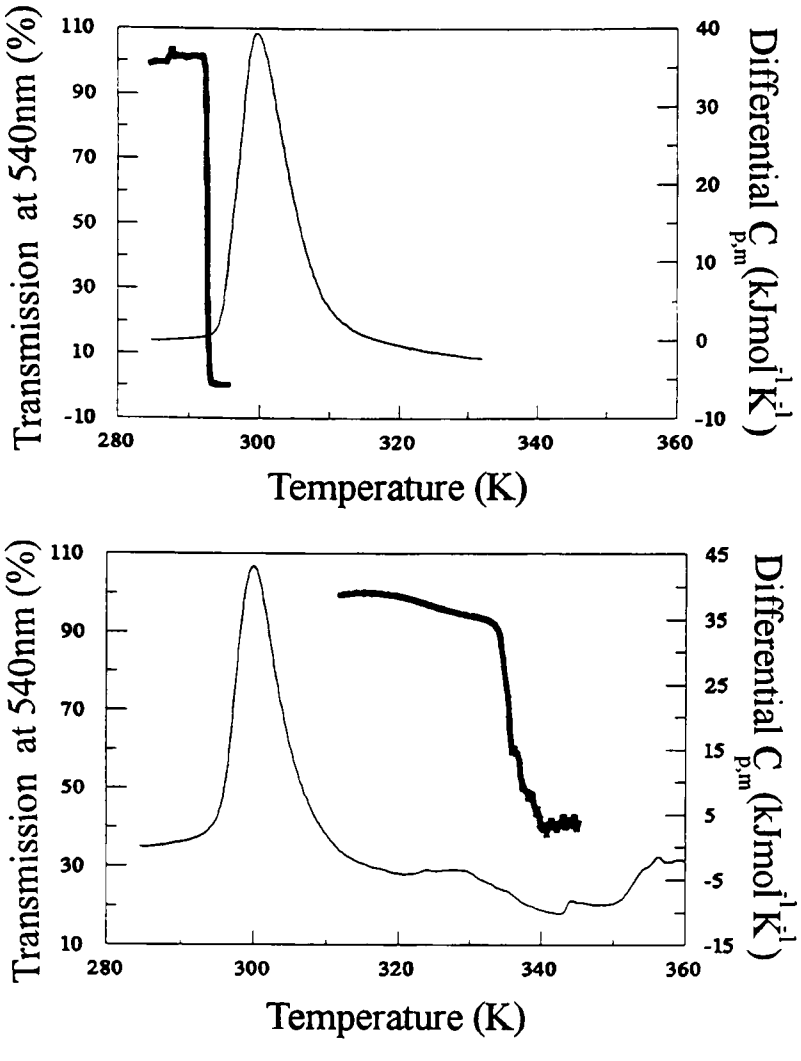

Figure 7.7 Turbidimetric scans of poloxamines T701 and T904 at 540nm and at a concentration of 5 mgmL^{-1} in double distilled water, scanned at a scan rate of 60Kh^{-1}. The corresponding calorimetric runs are superimposed showing the relationship between the two techniques.

7.6 Sodium Chloride Effects.

The effect of various concentrations of sodium chloride (0.51 to 3.08M) upon T304 (0.5% w/v) showed that with increasing salt concentration the T_m, of the LMPT was decreased. ΔH_{cal} , C_p^{max} and ΔS increased with increasing salt concentration (Figure 7.8). Extrapolation of the various thermodynamic parameters versus salt concentration to zero salt concentration allows the T_m , ΔH_{cal} , C_p^{max}, $\Delta T_{1/2}$, ΔS to be predicted for a 0.5% (w/v) of polymer in water (Table 7.6). The observed effect of salt upon the transition is similar to those effects observed for the "salting out" of a globular protein, where salts strongly affect the process of hydration of the hydrophobic residues. Since ions affect the structure of water, one would expect that the influence of sodium chloride on the observed phase transition for T304 would be partly because of the effect of the salt on the hydration shell of the polymer, allowing aggregation of the poloxamine to become thermodynamically more favourable. The effect of halide ions has been shown to have a far greater affect on the CP of POE systems than alkali metal ions, although the alkali metal ions interact directly with the POE but the extent of those contacts is very small and hence have only minor thermodynamic implications.[38] In contrast, hydrophobic solutes (e.g. pentanol) would preferentially interact

with the POP portion of the polymer and an increase in T_m of the LMPT would probably be observed. The observed effects of sodium chloride on the LMPT of a dilute aqueous solution of T304 are similar to those reported for the phase separation of aqueous solutions of ethyl(hydroxyethyl)cellulose and POE upon the addition of various cosolutes (alcohols, inorganic salts and surfactants).[11]

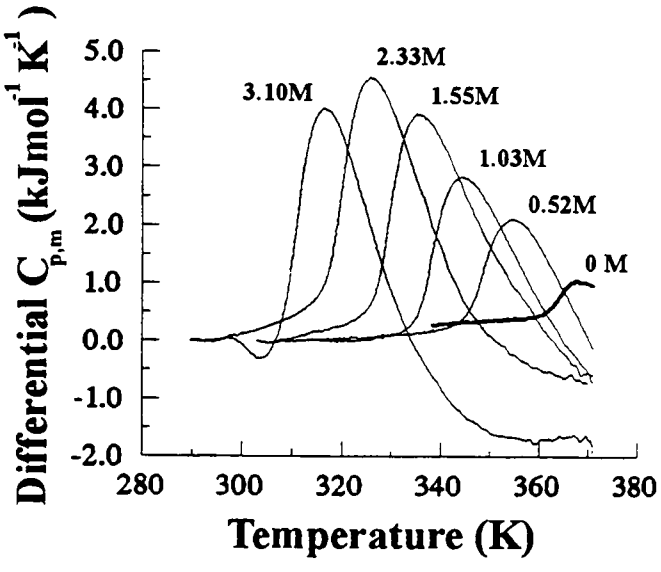

Figure 7.8 Calorimetric scans of T304 at a concentration of 5mgmL-1 in solutions of sodium chloride.

7.7 NMR Studies.

Proton and ^{13}C NMR of T701 and T904 (1% w/v in D_2O; Figure 7.9 and 7.10) show similar effects at temperatures around the LMPT to those observed for P237.[23] At the LMPT no significant shift is observed in either the ^1H or ^{13}C spectra for the POE $-CH_2-$ moieties of the polymers. However, after passing through the CP transition, line broadening occurs and additional broad lines appear. These effects are more marked for T701, where the onset of broadening occurs immediately upon passing through the CP transition, than for T904. The additional broad lines in the ^1H spectra are therefore associated with the CP transitions of the two poloxamines (T701 296.2K, T904 329.7K) and is due to aggregation of the polymer after the CP temperature has been exceeded. The ^1H NMR spectrum for T701 at 333K shows that there is an observed split in the population of the methyl group resonance between 1.1 and 1.4ppm. This indicates that both small aggregates (1.1ppm) and large aggregates (1.4ppm) forms co-exist at elevated temperatures. The largest shifts observed over the LMPT as the temperature is increased correspond to the methyl groups of the POP [δ ^1H = 1.17ppm to 1.16ppm (T701) and 1.17ppm to 1.14 ppm (T904)]. For T904 the ^{13}C NMR spectra show a shift for the methyl groups of the POP from 18.71 ppm at 283K to 19.93 ppm at 318K, although at the elevated temperature, a small peak at 18.71ppm is still observable. This

resonance may be due to a small number of hydrated hydrophobic oxypropylene units at the junction with the hydrophilic POE units constituting a partially hydrated area at the hydrophobe/hydrophile junction, rather than the existence of both monomolecular and aggregated forms at temperatures above the observed phase transition. This phenomenon is also observed for T701 although aggregation of the polymer tends to obscure this effect. For the HSDSC transition for T904 the baseline is observed to gently slope above the LMPT temperature, thus indicative of some form of aggregation corresponding to a gradual increase in aggregate size with increasing temperature. At elevated temperatures the observed shifts in both ^{1}H and ^{13}C spectra corresponds to hydrophobic interaction of the methyl group of the POP, which is probably associated with aggregation of the POP portion of the polymer.

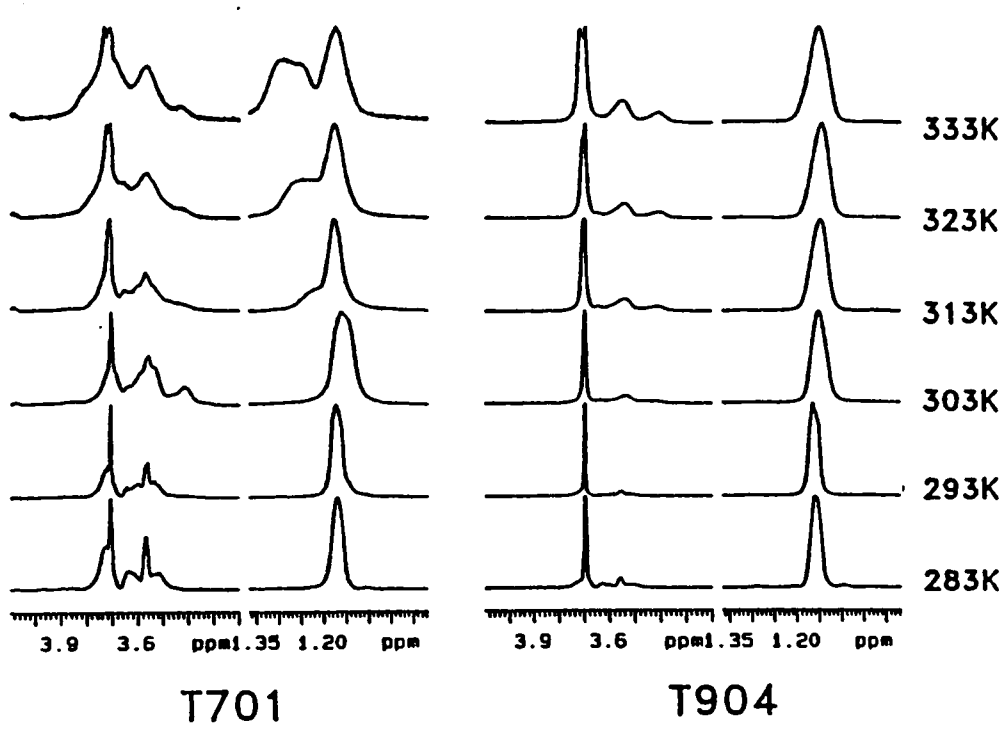

Figure 7.9 Proton NMR of T701 and T904 in D_2O as a function of temperature.

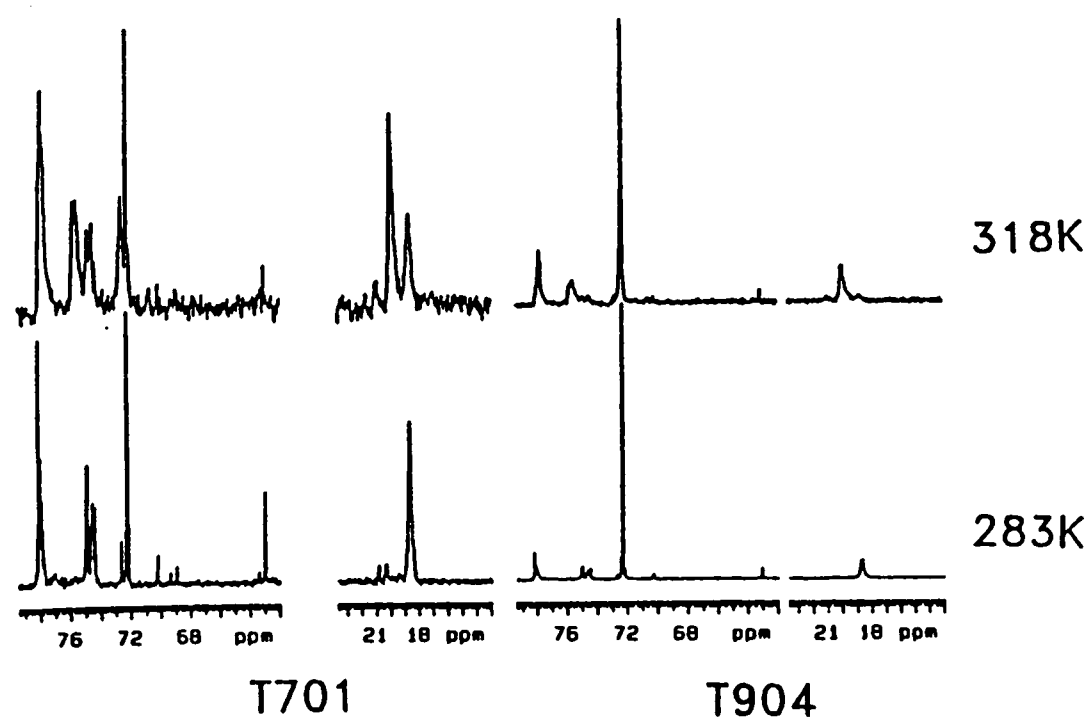

Figure 7.10 ^{13}C NMR of T701 and T904 in D_2O as a function of temperature.

7.8 Conclusions.

The observed LMPT's for poloxamines in dilute aqueous solution are due to several processes occurring almost simultaneously in the POP portion of the polymer. These processes being desolvation, conformational change involving hydrophobic interaction between the methyl groups and aggregation of the POP portion of the polymer. However, the order in which these processes occur cannot be determined by the methods used in this study. The observed LMPT appears to correspond to a monomolecular to aggregate transition where the POP constitutes a hydrophobic core bounded by the more hydrophilic POE with a partially hydrated area at the hydrophobe/hydrophile interface. The CP phase transition corresponds to a dehydration of the POE portion of the polymer resulting in phase separation and complements aggregation phenomena reported for other similar polymer-water systems.[10,11] The effect of pH upon the LMPT of T701 is related to deprotonation of the ethylene diamine moiety with increasing pH and is confirmed by the titrimetric analysis and by the observation that variations of pH are observed to have no effect on the LMPT of similar systems of dilute aqueous solutions of poloxamers.[22]

7.9 Tables.

Table 7.1 Thermodynamic parameters associated with the calorimetrically observed phase transitions of poloxamines at concentration of $5mgmL^{-1}$ in double distilled water, scanned at $60Kh^{-1}$.

Poloxamine	T_m (K)	CP (K)	ΔH_{cal} ($kJmol^{-1}$)	C_p^{max} ($kJmol^{-1}K^{-1}$)	$\Delta T_{1/2}$ (K)	ΔS_{cal} ($Jmol^{-1}K^{-1}$)
T701	299.6	296.2	296	37.2	7.5	988
T803	302.1	312.6	327	41.3	6.4	1082
T904	300.3	329.7	278	41.2	6.0	926
T1301	291.3	291.2	520	109.5	4.2	1785
T1302	294.7	303.5	512	92.7	4.5	1737
T304	368.2	-	-	-	-	-
T707	314.3	-	-	-	-	-
T908	306.0		-	-		

Table 7.2 Thermodynamic parameters associated with the calorimetrically observed phase transitions of poloxamines at constant oxypropylene concentration in double distilled water, scanned at $60Kh^{-1}$.

Poloxamine	Conc. ($mgmL^{-1}$)	T_m (K)	Cloud Point (K)	ΔH_{cal} ($kJmol^{-1}$)	C_p^{max} ($kJmol^{-1}K^{-1}$)	$\Delta T_{1/2}$ (K)	ΔS_{cal} ($Jmol^{-1}K^{-1}$)
T701	6.17	300.4	294.7	315	34.1	8.6	1050
T803	7.86	301.5	313.7	276	38.5	6.5	916
T904	10.25	299.4	326.2	351	49.2	6.2	1172
T1301	5.75	289.4	286.7	487	133.0	3.2	1682
T1302	6.17	294.1	302.2	483	111.8	3.8	1640
T304	8.25	364.2	-	-	-	-	-
T707	20.83	294.0	>370			-	
T908	32.50	398.9	>370	243	40.6	5.3	812

Table 7.3 The effects of scan rate on the thermodynamic parameters associated phase transitions of T701 at concentration of 5 $mgmL^{-1}$ in double distilled water.

Scan Rate (Kh^{-1})	T_m (K)	ΔH_{cal} ($kJmol^{-1}$)	C_p^{max} ($kJmol^{-1}K^{-1}$)	$T_{1/2}$ (K)	ΔS_{cal} ($Jmol^{-1}K^{-1}$)
10	300.3	248	28	8.6	826
30	300.3	272	28	9.1	907
60	299.6	296	37	7.5	988

Table 7.4 Reversibility of the phase transition of T904 at a concentration of 5$mgmL^{-1}$ in double distilled water, scanned at $\pm 30Kh^{-1}$.

Scan Rate (Kh^{-1})	Poloxamine	T_m (K)	ΔH_{cal} ($kJmol^{-1}$)	C_p^{max} ($kJmol^{-1}K^{-1}$)	$T_{1/2}$ (K)	ΔS_{cal} ($Jmol^{-1}K^{-1}$)
+30	T904	300.1	316	50	5.7	1053
-30	T904	300.6	-290	-44	5.9	-964

Table 7.5 The effects of copolymer concentration (1-20 $mgmL^{-1}$ in double distilled water) and pH (0.03M buffer at a copolymer concentration of 5 $mgmL^{-1}$)on the thermodynamic parameters associated with the phase transitions of T701, scanned at $60Kh^{-1}$.

Conc. ($mgmL^{-1}$)	T_m (K)	ΔH_{cal} ($kJmol^{-1}$)	C_p^{max} ($kJmol^{-1}K^{-1}$)	$\Delta T_{1/2}$ (K)	ΔS_{cal} ($Jmol^{-1}K^{-1}$)
1.0	302.6	264	30	8.6	873
2.5	301.0	278	33	7.9	922
5.0	299.6	296	37	7.5	988
7.5	299.0	303	38	7.3	1012
10.0	298.5	331	41	7.5	1109
15.0	297.7	337	43	7.2	1131
20.0	297.2	341	44	7.0	1146
pH					
2.5	315.9	225	19	10.6	713
4.3	311.3	264	24	10.2	847
5.0	306.0	307	30	9.6	1004
5.5	304.0	316	32	9.3	1039
6.8	303.1	344	36	8.9	1136
8.1	297.4	348	42	7.6	1170
11.1	298.8	313	39	7.4	1049

Table 7.6 The effects of sodium chloride on the thermodynamic parameters associated with the phase transition of T304 at a copolymer concentration of 5mgmL^{-1}, scanned at 60Kh^{-1}.

[NaCl] (M)	T_m (K)	ΔH_{cal} (kJmol^{-1})	C_p^{max} (kJmol^{-1}K^{-1})	$\Delta T_{1/2}$ (K)	ΔS_{cal} (Jmol^{-1}K^{-1})
0[1]	*(369.7)*	*(5)*	*(1)*	*(8.9)*	*(7)*
0.5	354.8	26	2	14.3	71
1.0	344.1	46	3	17.3	135
1.5	335.5	62	3	17.5	186
2.3	326.1	71	4	17.1	217
3.1	316.7	81	4	16.9	254

[1] Extrapolated data

7.10 References.

(1) Schmolka,I.R. *J.Am.Oil.Chem.Soc.* **1977**, *54*, 110.
(2) Synperonic PE and T series, *ICI Technical Literature,* **1991.**
(3) Lee,J.; Martin,P.A.; Tan,J.S., *J.Coll.Int.Sci*, **1989**, *131(1)*, 252.
(4) Tan,J.S.; Martin,P.A. *J.Coll.Int.Sci.,* **1990**, *36(2)*, 415.
(5) Douglas,S.J.; Davis,S.S.; Illum,L. *Int.J.Pharm.,* **1986**, *34*, 145.
(6) Illum,L.; Davis,S.S., Muller,R.H.; Mak,E.; West,P. *Life Sci.,* **1987**, *40*, 367.
(7) Davis,S.S.; Illum,L. *Drug Carrier Systems*, Roerdink, F.H.D. and Kroon, A.M. (Eds.), Wiley and Son Ltd., **1989**, 131.
(8) Illum,L.; Davis,S.S. *FEBS LETT.*, **1984**, *167*, 79.
(9) Pimienta,C.; Chouinard,F.; Labib,A., Lenaerts,V. *Int.J.Pharm,* **1992,** *80*, 1.
(10) Kjellander,R.; Florin,E. *J.Chem.Soc.Faraday Trans.*, **1981,** 77, *2053.*
(11) Karlstrom,G.; Carlsson,A.; Lindman,B. *J.Phys.Chem.,* **1990**, *94*, 5005.
(12) Vogel,A.I., *"Textbook of Quantitative Inorganic Analysis"*, 4th Edition, Revised by Bassett,J.; Denney,R.C.; Jeffery,G.H.; Mendham,J., (Longman Publ.)., **1983**, *Sect.X40,* 305.
(13) Eagland,D.; Crowther,N.J. *Faraday Symp.Chem.Soc.,* **1982**, *17*, 141.
(14) Blandamer,M.J.; Briggs,B., Burgess,J.; Cullis,P.M.; Eaton,G. *J.Chem.Soc. Faraday Trans.*, **1991**, *87(8)*, 1169.
(15) Schild,H.G.; Tirrel,D.A. *J.Phys.Chem.*, **1990**, *94*, 4352.
(16) Illum,L.; Hunneyball,I.M.; Davis,S.S. *Int.J.Pharm.*, **1986**, *29*, 53.
(17) Slepnev,V.I.; Kuznetsova,L.E.; Gubin,A.N.; Batrakova,E.V.; Alakhov,V.Y.; Kabanov,A.V. *Biochem. Int.,* **1991**, *26(4)*, 587.
(18) Johnston,T.P.; Punjabi,M.A.; Froelich,C.J. *Pharm.Res.,* **1992**, *9(3)*, 425.
(19) Guzman,M.; Garcia,F.F.; Molpeceres,J.; Aberturas,M.R. *Int.J.Pharm.*, **1992**, *80*, 119.
(20) Carter,C.; Fisher,T.C.; Hamai,H.; Johnson,C.S.; Meiselman,H.J.; Nash,G.B. *Clin.Hemorheol.*, **1992**, *12*, 109.

(21) Kumar,V.; Laouar,L.; Davey,M.R.; Mulligan,B.J.; Lowe,K.C. *J.Exp.Bot.*, **1992**, *43(249)*, 487.
(22) Mitchard,N.; Beezer,A.; Mitchell,J.; Leharne,S.; Chowdhry,B.; Buckton,G. *J.Chem.Soc.Chem.Comm.*, **1990**, 900.
(23) Beezer,A.; Mitchell,J.C.; Rees,N.; Armstrong,J.; Chowdhry,B.; Leharne,S.; Buckton,G. *J.Chem.Research,* **1991**,254.
(24) Brown,W.; Schillen,K.; Almgren,M.; Hvidt,S.; Bahadur,P. *J.Phys.Chem.*, **1991**, *95,* 1852.
(25) Zhou,Z.; Chu,B. *Macromolecules,* **1988,** *21*, 2548.
(26) Wang,Q.; Price,C., Booth,C. *J.Chem.Soc. Faraday Trans.*, **1992,** *88(10),* 1437.
(27) Wanka,G.; Hoffman,H.; Ulbricht,W. *J.Coll.Polym.Sci.*, **1990,** *268,* 101.
(28) Samii,A.; Karlstrom,G.; Lindman,B. *J.Phys.Chem.*, **1991**, *95,* 7887.
(29) Samii,A.; Karlstrom,G.; Lindman,B. *Langmuir,* **1991**, *7*, 1067.
(30) Gu,T.; Qin,S.; Ma,C. *J.Coll.Int.Sci.*, **1989**, *127(2)*, 586.
(31) Privalov,P.L.; Gill,S.J., *Adv.Protein Chem.*, **1989**, *39*, 191.
(32) Sturtevant,J.M., *Ann.Rev.Phys.Chem.*, **1987**, *38*, 463.
(33) Privalov,P.L., *Crit.Rev.Biochem. and Mol.Biol.*, **1990**, *25(4),* 281.
(34) Cole,S.C.; Chowdhry,B.Z., *TIBTECH,* **1989**, *7*, 11.
(35) Armstrong,J.K., Parsonage,J.R.; Chowdhry,B.Z.; Leharne,S.; Mitchell,J.; Beezer,A.E.; Löhner,K.; Laggner,P. *J. Phys. Chem,* **1993,** 97, 3904
(36) Williams,R.K.; Simard,M.A.; Jolicoeur,C. *J. Phys. Chem.*, **1985,** *89, 178.*
(37) Stark,J.G.; Wallace,H.G. *"Chemistry Data Book", (SI Edition),* John Murray Ltd. (Publ.) London, 1975 (Rev.), 98.
(38) Florin,E.; Kjellander,R.; Eriksson,J.C. *J.Chem.Soc.Faraday Trans. I,* **1984**, *80*, 2889.

CHAPTER 8 - MODELLING OF THE CALORIMETRIC PHASE TRANSITIONS

8.1 Introduction.

8.1.1 Modelling the Temperature Dependence of an Aggregation Process.

The mass action model of aggregation may be written as:[1]

$$K = \frac{[X_n]}{[X]^n} \qquad (1)$$

The extent of conversion, α, may be defined as the fraction of unimer present in aggregates. Thus $[X_n]=\alpha C/n$ and $[X]=(1-\alpha)C$, where C is the total concentration of polymer and n is the aggregation number. By substituting these expressions in the above equation the equilibrium expression becomes:

$$K = \frac{\alpha c}{n(1-\alpha)^n c^n} \qquad (2)$$

Differentiating lnK with respect to α at constant n and C gives the following expression:

$$\left(\frac{\partial \ln K}{\partial \alpha}\right)_{n,C} = \frac{1}{\alpha} + \frac{n}{1-\alpha} \qquad (3)$$

The HSDSC instrument measures the power required to keep the sample and reference cell temperatures equal whilst the temperature of the system (T) is raised as a linear function of time, t, i.e., the scan rate dT/dt is constant. The output of the instrument $(dq/dt)_p$ vs. t is readily converted to a plot of apparent excess heat capacity ($C_{p,xs}$) vs. temperature by multiplying the x axis by the scan rate and the y axis by its reciprocal.[2] This process is referred to as scan rate normalisation in the data analysis section. $C_{p,xs}$ at any point in the scan is related to the measured insrumental enthalpy (referred to as ΔH_{cal}) by the equation:

$$C_{p,xs} = \Delta H_{cal} \frac{d\alpha}{dT} \qquad (4)$$

Combining equations 3 and 4 allows the van't Hoff isochore to be written in the form:

$$\left(\frac{\partial \ln K}{\partial \alpha}\right)_{n,C} \frac{d\alpha}{dT} = \left(\frac{\partial \ln K}{\partial T}\right)_{n,C} = \left(\frac{1}{\alpha} + \frac{n}{1-\alpha}\right) \frac{C_{p,xs}}{\Delta H_{cal}} = \frac{\Delta H_{vH}}{RT^2} \qquad (5)$$

It should be noted that the derivation assumes that ΔH_{vH} is independent of temperature (i.e., the difference between pre- and post-transitional baseline , $\Delta C_{p,d}$, is equal to zero). ΔH_{vH} is obtained by setting α to 0.5 (the point at which the process is half completed) in equation 5. The equation after rearrangement then becomes:

$$\Delta H_{vH} = \frac{2(n+1)C_{p,1/2}RT_{1/2}^2}{\Delta H_{cal}} \qquad (6)$$

where $C_{p,1/2}$ and $T_{1/2}$ are the values of $C_{p,xs}$ and T when $\alpha = 0.5$.

An integrated form of the van't Hoff isochore is obtained from equation 5 and by evaluation of the integration constant using $\alpha = 0.5$ and $T = T_{1/2}$:

$$\ln\left(\frac{0.5^{n-1}\alpha}{(1-\alpha)^n}\right) = \frac{\Delta H_{vH}}{R}\left(\frac{1}{T_{1/2}} - \frac{1}{T}\right) \qquad (7)$$

An expression for $d\alpha/dT$ is then obtained by taking derivatives of equation 7:

$$\frac{d\alpha}{dT} = \frac{\Delta H_{vH}}{RT^2}\left(\frac{1}{\frac{1}{\alpha} + \frac{n}{1-\alpha}}\right) \qquad (8)$$

Substitution of this expression in equation 4 allows the excess C_p function to be calculated at any temperature T:

$$C_{p,xs} = \frac{\Delta H_{cal}\Delta H_{vH}}{RT^2}\left(\frac{1}{\frac{1}{\alpha} + \frac{n}{1-\alpha}}\right) \qquad (9)$$

8.1.2 **Modelling the Temperature Dependence of Phase Separation.**

Phase separation can be viewed as an aggregation process in which the aggregation number is infinitely large.[1,3] The assumption of an infinite aggregation number alters the equilibrium description of the process to give:[1,3]

$$K = \frac{1}{[X]} \qquad (10)$$

A similar expression is obtained by reference to the Gibbs phase rule.[3]

If one takes the natural logarithm of this expression and make appropriate substitutions into the integrated form of the van't Hoff isochore:

$$\ln K(T_2) - \ln K(T_1) = \frac{\Delta H_{vH}}{R}\left(\frac{1}{T_1} - \frac{1}{T_2}\right) \qquad (11)$$

If T_1 is set to equal the cloud point T_c and T_2 is any temperature T then one obtains:

$$-\ln[X]_{T_c} + \ln[X]_T = \frac{\Delta H_{vH}}{R}\left(\frac{1}{T_c} - \frac{1}{T}\right) \qquad (12)$$

At the cloud point:

$$\ln[X]_{T_c} = X_{total} \qquad (13)$$

Thus one may write:

$$[X] = [X]_{total}\, e^{\left[\frac{\Delta H_{vH}}{R}\left(\frac{1}{T} - \frac{1}{T_c}\right)\right]} \qquad (14)$$

α, the extent of conversion is defined as the fraction of material in the separated concentrated polymer phase; 1-α is thus the fraction in the dilute phase. Since:

$$1 - \alpha = \frac{[X]}{[X]_{total}} \qquad (15)$$

Then:

$$\alpha = 1 - e^{\left[\frac{\Delta H_{vH}}{R}\left(\frac{1}{T} - \frac{1}{T_c}\right)\right]} \qquad (16)$$

Differentiation of this expression with respect to T and substitution of the derivative into equation 4 yields an expression for the excess C_p:

$$C_{p,xs} = \frac{\Delta H_{cal}\Delta H_{vH}}{RT^2}\, e^{\left[\frac{\Delta H_{vH}}{R}\left(\frac{1}{T} - \frac{1}{T_c}\right)\right]} \qquad (17)$$

8.1.3 **Data Analysis.**

The HSDSC outputs obtained were initially analysed using the supplied DA-2 software. This consisted of scan rate normalisation, the process whereby the instrumental output was modified as outlined in the previous section. The $C_{p,xs}$ data were arithmetically transformed to give values with units of cal $mol^{-1} K^{-1}$. A baseline was then fitted to the data. This consisted of using the pre- and post-transitional data points to fit a spline curve. The calculated baseline data were subsequently subtracted from the HSDSC data.

The object of the second part of the data analysis was to obtain the thermodynamic parameters characterising the transitions by fitting the data to the aggregation model rather than the phase separation model and to estimate the values for n, the number of molecular species which come together to form an aggregate. This consisted of reading the data into a spreadsheet (Microsoft Excel 5.0) for which several applications were developed to carry out the following tasks.

The data were transformed once again to give the $C_{p,xs}$ axis units of $kJmol^{-1}K^{-1}$ and the temperature axis in units of K. The trapezoidal method of numerical integration was carried out for each data point resulting in a calculation of the enthalpy released up to that particular point, $\Delta H(T_i)$. The calorimetric enthalpy, ΔH_{cal} the total area under the curve, was obtained by summation of all $\Delta H(T_i)$. The extent of conversion, α, for each data point was calculated from the formula $\Delta H(T_i)/\Delta H_{cal}$. The values for C_p^{max} (the maximum value for $C_{p,xs}$), T_m, $C_{p,1/2}$ (the value of $C_{p,xs}$ when $\alpha = 0.5$), $T_{1/2}$ (the temperature when $\alpha = 0.5$) and $\Delta T_{1/2}$ (the peak width at half height) were then identified.

The estimation of n was carried out in the following way. ΔH_{vH} was calculated employing equation 6 and using an estimate for n. The extent of conversion data evaluated on the spreadsheet was used to calculate temperature values by rearranging equation 7 to give the following expression:

$$T = \frac{1}{\frac{1}{T_{1/2}} - \frac{R}{\Delta H_{vH}} \ln\left[\frac{0.5^{n-1}\alpha}{(1-\alpha)^n}\right]} \qquad (18)$$

Sturtevant[4] has pointed out that at the extremes of the transitions there may be a range of ΔH_{vH} values, thus only data for α between 0.1 and 0.9 were used for this exercise. The calculated temperature range was then compared to the experimental data. The closer the estimate of n to the true value, the closer the correspondence between the experimental temperature data and the calculated temperature data. Correspondence between the calculated and experimental temperature data was estimated in two ways: (A) by eye using a graph of α vs T_{calc} and T_{exp} as well as (B) by minimising the sum of the squared difference between the experimental and calculated temperature data sets by varying the value of n as the independent variable.

The excess heat capacity associated with the aggregation process, $\Delta C_{p,d}$, was obtained by fitting data points in the pre- and post-transitional parts of the trace to straight lines. The lines were the extrapolated to $T_{1/2}$. $\Delta C_{p,d}$ was then identified as the difference between the extrapolated post-transition $C_{p,xs}$ value and the extrapolated pre-transition $C_{p,xs}$ value.

8.2 Results and Discussion.

8.2.1 Establishing a Model for the Calorimetric Transitions.

It is possible to establish the underlying physico-chemical events comprising scanning calorimetric traces through simulation of the HSDSC output. For a process under strict thermodynamic control, this obliges the investigator to establish a reasonable equlibrium description of the process under analysis. Two reasonable schemes may be advanced for the phase transitions noted for POP solutions:

unimer ↔ aggregate ↔ separated phases (a)

unimer ↔ separated phases (b)

In the first scheme, aggregates in true solution are formed which then interact to form a separate concentrated polymer phase. In the second scheme, phase separation occurs without the formation of intermediate aggregates.

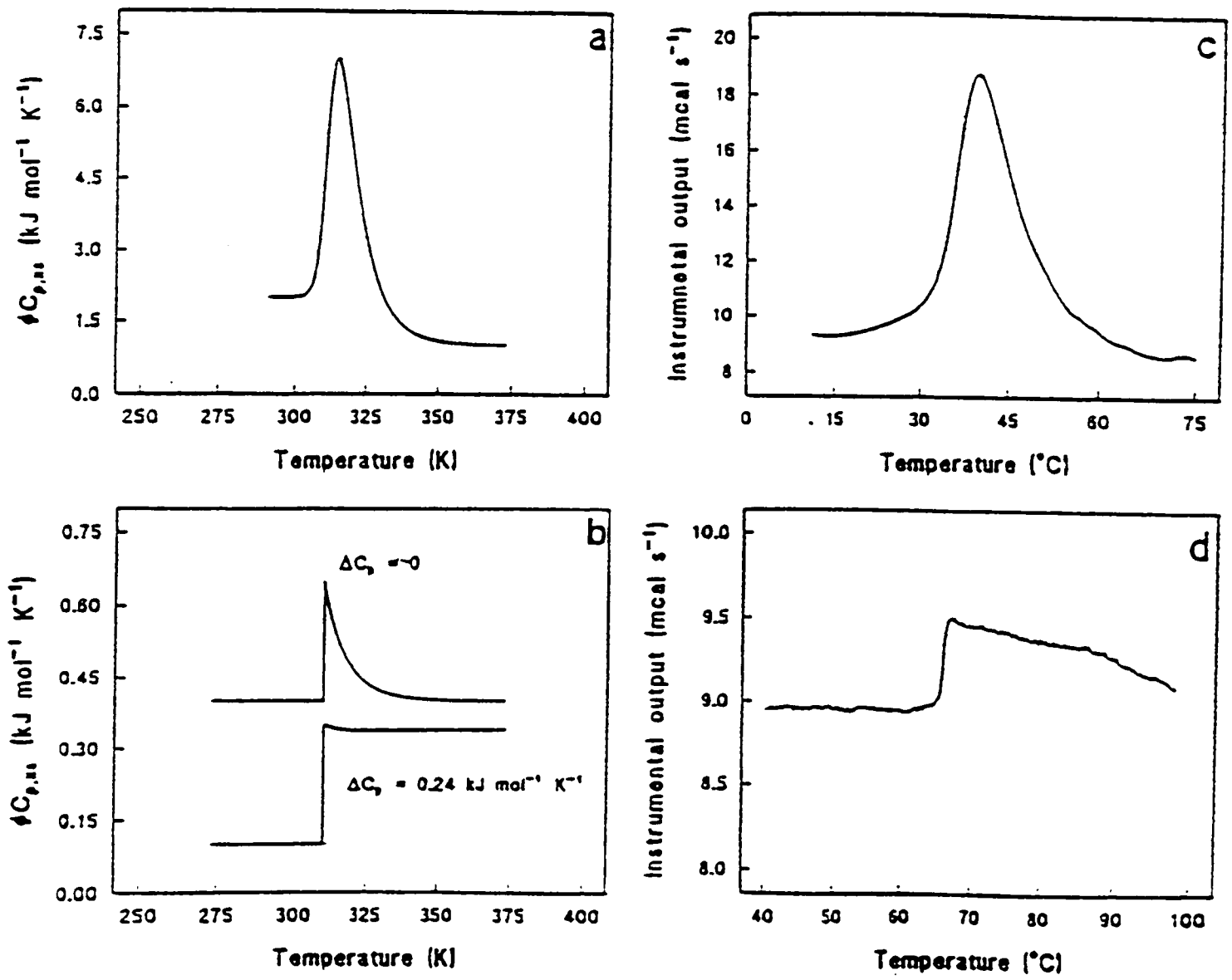

Figure 8.1 Simulated calorimetric traces for (a) aggregation and (b) phase separation. Calorimetric traces obtained for (c) P215 and (d) Polyoxyethylene (MW $1x10^6$ $gmol^{-1}$).

Figures 8.1a and b contain simulated HSDSC outputs obtained from the modelling described in the previous section. Figure 8.1a provides a simulation of the HSDSC output for an aggregation process in which the aggregation number, (n in the previous section) is 4. Figure 8.1b shows the possible output for phase separation. For both simulations the underlying change in heat capacity is incorporated into the plot. It is easily shown that the heat capacity change is merged with the plot of excess heat capacity by adding the term $\alpha\Delta C_{p,d}$.[2] Figure 8.1c shows a trace obtained for P215 which is thought to aggregate and 8.1d for POE (MW $1x10^6$ $gmol^{-1}$) which is believed to be phase separation. The simulations seem to capture some of the major features of the real data. In fact, the phase separation simulation in which the $\Delta C_{p,d}$ change for the process is zero readily compares with some of the phase separations noted by Schild and Tirrell.[5] It is noteworthy that the output for both processes is asymmetric. However, the simulated output for phase separation (see trace in which $\Delta C_{p,d}$ change for the process is zero) has a sharp, if not discontinuous, leading edge. From the shape of the POP traces I am persuaded to propose that scheme (a) is the more appropriate description of the events observed in the calorimeter. The question that should be immediately posed is: why suggest that aggregation occurs when phase separation is observed? The reasons are as follows: (1) the HSDSC output for the POP solutions is very similar to the output observed for the poloxamers (see figure 8.1c);[6] and the poloxamer transitions noted by us[6-10] and others[11] correspond with documented aggregation phenomena observed using other techniques;[12-17] (2) the HSDSC output obtained for the POP solutions is typical of other aggregation processes including proteins;[18] (3) HSDSC of phase separation in POE solutions gives a very different output. Figure 8.1d shows that in this case the trace is characterised by a very small calorimetric enthalpy, a relatively large positive increment in apparent $C_{p,xs}$ and a long gently sloping 'tail' which is a manifestation of the temperature dependence of the excess heat capacity[18] and may represent, mechanistically, the changing composition of the dilute and polymer rich phases. It is worth noting that the simulated HSDSC output for phase separation (see figure 8.1b) which incorporates a positive increase in $\Delta C_{p,d}$ for the transition seems to capture the most important aspects of the POE transition. It may be reasonable to assume that aspects of phase separation in POP solutions could produce similar outcomes. However, despite the close similarity of the transitions to aggregation traces, phase separation also occurs within the temperature window of the HSDSC transition as shown by the work of Schild and Tirrell.[5] It is therefore concluded that aggregation may precede phase separation; and it is considered possible that phase separation may occur as a result of interactions between POP aggregates.

It is not unknown for aggregates of these types of polymers to further interact. For instance, in concentrated solution the poloxamers will form gels. These gels arise from interactions between micellar aggregates. Calorimetric evidence indicates that the enthalpies for gelation are very small,[11,14] and that the enthalpy is possibly derived from partial desolvation of the POE blocks to facilitate adhesion between micelles. Since the enthalpy for gelation is weakly endothermic it is clear that the driving force for micellar aggregate interaction is entropic. For the proposed POP aggregates is possible that there will be a similar entropic driving force but this time resulting in phase separation. The enthalpy for the process could well be close to zero since for interaction between aggregates to occur desolvation is not a necessary precondition since it has already occurred (see Section 8.2.2).

Finally, in calorimetric terms, the aggregation and phase separation transitions will not simply be superimposed on each other but will be sequentially combined with each other. A treatment of sequential equilibria in HSDSC has been provided by Edge *et.al.*[19]

The apparent excess heat capacity functions for aggregation and phase separation have been formulated. Simulations using both formulae give rise to asymmetric endotherms with steep leading edges. For the aggregation model, it is easily shown that as the aggregation number increases in magnitude the leading edge becomes steeper. Tanford's suggestion that phase separation may be considered to be aggregation in which the aggregation number is infinite[3] leads to a trace that goes up extremely steeply and which appears as a discontinuous change in the heat capacity of the system. The phase separation model demonstrates the same behaviour. At some temperature infinitesimally smaller than the cloud point, the C_p of the system is governed by the polymer in water. At some temperature infinitesimally greater than the cloud point, the C_p of the system is related to the composition and relative proportions of the dilute and concentrated phases. This must result in a sudden change in C_p and produce a trace similar to the aggregation model using a large aggregation number.

The calorimetric outputs obtained for the various POP samples are shown in Figure 4.1 (Chapter 4). the HSDSC scans obtained are asymmetric with a pronounced leading edge. The leading edges do not, however, show any sudden changes and therefore may indicate that the calorimeter is detecting an aggregation process. The HSDSC data also include a gently sloping negative curve on the post-transitional side of the traces which may

be associated with the phase separation process. The overall thermodynamic values characterising the transitions are given in Table 8.1 and are displayed graphically in Figure 8.2. The trends associated with increasing molecular mass are immediately obvious. T_m decreases and ΔH_{cal} increases with increasing molecular mass. The decrease in T_m with increasing molecular mass is a trend also encountered in POE systems.[20] It may be explained by the fact that the decrease in entropy associated with the structured water surrounding the chains is offset by a gain in combinatorial entropy of mixing, given by the Flory Huggins theory. This is largest for small polymer chains. Small POE chains therefore have relatively smaller negative entropies of mixing with water compared to larger molecules. The entropy gain arising from hydrophobic interaction during aggregation and eventually phase separation thus tends to be smaller for small molecules compared to larger molecules and is thus offset to higher temperatures.

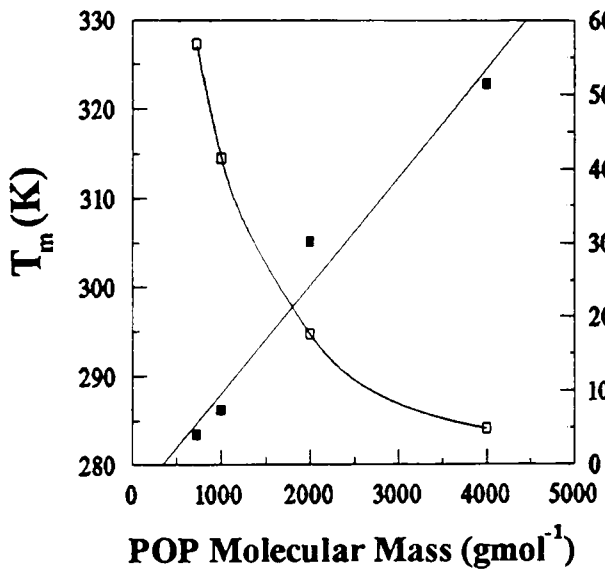

Figure 8.2 Effect of molecular mass on the thermodynamic parameters of T_m (□) and ΔH_{cal} (■).

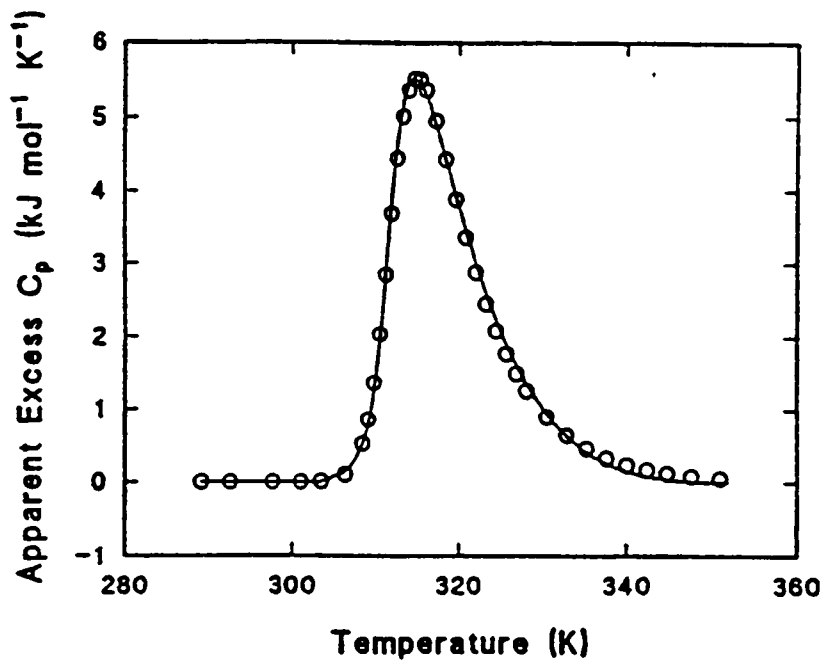

Figure 8.3 Variation of $C_{p,xs}$ with temperature for POP of molecular mass 1000. The open circles represent simulated $C_{p,xs}$ values; the solid line represents experimental data.

Thermodynamic parameters normally associated with descriptions of transition cooperativity, namely ΔH_{vH}, C_p^{max} and $\Delta T_{1/2}$, indicate that as molecular weight increases cooperativity of the transition increases. This is demonstrated by increasing values for ΔH_{vH} and C_p^{max} and decreasing values for $\Delta T_{1/2}$ as molecular mass increases. The van't Hoff enthalpy values are worthy of some comment since they are much larger than the values for ΔH_{cal}. Sturtevant[18]

points out that this is indicative of intermolecular cooperation; and in such a case the ratio of $\Delta H_{vH}/\Delta H_{cal}$ is a reflection of the number[21] of molecules which cooperate in the transition. The ratio is an indication of the base molar mass referred to in the enthalpy units.[21] The ratios however demonstrate that the cooperativity of the transitions decrease with increasing molecular mass. Thus for POP of molecular mass 725 $gmol^{-1}$ the ratio is 12, whilst that for POP of molecular mass 4000 $gmol^{-1}$ the ratio is 4.

The scans for POP 1000 were repeated several times at different scan-rates ranging from 10 to 90 Kh^{-1}. The thermodynamic properties obtained were independent of scan-rate which may be taken to indicate thermodynamically reversible processes[22] and which justifies the use of equilibrium thermodynamics to describe the phase transitions. Perfect reversibility was also demonstrated by the fact that samples could be heated, cooled and reheated. The scans obtained on reheating were identical to the initial scans.

8.2.2 **Phase Separation.**

Phase separation detected spectroscopically by the onset of turbidity, i.e., the cloud point, occurs quite close to the departure of the $C_{p,xs}$ function from the assumed base-line for the system.[5] Thus aggregation and phase separation are closely linked.

Very few reports in the literature deal with the phase separation behaviour of POP. However phase separation in POE[20] and POE-POP-POE[23] have been investigated. It seems reasonable to assume that the underlying molecular events for POP are likely to be similar to the phase separation behaviour of POE.[20] In Kjellander and Florin's statistical mechanical treatment, model building provides evidence that POE is capable of fitting into an ice-like lattice in which hydrogen bonds are readily established between water and the ether oxygens. At 35°C the interaction between polymer chains is low as revealed by the low negative values for w, a correction term for polymer/polymer interaction. As the temperature is raised w becomes more negative indicating greater polymer chain interaction. Experimental evidence[20] suggests that both the enthalpic and entropic contributions to w are large and positive. The coming together and interaction of two polymer chains results in the transfer of water molecules from hydration shells surrounding the polymer chains to the bulk. Thus transfer increases entropy since the restrictions on thermal motion of water molecules in the shell is, to a certain extent, lifted in the bulk. However the loss of thermal stabilisation energy associated with the hydrogen bonded structure results in a positive enthalpy change.

The Lund[24,25] group have interpreted the thermal behaviour of POE in terms of conformational adaptation. They argue that at low temperatures polar conformers of the polymer chains are favoured. At higher temperatures, however, non-polar conformers predominate. It is tempting to consider that such conformational changes may affect interaction with water. Nevertheless, conformational changes occur also in the absence of water[25] which precludes any suggestion that changing interaction with water is the driving force for conformational change. However it is likely that the decrease in polarity associated with the thermally induced change in conformation will affect interaction with water. Similar arguments have been presented by Hergeth *et.al.* for phase separation in the poloxamers.[23]

In POE-POP-POE block copolymers aggregation is associated with desolvation of the POP block. If large enough the POE blocks maintain the co-polymer in solution. Above the aggregation temperature the aggregates exists as dimers with small numbers of unimers and trimers.[23] Raising the temperature high enough causes phase separation. This happens because the POE blocks become desolvated. Phase separation is accompanied by an increase in aggregation number to about 100.[23]

8.2.3 **Solubility Behaviour of POP.**

For proteins, thermal unfolding gives rise to solvent exposure of hydrophobic amino acid residues. Such exposure tends to reinforce the hydrogen bonded structure of water. This is demonstrated by a positive value for $\Delta C_{p,d}$ the heat capacity change associated with the phase transition.[26] If the phase separation process in POP involves the partial destruction of the hydrogen bonded structure of water shells surrounding the POP chains, then this should be reflected in negative values for $\Delta C_{p,d}$. Figure 4.1 (Chapter 4) shows this to be the case for all the POP homo-polymers under investigation.

The practical effect of the negative $\Delta C_{p,d}$ values for the transition is that it gives rise to an upper transition in which the polymer redissolves. An upper phase transition temperature may be demonstrated by use of a combined form of the van't Hoff isochore and Kirchoff equation (i.e., the derivation assumes that ΔH_{vH} is temperature dependent and as a consequence $\Delta C_{p,d}$ is non-zero):

$$\ln\left(\frac{0.5^{n-1}\alpha}{(1-\alpha)^n}\right)=\ln\left(\frac{K(T)}{K(T_{1/2})}\right)=\frac{\Delta H_{vH}}{R}\left(\frac{1}{T_{1/2}}-\frac{1}{T}\right)+\frac{\Delta C_{p,d}}{R}\left(\ln\left(\frac{T}{T_{1/2}}\right)+\frac{T_{1/2}}{T}-1\right) \quad (18)$$

$$\ln\left(\frac{0.5^{n-1}\alpha}{(1-\alpha)^n}\right)=\ln\left(\frac{K(T)}{K(T_{1/2})}\right)=\frac{\Delta H_{vH}}{R}\left(\frac{1}{T_{1/2}}-\frac{1}{T}\right)+\frac{\Delta C_{p,d}}{R}\left(\ln\left(\frac{T}{T_{1/2}}\right)+\frac{T_{1/2}}{T}-1\right) \quad (18)$$

where K(T) is the value of the equilibrium constant at temperature T, and $K(T_{1/2})$ is the value of the equilibrium constant at $T_{1/2}$. When $\alpha = 0.5$ the eequation evaluates to zero. Clearly this occurs for two values of T. One value is $T_{1/2}$, the other, is in effect, an upper $T_{1/2}$ value.

The $\Delta C_{p,d}$ values used for the calculations were scaled up by multiplying the $\Delta C_{p,d}$ values obtained from the scanning calorimetric traces with the $\Delta H_{vH}/\Delta H_{cal}$ ratio. This had the effect of converting the values from $kJmol^{-1}$ (of chains)K^{-1} to $kJmol^{-1}$ (of molecular clusters)K^{-1} thereby providing parity with units of ΔH_{vH}. Solubility gaps in phase diagrams of solutions of POE have been identified.[20] The above thermodynamic analysis implies that POP aggregates should dissociate at higher temperatures. Dissociation presumably resulting in a disappearence of the polymer rich phase. The magnitude of the upper $T_{1/2}$ values are sensitive to the values estimated for $\Delta C_{p,d}$. Thus, in the absence of a proper error analysis for the $\Delta C_{p,d}$ values it is probably not worthwhile commenting on the values obtained.

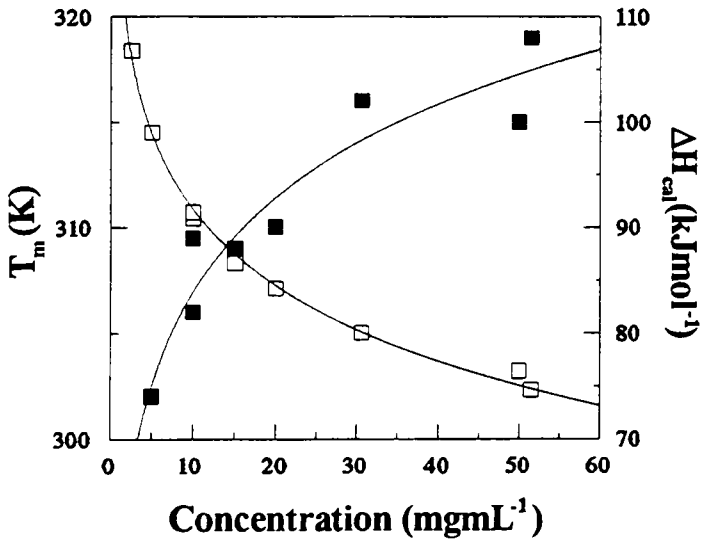

Figure 8.4 Effect of concentration of aqueous solutions of POP 1000 on the thermodynamic parameters of T_m (□) and ΔH_{cal} (■).

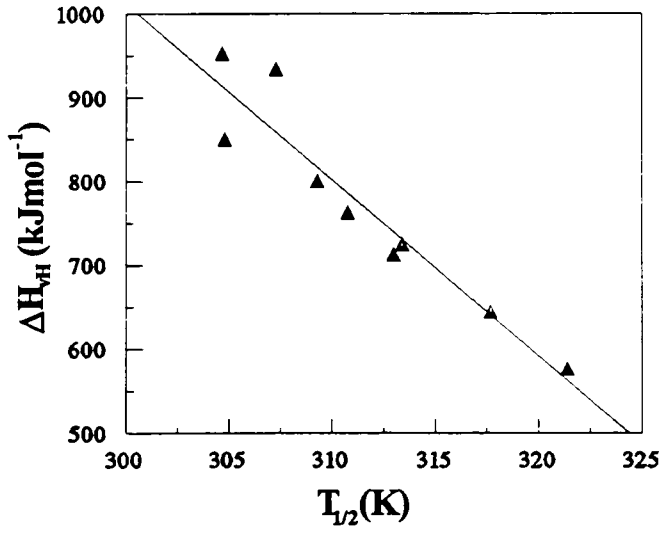

Figure 8.5 The variation of ΔH_{vH} with $T_{1/2}$. The data was obtained for POP 1000 solutions of various concentrations.

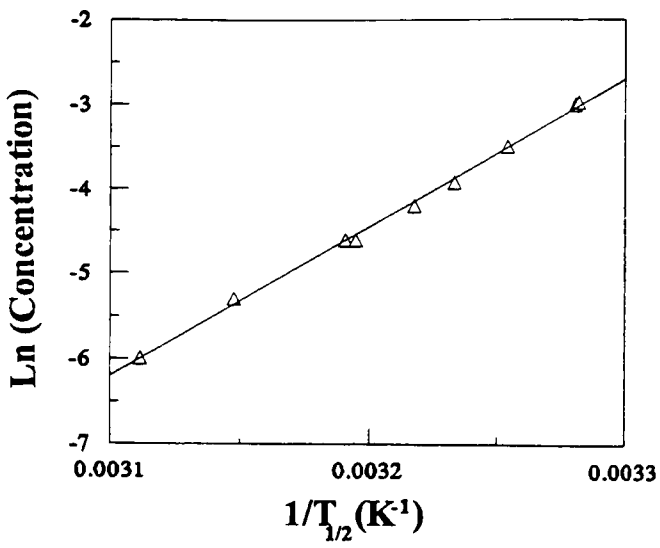

Figure 8.6 van't Hoff plot for aqueous solutions of POP 1000.

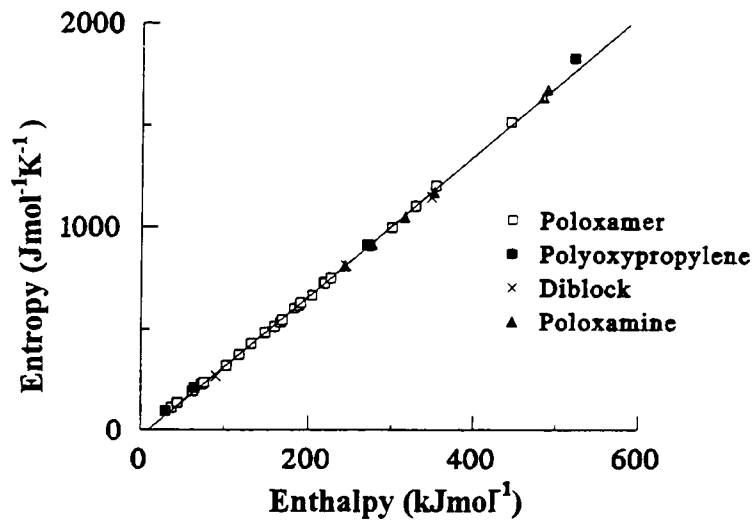

Figure 8.7 Enthalpy-entropy compensation plot for all polymer solutions investigated.

8.2.4 **Simulations of $C_{p,xs}$ Temperature Plots.**

Simulations of the scans were produced by using equations 7 and 9. Equation 7 was used to calculate a as a function of temperature. The equation was solved using the Newton-Raphson procedure on a spreadsheet. The computed values for a together with the corresponding temperatures plus values for n obtained as outlined in the data analysis section were inserted into equation 9 to compute values for $C_{p,xs}$. The excellent correspondence between simulations and calorimetric traces is shown by the example in Figure 8.3 and seems to indicate the appropriateness of the model assumptions. The data analysis suggests that aggregation involves molecular clusters. The ratio of the van't Hoff and calorimetric enthalpies shows that a number of molecules form the base cooperative unit involved in the aggregation process. The plot simulation provides evidence that the transition process involves the aggregation of these clusters. Table 8.2 contains estimates for the overall number of molecules involved in the aggregation process. It must be noted that these values represent average values for the system under investigation. The Table reveals that as molecular weight increases the size of the cluster in terms of monomeric content decreases. On the other hand the number of clusters involved in the aggregation process apparently show no significant changes with molecular weight.

8.2.5 **The Effect of Concentration on the Thermodynamics of the Phase Transitions.**

The thermodynamic parameters for POP 1000 solutions of different aqueous concentrations (Table 8.3; Figure 8.4) show that increasing concentration produces a decrease in T_m. The fact that an increase in solution concentration produces a decrease in T_m provides supporting evidence that the process under investigation involves association.[18] This effect of concentration on T_m is presumably a manifestation of Le Chatelier's principle in that an increase in the concentration of starting species forces the equilibrium in the direction of producing more aggregates. Since the aggregation process is endothermic this must result in a decrease in the temperature at which the transition occurs.

The simulated values for n (Table 8.3) are fairly constant and would thus appear to indicate that the change in concentration does not affect the number of clusters participating in the aggregation process. The $\Delta H_{vH}/\Delta H_{cal}$ ratio indicates that the average number of monomeric species participating in the pre-aggregation clusters is between 7 and 9 and is relatively unaffected by changes in concentration. This would suggest that the decrease in ΔH_{cal} and ΔH_{vH} with decreasing concentration and hence increasing temperature is merely a manifestation of the temperature dependence of these two enthalpy values. A plot of ΔH_{vH} against $T_{1/2}$ (Figure 8.5) provides an estimate of $\Delta C_{p,d}$ for the transition. The approximate linearity of the plot ($r^2 = 0.872$) suggests that $\Delta C_{p,d}$ is independent of temperature. The gradient yields a value of -19.3 kJ mol(of molecular clusters)$^{-1}$.K^{-1} for $\Delta C_{p,d}$. This is larger than the other value quoted for POP 1000 in Table 8.1 (i.e., -0.5 kJ mol(of monomer)$^{-1}$.K^{-1} or -4.36 kJ mol(of molecular clusters)$^{-1}$.K^{-1}). It does however allow prediction of a much lower upper $T_{1/2}$ value of 396.3 K. The difference in these $\Delta C_{p,d}$ values is possibly a reflection of the fact that $\Delta C_{p,d}$ obtained from the calorimetric data represents the sum of the negative $\Delta C_{p,d}$ value for aggregation and the positive $\Delta C_{p,d}$ value for phase separation.

If one reconsiders equation 2 differentiation of lnK with respect to lnc at a constant value for n and α (set equal to 0.5) one obtains the following:

$$\left(\frac{\partial \ln K}{\partial \ln c}\right)_{n,T} = -(n-1) \qquad (20)$$

Combining equation 20 with the following expression:

$$\left(\frac{\partial \ln K}{\partial \ln c}\right)_{n,T}\left(\frac{\partial \ln c}{\partial\left(\frac{1}{T}\right)}\right)_n = \left(\frac{\partial \ln K}{\partial\left(\frac{1}{T}\right)}\right)_n = -\frac{\Delta H_{vH}}{R} \qquad (21)$$

gives:

$$\left(\frac{\partial \ln c}{\partial\left(\frac{1}{T}\right)}\right)_n = \frac{\Delta H_{vH}}{R(n-1)} \qquad (22)$$

A plot of ln c vs $1/T_{1/2}$ gives a good linear plot (Figure 8.6, $r^2 = 0.997$) of gradient $18000K^{-1}$. Substitution of ΔH_{vH} values, obtained for the various solutions, into equation 22 allows an estimation of the values of n. These are shown in Table 8.3. Perhaps not unsurprisingly these computed n values are very close to the simulated n values.

8.2.6 **Comparison with Block Copolymers.**

By way of comparison selected thermodynamic parameters for the block copolymers P215 and P217 are presented in Table 8.6. Both copolymers have POP blocks close to a molecular weight of 2000 and thus invite comparison with the homopolymer of the same molecular weight. P215 contains 50% POE and P217 contains 70% POE. It is evident that the incorporation of ethylene oxide into the polymer dramatically reduces the calorimetric and van't Hoff enthalpies and increases the phase transition temperature. The ratio of ΔH_{vH} to ΔH_{cal} for both polymers is three indicating that three molecules form the base mole cooperative unit in the aggregation process. The number of clusters involved in the process is, in both cases, also equal to 3. Thus ethylene oxide seems to decrease the cooperativity of the transition and decrease the number of clusters involved in the process. This possibly indicates the role of ethylene oxide in increasing the repulsion between the POP segments of the copolymers.

8.2.7 **Entropy-Enthalpy Compensation.**

The free energy of the systems under consideration may be calculated at $T_{1/2}$ through the application of the following equation:

$$\Delta G = RT_{1/2} \ln(nc^{n-1}0.5^{n-1}) \qquad (23)$$

where c is the concentration of molecular clusters in mol L^{-1}

Using values for the van't Hoff enthalpy enables the computation of entropy values at $T_{1/2}$. These values have been plotted against each other in the form of an entropy-enthalpy compensation plot. The gradient of the plot yields the compensation temperature which characterises solvent-solute interaction.[27]

The compensation plot in Figure 8.7 is an excellent linear plot ($r^2 = 0.9998$). The most interesting feature of the plot is that it contains enthalpy-entropy data for all the solutions examined in this study including the pluronic solutions. Thus the linearity of the plot implies that all the phase transitions investigated are manifestations of the same interaction between the aqueous solvent and poly (oxypropylene). The compensation temperature obtained is 275 K.

8.2.8 **Modelling of the Phase Transitions for Diblocks, Poloxamers and Poloxamines.**

The data derived for the phase transitions for diblocks, poloxamers and poloxamines in Chapters 4, 5 and 6 have been re-analysed to determine values for ΔH_{vH} and n using equations 6 and 18. The data are presented in Tables 8.4-8.9.

8.2.8.1 **Copolymers in Water at a Concentration of 5mgmL^{-1}.**

The number of molecules comprising each cluster for the diblocks, poloxamers and poloxamines in water at a concentration of 5mgmL^{-1} (ΔH_{vH}/ ΔH_{cal}, Tables 8.4, 8.5 and 8.6) are lower than those observed for the POP homopolymers. The value of ΔH_{vH} increases with increasing POP content as observed for the POP hompolymers. The ratios of ΔH_{vH}/ ΔH_{cal} for the diblocks, poloxamers and poloxamines are 3.1(±1.0), 2.8 (±1.0) and 2.4 (±0.8) respectively compared to 7.7 (±3.4) for the POP homopolymers. These lower values reflect the effect of POE in increasing repulsion between the POP segments of the copolymers, and there is a slight trend of decreasing ΔH_{vH}/ ΔH_{cal} with increasing number of POE chains per molecule although the averaged values are not significantly different. The number of clusters involved in the aggregation process ranges from 1 to 9 for the POE containing block copolymers and averages 3-4 for each copolymer group (diblocks (3.1 (±0.7), poloxamers 2.8 (±1.3), poloxamines 3.9 (±2.6)), which again, are lower than those values observed for the POP homopolymers. The observation that the POP hompolymers precipitate upon aggregation and POE containing copolymers remain in solution also reflect that the number of molecules per cluster and aggregate are higher for POP homopolymers.

8.2.8.2 **Concentration Effects.**

The effects of concentration for P237 (1-50mgmL^{-1}) and P333 (0.1-20mgmL^{-1}) is shown in Table 8.7. There is a slight increase in ΔH_{vH} with increasing concentration, and this is merely a reflection of the temperature dependence of the phase transition (T_m decreases with increasing concentration). The values for $\Delta H_{vH}/ \Delta H_{cal}$ and n do not significantly change with increasing concentration indicating that the nature of the aggregation is unaffected by the number of molecules present in solution. The difference in the number of molecules comprising each cluster between P237 and P333 (4.5 (±0.6) and 2.3 (±0.5) respectively) may indicate that the initial core size of the aggregate is the same (increasing n with decreasing POP molecular mass). However, by comparison of these values to other poloxamers (Table 8.6) by grouping the copolymers in terms of constant POP molecular mass and percentage POE content show a slight, but insignificant, decrease in $\Delta H_{vH}/ \Delta H_{cal}$ with increasing POP content (excluding copolymers close to the solubility limit of POP i.e., with a POP content of 950gmol^{-1}).

8.2.8.3 **Cosolute and Cosolvent Effects.**

The effects of cosolutes and cosolvents on the phase transition of P237 at a concentration of 5mgmL^{-1} are shown in Tables 8.8 and 8.9. The presence of salts and urea appear to have no significant effect on ΔH_{vH}, the number of molecules per cluster or the number of clusters that initially aggregate (Table 8.8), and this may reflect that the cosolutes (NaCl, NaH_2PO_4/Na_2HPO_4 and urea) interact with the solvent and not directly with the POP block - the effects on T_m reflecting the change in the nature of the solvent and water structure which indirectly effects the aggregation process. The effects of alcohols and formamide (Table 8.9) show significant changes in $\Delta H_{vH}/ \Delta H_{cal}$ and n with increasing cosolvent concentration, however, fairly large quantities of cosolvent are required to significantly effect the thermodynamics associated with the aggregation process. Increasing concentrations of methanol, ethanol and formamide raise the T_m and increase the number of molecules per cluster, although the value of n does not significantly alter. A slight decrease in T_m and a large increase of the $\Delta H_{vH}/ \Delta H_{cal}$ ratio is observed with increasing propanol concentration. The value of ΔH_{vH} did not significantly alter with increasing propanol concentration. Butanol decreased the T_m and $\Delta H_{vH}/ \Delta H_{cal}$ with increasing concentration. These effects may reflect

that the cosolvents replace water molecules in the solvation sphere of the POP block, and may also reflect that they act as water strucure promoters or breakers as observed for cosolutes.

8.3 Concludimg Remarks.

This study has suggested that phase transitions investigated by HSDSC provide evidence of a thermally induced aggregation process taking place between several molecular clusters It is believed that this process is a precursor to phase separation. The number of clusters involved in the process varies between 3 and 7. The number of polymer molecules incorporated in each cluster ranges from 3 to 11 molecules for the homopolymers and block copolymers in water. These parameters vary with molecular mass for the POP hompolymers but remain constant with changes in concentration. The incorporation of POE blocks into the molecules also has an affect on cluster size and aggregation number reducing the number of molecules per cluster and per aggregate to approximately 3 and 3-4 respectively. Cosolutes and cosolvents dramatically affect the temperature at which aggregation occurs and may reflect changes in water structure or replacement of water molecules associated with the POP block. Cosolutes (NaCl, phosphate and urea) do not appear to affect the number of molecules or clusters of molecules involved in the aggregation process and may reflect changes in solvent structure only, but high cosolvent concentrations dramatically affect the number of molecules associated in each molecular cluster (MeOH, EtOH PrOH and formamide increase the number of molecules per cluster, and BuOH decrease the number of molecules per cluster with increasing cosolvent concentration) which may reflect changes in solvent structure as well as the formation of solvent-rich zones around the POP block of the copolymer. However an enthalpy-entropy compensation plot shows that the chemical driving force of aggregation and the solvent POP interaction is the same for all the systems investigated.

8.4 Tables

Table 8.1 The Effect of Molecular Mass on the Overall Thermodynamic Parameters for the Observed Phase Transitions of Poloyoxypropylene in Aqueous Solution.

Molecular Mass ($gmol^{-1}$)	T_m (K)	$T_{1/2}$ (K)	ΔH_{cal} ($kJmol^{-1}$)	C_p^{max} ($kJmol^{-1}K^{-1}$)	$\Delta T_{1/2}$ (K)	$\Delta C_{p,d}$ ($kJmol^{-1}K^{-1}$)	ΔH_{vH} ($kJmol^{-1}K^{-1}$)
725	327.3	331.3	41	2.3	15.2	-0.3	487
1000	314.5	317.7	74	5.5	11.5	-0.5	645
2000	294.7	296.0	302	56.3	4.2	-4.5	1790
4000	284.1	284.4	514	215.7	2.0	-6.6	2109

Table 8.2 Values for Number of POP Molecules in Clusters and Number of Clusters Involved in Aggregation.

Molecular Mass ($gmol^{-1}$)	$\Delta H_{vH}/\Delta H_{cal}$	n
725	11.9	4.5
1000	8.7	5
2000	5.9	7
4000	4.1	3

Table 8.3 Thermodynamic Parameters for POP 1000 as a Function of Concentration.

Conc. ($mgmL^{-1}$)	T_m (K)	$T_{1/2}$ (K)	ΔH_{cal} ($kJmol^{-1}$)	C_p^{max} ($kJmol^{-1}K^{-1}$)	$\Delta T_{1/2}$ (K)	ΔH_{vH} ($kJmol^{-1}$)	$\Delta H_{vH}/\Delta H_{cal}$	n^a	n^b
2.5	318.4	321.4	88	4.1	11.5	577	6.6	3.5	4.9
5.0	314.5	317.7	74	5.5	11.5	645	8.7	5	5.3
10.0	310.4	313.0	89	7.5	10.3	713	8.0	5	5.8
10.0	310.7	313.4	82	7.0	10.2	725	8.9	5	6.1
15.0	308.3	310.8	88	8.1	9.4	763	8.7	5	6.1
20.0	307.1	309.3	90	8.8	9.0	801	8.9	5	6.4
30.6	305.0	307.3	102	10.3	8.5	934	9.1	6	7.2
50.0	303.2	304.8	100	10.5	8.2	850	8.5	5	6.7
51.5	302.3	304.7	108	11.3	8.1	953	8.8	6	7.4

[a]n values simulated from fitting of $C_{p,xs}$ data, [b]n values computed from equation 22

Table 8.4 Thermodynamic Parameters for the Diblock Copolymers in Water at a Concentration of 5mgmL^{-1} .

Diblock MW (gmol^{-1})	T_m (K)	$T_{1/2}$ (K)	ΔH_{cal} (kJmol^{-1})	C_p^{max} (kJmol^{-1}K^{-1})	$C_{p,1/2}$ (kJmol^{-1}K^{-1})	$\Delta T_{1/2}$ (K)	ΔH_{vH} (kJmol^{-1})	$\Delta H_{vH}/\Delta H_{cal}$	n
3438	300.2	301.9	253	26.6	25.0	8.3	533	2.1	2.6
8750	336.8	339.2	99	5.5	5.4	15.6	404	4.1	2.9
13333	302.5	303.7	351	55.5	49.6	5.4	1052	3.0	3.9

Table 8.5 Thermodynamic Parameters for the Phase Transitions Observed for Poloxamines in Water at a Concentration of 5mgmL^{-1} .

Poloxamine	T_m (K)	$T_{1/2}$ (K)	ΔH_{cal} (kJmol^{-1})	C_p^{max} (kJmol^{-1}K^{-1})	$C_{p,1/2}$ (kJmol^{-1}K^{-1})	$\Delta T_{1/2}$ (K)	ΔH_{vH} (kJmol^{-1})	$\Delta H_{vH}/\Delta H_{cal}$	n
T701	299.6	301.1	324	37.2	34.8	7.5	668	2.1	3.1
T803	302.1	304.3	357	41.3	33.3	6.4	1361	3.8	8.5
T904	299.9	300.8	293	41.2	39.2	6.0	695	2.4	2.5
T1301	291.3	291.9	529	109.5	105.2	4.2	917	1.7	2.3
T1302	294.7	295.6	529	92.7	83.7	4.5	989	1.9	3.3

Table 8.6 Thermodynamic Parameters for the Phase Transitions Observed for Poloxamers in Water at a Concentration of 5mgmL^{-1} .

Poloxamer	T_m (K)	$T_{1/2}$ (K)	ΔH_{cal} (kJmol^{-1})	C_p^{max} (kJmol^{-1}K^{-1})	$C_{p,1/2}$ (kJmol^{-1}K^{-1})	$\Delta T_{1/2}$ (K)	ΔH_{vH} (kJmol^{-1})	$\Delta H_{vH}/\Delta H_{cal}$	n
P101	324.2	328.5	61.6	3.3	3.0	17.6	670	10.9	6.6
P105	346.2	348.2	36.3	1.6	1.7	20.6	229	6.3	1.5
P108	354.9	355.2	19.8	1.2	1.2	16.9	249	12.6	0.9
P122	326.6	328.6	93.2	3.9	3.9	20.8	178	1.9	1.4
P123	325.2	328.1	83.3	4.6	4.4	15.8	343	4.1	2.6
P124	313.8	316.9	120.2	8.3	7.6	11.2	525	4.4	4.0
P181	303.5	306.7	187.3	13.6	12.2	13.0	541	2.9	4.3
P182	312.2	314.3	156.9	11.4	10.8	11.6	444	2.8	2.9
P184	313.9	316.8	163.4	12.3	10.3	12.6	503	3.1	3.8
P188	330.5	332.1	87.9	5.5	5.2	14.8	289	3.3	1.6
P215	315.0	316.8	158.6	11.9	11.8	11.1	436	2.7	2.5
P217	323.0	325.4	96.7	7.1	6.2	14.4	388	4.0	2.4
P231	301.5	302.4	252.6	21.8	23.5	10.4	383	1.5	1.7
P234	306.6	308.2	193.6	22.5	20.4	7.4	876	4.5	4.3
P235	309.4	310.8	175.3	18.7	16.8	9.2	575	3.3	2.7
P237	314.8	317.3	194.8	18.2	15.9	9.9	817	4.2	5.0
P238	310.1	311.0	140.5	14.8	13.2	9.9	416	2.9	1.8
P282	300.3	301.8	283.4	31.1	29.0	8.2	726	2.6	3.7
P284	308.9	310.1	224.6	19.1	18.8	10.1	431	1.9	2.2
P331	293.1	293.8	374.3	59.4	56.9	5.5	604	1.6	1.8
P333	298.5	299.3	353.6	52.2	50.2	5.7	746	2.1	2.5
P335	300.7	301.6	316.4	45.8	43.9	6.1	710	2.2	2.4
P338	304.9	305.6	227.2	22.6	22.2	8.6	385	1.7	1.5
P401	291.5	292.1	434.6	74.9	75.5	4.6	723	1.7	1.9
P407	300.6	301.7	176.8	26.4	25.0	5.4	960	5.4	3.5

Table 8.7 The Effects of Concentration on the Thermodynamic Parameters for the Phase Transitions of Poloxamers in Water.

Conc. ($mgmL^{-1}$)	T_m (K)	$T_{1/2}$ (K)	ΔH_{cal} ($kJmol^{-1}$)	C_p^{max} ($kJmol^{-1}K^{-1}$)	$C_{p,1/2}$ ($kJmol^{-1}K^{-1}$)	$\Delta T_{1/2}$ (K)	ΔH_{vH} ($kJmol^{-1}$)	$\Delta H_{vH}/\Delta H_{cal}$	n
P237									
1.0	319.7	321.7	160	13.0	12.8	10.4	610	3.8	3.4
2.5	316.9	319.2	187	15.4	15.0	9.6	705	3.8	4.2
5.0	314.8	317.3	195	18.2	15.9	9.9	817	4.2	5.0
7.5	313.9	316.0	191	17.9	16.2	9.2	788	4.1	4.6
10.0	312.9	315.1	196	18.5	15.9	8.9	831	4.2	4.9
15.0	311.7	314.1	206	19.4	17.4	8.7	923	4.5	5.7
17.1	311.3	313.3	185	18.6	17.0	8.3	830	4.5	4.6
20.0	310.7	312.9	191	19.2	17.5	8.5	859	4.5	4.8
25.0	310.5	312.9	181	17.6	15.5	8.8	896	5.0	5.4
34.1	309.3	311.4	189	19.9	17.5	8.2	1098	5.8	6.4
50.0	307.8	310.0	192	19.3	17.4	8.0	927	4.8	5.4
P333									
0.1	303.8	304.2	207	24.0	34.5	3.8	731	3.5	1.8
0.5	301.6	302.6	268	44.1	46.0	6.6	603	2.3	2.2
1.0	301.0	301.8	327	41.7	42.2	6.5	573	1.8	1.9
2.5	299.7	300.5	345	46.4	45.8	6.2	663	1.9	2.3
5.0	298.4	299.3	354	52.2	50.2	5.7	746	2.1	2.5
10.0	297.2	298.1	340	53.0	51.6	5.4	759	2.2	2.4
15.0	296.6	297.5	344	54.0	52.5	5.2	818	2.4	2.6
20.0	296.1	296.7	341	57.2	53.4	5.3	809	2.4	2.5

Table 8.8 The Effects of Cosolutes on the Thermodynamic Parameters Derived for P237 in Aqueous Solution at a Concentration of 5mgmL^{-1}.

Conc. (M)	T_m (K)	$T_{1/2}$ (K)	ΔH_{cal} (kJmol^{-1})	C_p^{max} (kJmol^{-1}K^{-1})	$C_{p,1/2}$ (kJmol^{-1}K^{-1})	$\Delta T_{1/2}$ (K)	ΔH_{vH} (kJmol^{-1})	ΔH_{vH} /ΔH_{cal}	n
NaCl									
0	314.8	317.3	195	18.2	15.9	9.9	817	4.2	5.0
0.34	309.9	312.0	194	20.3	18.8	8.9	762	3.9	4.2
0.69	305.8	307.7	201	22.1	20.0	8.4	802	4.0	4.2
1.03	301.9	304.1	209	23.4	20.9	8.1	884	4.2	5.3
1.38	297.8	299.6	230	26.1	24.1	8.1	767	3.3	4.2
1.71	294.1	295.9	243	27.9	25.3	8.0	777	3.2	4.3
Phosphate									
0.10	313.8	315.8	160	13.1	12.0	11.2	545	3.4	3.5
0.15	311.4	314.4	166	14.5	13.1	10.5	664	4.0	5.3
0.20	307.5	309.7	153	15.4	14.0	9.2	697	4.6	4.0
0.35	303.0	304.4	161	17.4	16.8	8.5	607	3.8	3.1
0.50	297.9	299.5	145	17.7	16.3	7.7	685	4.7	3.4
Urea									
1.04	319.2	321.5	167	13.0	10.5	11.7	486	2.9	3.1
1.58	322.3	325.1	146	11.3	9.0	12.2	526	3.6	3.4
2.86	324.1	325.9	173	13.7	9.8	12.0	501	2.9	2.8
4.05	326.7	328.9	136	10.0	8.0	13.2	442	3.3	2.7
7.83	331.7	334.1	98	6.7	5.4	13.9	439	4.5	2.8

Table 8.9 The Effects of Cosolvents on the Thermodynamic Parameters Derived for P237 in Aqueous Solution at a Concentration of 5mgmL^{-1}.

Cosolvent Conc. (%)	T_m (K)	$T_{1/2}$ (K)	ΔH_{cal} (kJmol^{-1})	C_p^{max} (kJmol^{-1}K^{-1})	$C_{p,1/2}$ (kJmol^{-1}K^{-1})	$\Delta T_{1/2}$ (K)	ΔH_{vH} (kJmol^{-1})	ΔH_{vH} /ΔH_{cal}	n
Methanol									
0	315.2	317.3	170	17.3	15.8	9.3	719	4.2	3.6
5.0	317.0	319.1	145	13.1	11.9	10.5	633	4.4	3.5
10.0	319.3	321.4	119	10.1	9.1	11.9	568	4.8	3.3
15.0	322.4	324.3	109	7.5	7.2	12.7	381	3.5	2.3
17.5	323.1	325.1	70	5.0	4.9	12.4	379	5.4	2.1
20.0	326.9	328.3	38	3.4	2.8	13.1	508	13.4	2.8
22.5	329.5	331.0	24	2.5	1.8	13.5	471	19.6	2.5
25.0	331.9	333.9	21	1.9	1.5	13.5	366	17 4	1.7
Ethanol									
5.0	317.1	319.4	155	13.0	11.6	11.3	552	3.4	3.4
10.0	319.1	321.3	99	7.9	7.4	11.0	545	5.5	3.3
15.0	322.6	324.5	60	4.1	4.0	12.1	449	7.5	2.8
20.0	328.9	331.4	14	1.5	1.0	13.6	705	50.4	4.1
Propanol									
2.5	314.9	317.3	179	14.8	14.1	9.5	767	4.3	4.8
5.0	314.4	316.3	149	13.5	12.5	9.8	694	4.7	4.0
7.5	313.4	315.8	100	9.8	8.5	9.3	826	8.3	4.9
10.0	313.3	314.9	79	7.8	7.0	9.7	601	7.6	3.1
Butanol									
2.5	310.1	312.0	191	18.5	16.8	8.8	718	3.8	4.0
5.0	303.5	304.8	216	20.4	21.3	7.8	534	2.5	2.5
7.5	295.0	296.4	288	30.0	29.5	7.1	574	2.0	2.8
Formamide									
10	318.2	320.1	139	11.0	10.6	11.4	542	3.9	3.2
20	321.5	323.8	108	8.1	7.6	12.5	480	4.4	2.9
30	326.1	328.6	99	5.7	5.8	14.4	426	4.3	3.1
40	329.2	332.4	52	3.5	3.3	14.2	447	8.6	2.9
50	336.8	337.2	17	1.5	1.5	11.7	405	23.8	1.5
60	344.2	344.4	17	1.0	1.2	12.6	416	24.5	2.0

8.5 References.

(1) Shaw, D.J. *Introduction to Colloid and Surface Chemistry*, Butterworths, London, (1980).
(2) Chang, L-H.; Li, S-J.; Ricca, T.L.; Marshall, A.G. *Anal. Chem.* **1984**, *56*, 1502.
(3) Tanford, C. *The Hydrophobic Effect*, 2nd Edition, Wiley, New York, **1980**.
(4) Sturtevant, J.M. *Proc. Natl. Acad. Sci. USA*, **1982**, *79*, 3963.
(5) Schild, H.G.; Tirrell, D.A. *J. Phys. Chem.*, **1990**, *94*, 4352.
(6) Mitchard, N.M.; Beezer, A.E.; Rees, N.H.; Mitchell, J.C.; Leharne, S.; Chowdhry, B.Z.; Buckton, G. *J. Chem. Soc. Chem. Commun.* **1990**, 900.
(7) Mitchard, N.M. Ph.D. Thesis, University of London, 1990.
(8) Beezer, A.E.; Mitchell, J.C.; Rees, N.H.; Armstrong, J.K.; Chowdhry, B.Z.; Leharne, S.; Buckton, G. *J. Chem. Res.* **1991**, 254.
(9) Beezer, A.E.; Mitchard, N.M.; Mitchell, J.C.; Armstrong, J.K.; Chowdhry, B.Z.; Leharne, S.; Buckton, G. *J. Chem. Res.* **1992**, 236.
(10) Mitchard, N.M.; Beezer, A.E.; Mitchell, J.C.; Armstrong, J.K.; Chowdhry, B.Z.; Leharne, S.; Buckton, G. *J. Phys. Chem.* **1992,** *96*, 9507.
(11) Yu, G.-E.; Deng, Y.; Dalton, S.; Wang, Q.-G.; Attwood, D.; Price C.; Booth, C. *J. Chem. Soc. Faraday Trans.*, **1992**, *88*, 2537.
(12) Wanka, G.; Hoffmann, H.; Ulbricht, U. *Colloid Polym. Sci.*, **1990**, *268*, 101.
(13) Wang, Q.; Price C.; Booth, C. *J. Chem. Soc. Faraday Trans.*, **1992**, *88*, 1437.
(14) Brown, W.; Schillén, K.; Almgren, M.; Hvidt, S.; Bahadur, P. *J. Phys. Chem.*, **1991**, *95*, 1850.
(15) Brown, W.; Schillén K.; Hvidt, S. *J. Phys. Chem.*, **1992**, *96*, 6038.
(16) Malmsten M.; Lindman, B. *Macromolecules*, **1992**, *25*, 5440.
(17) Linse P.; Malmsten, M. *Macromolecules*, **1992**, *25*, 5434.
(18) Sturtevant, J.M. *Ann. Rev. Phys. Chem.* **1987**, *38*, 463.
(19) Edge, V.; Allewell N.M.; Sturtevant, J.M. *Biochemistry*, **1985**, *24*, 5899.
(20) Kjellander, R.; Florin, E. *J. Chem. Soc. Faraday Trans.*, **1981**, *77*, 2053.
(21) Blandamer, M.J.; Briggs, B.; Brown, H.R.; Burgess, J.; Butt, M.D.; Cullis, P.M.; Engberts, J.B.F.N. *J. Chem. Soc. Faraday Trans.*, **1992**, *88*, 979.
(22) Sanchez-Ruiz, J.M.; Lopez-Lacomba, J.L.; Cortijo, M.; Mateo, P.L. *Biochem.*, **1988**, *27*, 1648.
(23) Hergeth, W.-D.; Alig, I.; Lange, J.; Lochmann, J.R.; Scherzer T.; Wartewig, S. *Makromol. Chem. Macromol. Symp.*, **1991**, *52*, 289.
(24) Karlström, G. *J. Phys. Chem.* **1985**, *89*, 4962.
(25) Björling, M.; Karlström, G.; Linse, P. *J. Phys. Chem.* **1991**, *95*, 6706.
(26) Privalov, P.L. *Crit. Rev. Biochem. Mol. Biol.* **1990**, *25*, 281.
(27) Bedö, Zs.; Berecez, E.; Lakatos, I. *Colloid Polym. Sci.*, **1992**, *270*, 799.

CHAPTER 9 - SUMMARY

The studies presented in this thesis, demonstrate that the phase behaviour of all of the block copolymers studied is dependent on changes associated with the solvation and aggregation state of the POP block. Figure 9.1 shows the relationship between the observed phase transition temperature and POP content of all of the homopolymers and block copolymers studied at a concentration of 5 $mgmL^{-1}$ in double distilled water and at a scan rate of 60 Kh^{-1}. The T_m decreases with increasing POP content and there is no apparent relationship to the POE content.

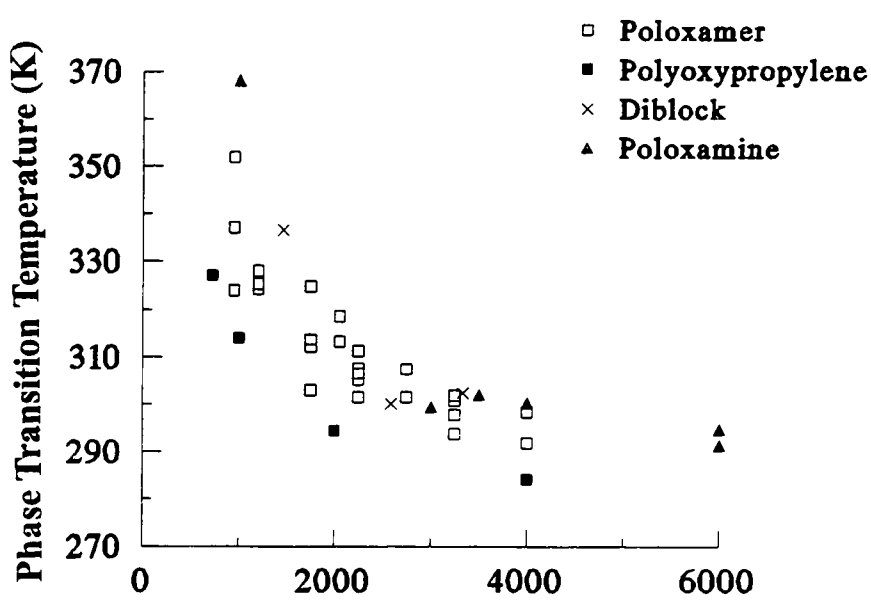

Figure 9.1 A plot of the calorimetrically observed phase transition temperature versus POP content for all of the polymer samples investigated at a concentration of 5 $mgmL^{-1}$ and at a scan rate of 60Kh^{-1}.

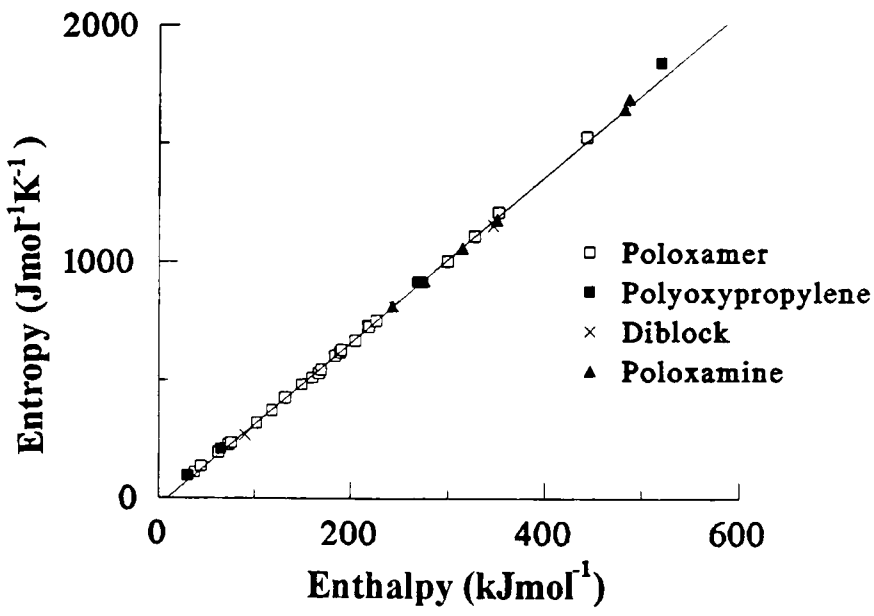

Figure 9.2 Entropy-enthalpy compensation plot for the observed phase transition of the polymers studied in dilute aqueous solution by HSDSC.

The observation that the calorimetrically observed phase transition is solely due to changes in the interaction between the solvent and POP blocks can be further demonstrated in the form of an enthalpy-entropy compensation plot (Figure 9.2). The plot is linear ($r^2 = 0.999$) and strongly implies that all of the phase transitions examined in this thesis reflect the same interaction between the aqueous solvent and POP.

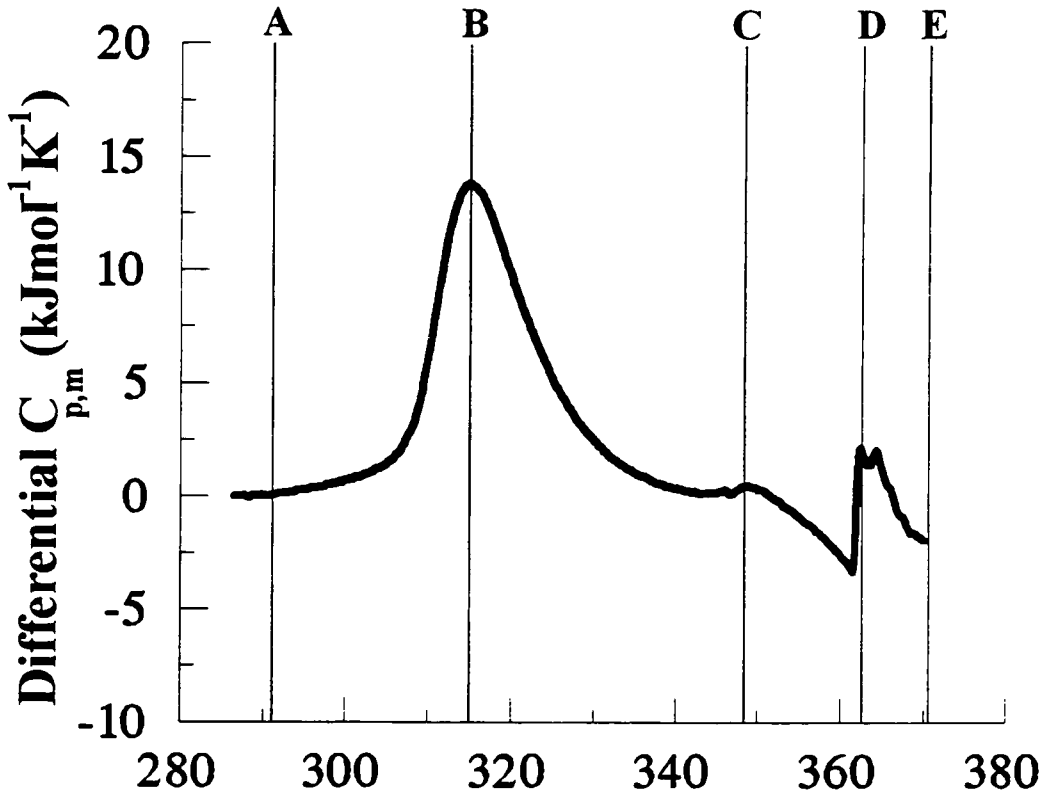

Figure 9.3 Summary of the different solvation states observed for block copolymers of POP and POE in dilute aqueous solution.

Figure 9.3 shows the different states of solvation and aggregation observed for copolymers of POE and POP in dilute aqueous solution and are described as follows:

(1) Below A - At temperatures below A, the copolymer samples exist mainly as single copolymer chains with hydrated and extended POE chains and partially hydrated POP chains.

(2) From A to B - At temperatures above A, the population of dimeric and low chain number clusters increases, with weakly associated and hydrated POP blocks. At temperatures close to A and at temperatures below the start of the observed phase transition the hydration state of the copolymers in the clusters and single chains are essentially the same. As the temperature increases through the phase transition and up to B, the POP dehydrates and

the clusters aggregate to form larger aggregates with a dehydrated POP core bounded by POE which remains hydrated and in the same state as single hydrated polymer chains.

(3) From B to C - At temperatures above B, the size of the molecular aggregate increases in size, the number of chains per aggregate dependent on the POE content. The core of the aggregate becomes more POP rich, as water trapped in the hydrophobic core moves to the bulk phase. The molecular mass of the aggregates is of the order of 10^6 $gmol^{-1}$. At C the aggregates are no longer stable in solution due to size and precipitate from solution observed as the cloud point. The POE chains remain predominantly hydrated.

(4) From C to D - At temperatures above C phase separation of the aggregates continues and complete phase separation of the POP blocks is observed, in which the terminal blocks of the POP (which behave as POE) phase separate. At D, dehydration of the POE chains is observed.

(5) From D to E - At temperatures above D phase separation of the aggregates continues involving dehydration of the POE blocks. The phase separation constitutes supramacromolecular formation resulting in a distinct oil phase and aqueous phase.

Increasing copolymer concentration decreases the T_m and raises the ΔH_{cal} and the change in enthalpy merely reflects the concentration dependence of the aggregation process. The presence of cosolutes and cosolvents effect the aggregation process dependent on the nature of the cosolute/cosolvent. Salts that increase water structure (NaCl, phosphate) lower the temperature at which aggregation is observed, and the enthalpy increases with increasing salt concentration. The opposite trend is observed in the presence of water structure breakers (urea, guanidinium chloride). Increasing concentrations of methanol, ethanol and formamide increase the T_m and decrease ΔH_{cal} , propanol slightly decreases T_m and ΔH_{cal} , and butanol decreases the T_m and raises ΔH_{cal} . The effect of cosolvents on the aggregation behaviour of poloxamers in aqueous solution may reflect changes in the nature of the solvent as well as direct interaction with the POP block, forming a cosolvent-rich phase in the core of the aggregate.

Modelling of the phase behaviour of POP homopolymers, POP/POE diblock copolymers, poloxamers and poloxamines using a mass action model, demonstrates that the

aggregation process is cooperative, and in constant equilibrium between single chains, clusters and aggregates. The number of chains per cluster ($\Delta H_{vH} / \Delta H_{cal}$) and aggregate (n) decrease when POE is incorporated in the molecule compared to POP homopolymers. Increasing copolymer concentration and the presence of salts (NaCl, phosphate) and urea do not effect the number of molecules per cluster or number of clusters per aggregate. The presence of relatively high concentrations of methanol, ethanol, propanol and formamide increases the $\Delta H_{vH} / \Delta H_{cal}$ and the number of clusters per aggregate slightly decreases with increasing cosolvent concentration. With increasing butanol concentration the $\Delta H_{vH} / \Delta H_{cal}$ and n decrease.

Overall, the aggregation behaviour of POP homopolymers, diblocks, poloxamers and poloxamines is associated solely with changes in the solvation and conformation of the POP block, the POE block allows the aggregated from of the copolymer to remain in solution. The aggregation behaviour is sensitive to changes in copolymer concentration, which is a manifestation of the principle of LeChatelier and Braun in that an increase in the concentration of single polymer chains will result in an increase in the concentration of aggregates i.e., a decrease in T_m. The aggregation behaviour of the copolymers is dramatically effected by changes in the nature of the solvent by the addition of cosolutes or cosolvents, additives that increase polymer-solvent interactions or reduce hydrogen bonding (water structure "breakers") raise the temperature at which aggregation occurs (lowering the enthalpy). Conversely, additives that either displace water from the POP block or increase water structure, destabilise the POP block and favours polymer-polymer interactions (shifting the equilibrium towards the aggregated form from single chains), and hence lowers the T_m and increases the ΔH_{cal} of aggregation.

ADDENDUM

CONFERENCE PRESENTATIONS.

Conference:	International Conference on Thermodynamics of Solutions and Biological Systems.
Location:	New Delhi, India. 3rd-6th January, 1993.
Title:	**Scanning Calorimetric Studies of Poly(ethylene oxide)/Poly(propylene oxide)/Poly(ethylene oxide) Triblock Copolymers (Poloxamers) and Poly(propylene oxide) in Dilute Aqueous Solution. (Paper).**
Authors:	Armstrong,J.K.; Leharne,S.A.; Chowdhry,B.Z.; Beezer,A.E.; Mitchell,J.C.

Conference:	Macromolecules '92, Third Euro-American Conference on 'Functional Polymers and Biopolymers'.
Location:	University of Kent, Canterbury, Kent, UK. 7th-11th September, 1992.
Title:	**Scanning Calorimetric Studies of Poly(ethylene oxide)/Poly(propylene oxide)/Poly(ethylene oxide) Triblock Copolymers (Poloxamers) in Dilute Aqueous Solution. (Paper).**
Authors:	Armstrong,J.K.; Leharne,S.A.; Mitchell,J.C.; Beezer,A.E.; Chowdhry,B.Z.

Conference:	Chemistry Research for Britain,'Highlights of Postgraduate Chemistry'.
Location:	The Royal Society, 6 Carlton Terrace, London, UK. 16th September 1992.
Title:	**Scanning Calorimetric Studies of ABA Triblock Copolymers (Poloxamers) in Dilute Aqueous Solution. (Poster + COPUS Report).**
Authors:	Armstrong,J.K.; Chowdhry,B.Z.

Conference:	46th Annual Calorimetry Conference.
Location:	DeKalb, Illinois,USA. 28th July-1st August, 1991.
Title:	**Novel Phase Transitions of Poloxamines in Dilute Aqueous Solution Detected by High Sensitivity Differential Scanning Calorimetry. (Paper).**
Authors:	Armstrong,J.K.; Leharne,S.A.; Mitchell,J.C.; Beezer,A.E.; Chowdhry,B.Z.

Conference:	20th Meeting of the Federation of European Biochemical Societies.
Location:	Budapest,Hungary. 19th-24th August, 1990.
Title:	**Calorimetric Study of Surfactants. (Poster).**
Authors:	Armstrong,J.K.; Leharne,S.A.; Mitchell,J.C.; Chowdhry,B.Z.

FULL PUBLICATIONS

1. **Thermodynamic Model-Fitting of the Calorimetric Output Obtained for Aqueous Solutions of Oxyethylene-Oxypropylene-Oxyethylene Triblock Copolymers.** Paterson,I.; Armstrong,J.; Chowdhry,B.; Leharne,S., *Langmuir*, **1997**, *13(8)*, 2219-2226.

2. **Effect of Cosolvents and Cosolutes upon Aggregation Transitions in Aqueous-Solutions of the Pluronic F87 (Poloxamer P237): A High Sensitivity Differential**

Scanning Calorimetry Study. Armstrong,J.K.; Chowdhry,B.Z ; Mitchell,J.C.; Beezer,A.E; Leharne,S.A., *J.Phys.Chem.*, **1996**, *100(5)*, 1738-1745.

3. **Scanning Microcalorimetric Investigations of Phase Transitions in Dilute Aqueous Solutions of Poly(oxypropylene).** Armstrong,J.; Chowdhry,B.; O'Brien,R.; Beezer,A.; Mitchell, J.; Leharne,S., *J.Phys.Chem.*, **1995**, *99(13)*, 4590-4598.

4. **An Investigation of Dilute Aqueous Solution Behavior of Poly(oxyethylene) + Poly(oxypropylene) + Poly(oxyethylene) Block-Copolymers.** Beezer,A.E.; Loh,W.; Mitchell,J.C.; Royall,P.G.; Smith,D.O.; Tute,M.S.; Armstrong,J.K.; Chowdhry,B.Z.; Leharne,S.A.; Eagland,D.; Crowther,N.J., *Langmuir*, **1994**, *10(11)*, 4001-4005.

5. **Scanning Calorimetric Studies of Poly(ethylene oxide)-Poly(propylene oxide)-Poly(ethylene oxide) Triblock Copolymers (Poloxamers) and Poly(propylene oxide) in Dilute Aqueous Solution.** Armstrong,J.K.; Leharne,S.; Mitchell,J.C.; Beezer,A.E.; Chowdhry,B.Z., *J.Macromol.Sci.-Pure and Appl.Chem.*, **1994**, *A31 suppl.6-7*, 1299-1306.

6. **Thermodynamic Model-Fitting of Differential Scanning Calorimetry Traces Obtained for Aqueous Solutions of Oxyethylene Oxypropylene ABA Block-Copolymers.** Armstrong,J.K.; Chowdhry,B.Z.; Beezer,A.E.; Mitchell,J.C.; Leharne,S.A., *J.Chem.Res.(S)*, **1994**, *9*, 364-365.

7. **Scanning Densitometric and Calorimetric Studies of Poly(ethylene oxide)/Poly(propylene oxide)/Poly(ethylene oxide) Triblock Copolymers (Poloxamers) in Dilute Aqueous Solution.** Armstrong,J.K.; Parsonage,J.R.; Chowdhry,B.Z.; Leharne,S.A.; Mitchell,J.C.; Beezer,A.E.; Löhner,K.; Laggner,P., *J.Phys.Chem.*, **1993,** *97(15)*, 3904-3909.

8. **Thermodynamic Analysis of Scanning Calorimetric Transitions Observed for Dilute Aqueous Solutions of ABA Block Copolymers.** Mitchard,N.M.; Beezer,A.E.; Mitchell,A.E.; Armstrong,J.K.; Chowdhry,B.Z.; Leharne,S.A.; Buckton,G., *J.Phys.Chem.*, **1992,** *96(23)*, 9507-9512.

9. **High Sensitivity Differential Scanning Microcalorimetry of Phase Transitions in Dilute Aqueous Solutions of Poly(oxyethylene)+Poly(oxypropylene)+ Poly(oxyethylene) Block Copolymers.** Beezer,A.E.; Mitchard,N.M.; Mitchell,J.C.; Armstrong,J.K.; Chowdhry,B.Z.; Leharne,S.A.; Buckton,G., *J.Chem.Res.(S)*, **1992,** 7, 236-237.

10. **NMR Evidence for a Novel Phase Transition in Dilute Aqueous Solution of Pluronic F87 (Poloxamer 237).** Beezer,A.E.; Mitchell,J.C.; Rees,N.H.; Armstrong,J.K.; Chowdhry,B.Z.; Leharne,S.A.; Buckton,G., *J.Chem.Res.(S)*, **1991,** *9*, 254- 255.